University of Alberta

Design, Synthesis and Evaluation of Severe Acute Respiratory Syndrome Coronavirus 3C-Like Protease Inhibitors

by

Jianmin Zhang

A thesis submitted to the Faculty of Graduate Studies and Research in partial fulfillment of the requirements for the degree of Doctor of Philosophy

Department of Chemistry

Edmonton, Alberta

Fall 2007

Your file Votre référence
ISBN: 978-0-494-33100-2
Our file Notre référence
ISBN: 978-0-494-33100-2

ABSTRACT

Seven classes of compounds have been designed, synthesized and evaluated as potential SARS-CoV $3CL^{pro}$ inhibitors. The cyclic peptidyl keto-glutamine (*S*)-2-((2*S*,3*S*)-2-((*S*)-2-acetamido-3-methylbutanamido)-(benzyloxy)butanamido)-*N*((*S*)-4-(1,4-dioxo-3,4-dihydrophthalazin-2(1*H*)-yl)-3-oxo-1-((*S*)-2-oxopyrrolidin-3-yl)butan-2-yl)-4-methylpentanamide (**21**) and three related analogues were synthesized. This type of compound displays very potent inhibition against $3CL^{pro}$ with IC_{50} values ranging from 0.6 to 3.4 μM. Enzyme kinetics, ESI-MS and crystal structure studies suggest that Ac-Val-Thr(OBn)-Leu-γ-lactamglutamine-phthalhydrazide (**21**) (IC_{50} = 2.7 μM, K_i = 0.25 μM) initially inhibits the $3CL^{pro}$ in a competitive and reversible fashion, and subsequently inactivates the $3CL^{pro}$ by the formation of a covalent thioether bond in a long time course. Furthermore, the Ac-Val-Thr(OBn)-Leu-*N*,*N*-dimethylglutamine-phthalhydrazide (**25**) was also synthesized, by the replacement of the γ-lactam moiety of **21** with a *N*,*N*-dimethyl amide. This compound shows moderate inhibition against $3CL^{pro}$ with an IC_{50} value of 64 μM. Using a similar method, a related analogue, Ac-Val-Thr(OBn)-Leu-Phe-phthalhydrazide (**29**), was prepared. Compound **29** shows weaker inhibition against $3CL^{pro}$ (72% inhibition at 100 μM) compared to compound **21** (94% inhibition at 100 μM). In addition, the cyclic peptidyl keto-glutamines Ac-Val-Thr(OBn)-Leu-γ-lactamglutamine-thiophene (**30**), its benzyl deprotected analogue **31**, and Ac-Val-Thr(OBn)-Leu-γ-lactamglutamine-5-chloro-3-pyridinol (**32**) were synthesized. All of them exhibit very weak inhibition against $3CL^{pro}$ (<10% to 23% inhibition at 100 μM). These results suggest that both the γ-lactam and the phthalhydrazide moieties are

important structural features for the peptidyl keto-glutamines as SARS $3CL^{pro}$ inhibitors. Next, a library of non-peptidyl heteroaromatic esters and their analogues were prepared. The pyridinyl ester 5-bromo-pyridin-3-yl furan-2-carboxylate (**34**) is one of the most potent inhibitors, with an IC_{50} of 50 nM, K_m of 26×10^{-9} M, K_{cat} of 17×10^{-5} s^{-1} and K_{cat}/K_m of 6.5×10^3 M^{-1} s^{-1}. ESI-MS studies suggest a mechanism involving acylation of the active site cysteine thiol. Finally, a series of methylene ketones and fluorinated methylene ketones were synthesized, based on the modification of pyridinyl ester inhibitors. The most potent inhibitor 2-(5-bromopyridin-3-yl)-1-(5-(4-chlorophenyl)furan-2-yl)ethanone (**58**) has an IC_{50} of 13 μM against SARS-CoV $3CL^{pro}$ in a non-covalent and reversible fashion.

ACKNOWLEDGEMENTS

I would like to thank my supervisor, Professor John C. Vederas, for his excellent guidance, support and encouragement throughout my studies. It is such a rewarding and memorable time spent in his lab. I thank all the Vederas group members, both past and present, for their help in this work and their friendship that makes working in this lab so enjoyable. I especially thank Drs. Steven Cobb and Matt Clay for the proofreading of my thesis. I would also like to thank Dr. Hanna Pettersson, Dr. Rajendra Jain, Mr. Reuben Mahaffy and Mr. Sean Ferland for their synthetic work related to this project.

I would like to thank Professor Michael N. G. James (Department of Biochemistry, University of Alberta), Professor Lindsay D. Eltis (Department of Microbiology and Immunology, University of British Columbia), Dr. Jonanthan Parrish, Dr. Jiang Yin, Dr. Chunying Niu and Ms. Carly Huitema for their collaborative efforts and helpful suggestions.

I thank Professor Dennis Hall and Dr. Eric Pelletier for help with combinatorial synthesis and HPLC-MS purification. Dr. Randy Whittal, Dr. Angie Morales-Izquierdo and Ms. Jing Zheng are thanked for help with mass spectra. Financial assistance from the University of Alberta is gratefully acknowledged.

Finally, I would like to thank my family for their great patience and invaluable support, which is especially encouraging during my studies.

TABLE OF CONTENTS

LIST OF TABLES

LIST OF FIGURES

LIST OF SCHEMES

LIST OF ABBREVIATIONS

[α]	specific rotation
Ac	acetyl
AcOH	acetic acid
APE	aza-peptide epoxides
aq	aqueous
atm	atmosphere
Ar	aryl
Bis-Tris	2-(bis(2-hydroxyethyl)imino)-2-(hydroxymethyl)-1,3-propanediol
Bn	benzyl
Boc	*tert*-butoxycarbonyl
br	broad
tert-Bu	*tertiary*-butyl
c	concentration
calcd	calculated
Cbz	benzyloxycarbonyl
CDI	1,1'-carbonyldiimidazole
$3CL^{pro}$	3C-like protease
CMK	chloromethyl ketone
CoV	coronavirus
CPE	cytopathogenic effect
Cys	cysteine

δ	chemical shift in parts per million downfield from tetramethylsilane
d	doublet
DCC	1,3-dicyclohexylcarbodiimide
DCM	dichloromethane
DEAD	diethyl azodicarboxylate
DIPEA	diisopropylethyl amine
DMAP	4-(dimethylamino)pyridine
DMF	dimethylformamide
DMSO	dimethylsulfoxide
DTT	dithiothreitol
EC_{50}	concentration causing 50% of a maximum effect
EDCI	1-(3-dimethylaminopropyl)-3-ethylcarbodiimide
EDTA	ethylenediaminetetraacetic acid
EI	electron impact ionization
Enz	enzyme
ES	electrospray ionization
Et	ethyl
Et_2O	diethyl ether
EtOAc	ethyl acetate
EtOCOCl	ethyl chloroformate
eq.	equivalents
FMK	fluoromethyl ketone
FRET	fluorescence resonance energy transfer

Gln	glutamine
Glu	glutamic acid
HAV	hepatitis A virus
HBTU	o-Benzotriazol-1-tetramethyluroniumhexafluorophosphate
His	histidine
HIV	human immunodeficiency virus
HOBt	*N*-hydroxybenzotriazole
HPLC	high performance liquid chromatography
HRMS	high resolution mass spectrometry
HRV	human rhinovirus
HTS	high throughput screening
IC_{50}	concentration causing 50% inhibition
IR	infrared
J	coupling constant
KDa	kiloDalton
K_i	dissociation constant of enzyme-inhibitor complex
k_{inact}	rate of enzyme inactivation
K_m	Michaelis-Menten constant
k_{obs}	first order rate constant for the enzyme inactivation
LDA	lithium diisopropylamine
Leu	leucine
LiHMDS	lithium bis(trimethylsilyl) amide
m	multiplet

Me	methyl
MeCN	acetonitrile
MeOH	methanol
MHz	megahertz
MS	mass spectrometry
m/z	mass to charge ratio
μM	micromolar
nM	nanomolar
NFSi	*N*-fluorobenzenesulfonimide
NMR	nuclear magnetic resonance
Ph	phenyl
Phe	phenylalanine
PPh_3	triphenylphosphine
ppm	parts per million
psi	pounds per square inch
Py or Pyr	pyridine
q	quartet
quant.	quantitative
rt	room temperature
s	singlet
SARS	severe acute respiratory syndrome
t	triplet
$t_{1/2}$	half life

TFA	trifluoroacetic acid
THF	tetrahydrofuran
TLC	thin layer chromatography
Thr	threonine
TMS	tetramethylsilane
TMSCl	trimethylsilyl chloride
Val	valine

INTRODUCTION

The last 20 years have seen rapid progress in the development of new antiviral agents targeting viral proteases that are essential to the life cycle of a number of viruses, such as human immunodeficiency virus (HIV), hepatitis B and C viruses, influenza A and B viruses, human rhinovirus (HRV) and respiratory syncytial virus (RSV).[1a,2] Viral proteases, which selectively cleave peptide bonds and thus are essential to the life cycle of many viruses, are very attractive targets for antiviral drug design.[3] A notable example is the successful development of HIV protease inhibitors as antiviral drugs for the treatment of acquired immune deficiency syndrome (AIDS). Only 4 years after the first isolation of HIV in 1983, a few antiviral drugs were approved for use. From 1995 to 2007, 10 novel antiviral drugs from HIV protease inhibitors were approved for use in the United States, including Tipranavir (2005) **1** and Darunavir **2** (2006) (Figure 1).[1a,1b,4]

Figure 1 HIV protease inhibitors as antiviral drugs

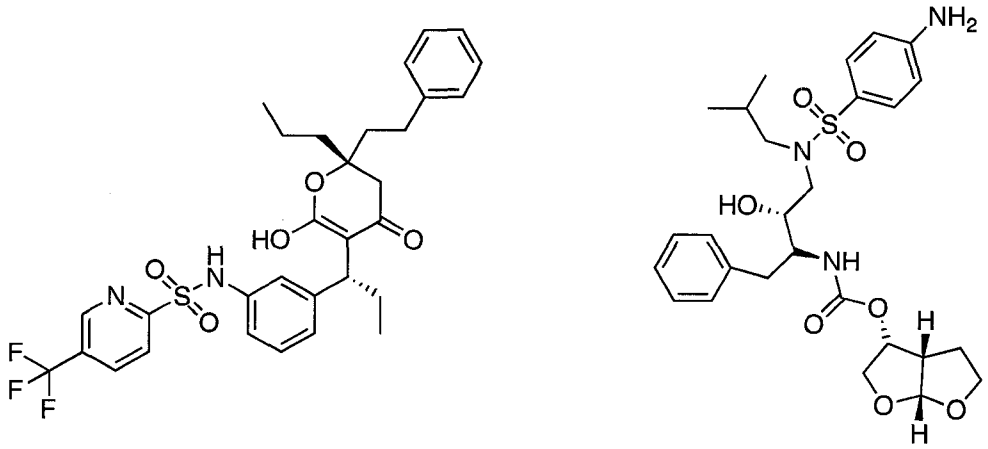

Tipranavir **1** Darunavir **2**

1. SARS Coronavirus (SARS-CoV)

In the 20th century, in 1918, 1957 and 1968 there were three global outbreaks of influenza, which caused total deaths of 50, 5 and 2 million people, respectively.[5] In November 2002, severe acute respiratory syndrome (SARS) occurred as a life-threatening form of atypical pneumonia originally in Guangdong province in China. It rapidly spread through 32 countries in other parts of the world in 2003.[6,7] SARS is characterized by high fever, malaise, rigor, headache and non-productive cough or dyspnea, and may progress to generalized interstitial infiltrates in the lung, requiring intubation and mechanical ventilation.[8] Due to a rapid international response to this infectious disease, the crisis was eventually restrained in 2003. However, around 8500 people worldwide were affected and over 900 died in the first wave of the SARS outbreak. The re-emergence of SARS in Southern China was reported in December 2003 and again in the spring of 2004.[9]

The causative agent of SARS has been identified as a novel human coronavirus.[6-7,10-12] The SARS coronavirus (Figure 2),[13] including the human CoV 229E (HCoV), as well as porcine transmissible gastroenteritis virus (TGEV), mouse hepatitis virus (MHV), bovine coronavirus (BCoV) and porcine epidemic diarrhea virus (PEDV) are enveloped and positive-stranded RNA viruses possessing the largest viral RNA genomes known to date (27 to 31 kb).[14] Studies show that genes of SARS-CoV have 70% or less identity with the corresponding genes of other coronaviruses.[11] Therefore, SARS-CoV is not closely related to the known coronaviruses of humans and animals. Phylogenetic analysis based

on the polymerase gene suggests that SARS coronavirus is a novel virus different from any of the previously known coronaviruses (Group 1, 2 and 3, Figure 3).[6,11,12] It is relatively similar to the murine, bovine, porcine, and human coronaviruses in group 2 and avian coronavirus IBV in group 3 (Figure 3).

Figure 2 Model of SARS coronavirus (adapted with permission from Oxford *et al.*[13])

Figure 3 Phylogenetic analysis suggests that SARS coronavirus is different from any of the previously known coronaviruses (adapted with permission from Rota *et al.*[11])

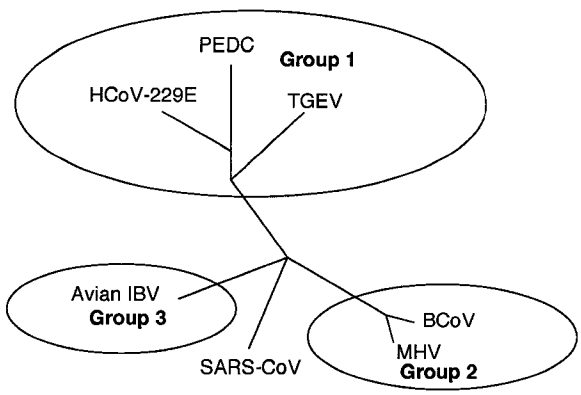

The first step of SARS-CoV infection is binding of the spike protein (S) to a specific receptor on the cell membrane.[15] After the initial binding and the following cellular entry, SARS-CoV undergoes a rapid replication cycle through several processes including transcription, translation and proteolytic processing, which lead to the virus maturation and release (Figure 4).[16-18] Many processes essential to the viral replication could be potential targets for the development of antiviral drugs and vaccines (Figure 4).[19,20] For example, the spike glycoprotein S could be a good target for the design of vaccines. Antibodies can potentially prevent the virus entry through blocking the binding interaction between the viral spike protein S and the specific virus receptor on the host cell.[19-21]

Figure 4 Major processes that are essential to the viral replication and are good targets for antiviral drugs and vaccines (adapted with permission from Holmes *et al.*[19])

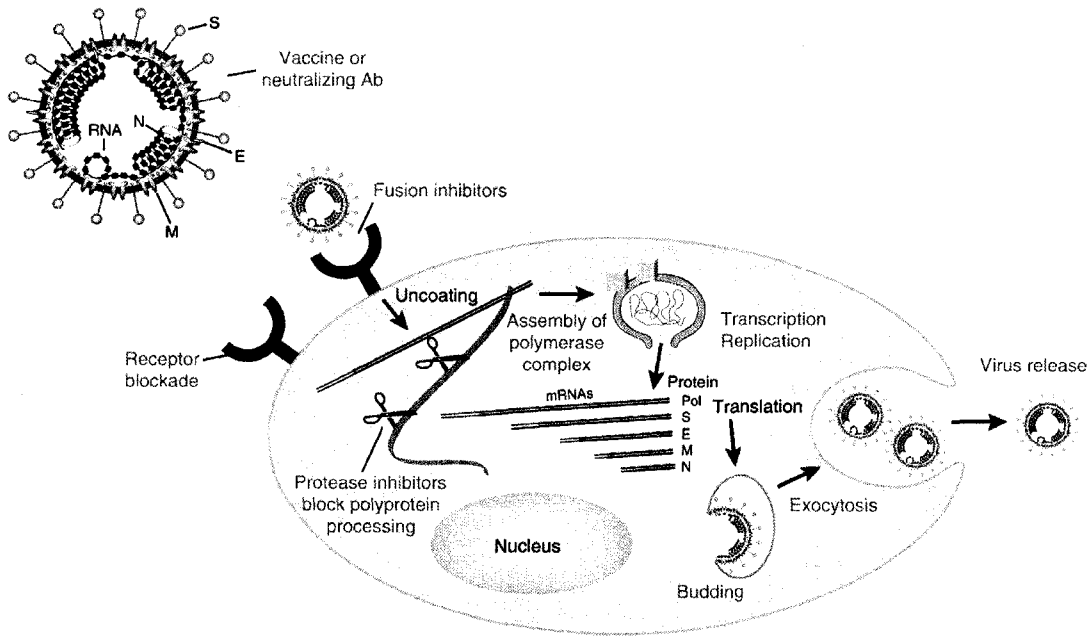

2. SARS Coronavirus 3C-Like Protease ($3CL^{pro}$)

Studies of SARS coronavirus, as well as the relatively well-characterized human CoV 229E (HCoV) and porcine transmissible gastroenteritis (TGEV), suggest that at least three major processes are essential to viral replication and thus are good targets for drug design: viral entry, transcription of the viral genome, and proteolytic processing.[16-18,22] The latter two processes are mediated by the functional subunits encoded by the replicase gene. The replicase gene encodes two overlapping polyproteins, pp1a (~486 KDa) and pp1ab (~790 KDa) in SARS-CoV.[16]

The two polyproteins pp1a and pp1ab are processed by viral proteases to produce the functional subunits of the replicase. Major replicase components include an RNA polymerase, an NTPase/helicase and two proteases that process the polyproteins.[16] The RNA polymerase replicates the viral genome and the NTPase/helicase unwinds the resultant RNA duplex intermediates. The main protease of the two proteases is a cysteine protease called $3CL^{pro}$, cleaving pp1a/pp1ab at central and C-proximal regions at 11 well-conserved sites. The other protease is a papain-like protease called PL^{pro}, cleaving pp1a/pp1ab at three N-proximal sites. This is similar to infectious bronchitis virus (IBV) where only one protease $PL2^{pro}$ cleaves two sites in this region, and is contradictory to other coronaviruses (*e.g.* HCoV 229E and MHV) where two proteases $PL1^{pro}$ and $PL2^{pro}$ cleave the active sites (Figure 5).

Figure 5 The positions of cleavage sites predicted to be processed by PL2^{pro} (blue) and 3CL^{pro} (red) (adapted with permission from Thiel *et al.*[16])

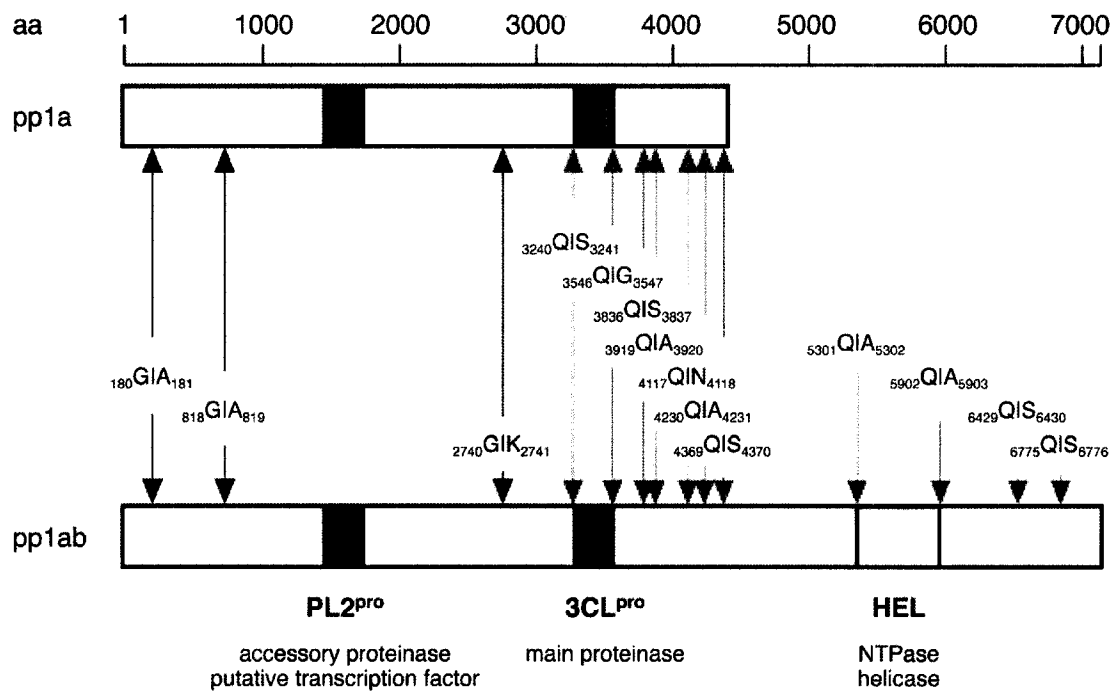

Because of its similarity to 3C protease (3C^{pro}) of the picornavirus family, the main protease (M^{pro}) is also called 3CL^{pro}.[10,23] 3CL^{pro} is a cysteine protease with the sulfur of Cys145 acting as a nucleophile and the imidazole ring of His41 acting as a general base in the active site (Figure 6).[10,23,24] The 306 residues of this protease fold into 3 domains. Domain I and II are β-barrels similar to that of the chymotrypsin-like serine proteases and the picornaviral 3C^{pro}.[25] Domain I and II possess the catalytically functional units in the active site: a nucleophile (Cys145 in the 3CL^{pro}), a general acid-base catalyst (His41 in the 3CL^{pro}), and an electrophilic oxyanion hole, as is also common for the picornaviral

$3C^{pro}$. Domain III possesses ~100 residues which fold into 5 α-helice. No counterpart of domain III has been identified in $3C^{pro}$. Domain III may play an important role in dimerization, which is essential to enzyme activity. Many inter-subunit contacts within the dimer occur between the respective domains III of the protomers.[26a,b]

Figure 6 X-ray crystal structure of the SARS-CoV $3CL^{pro}$ dimer with Cys145 as a nucleophile and His41 as a general base in the active site (http://www.rscb.org)[27]

Similar to other coronaviruses, sequence analysis suggests that the $3CL^{pro}$ cleaves 11 peptide bonds in all the 11 conserved cleavage sites with different efficiency.[16,28] The two peptides between the P_1 and P_1' positions are cleaved with the highest efficiency. In addition, cleavage sites were found to be mainly determined by the P_2, P_1 and P_1'

residues. The P_1 position has a well-conserved Gln residue for the $3CL^{pro}$, as is for the $3C^{pro}$. The P_2 position has a preference of large hydrophobic residues such as Leu/Ile residues, and the P_1' position seems to be tolerant of residues such as Arg, Ser, Gly, Asn or Cys.

As the peptide-based inhibitors mimic natural substrates, a good understanding of substrate specificity will aid in the design of the structure-based $3CL^{pro}$ inhibitors. The standard nomenclature[29] shown in Figure 7 is in general use for designation of substrate/inhibitor residues (*e.g.* P_3, P_2, P_1, P_1', P_2', P_3') that bind to corresponding enzyme subsites (*e.g.* S_3, S_2, S_1, S_1', S_2', S_3').

Figure 7 The standard nomenclature for substrate residues and their corresponding binding sites[29]

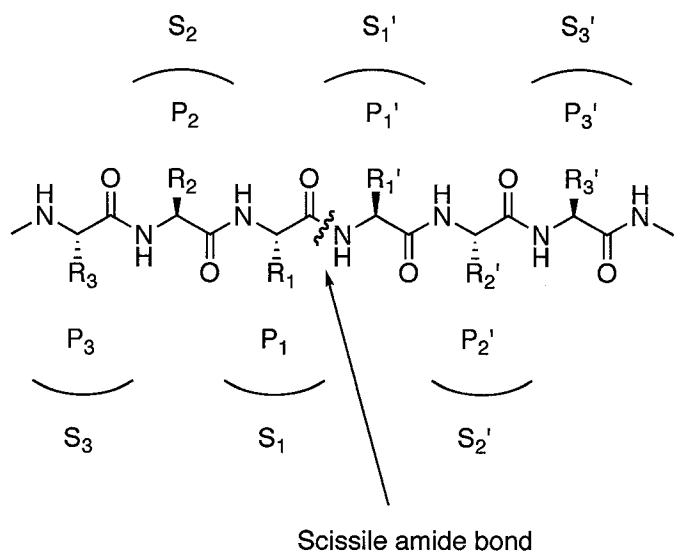

3. SARS 3C-Like Protease ($3CL^{pro}$) Inhibitors

3.1. Inhibitor Design

Due to its pivotal role in the viral replication and transcription, SARS $3CL^{pro}$ has been identified as a key target for anti-SARS drug design. The substrate specificity of SARS $3CL^{pro}$ is very similar to that of the picornaviral $3C^{pro}$ enzymes at the P_1, P_1' and P_4 sites. Interestingly, sequence similarity was also found between the substrate-binding sites of SARS $3CL^{pro}$ and other related coronavirus main proteases. This is supported by studies indicating that the porcine transmissible gastroenteritis (TGEV) main protease substrate can be cleaved by SARS $3CL^{pro}$,[10] and the reported co-crystal structure of a TGEV inhibitor, Cbz-Val-Asn-Ser-Thr-Leu-Gln-CMK **3** (Figure 8), with the SARS $3CL^{pro}$.[16] Apparently, screening and modification of known protease inhibitors is a good starting point for the development of anti-SARS drugs. For example, some molecular modeling studies suggest that AG7088 **4** (Figure 8),[30] an available human rhinovirus $3C^{pro}$ inhibitor, could be modified to be useful for treating SARS.[10]

Figure 8 Structures of hexapeptidyl CMK **3** and AG7088 **4**

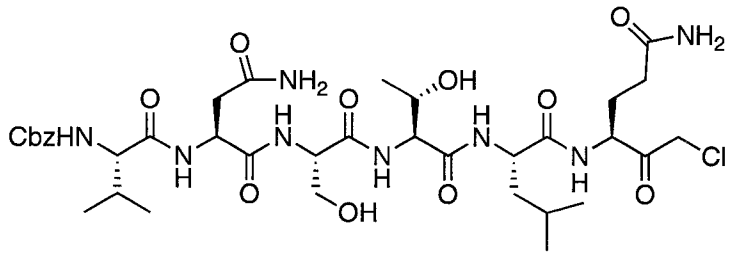

3

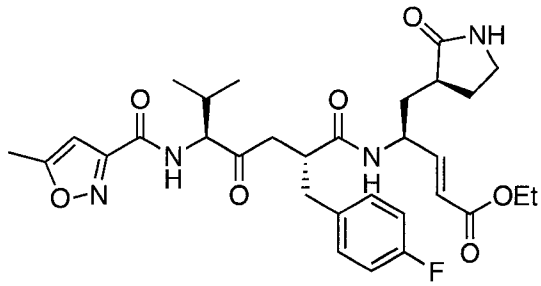

4

A number of small molecules have been reported that are potent inhibitors of $3CL^{pro}$, such as the HIV protease inhibitor TL-3,[31] metal-conjugated compounds,[32] bifunctional aryl boronic acids,[33] thiophenylcarboxylate,[34] AG7088 analogues,[35,36] anilides,[37] isatin derivatives,[38,39] and benzotriazole esters.[40] Some of them display very potent inhibition against SARS $3CL^{pro}$ with low micromolar or nanomolar activities.

Development of the SARS 3CL^{pro} inhibitors has mainly been approached by two routes: rational design and library-based high throughput screening.[41-43] A few strategies are commonly used for the rational design approach: design of transition state analogs for the studies of inhibition mechanisms; design of affinity labels or mechanism-based inactivators as covalent and irreversible inhibitors for inactivation of the protease; or structure-based design of protease inhibitors with assistance of three-dimensional structural information. Three representative SARS 3CL^{pro} inhibitors **5**, **6**, **7** prepared by the rational design approach are shown in Table 1.[33,37,38]

The library-based high throughput screening approach provides a rather random but effective way in the development of drugs. This strategy is based on rapidly examining large libraries of naturally occurring and synthetic compounds. It typically uses a cell-based assay to detect the protective effect of the compounds on the SARS-CoV infected VeroE6 cells, or uses a protease-based assay to observe the inhibitory activities of the compounds against the SARS-CoV 3CL^{pro}. Two representative SARS 3CL^{pro} inhibitors **8**, **9** from the library-based high throughput screening approach are also shown in Table 1.[22,34] Both strategies have elements of logic in the design and can complement each other. Mechanistic and structural insight from rational design can assist in the design of synthetic libraries and the interpretation of screening results, and library-based high throughput screening can provide a good starting point for optimization of successful lead compounds.

Table 1 Some potent SARS 3CL^{pro} inhibitors based on a rational design approach (**5**, **6**, **7**) or a library-based high throughput screening approach (**8**, **9**)

Inhibitor	Structure	IC_{50} (μM)	Ki (μM)
5	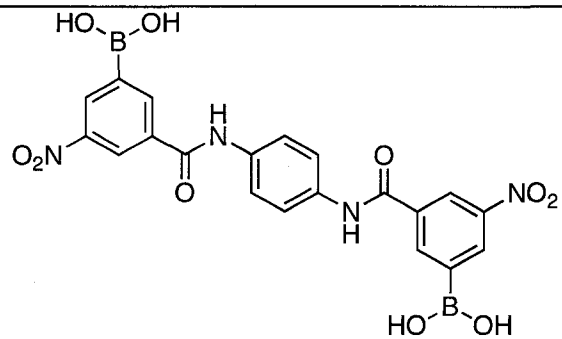		0.04
6	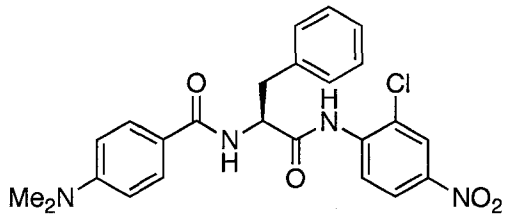		0.03
7	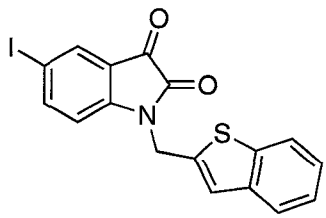	0.95	
8	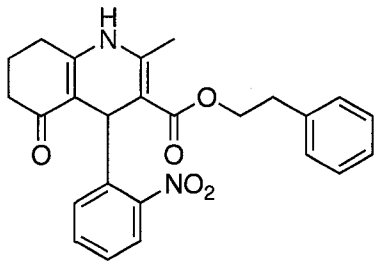	2.5	
9	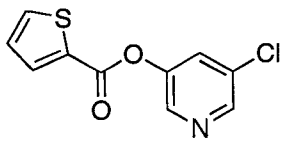	0.5	

3.2. SARS 3CL^{pro} Inhibitors from Rational Design Approach

The substrate specificity of SARS 3CL^{pro} is very similar to that of picornaviral 3C^{pro} enzymes.[10] This suggests the strategy for the discovery of effective anti-SARS drugs through screening and modification of known picornavirus 3C^{pro} inhibitors. Many reported SARS 3CL^{pro} inhibitors are analogues derived from the available picornavirus 3C^{pro} inhibitors. For example, quite a few potent SARS 3CL^{pro} inhibitors reported in the literature are modified analogues of AG7088 **4** and isatin derivative **10** (Figure 9), both of which are very potent human rhinovirus (HRV) 3C^{pro} inhibitors with an IC_{50} of 13 nM and a K_i of 11 nM, respectively.[30,44]

Figure 9 Structures of AG7088 **4** and isatin derivative **10**

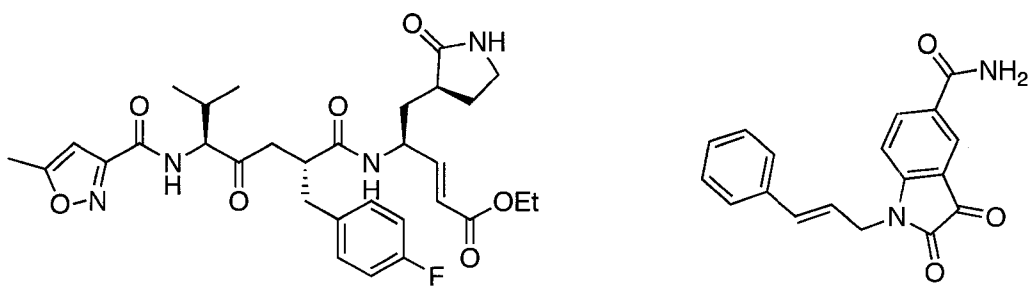

4 **10**

3.2.1. Michael Acceptors: AG7088 Analogues

Michael acceptors are known as mechanism-based inactivators of cysteine proteases.[30] This class of inhibitors has a substrate-derived recognition peptide that provides specific binding affinity to the target protease, and an α,β-unsaturated ester in the P_1 position as a Michael acceptor. The Michael acceptor can form a covalent bond by the nucleophilic attack from the sulfur atom of the target protease, which leads to the inactivation of the target protease. Both the HRV $3C^{pro}$ inhibitor AG7088 **4** and its analogue **11**, a reported SARS $3CL^{pro}$ inhibitor,[35] belong to this family (Figure 10).

Figure 10 Inactivation of SARS $3CL^{pro}$ by inhibitor **11**, derived from the HRV $3C^{pro}$ inhibitor AG7088 **4**[30,35]

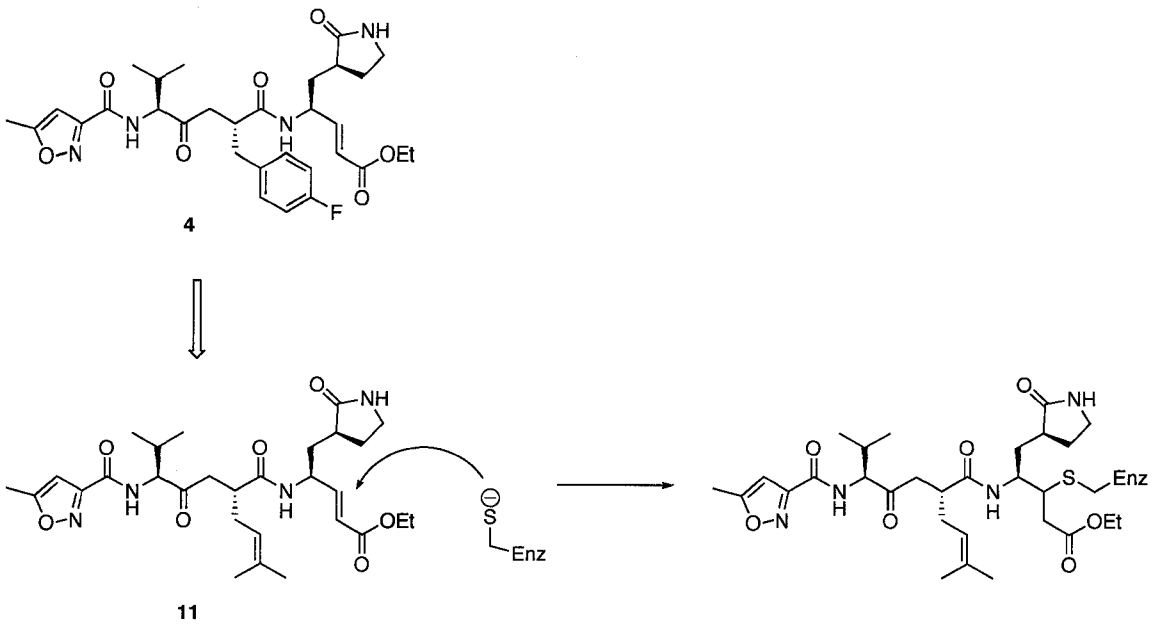

Interestingly, Shie *et al.* recently reported that AG7088 itself has no inhibition against SARS $3CL^{pro}$ even at 100 μM concentration.[36] However, Ghosh *et al.* found that by replacing the *p*-fluorobenzyl group in the P_2 position with a prenyl substituent, this modified AG7088 analogue **11** (Figure 10) shows modest inhibition against SARS $3CL^{pro}$ with IC_{50} of 70 μM and k_{inact} of 0.014 min^{-1}.[35] The X-ray crystal structure of $3CL^{pro}$-inhibitor **11** complex has confirmed a covalent bond between inhibitor **11** and $3CL^{pro}$, and provides evidence of crucial hydrogen bonds between inhibitor **11** and His 164 and Glu 166 of the enzyme.[35]

Shie *et al.* also reported a series of Michael acceptors as SARS $3CL^{pro}$ inhibitors based on the modification of AG7088.[36] Replacement of the γ-lactam moiety by a phenyl group generated the modified AG7088 analogue **12** (Figure 11, IC_{50} = 39 μM) that has significantly improved inhibition against $3CL^{pro}$ (IC_{50} >> 100 μM for AG7088). The further modified analogue **13** (Figure 11) is a very potent SARS $3CL^{pro}$ inhibitor with an IC_{50} of 1 μM and a K_i of 0.52 μM. Inhibitor **13** is also non-toxic in the cellular system with an EC_{50} of 0.18 μM.

Figure 11 Michael acceptors **12** and **13** as SARS $3CL^{pro}$ inhibitors

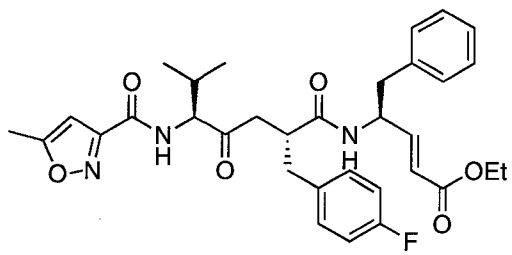

12

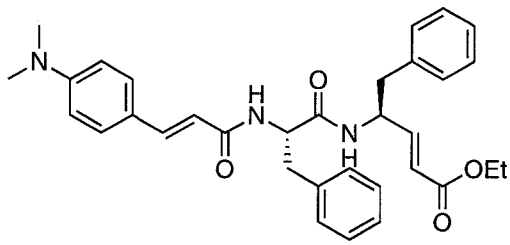

13

More recently, Yang *et al.* reported another AG7088 analogue, Michael acceptor **14** (Figure 12) as a SARS 3CL^{pro} inhibitor with K_i of 9 μM in the enzymatic assay and IC_{50} of 6 μM in the cell-based assay with very low cytotoxicity.[45] The x-ray crystal structure of 3CL^{pro}-inhibitor **14** complex indicates that the P_1, P_2, P_4, and P_1' residues of inhibitor **14** fit into the corresponding subsites of the enzyme very well.

Figure 12 Michael acceptor **14** as a SARS 3CL^{pro} inhibitor

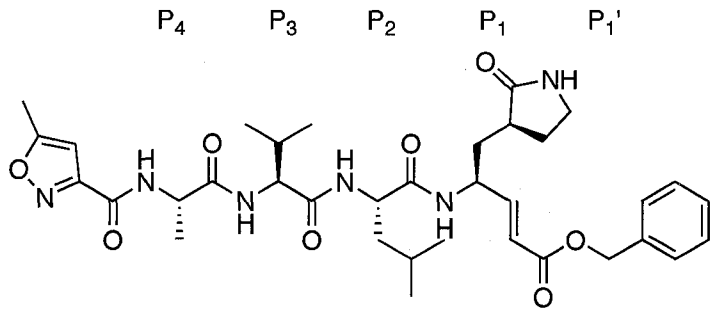

3.2.2. Aza-peptide Epoxides (APE)

Aza-peptide epoxides (APE) were initially introduced as a class of inhibitors for clan CD cysteine peptidases, including the legumains and the caspases.[46-48] This class of inhibitors has an aza-peptide and an epoxide moiety attached to the carbonyl group in the P_1 position, and a substrate-derived recognition peptide in the side chain of the P_1 position. For the APE, replacement of the α-carbon atom of the P_1 residue with a nitrogen atom induces trigonal planar geometry at the site normally occupied by the α-carbon atom of the P_1 residue and reduces the electrophilicity of the carbonyl group of the P_1 residue, thereby resulting in the carbonyl group being resistant to nucleophilic attack.

It has been proposed that APE inhibit the target proteases irreversibly with a mechanism through either pathway I or II (Figure 13).[46,48] The sulfur atom of the catalytic Cys145 attacks C3 (pathway I) or C2 (pathway II) of the epoxide carbon atoms, depending on the orientation of the APE in the active site of the target protease. This nucleophilic attack leads to the opening of the epoxide ring and the formation of a covalent bond, and thus the irreversible inhibition of the target protease.

Figure 13 Inactivation of SARS 3CL^{pro} by the aza-peptide epoxide (APE) **15** through pathway I[49a]

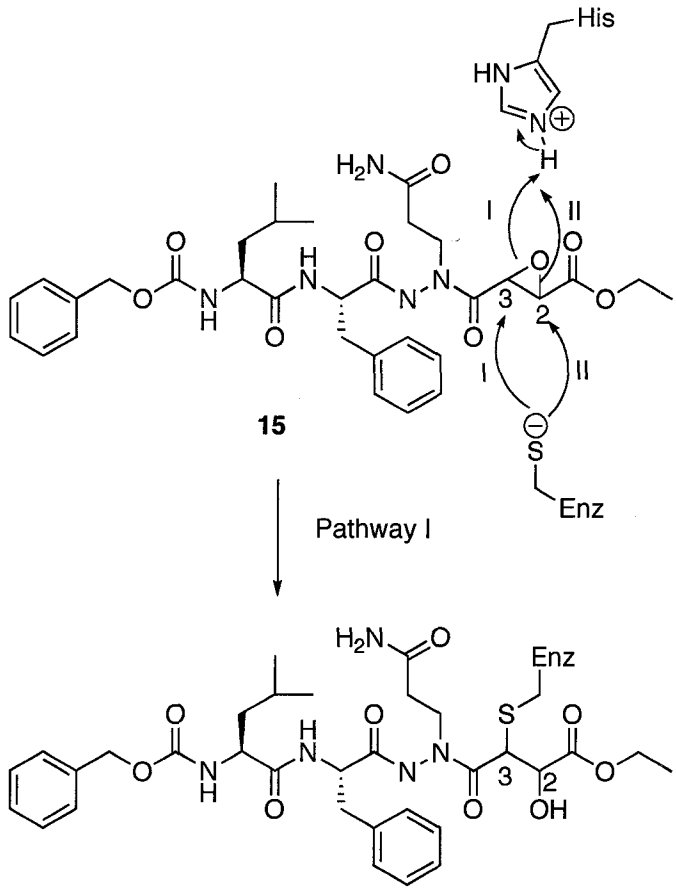

Professor Michael James' group at the University of Alberta has reported that the (S,S) diastereomer of the APE **15** (Figure 13) has the best inhibition against SARS $3CL^{pro}$ with a k_{inact}/K_i value of 1900 M^{-1} s^{-1}.[49a,b] The crystal structure studies reveal covalent bond formation between the sulfur atom of the catalytic Cys145 residue and carbon-3 of APE **15** (Figure 14).

Figure 14 A diagram of the interactions from the X-ray crystal structure of SARS $3CL^{pro}$-inhibitor **15** complex. Hydrogen bonds (2 molecules / asymmetric unit) are shown as lines with their distances (in Å) given alongside. The residues of $3CL^{pro}$ in contact with the APE **15** are shown in arcs (from Lee *et al.*[49a])

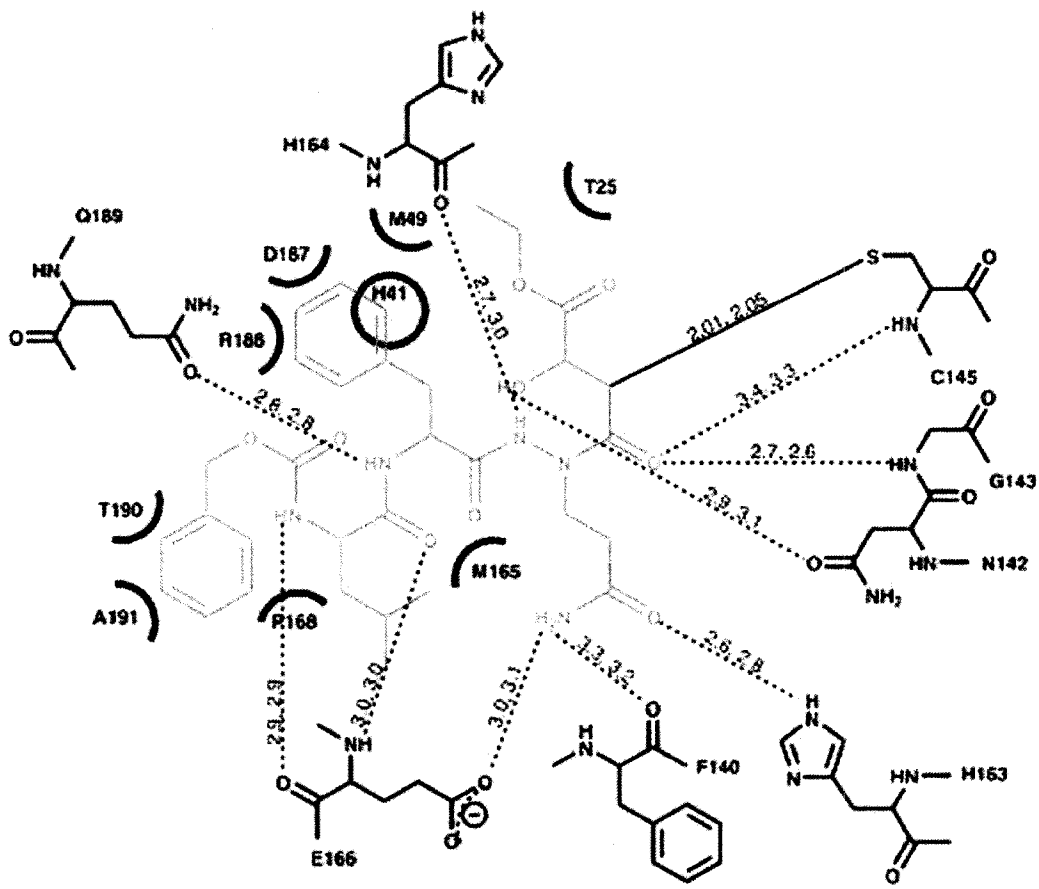

3.2.3. Peptidyl Fluoromethyl Ketones (FMK)

Peptidyl fluoromethyl ketones are known as irreversible inhibitors of cysteine proteases that inactivate the enzymes through the formation of thioether bonds.[50] Due to the inherently low reactivity of the carbon-fluorine bond,[51] peptidyl fluoromethyl ketones are very selective and rapid inhibitors of cysteine proteases, but rather poor inhibitors of serine proteases. Hence, peptidyl fluoromethyl ketones are very promising leads as cysteine protease inhibitors, and may reduce non-specific reactions with other nucleophiles, thereby decreasing toxicity in cellular systems.

The detailed inhibition mechanism of cysteine proteases by peptidyl halomethyl ketones, including the peptidyl fluoromethyl ketones, is still not completely clear. However, crystal structure studies with cysteine proteases[52] (*e.g.* cruzain, caspase-1, -3 and -8) inactivated by peptidyl halomethyl ketones have confirmed the formation of thioethers from the covalent-bond products of enzyme-inhibitor complexes.

Two possible mechanisms[53] (Figure 15) have been proposed for the inhibition of cysteine proteases by peptidyl halomethyl ketones, either of which could lead to the final product thioethers. Mechanism 1 suggests a direct displacement of the halide group by an S_N2 nucleophilic attack from the sulfur atom of the cysteine residue of the target protease, to provide the thioether product. Mechanism 2 suggests formation of a thiohemiketal in the first step, followed by formation of a three-membered episulfide intermediate, and then a rearrangement of the three-membered episulfide to the thioether product. However, prior

to our work there was no evidence of the formation of this proposed three-membered episulfide intermediate.

Figure 15 Proposed mechanisms of inhibition of cysteine proteases by peptidyl fluoromethyl ketones

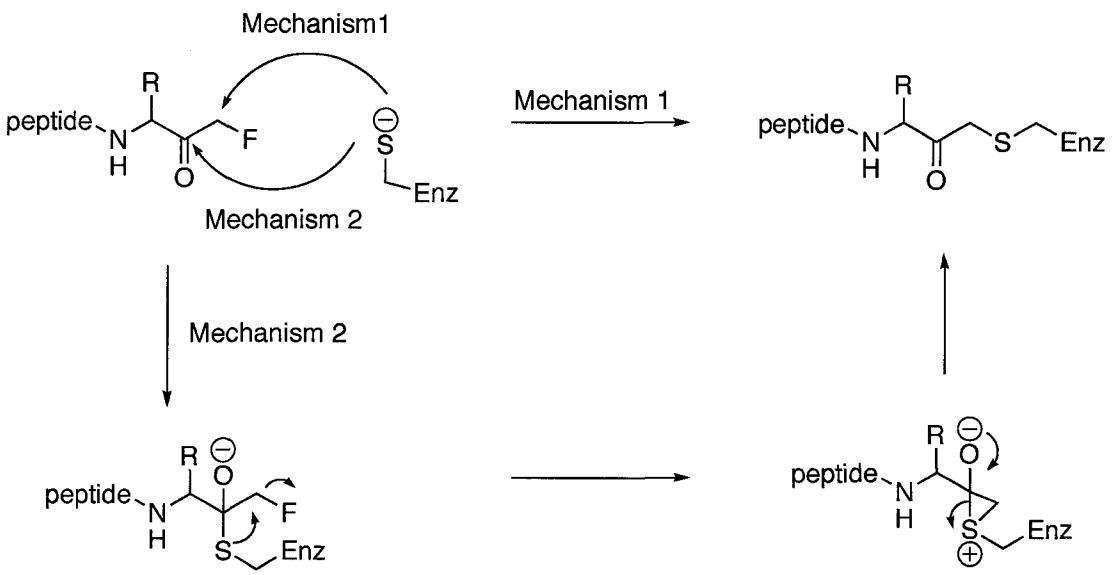

Zhang *et al.* of Maxim Pharmaceuticals recently reported a series of dipeptidyl fluoromethyl ketones as SARS 3CL^{pro} inhibitors derived from MX1013 **16** (Figure 16), a potent inhibitor of caspase-3 that belongs to a family of cysteine proteases and plays a crucial role in apoptosis.[54] The most potent inhibitor **17** (Figure 16) has an EC_{50} of 2.5 μM and a selectivity index (SI) of larger than 40 for cytopathogenic effect (CPE) inhibition in SARS-CoV infected Vero or CaCo-2 cells.

Figure 16 Inactivation of SARS 3CL^{pro} by the dipeptidyl fluoromethyl ketone **17** derived from a caspase-3 inhibitor **16**

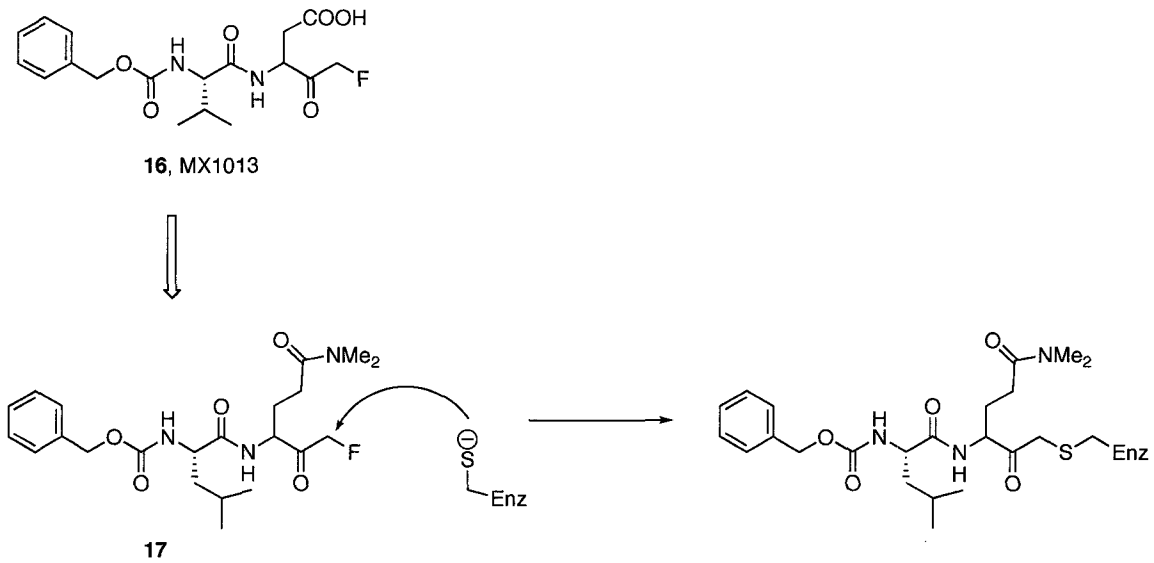

3.2.4. Trifluoromethyl Ketones

Trifluoromethyl ketones are reversible inhibitors of both serine and cysteine proteases.[55-57] The trifluoromethyl group can thermodynamically stabilize the hemiketal or hemithioketal intermediate resulting from the nucleophilic attack of the oxygen atom of a serine protease or the sulfur atom of a cysteine protease. This hemiketal or hemithioketal intermediate is believed to be a mimic of the substrate-enzyme intermediate, namely the tetrahedral analogue formed during the substrate peptide bond hydrolysis (Figure 17).

Figure 17 The trifluoromethyl ketone **18**, interaction with SARS 3CL^{pro}

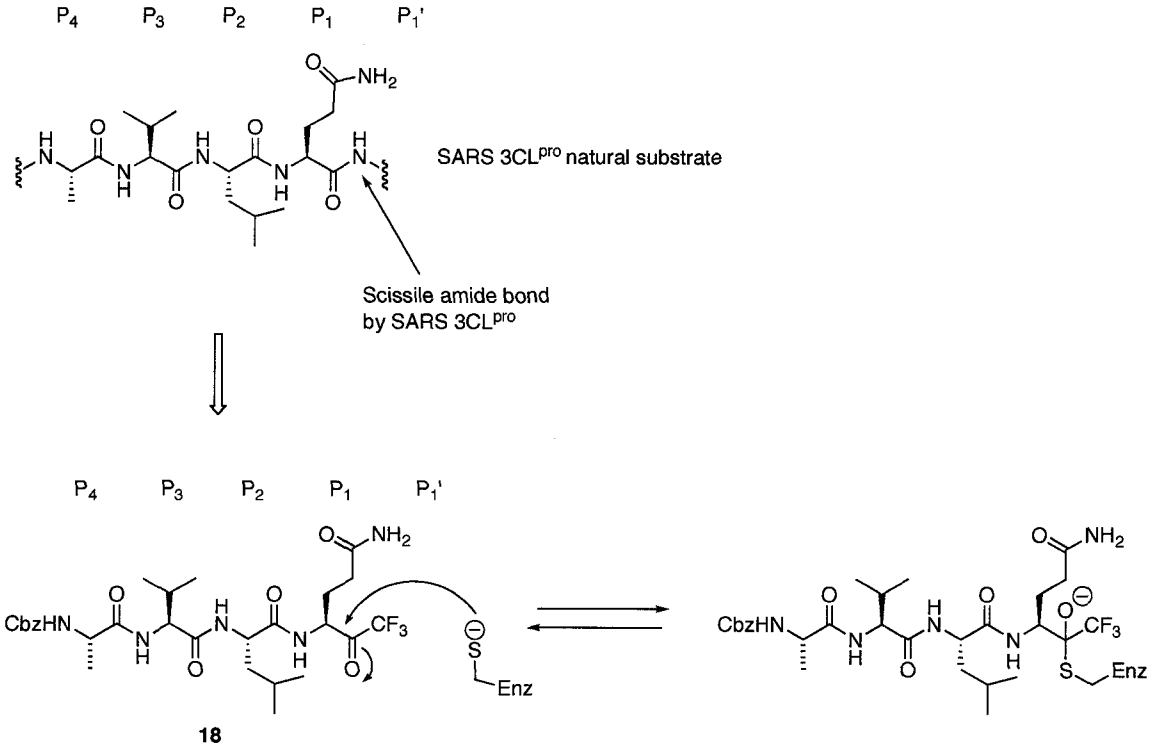

Sydnes *et al.* reported a series of peptidyl trifluoromethyl ketones as SARS 3CL^{pro} inhibitors with K_i values ranging from 116 μM to > 1000 μM.[58] One representative from this class of inhibitors, compound **18** (Figure 17) has a K_i of 135 μM against SARS-CoV 3CL^{pro}.

3.2.5. Isatin Derivatives

Isatin derivatives have long been known as potent and covalent inhibitors for the picornavirus enzyme, human rhinovirus (HRV) 3C^{pro}.[44] A good example is the isatin derivative **19**, an extremely potent HRV-14 3C^{pro} inhibitor with K_i of 2 nM. Isatin **19**

(Figure 18) appears to be a good mimic of the HRV $3C^{pro}$ natural substrate from the view of structure-based design: the benzamide group is a mimic of the Gln with more restricted conformation in the P_1 position; the α-keto amide mimics the scissible amide bond in the cleavage site; and the benzothiophene group mimics the Phe in the P_2 position (Figure 18). Because of the similarity of SARS $3CL^{pro}$ and HRV $3C^{pro}$ as cysteine proteases, isatin derivatives can be good starting points for the discovery of SARS $3CL^{pro}$ inhibitors. However, most of the isatin derivatives are also known as very toxic agents in cellular systems, possibly due to the high reactivity of the α-keto amide group that will lead to non-specific reactions with other thiols and nucleophiles.

Figure 18 The isatin derivative **19** mimics HRV $3C^{pro}$ natural substrate

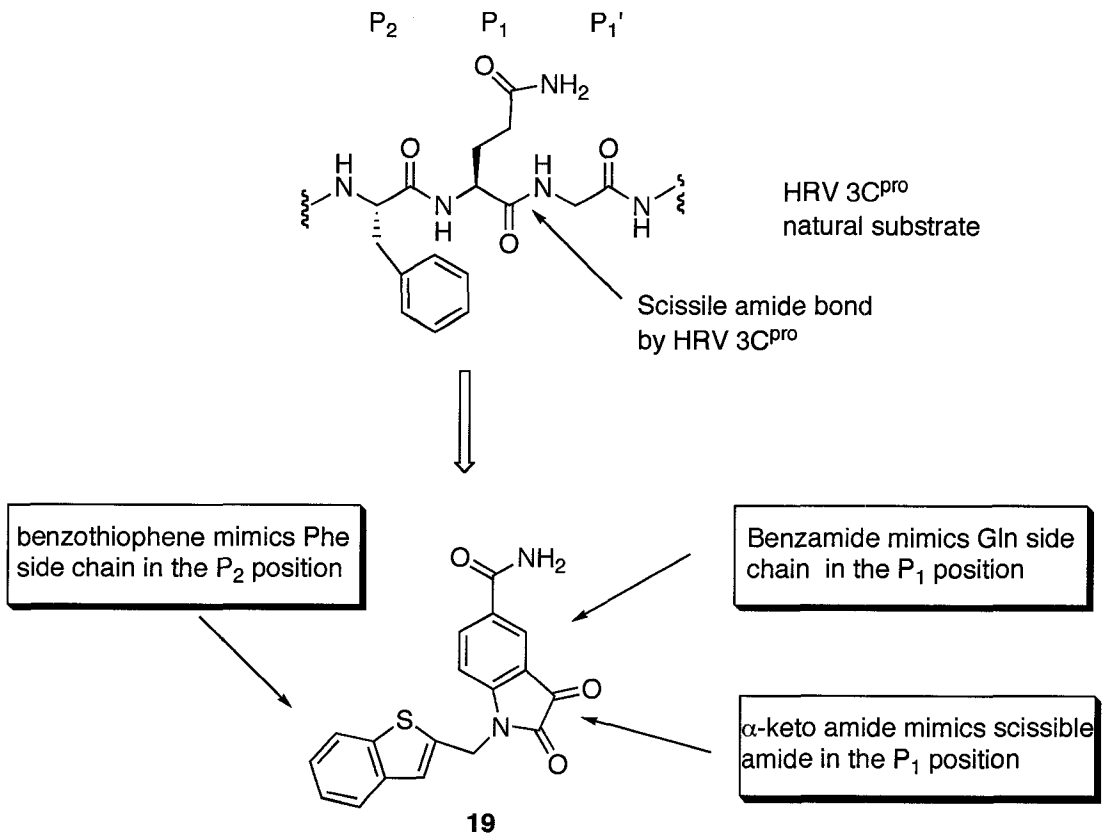

Several isatin derivatives have been synthesized and evaluated as SARS $3CL^{pro}$ inhibitors by different research groups.[38,39] One of the most potent inhibitors prepared by replacing the benzothiophenyl group of **19** with a napthenyl group has an IC_{50} value of 0.4 μM against SARS $3CL^{pro}$. Interestingly, this class of inhibitors displays non-covalent and reversible inhibition against SARS $3CL^{pro}$, which suggests a completely different inhibition mechanism from that of HRV-14 $3C^{pro}$.

3.3. SARS $3CL^{pro}$ Inhibitors from Library-based High Throughput Screening

With the development of more sensitive techniques such as the fluorescence resonance energy transfer (FRET) assay,[34] high throughput screening (HTS) has become a powerful tool to identify structural leads for novel therapeutics from small molecules with biologically promising motifs. A major advantage of HTS is that once a successful lead is identified from the screening, less effort may be required for further modification. Several groups have reported a few SARS $3CL^{pro}$ inhibitors from high throughput screening recently. [22,31,34,59-64]

Wu *et al.* have screened nearly 10,000 targets from approved drugs and synthetic compounds using a Vero cell-based assay, and found that ~ 50 are biologically active as anti-SARS agents at 10 μM.[31] Among these 50 active compounds, the best lead **20** (Figure 19), a very potent HIV protease inhibitor (K_i = 1.5 nM) called TL-3, displays potent inhibition against SARS $3CL^{pro}$ with K_i of 0.6 μM.

Figure 19 The HIV protease inhibitor TL-3 as a SARS 3CL^{pro} inhibitor

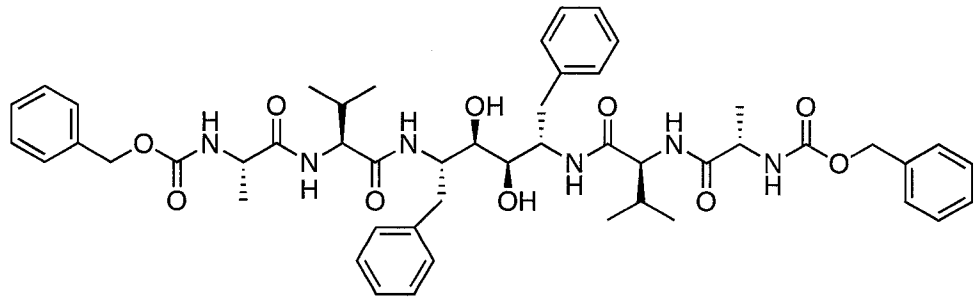

20

Kao *et al.* have screened 50,240 small molecules in a Vero cell-based assay, and found 104 compounds with biological activity against SARS 3CL^{pro}.[22] The most potent inhibitor **8** (Figure 20, also shown in Table 1) has an IC_{50} of 2.5 μM and an EC_{50} of 7 μM. Blanchard *et al.* have also screened about 50,000 small molecules using a FRET assay, and identified 5 lead compounds as SARS 3CL^{pro} inhibitors with IC_{50} values ranging from 0.5 to 7 μM.[34] Ester **9** (Figure 20, also shown in Table 1) was among the 5 compounds and has an IC_{50} of 0.5 μM against 3CL^{pro}.

Figure 20 SARS 3CL^{pro} inhibitors **8** and **9** from library-based high throughput screening

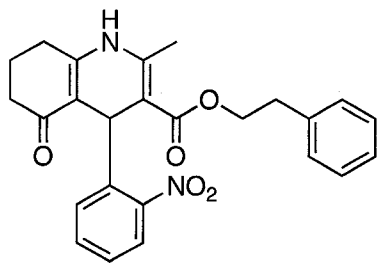

8

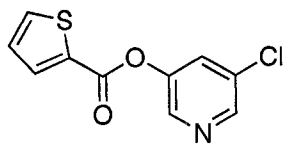

9

4. Project Goal: Design, Synthesis and Evaluation of SARS 3CL^{pro} Inhibitors.

The main objective of this thesis is to discover novel potent SARS 3CL^{pro} inhibitors as potential anti-SARS drugs. Three classes of compounds have been designed, synthesized and evaluated as potent SARS 3CL^{pro} inhibitors: peptidomimetics (Targets **A-E**, Figures 21 and 22), heteroaromatic esters and aldehydes (Targets **F** and **G**, Figure 23), methylene ketones and fluorinated methylene ketones (Target **H**, Figure 24). Clearly a good understanding of inhibition mechanisms for SARS 3CL^{pro} with these inhibitors will assist the discovery of more effective inhibitors for both the coronavirus SARS 3CL^{pro} and other picornavirus 3C^{pro} such as those from HAV and HRV.

Target **A** (**21-24**, Figure 21) is a series of cyclic keto-glutamine tetrapeptides, composed of a substrate-derived recognition tripeptide, a phthalhydrazide moiety which is an important structural feature for the potent inhibition of HAV $3C^{pro}$ for this class of compounds,[65a-e] and a γ-lactam moiety, which is a key structural feature for the potent inhibition of HRV-14 $3C^{pro}$ by AG7088.[30] Target **B** (**25-28**, Figure 21) is a series of acyclic keto-glutamine tetrapeptide analogues of target A, with replacement of the cyclic γ-lactam moiety with an acyclic dimethyl amide moiety. Because of the similarity of SARS $3CL^{pro}$ to $3C^{pro}$ in the picornavirus family (*e.g.* HAV and HRV), targets **A** and **B** are expected to be SARS $3CL^{pro}$ inhibitors. Furthermore, some important structure-activity relationships might be revealed for this class of inhibitors based on the evaluation of their inhibitory activities against $3CL^{pro}$.

Figure 21 Targets **A** and **B**: Keto-glutamine tetrapeptides

Target **A:** Cyclic keto-glutamines

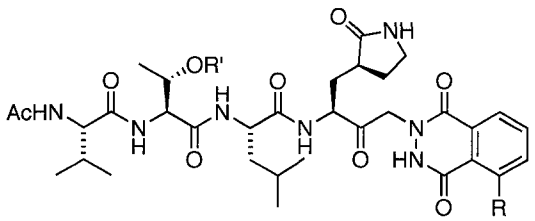

21: R = H, R' = Bn

22: R = H, R' = H

23: R = NO_2, R' = Bn

24: R = NO_2, R' = H

Target **B:** Acyclic keto-glutamines

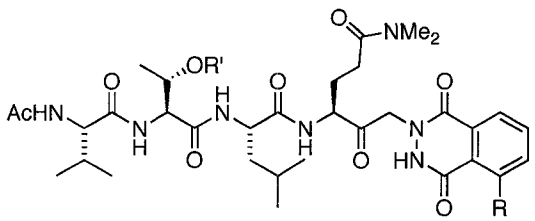

25: R = H, R' = Bn

26: R = H, R' = H

27: R = NO_2, R' = Bn

28: R = NO_2, R' = H

Target **C** (**29**, Figure 22) is a modified keto-phenylalanine tetrapeptide of target **A** that has a phenyl group to mimic the γ-lactam moiety.[29] Targets **D** and **E** (**30-32**, Figure 22) are also keto-glutamine tetrapeptides that are structurally "mix-and-match" combinations of target **A** and thiophenecarboxylate **9** (Figure 20), a potent inhibitor for both SARS $3CL^{pro}$ and HAV $3C^{pro}$.[34] Compound **9** is believed to bind at the active sites of these two cysteine enzymes, and both the thiophenyl and pyridinyl moieties may structurally play crucial roles for the potent inhibition of SARS $3CL^{pro}$ and HAV $3C^{pro}$.

Figure 22 Targets **C-E**: Modified keto-glutamine tetrapeptides

Target **C**: Keto-phenylalanine

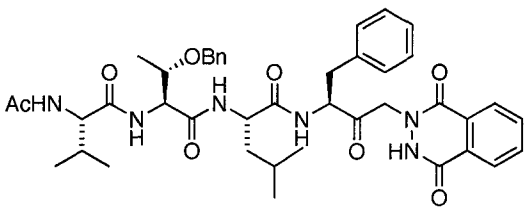

29

Target **E**: Cyclic keto-glutamine

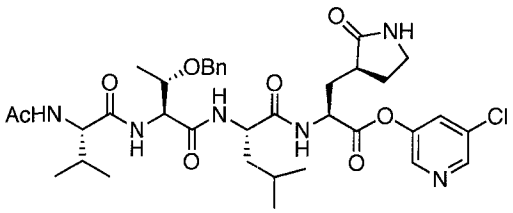

32

Target **D**: Cyclic keto-glutamines

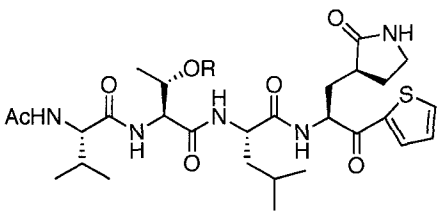

30: R = Bn

31: R = H

Target **F** (**33-40**, Figure 23) is a series of heteroaromatic esters that are identified from library-based screening or synthesized by further modification of the successful leads

identified from library-based screening. They are expected to be affinity labels of SARS 3CL^{pro}, and structure-activity relationship studies may shed light on the discovery of more effective and non-covalent reversible inhibitors. Target **G** (**41-45**, Figure 23) is a series of aldehyde analogues of Target **F**. Aldehydes are known to be chemically more reactive towards nucleophiles and are potentially good inhibitors for cysteine proteases through formation of hemithioacetals.[66]

Figure 23 Targets **F** and **G**: Heteroaromatic esters and aldehydes

Target **F**: Heteroaromatic esters **33-40**

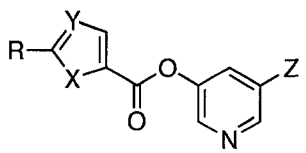

33: X = O, Y = C, Z = Cl, R = H

34: X = O, Y = C, Z = Br, R = H

35: X = N, Y = S, Z = Cl, R = H

36: X = O, Y = C, Z = Cl, R = 4-Chlorophenyl

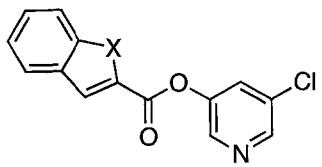

37: X = O

38: X = N

39: X = S

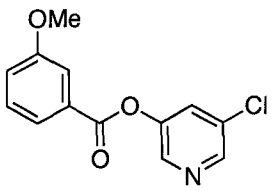

40

Target **G**: Heteroaromatic aldehydes **41-45**

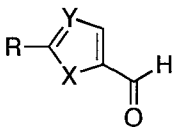

41: X = S, Y = C, R = H

42: X = O, Y = C, R = H

43: X = N, Y = S, R = H

44: X = O, Y = C, R = 4-Chlorophenyl

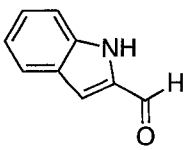

45

Target **H** (**46-62**, Figure 24) is a class of methylene ketones and fluorinated methylene ketones. The methylene ketones were initially designed and synthesized for the development of more stable and non-covalent inhibitors based on the heteroaromatic esters (target **F**). Fluorinated methylene ketones are also designed based on the concept that they possess the combined effects of suitable structure and chemical reactivity, and that the difluoromethylene moiety is well known as a mimic of oxygen in biological systems.[67]

Figure 24 Target **H**: Methylene ketones and fluorinated methylene ketones.

Target **H**: Methylene ketones and fluorinated methylene ketones

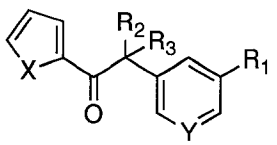

46: X = S, Y = N, R_1 = H, R_2 = H, R_3 = H

47: X = S, Y = N, R_1 = H, R_2 = H, R_3 = F

48: X = S, Y = N, R_1 = H, R_2 = F, R_3 = F

49: X = O, Y = N, R_1 = Cl, R_2 = H, R_3 = H

50: X = O, Y = N, R_1 = Cl, R_2 = H, R_3 = F

51: X = O, Y = N, R_1 = Cl, R_2 = F, R_3 = F

52: X = O, Y = C, R_1 = Cl, R_2 = H, R_3 = H

53: X = O, Y = C, R_1 = Cl, R_2 = H, R_3 = F

54: X = O, Y = C, R_1 = Cl, R_2 = F, R_3 = F

55: X = O, Y = N, R_1 = Br, R_2 = H, R_3 = H

56: X = O, Y = N, R_1 = Br, R_2 = H, R_3 = F

57: X = O, Y = N, R_1 = Br, R_2 = F, R_3 = F

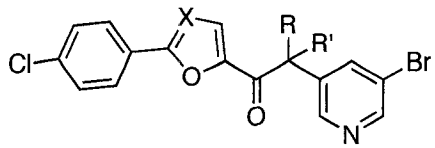

58: X = C, R = H, R' = H

59: X = C, R = H, R' = F

60: X = C, R = F, R' = F

61: X = N, R = H, R' = H

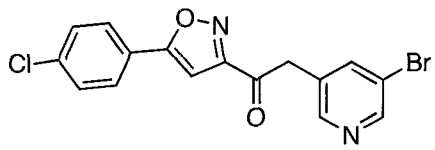

62

RESULTS AND DISCUSSION

1. Cyclic Peptidyl Keto-Glutamines – Target A

1.1. Design of Target A (21-24)

In the last 10 years, many studies have been done in our group on picornavirus 3C proteases ($3C^{pro}$), especially on that of human rhinovirus-14 (HRV-14) and hepatitis A virus (HAV).[65a-e] Our previous studies have indicated that the keto-glutamine **63** (Figure 25) with a phthalhydrazide moiety is a potent HAV $3C^{pro}$ inhibitor with IC_{50} of 13 μM and K_i of 9 μM, and displays reversible inhibition after 45 min pre-incubation with the HAV 3C protease.[65b] The structure-activity relationship studies suggest that the phthalhydrazide moiety is an important structural feature for the potent inhibition of HAV $3C^{pro}$. The nature of reversible inhibition of compound **63** is very attractive, which suggests that non-specific reactions will not occur with other thiols and nucleophiles, and thus the compound may have low cytotoxicity.

AG7088 (Figure 25) is a very potent HRV $3C^{pro}$ inhibitor discovered by Agouron Pharmaceutics Company with IC_{50} of 13 nM.[30] Crystal structure studies indicate that the γ-lactam moiety is a key structural factor for the binding affinity to the HRV $3C^{pro}$. Due to the similarity of SARS $3CL^{pro}$ and picornavirus $3C^{pro}$ (e.g. HAV and HRV $3C^{pro}$), a series of cyclic peptidyl keto-glutamines (target **A**, **21-24**, Figure 21) were designed as SARS

3CL^{pro} inhibitors, containing the substrate-derived recognition tripeptide, the phthalhydrazide moiety and the γ-lactam moiety (Figure 25).

Figure 25 Rational design of cyclic keto-glutamine tetrapeptides (*e.g.* **22**) as SARS 3CL^{pro} inhibitors based on an HRV inhibitor AG7088 **4** and an HAV inhibitor **63**

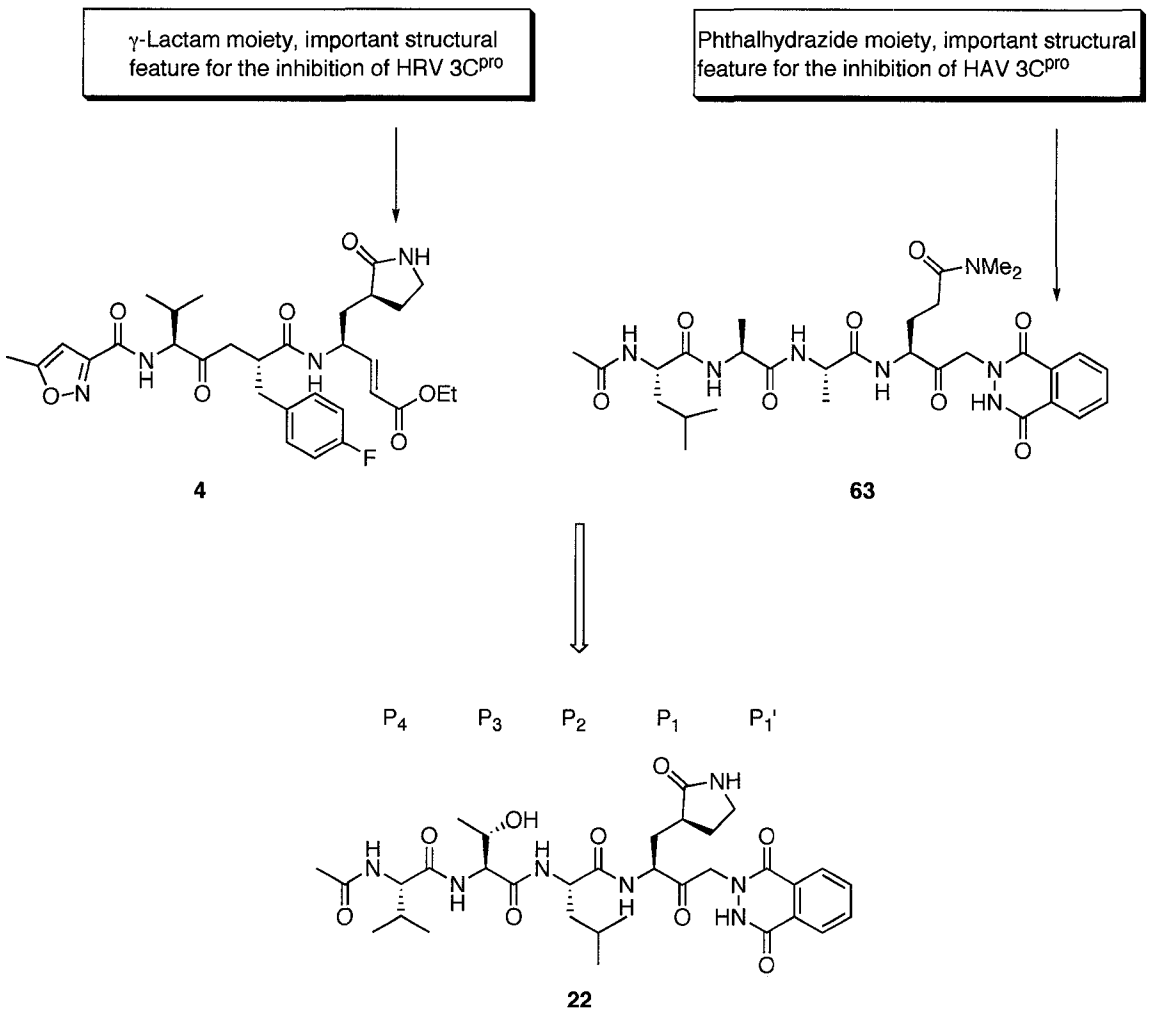

1.2. Synthesis of Target A (21-24)

A retrosynthetic analysis of target **A** (**21-24**) is shown in Figure 26, with the cyclic keto-glutamine tetrapeptide **21** used as an example. The cyclic keto-glutamine tetrapeptide **21** can potentially be synthesized from the cyclic keto-glutamine **64** and the tripeptide **65**. The cyclic keto-glutamine **64** can be prepared from the cyclic glutamic acid derivative **66** by a modified literature method established in our group previously,[65b] and the tripeptide **65** can be prepared by standard peptide synthesis.

Figure 26 Retrosynthetic analysis of target **A** (*e.g.* **21**)

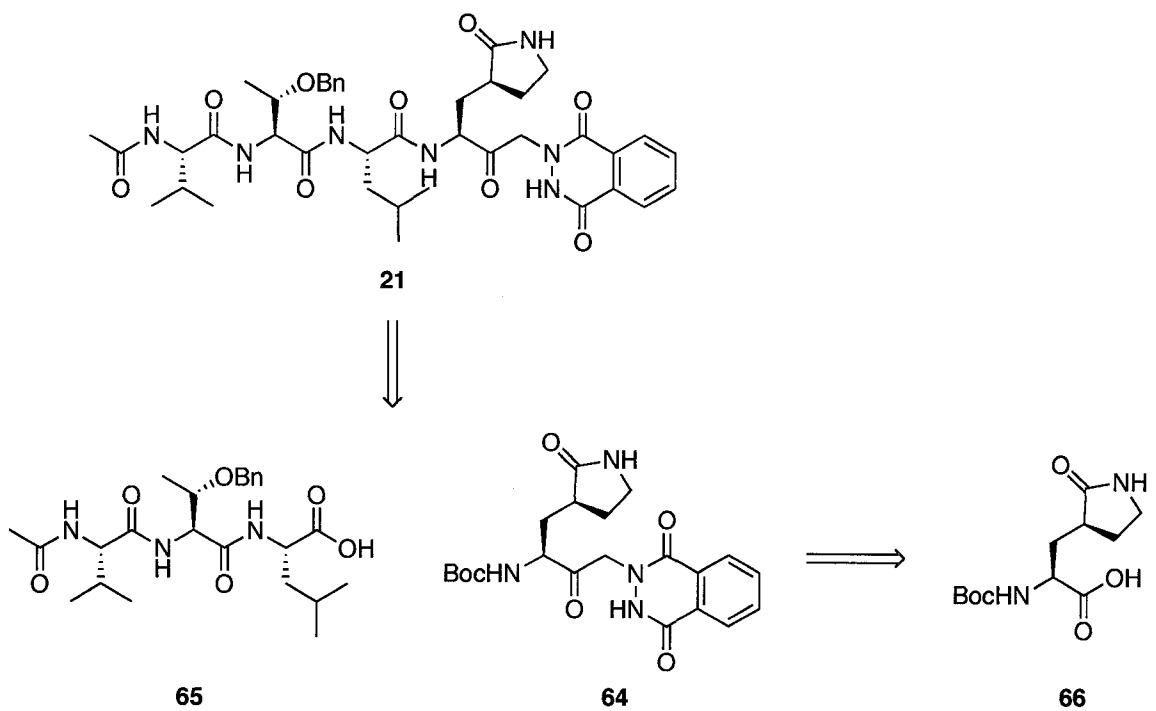

1.2.1. Synthesis of the Cyclic Glutamic Acid Derivative 66

The key cyclic glutamic acid derivative **66** was synthesized by a modified literature procedure (Scheme 1).[68] Esterification of the L-glutamic acid **67** with TMSCl/MeOH, followed by the Boc protection of the free amine, provides the *N*-Boc-L-glutamic acid dimethyl ester **68**. The resulting dimethyl ester **68** is deprotonated with LiHMDS and then bromoacetonitrile is added for alkylation, which yields the nitrile **69**. Hydrogenation of the nitrile **69** with platinum oxide, followed by a cyclization reaction in the presence of sodium bicarbonate, gives the cyclic methyl ester **70**. Hydrolysis of the ester **70** by LiOH generates the desired cyclic glutamic acid derivative **66**.

Scheme 1 Synthesis of the cyclic glutamic acid derivative **66**

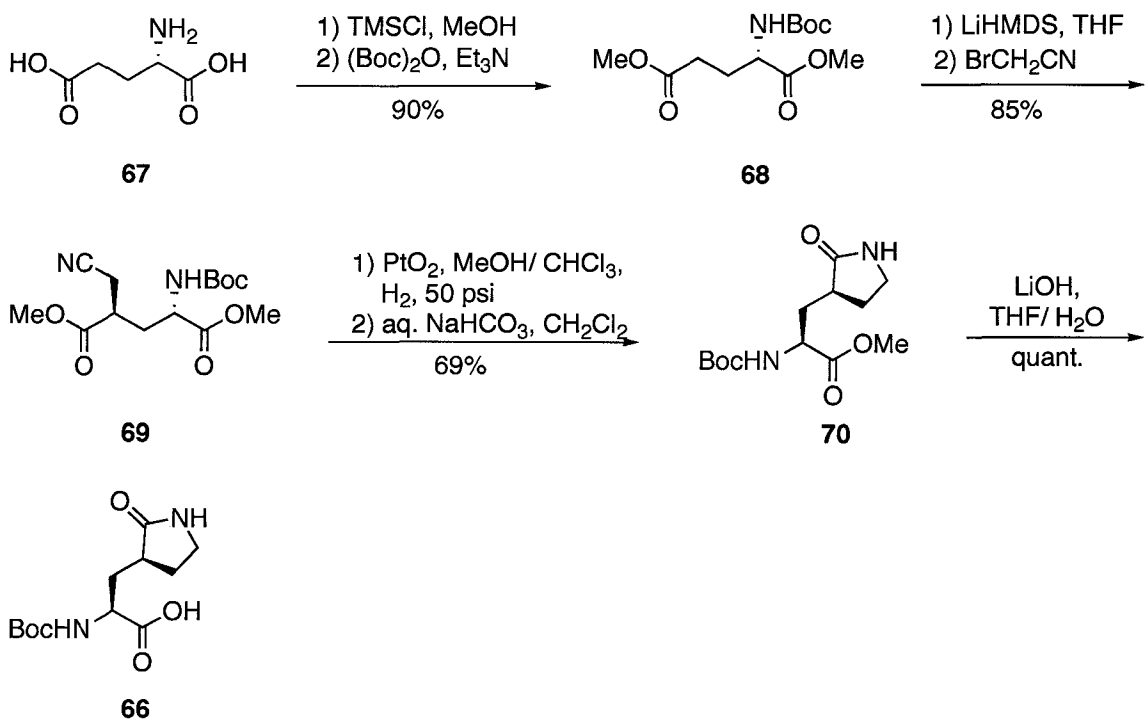

1.2.2. Synthesis of the Cyclic Keto-Glutamines 64 and 74

The cyclic keto-glutamine **64** was synthesized from **66** by a modified literature method established in our group previously (Scheme 2).[65b] Activation of the free carboxylic acid functional group of **66** with ethyl chloroformate, followed by diazomethane substitution, provides the diazo compound **71**. Treatment of **71** with 48% HBr generates the bromide **72**. Nucleophilic substitution of the bromide **72** with sodium phthalhydrazide yields the desired cyclic keto-glutamine **64**, and the dimer **73** as a side product. The moderate yield of the desired product **64** in this substitution reaction is partly due to formation of **73**.

Scheme 2 Synthesis of the cyclic keto-glutamine **64**

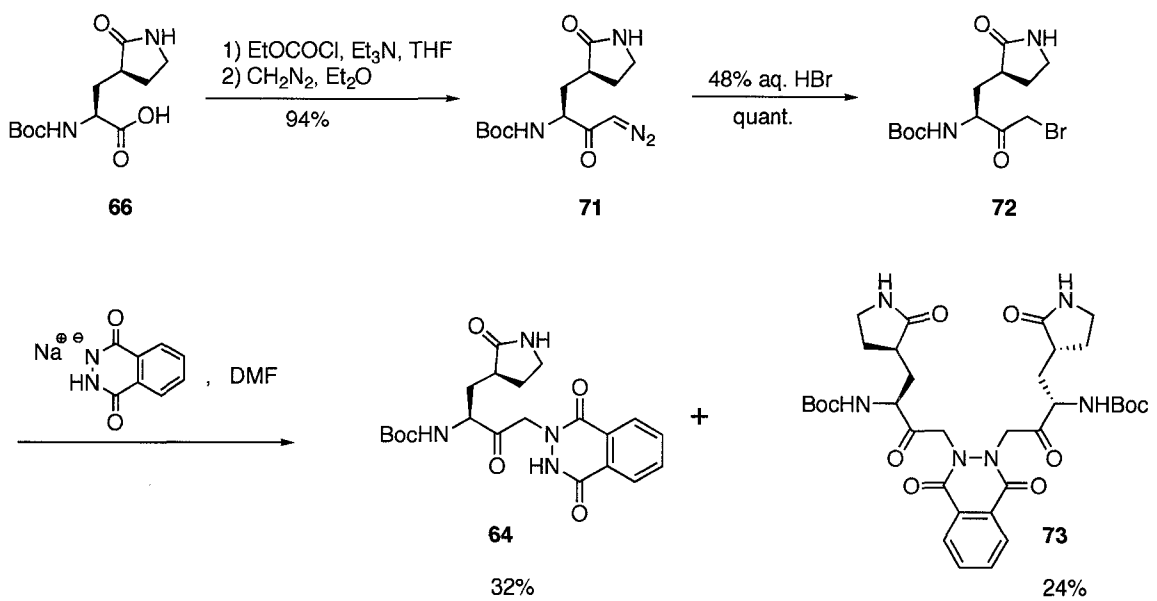

To examine further the phthalhydrazide moiety, nitro compound **74** analogous to the keto-glutamine **64**, was also synthesized (Scheme 3). Treating the bromide **72** with sodium nitro-phthalhydrazide yields the cyclic keto-glutamine **74** in modest yield.

Scheme 3 Synthesis of the cyclic keto-glutamine **74**

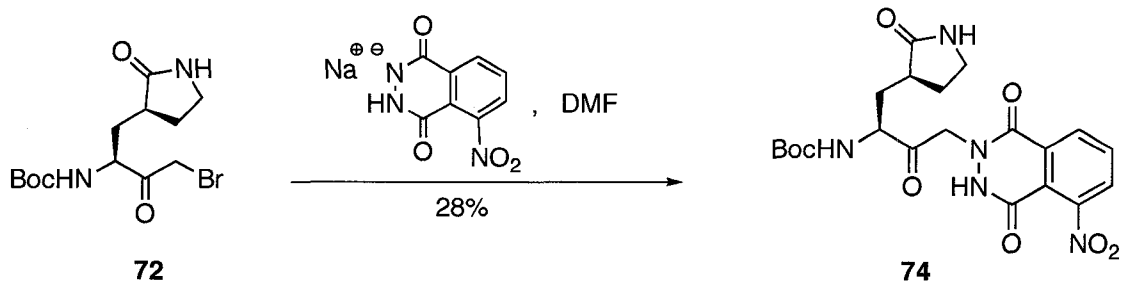

1.2.3. Synthesis of the Recognition Tripeptide 65

The tripeptide **65** was prepared as described in Scheme 4. Esterification of commercially available L-leucine **75** with $SOCl_2$/MeOH provides the L-leucine methyl ester **76**, which is then treated with the pre-activated Boc-Thr(OBn)-OH/EtOCOCl solution to generate the dipeptide **77**. Removal of the Boc protective group of **77** with trifluoroacetic acid, followed by the reaction with Boc-Val-OH using EDCI and HOBt as the coupling reagents, affords the tripeptide **78**. Deprotection of the Boc group with TFA, and then blocking of the resulting free amine with acetic anhydride gives the *N*-acetyl tripeptide **79**. Hydrolysis of the ester functional group of **79** by LiOH provides the desired tripeptide Ac-Val-Thr(OBn)-Leu-OH **65**.

Scheme 4 Synthesis of the recognition tripeptide **65**

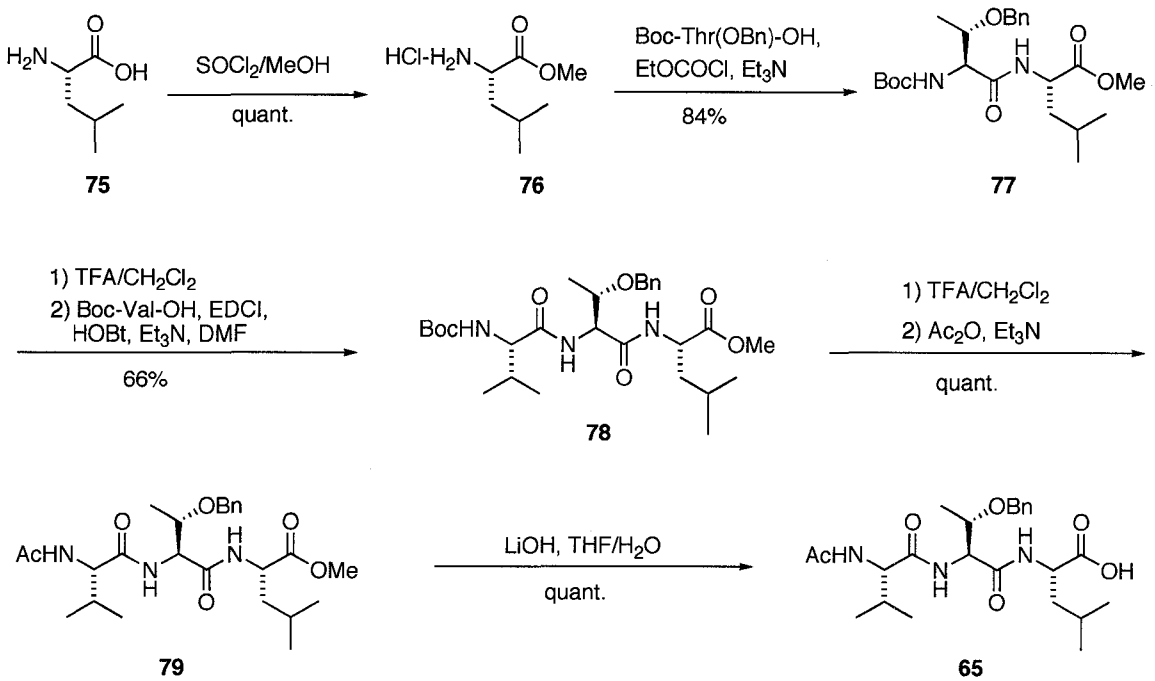

1.2.4. Synthesis of the Cyclic Keto-Glutamine Tetrapeptides 21-24

With the cyclic keto-glutamines **64** and **74** and the recognition tripeptide **65** available, the next coupling reaction can proceed for the target **A**: cyclic keto-glutamine tetrapeptides **21-24**. Removal of the Boc protective groups of **64** and **74** with TFA, followed by coupling with the tripeptide Ac-Val-Thr(OBn)-Leu-OH **65** affords the tetrapeptides **21** and **23** in 67% and 28% yields, respectively (Scheme 5). Debenzylation of **21** to generate the tetrapeptide **22** is achieved by palladium hydrogenation (H_2, Pd/C), while debenzylation of **23** to provide the tetrapeptide **24** is accomplished by Lewis acid (TFA/TMSOTf), because of the presence of the sensitive nitro group in **23** (Scheme 6).

The tetrapeptides **23** and **24** were prepared by previous postdoctoral fellows in our group, Dr. Rajendra Jain and Dr. Hanna Pettersson.

Scheme 5 Synthesis of the cyclic keto-glutamine tetrapeptides **21** and **23**

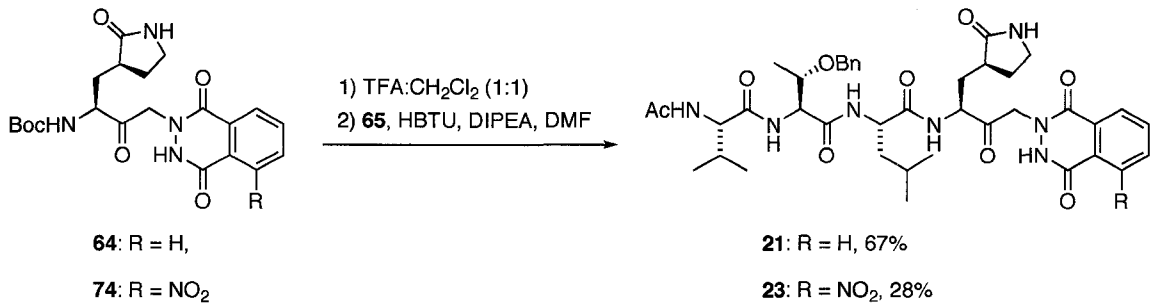

Scheme 6 Synthesis of the cyclic keto-glutamine tetrapeptides **22** and **24**

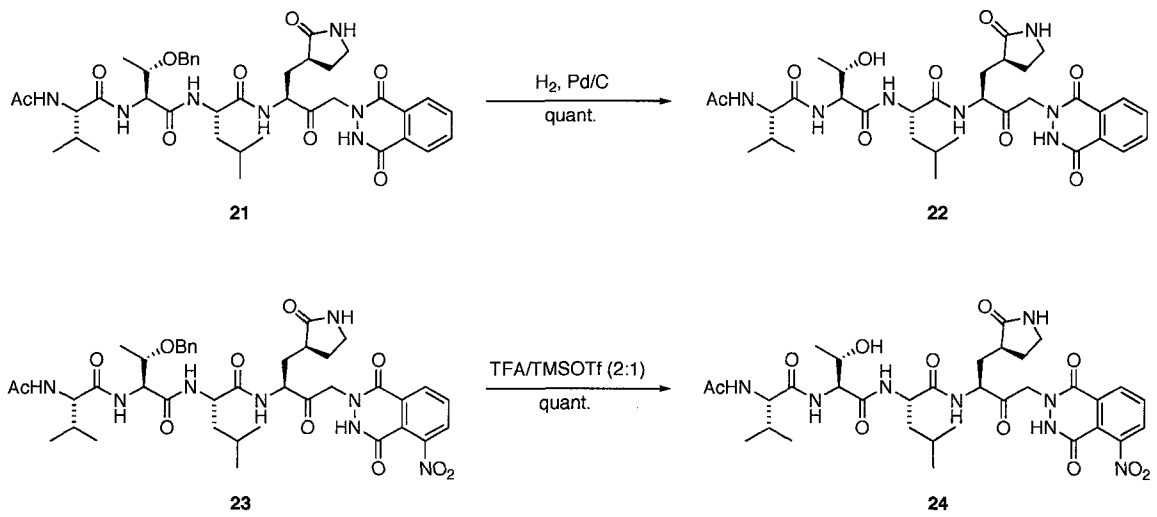

1.3. Evaluation of Target A as SARS 3CL^{pro} Inhibitors

Compounds **64**, **74**, **21-24** were tested as SARS 3CL^{pro} inhibitors using a continuous fluorometric assay and 1.0 μM His-tagged protease, as described in the experimental section (Part 5). The shorter keto-glutamine monomers **64** and **74** show rather poor inhibition against 3CL^{pro} (15% and 24% at 100 μM, respectively). However, the corresponding extended tetrapeptides **21** and **23** are very potent inhibitors with IC_{50} values of 2.7 μM and 0.6 μM, respectively. This indicates that the recognition tripeptide is important for the binding affinity to SARS 3CL^{pro}. The tetrapeptide **22** (IC_{50} of 2.9 μM) derived from the compound **21**, by removal of the benzyl-protecting group in the P_3 threonine residue, is approximately the same potent to the inhibitor **21** (IC_{50} of 2.7 μM). Interestingly, the tetrapeptide **24** (IC_{50} of 3.4 μM), which is derived from the compound **23** by removal of the benzyl protecting group in the P_3 threonine residue, is around four-fold less potent than **23** (IC_{50} of 0.6 μM).

Hence, these cyclic peptidyl keto-glutamines are a new class of potent SARS 3CL^{pro} inhibitors, and removal of the threonine O-benzyl group of the corresponding keto-glutamine inhibitor slightly increases the IC_{50} values, but still gives low micromolar inhibition against 3CL^{pro}.

1.4. Modeling Studies of Target A (21-24)

Modeling studies (Figure 27) of $3CL^{pro}$ with inhibitors **21-24** were conducted as described in the experimental section (Part 8), by Dr. Jonathan Parrish in Prof. Michael James' group at the Department of Biochemistry, University of Alberta.

Figure 27 Modeling studies indicating inhibitors **21-24** (A-D, respectively) in the active site of $3CL^{pro}$. Key active site side chains are shown in two shades: lighter for the protease/inhibitor complex and darker for the enzyme in the absence of inhibitor (done by Dr. Jonathan Parrish).

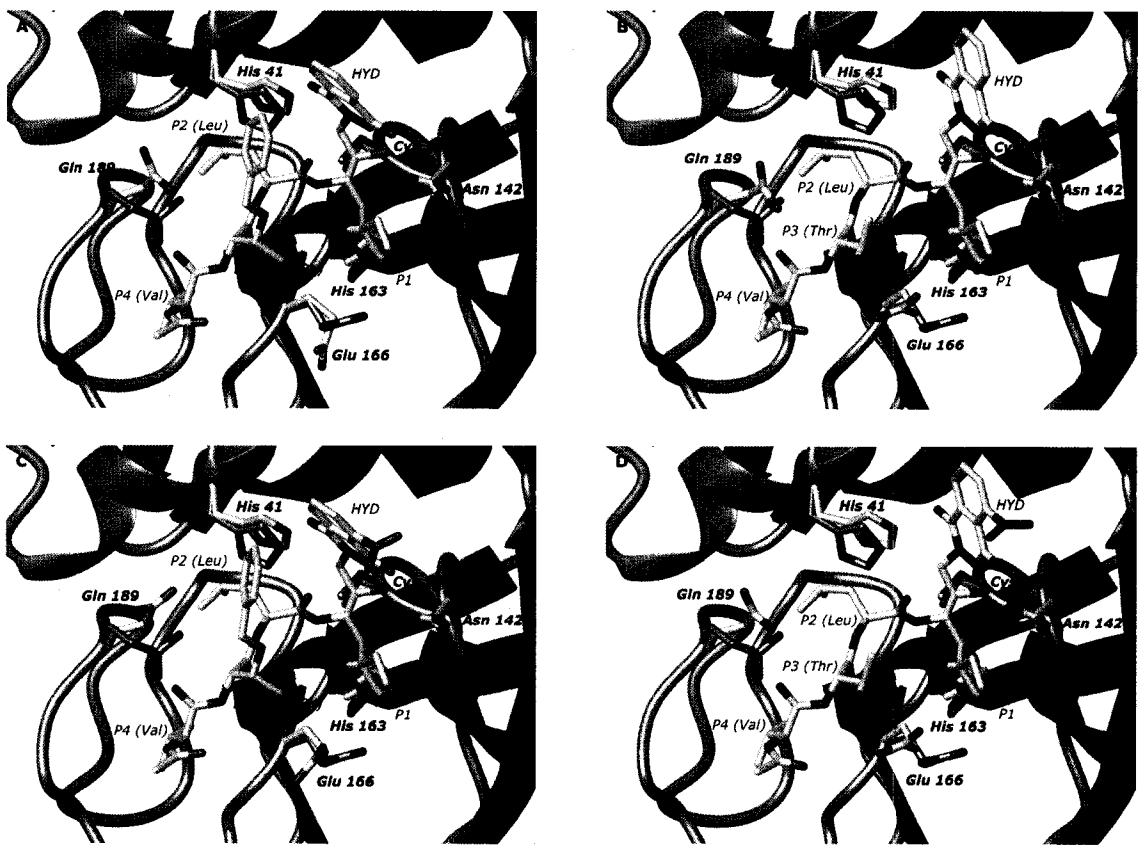

The inhibitors are shown binding in an extended conformation, forming a partial β-sheet interaction with residues 163-166 in the protease and a hydrogen bond between residue His163 and the P_1 side chain (Figure 27). The last hydrogen bond is responsible for the protease specificity for Gln in the P_1 position. The modeling studies indicate that the active site of the enzyme has enough room to accommodate the phthalhydrazide group.

Specific interactions relating to the different substituents on the inhibitors are noted from the modeling, particularly with the nitro group attached to the phthalhydrazide (**23**, **24**) and the benzyl group on the threonine (**21**, **23**). The oxygens on the nitro group are in a position to hydrogen bond to the side chain nitrogen of Asn142. The benzyl group, attached to the threonine at P_3, fits into a small pocket above the leucine at P_2. In addition to filling a small hydrophobic pocket, the phenyl ring forms a favorable aromatic-aromatic stacking interaction with the phthalhydrazide group of the inhibitor. For the inhibitors with no benzyl group (**22**, **24**), the free hydroxyl group in the threonine side chain is in a position to form a hydrogen bonding interaction with Glu166.

In light of the interactions in the models, it is possible to rationalize the increased inhibition of **23** relative to **21**. The nitro group on the phthalhydrazide, in addition to an interaction with Asn142, may contribute to the binding of **23** by presenting the hydrophilic atoms towards the solvent. These three major effects, the increased hydrophilicity of the phthalhydrazide moiety, the packing of a hydrophobic pocket, and the aromatic-aromatic stacking may explain the synergistic contributions to inhibition parameters for these two chemical groups.

1.5. Inhibition Mechanism Studies of Target A

To gain further insight into the inhibition mechanism for this class of inhibitors, more detailed enzyme kinetics studies were done with inhibitor **21** and SARS $3CL^{pro}$. Inhibitor **21** displays potent inhibition against SARS $3CL^{pro}$ with IC_{50} of 2.7 μM and K_i of 0.25 μM. Initially a competitive and reversible inhibition is observed over a short period of time (15 min to 1 h). The inhibitor **21** (Figure 28) appears to be a potent reversible inhibitor for SARS $3CL^{pro}$ in a short time course, probably due to the relatively low reactivity of carbon-nitrogen bond and apparent poor leaving group ability of the phthalhydrazide.

However, recent crystal structure studies of SARS $3CL^{pro}$-inhibitor **21** complex by Michael James' group revealed formation of a covalent thioether bond, with departure of the phthalhydrazide moiety (Figure 28).[69a] This is probably due to the fact that crystals used in these studies were grown over a longer time period (24-72 hours). More interestingly, two species of modified enzymes have been detected by high resolution x-ray crystallography: an alkylated species similar to those reported in other covalently inhibited $3C^{pro}$ and $3CL^{pro}$ (**A**, Figure 28), and a species in which the inhibitor is linked to $3CL^{pro}$ by an episulfide cation ring (**B**, Figure 28). If preformed SARS $3CL^{pro}$ crystals are soaked with **21**, **B** is formed. However, if the same enzyme is inhibited in solution and the enzyme-inhibitor complex is crystallized, **A** is observed. Presumably the crystallized active protease conformation favors episulfide formation. In the **B** complex, the sulfur atom of the catalytic Cys145 is directly attached to the carbonyl carbon, leading to the

formation of an episulfide cation ring and an oxyanion in the active site. Similar three-membered episulfide intermediates were also trapped in the co-crystal structures of this class of peptidyl keto-glutamines with HAV $3C^{pro}$.[69b] To the best of our knowledge, these are the first crystal structures showing the evidence of formation of the three-membered episulfide intermediate. [69a,b]

Figure 28 The interactions between inhibitor **21** and SARS $3CL^{pro}$. **A**: the alkylated form of SARS $3CL^{pro}$-inhibitor **21** complex; **B**: the episulfide form of SARS $3CL^{pro}$-inhibitor **21** complex (modified from Yin *et al.*)[69a]

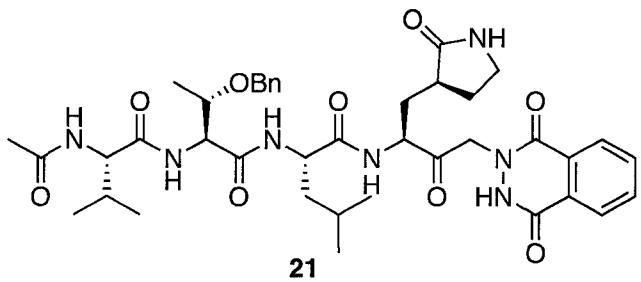

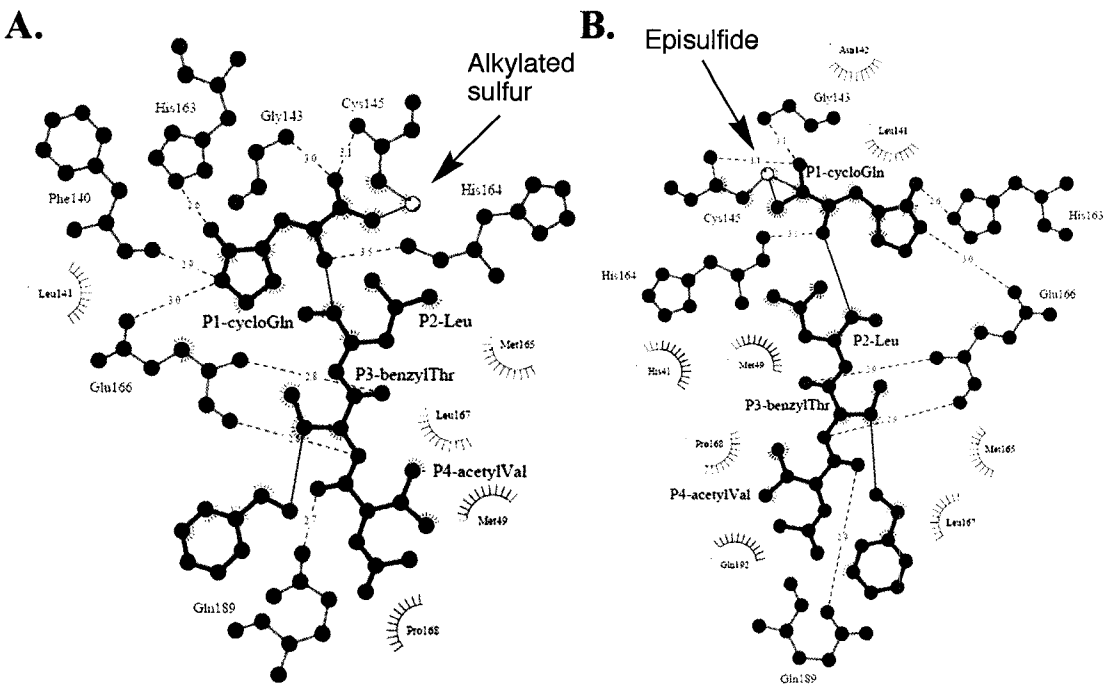

The inhibition mechanism of compound **21** with SARS 3CL^{pro} was further examined by electrospray ionization-mass spectrometry (ESI-MS) studies with co-crystals of the SARS 3CL^{pro}-inhibitor **21** complex (Figure 29). Two major peaks are obvious in the mass spectrum of the SARS 3CL^{pro}-inhibitor **21** complex: the peak with a mass 33844 for the 3CL^{pro} and the peak with a mass 34460 for the 3CL^{pro}-inhibitor **21** complex. The mass difference of 616 Dalton of the two peaks suggests a covalent bond formation between 3CL^{pro} and inhibitor **21**, with departure of the phthalhydrazide moiety. This result is consistent with the crystallographic observations.

Figure 29 ESI-MS of the SARS 3CL^{pro}-Inhibitor **21** Complex.

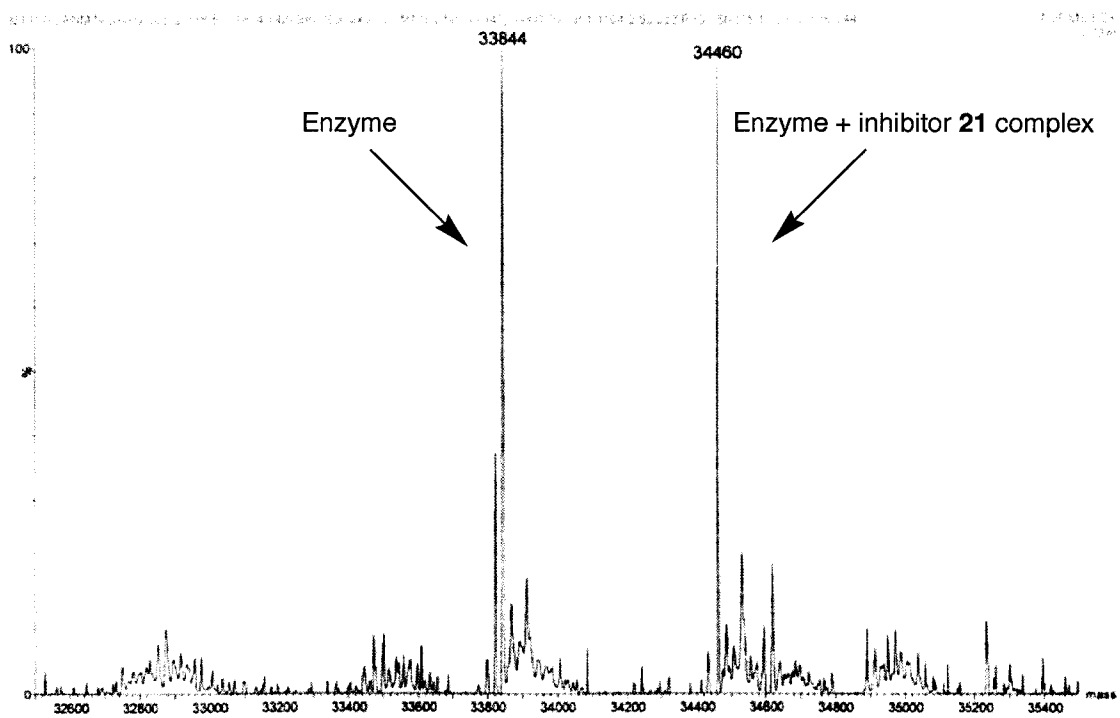

A mechanism of inhibition is proposed to interpret the discrepancy between the enzyme kinetics results and the crystallography/mass spectrometry results (Figure 30). Cyclic peptidyl keto-glutamines (*e.g.* **21**) may function as competitive inhibitors and were initially designed as reversible inhibitors for SARS $3CL^{pro}$, due to the relatively robust carbon-nitrogen bond of the phthalhydrazide moiety. In the first step of inhibition, the sulfur atom of the catalytically active Cys145 residue attacks the carbonyl group of inhibitor **21**, leading to the formation of the tetrahedral intermediate **21a**. The tetrahedral intermediate **21a** is not very thermodynamically stable, so it can break down to inhibitor **21** and the reactivated enzyme. This equilibrium takes place in a rapid and reversible way in a short time course, as described in pathway 1 (Figure 30). However, over a longer time, the tetrahedral intermediate **21a** can undergo a slow reaction to form the unfavorable three-membered episulfide intermediate **21b** (observed by crystallography, B, Figure 28). This high-energy intermediate **21b** is then converted to the thermodynamically stable product **21c** in solution (observed by crystallography, A, Figure 28). Formation of this thermodynamically stable product **21c** drives the reaction to favor pathway 2 (Figure 30).

Figure 30 Proposed inhibition mechanism of SARS 3CL^{pro} by inhibitor **21**. Pathway 1: reversible and competitive inhibition. Pathway 2: irreversible and covalent inhibition.

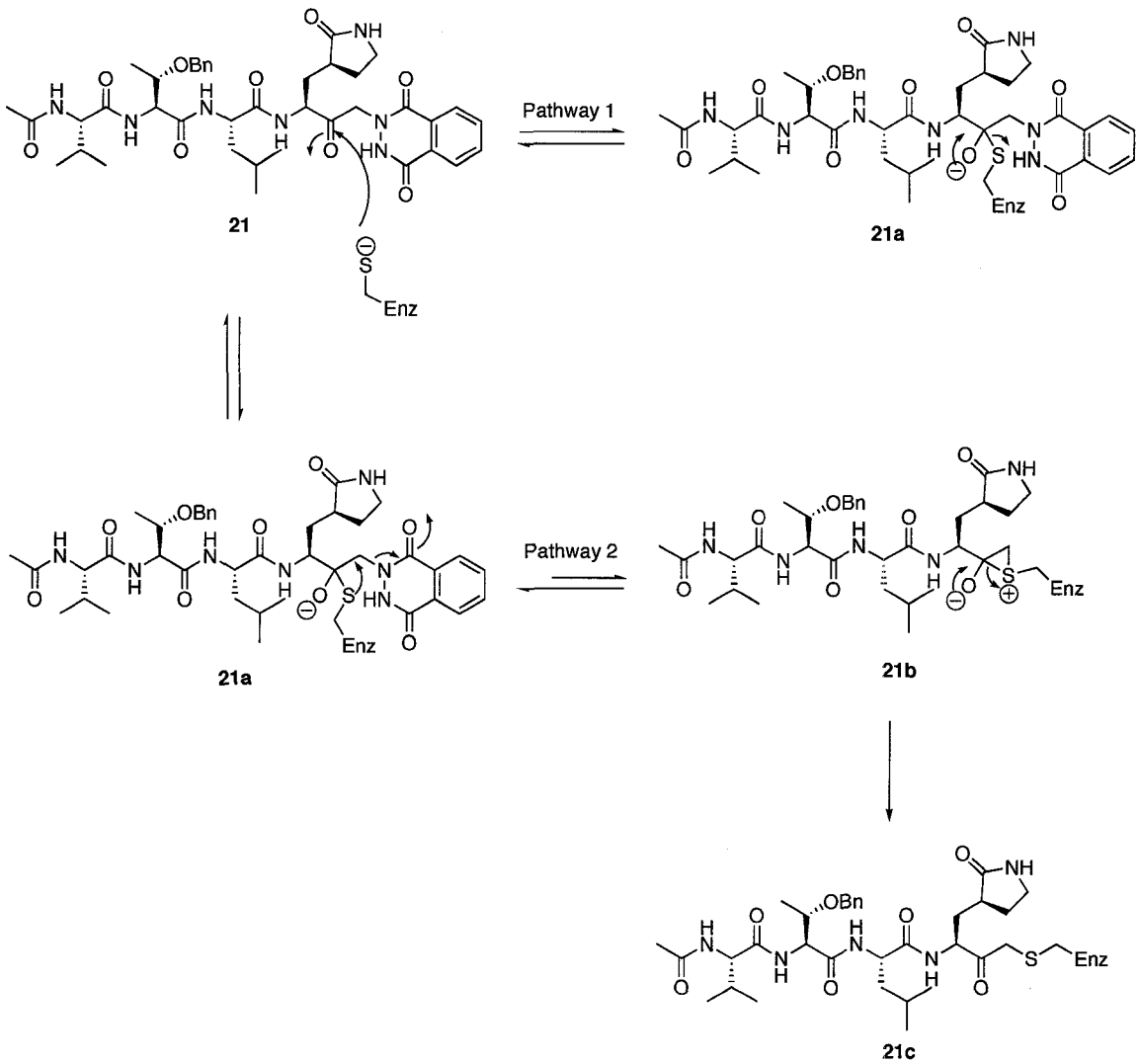

2. Acyclic Peptidyl Keto-Glutamines – Target B (25-28)

2.1. Design and Synthesis of Target B (25-28)

To gain further insight into the structure-activity relationships, target **B** (**25-28**) was designed and synthesized for the examination of peptidyl keto-glutamines. Previous studies with HAV 3C protease have shown that replacement of the glutamine residue by the *N,N*-dimethyl glutamine has no impact on substrate peptide recognition or cleavage.[70] This modification simplifies the synthesis by avoiding the primary amide protection and deprotection steps that are otherwise essential to prevent the side-chain cyclization reaction (Figure 31).[71]

Figure 31 Side-chain cyclization reaction for halomethyl glutamines

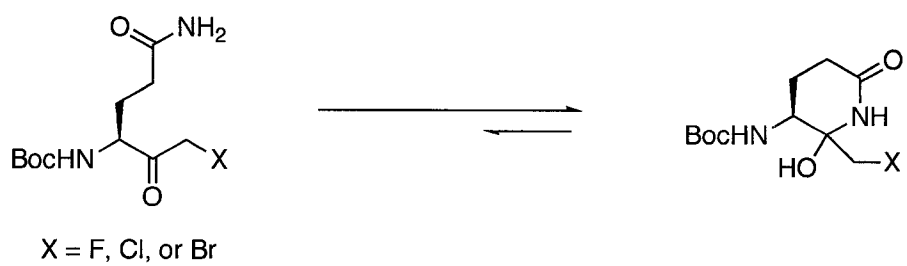

The synthetic strategy for target **B** (**25-28**) is similar to that for target **A** (**21-24**), as illustrated in Figure 32 with **25** as an example. The acyclic keto-glutamine tetrapeptide **25** can be synthesized from the tripeptide **65** and the acyclic keto-glutamine **80**, which can be prepared by a method established in our group previously.[65b]

Figure 32 Retrosynthetic analysis of target **B** (*e.g.* **25**)

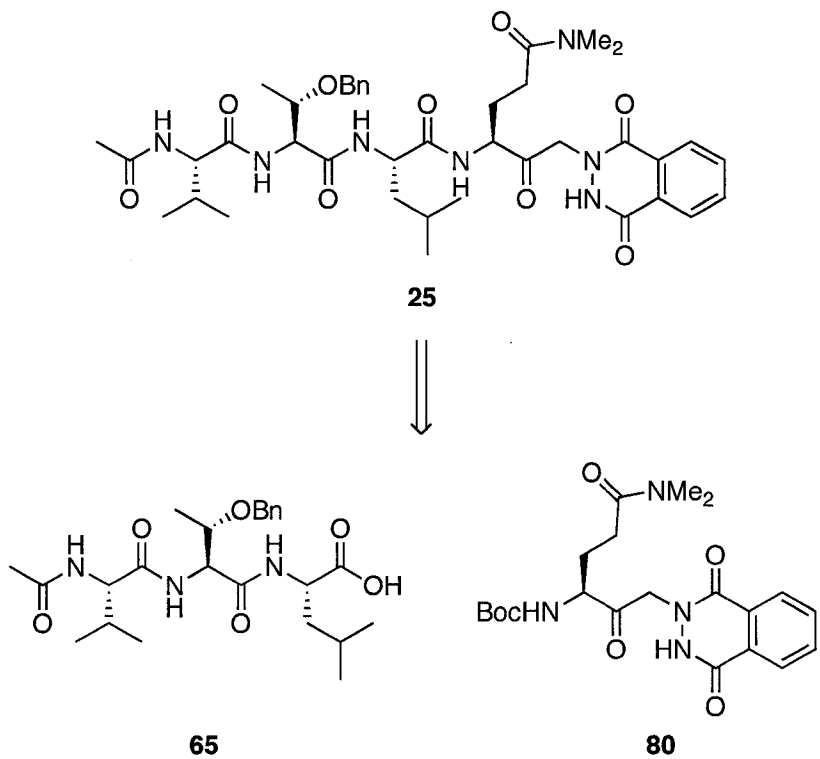

2.1.1. Synthesis of the Acyclic Keto-Glutamines 80 and 86

The acyclic keto-glutamines **80** and **86** were prepared by a literature method established in our group previously (Scheme 7).[65b] Treatment of commercially available L-glutamic acid derivative **81** with ethyl chloroformate, followed by the addition of $NHMe_2$•HCl and Et_3N generates the amide **82**. Removal of the benzyl protecting group of **82** by palladium hydrogenolysis provides the carboxylic acid **83**. Activation of **83** with ethyl chloroformate, followed by treatment with diazomethane, gives the diazo compound **84**,

which is readily transformed to the bromide **85** using 48% HBr. Nucleophilic substitution of the bromide **85** with sodium phthalhydrazide or nitrophthalhydrazide affords the acyclic keto-glutamines **80** and **86** in 41% and 34% yields, respectively. The relatively moderate yields for the substitution reactions are due to side reactions that lead to the dimer products, as reported previously.[65b]

Scheme 7 Synthesis of the acyclic keto-glutamines **80** and **86**

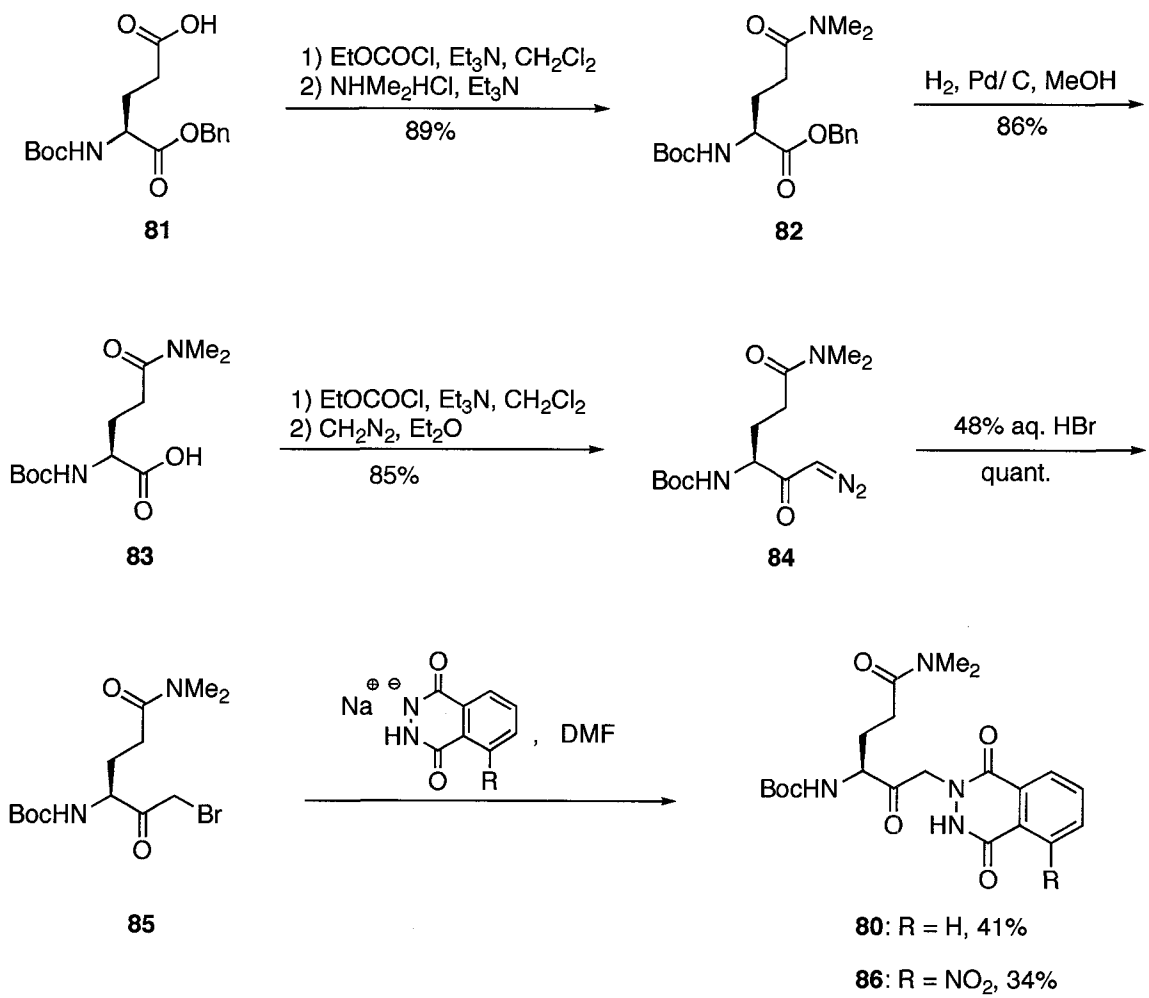

2.1.2. Synthesis of the Acyclic Peptidyl Keto-Glutamines 25-28

The acyclic keto-glutamine tetrapeptides **25-28** were prepared by coupling of the recognition tripeptide **65** to the corresponding keto-glutamine monomers (**80** and **86**). Removal of Boc protective groups of **80** and **86** with TFA, and then coupling of the tripeptide Ac-Val-Thr(OBn)-Leu-OH **65** yields the tetrapeptides **25** and **27** in 28% and 33% yields, respectively (Scheme 8). The tetrapeptide **27** was prepared by previous postdoctoral fellows in our group, Dr. Rajendra Jain and Dr. Hanna Pettersson.

Scheme 8 Synthesis of the acyclic peptidyl keto-glutamines **25** and **27**

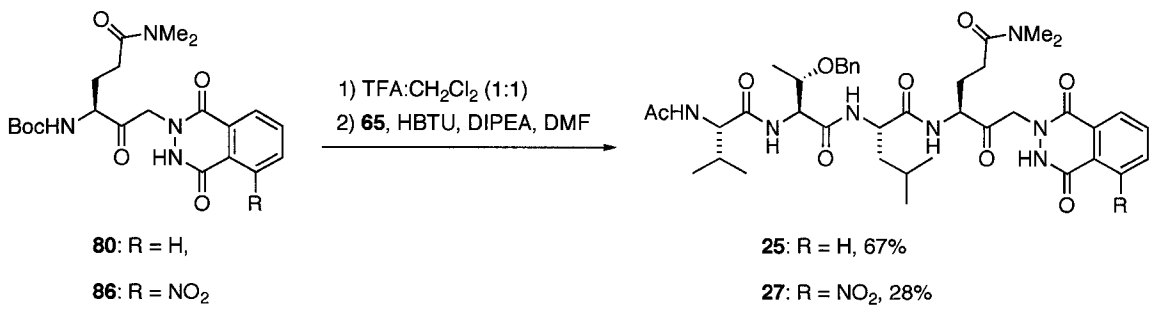

Debenzylation of **25** to generate the tetrapeptide **26** is achieved by palladium hydrogenation (H_2, Pd/C). Debenzylation of **27** to give **28** employed Lewis acid (TFA/TMSOTf), due to the presence of the sensitive nitro group in **27**, as mentioned earlier (Scheme 9). The tetrapeptide **28** was prepared by previous postdoctoral fellows in our group, Dr. Rajendra Jain and Dr. Hanna Pettersson.

Scheme 9 Synthesis of the acyclic peptidyl keto-glutamines **26** and **28**

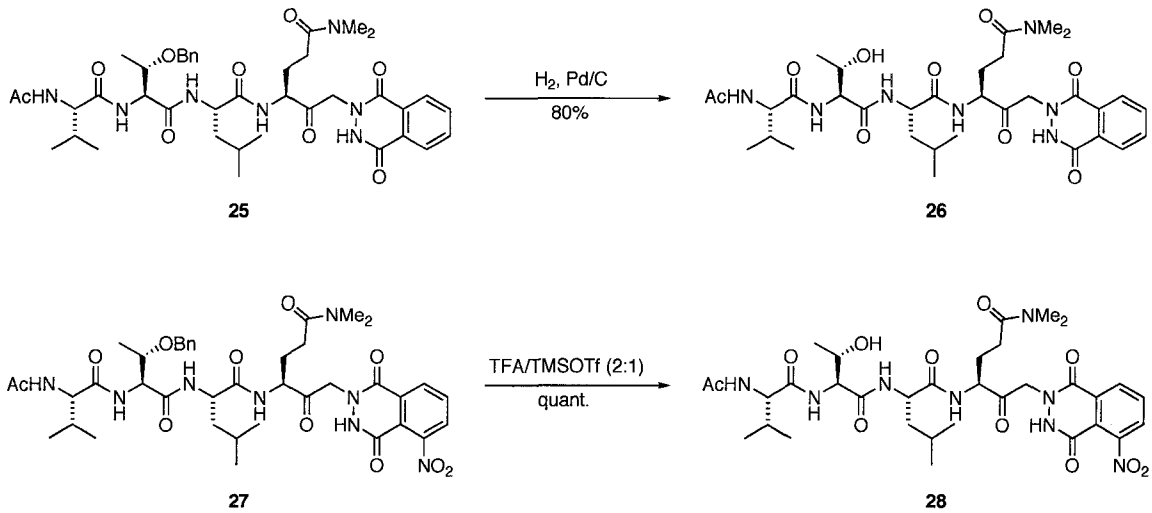

2.2. Evaluation of Target B as SARS 3CL^{pro} Inhibitors

Compounds **80**, **86**, **25-28** were tested as SARS 3CL^{pro} inhibitors using a fluorometric assay and 1.0 μM His-tagged protease, as described in the experimental section (Part 5). The keto-glutamine monomers **80** and **86** show very weak inhibition against 3CL^{pro} (less than 10% at 100 μM). The corresponding extended tetrapeptides **25** and **27** display much improved inhibition with IC_{50} values of 64 μM and 28 μM, respectively. This indicates that the recognition tripeptide is crucial for the binding affinity to SARS 3CL^{pro}. In addition, the tetrapeptides **26** and **28** have IC_{50} values of 70 μM and 53 μM, respectively. This suggests that removal of the benzyl-protecting group in the P_3 threonine residue slightly decreases inhibitory activity against 3CL^{pro} for this class of compounds. However, compared to the cyclic peptidyl keto-glutamines (**21-24**), the acyclic analogues

(**25-28**) exhibit much weaker inhibition, suggesting that the γ-lactam moiety is an important structural feature for the peptidyl keto-glutamines as SARS $3CL^{pro}$ inhibitors.

3. Peptidyl Keto-Phenylalanine – Target C (29)

3.1. Design of Target C (29)

As described earlier, the structure-activity relationship studies and crystal structure studies indicate that the γ-lactam moiety is an important structural feature for the cyclic peptidyl keto-glutamines to be potent inhibitors of SARS $3CL^{pro}$. Interestingly, AG7088 **4** has been reported to show no inhibition against SARS $3CL^{pro}$ even at 100 μM concentration. However, replacement of the γ-lactam moiety by a phenyl group provided modified AG7088 analogues that have significantly improved inhibition (*e.g.* **12**, IC_{50} = 39 μM, Figure 33).[36] It is known that the phenyl group can fit in the P_1 position at the active site of papain proteases.[29] Based on this concept, we decided to examine a modified keto-glutamine analogue **29**, in which the γ-lactam is replaced with a phenyl group in the P_1 position (Figure 33).

Figure 33 Rational design of target **C** (**29**)

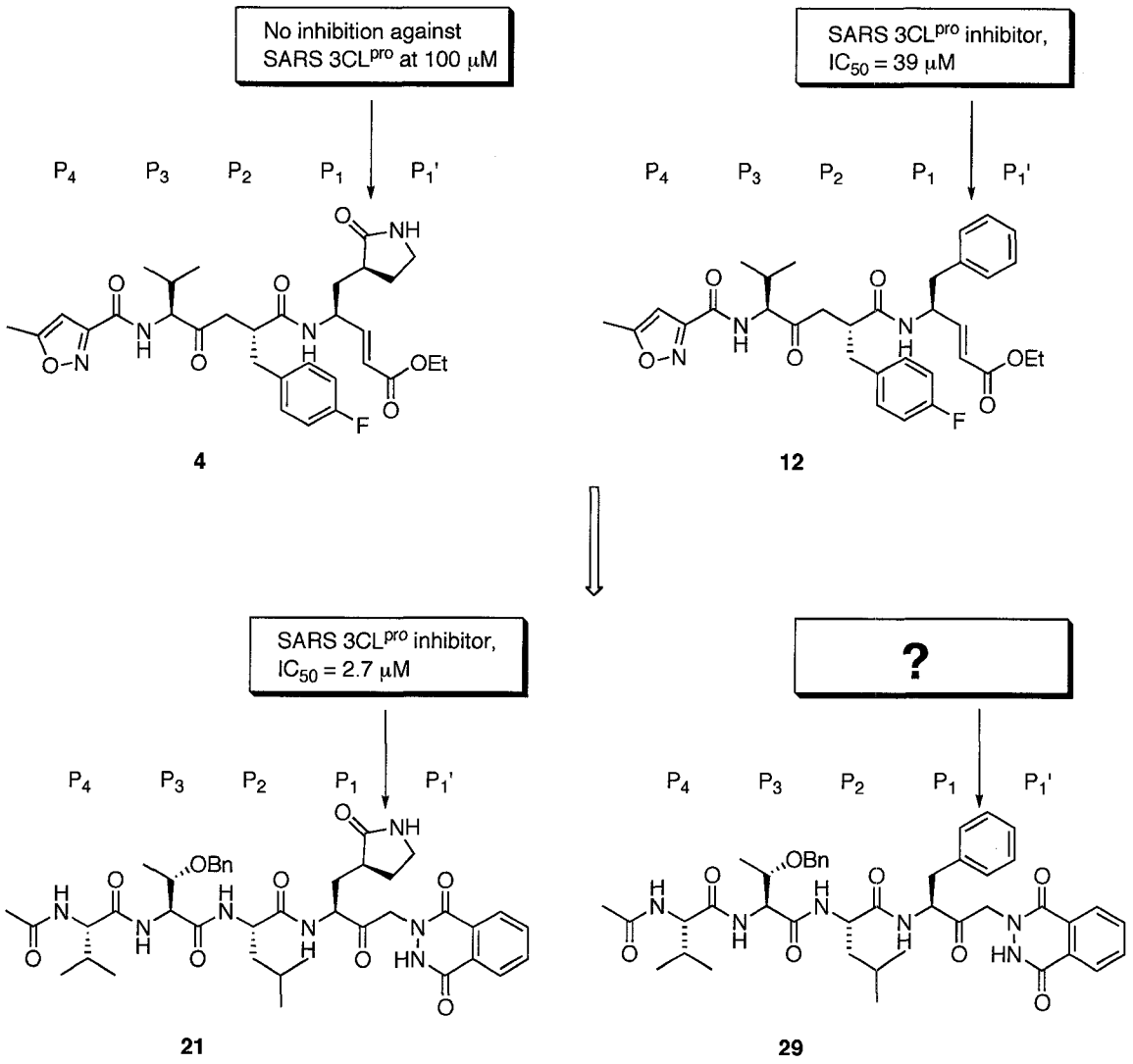

3.2. Synthesis of Target C

The keto-glutamine analogue **29** with a phenyl substituent in the P1 position was synthesized using a method similar to that used for targets **A** and **B** (Scheme 10). Activation of the carboxylic acid of *N*-Boc-L-phenylalanine **87** with ethyl chloroformate,

followed by diazomethane substitution provides the diazo compound. Treating the diazo intermediate with 48% aqueous HBr gives compound **88** in 76% yield over three steps. Nucleophilic substitution of the bromide **88** with sodium phthalhydrazide produces compound **89** in 34% yield. Removal of the Boc group with TFA, followed by coupling with the recognition tripeptide Ac-Val-Thr(OBn)-Leu-OH affords the desired tetrapeptide **29** in 45% yield.

Scheme 10 Synthesis of target **C** (**29**) from *N*-Boc-L-phenylalanine **87**

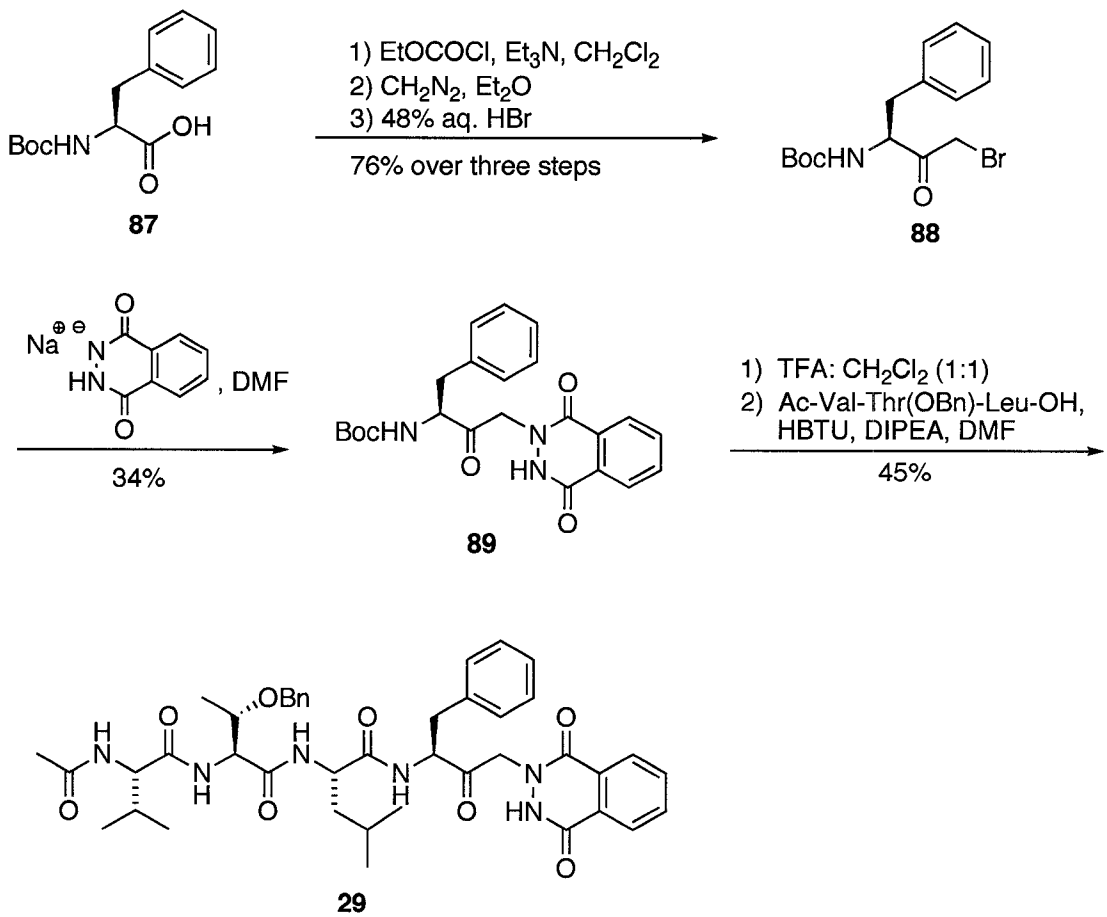

3.3. Evaluation of Target C as a SARS 3CL^{pro} Inhibitor

Compound **29** was tested as a SARS 3CL^{pro} inhibitor using a continuous fluorometric assay and 1.0 μM His-tagged protease, as described in the experimental section (Part 5). In contrast to the keto-glutamine **21** with the γ-lactam moiety (94% inhibition at 100 μM), the analogue **29** with a phenyl substituent does not show improved inhibition (72% inhibition at 100 μM) (Figure 34). This is unexpected in view of the better inhibition of SARS 3CL^{pro} by **12** compared to **4** (Figure 33).[36] The testing results suggest that for this class of peptidyl keto-glutamines, the γ-lactam moiety is an important structural feature to achieve good SARS 3CL^{pro} inhibition.

Figure 34 Compounds **21** and **29** as SARS 3CL^{pro} inhibitors

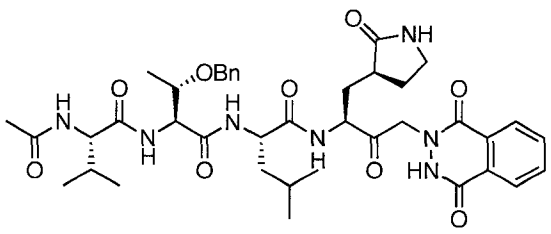

21, 94% inhibition at 100 μM

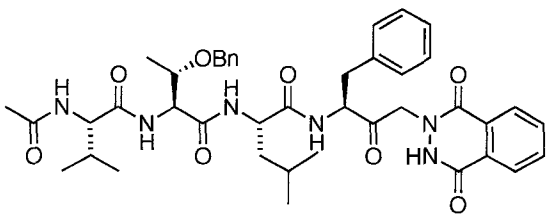

29, 72% inhibition at 100 μM

4. Peptidyl Keto-Glutamine Analogues – Targets D & E

4.1. Design of Targets D & E

As described in the structure-activity relationship studies with targets **A**, **B** and **C** earlier, the γ-lactam moiety is an important structural feature for peptidyl keto-glutamines as potent inhibitors of SARS $3CL^{pro}$. Screening of compound libraries has demonstrated that aromatic ester **9** (Figure 35, IC_{50} = 0.5 μM) is approximately equipotent to keto-glutamine **23** (IC_{50} = 0.6 μM) as a $3CL^{pro}$ inhibitor.[34] Both the thiophenyl and pyridinyl moieties are believed to play important roles in such effective inhibition. Hence, it seemed reasonable to prepare "mix-and-match" combinations based on the assumption that the ketone of **23** and the carbonyl of **9** could bind at the same enzyme site (*i.e.* at or near the Cys145 nucleophile). This assumption is supported by the observation that compound **9** inhibits HAV $3C^{pro}$ as strongly as it does SARS-CoV $3CL^{pro}$. Although the two proteases have low sequence identity, they appear to accept similar substrate analogues in their active sites. Targets **D** (**30**, **31**) and **E** (**32**) were thus designed and synthesized based on this "mix-and-match" combination concept (Figure 35).

Figure 35 Rational design of targets **D** & **E** (*e.g.* **30** and **32**, respectively)

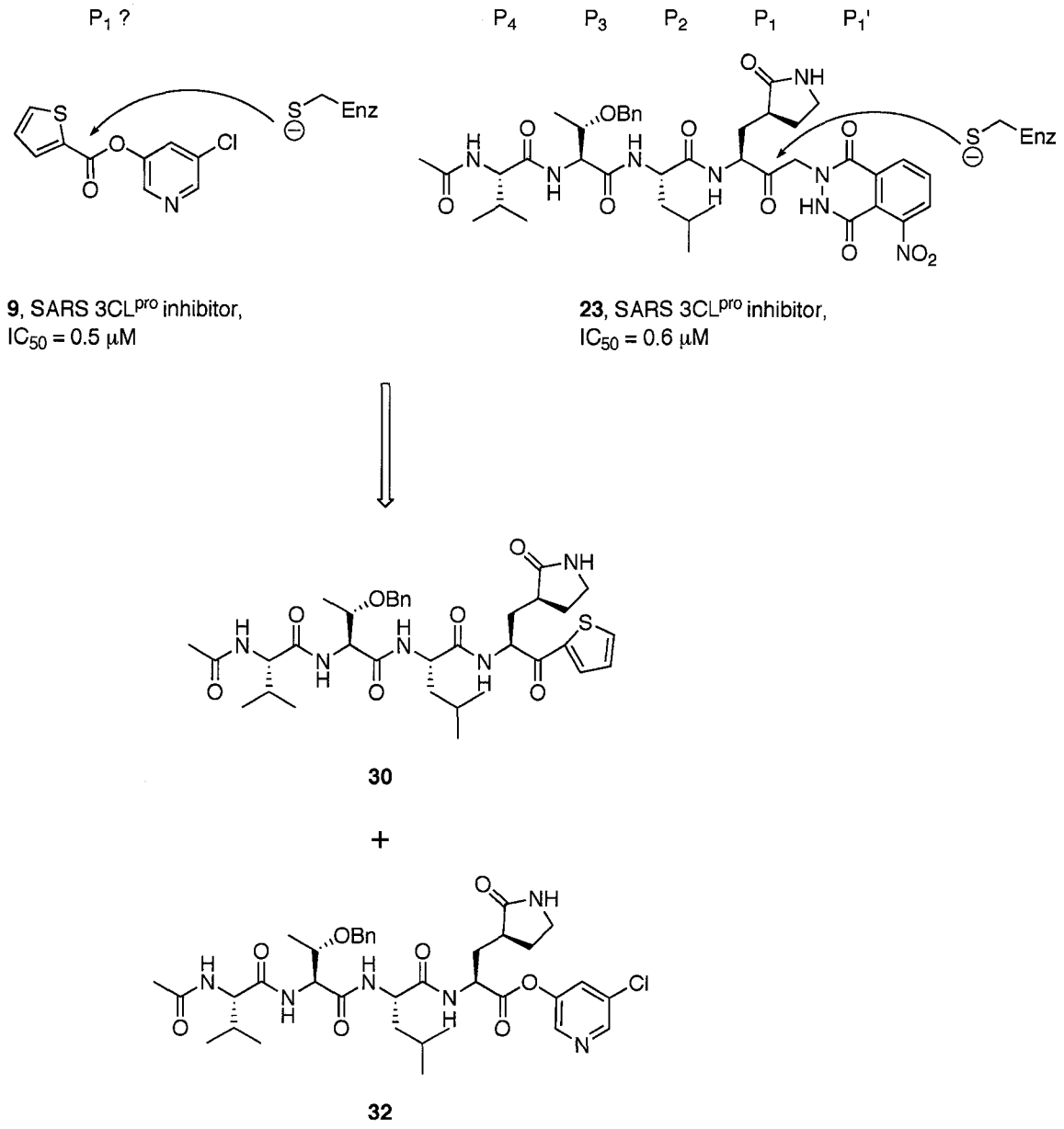

4.2. Synthesis of Target D (30, 31)

The proposed synthetic route to target **D** (**30**, **31**) is similar to that for targets **A**, **B** and **C**, as shown in Figure 36 with **30** as an example. Compound **30** could be prepared from the tripeptide **65** and the cyclic keto-glutamine derivative **90**. Compound **90** may be prepared from the readily available cyclic glutamic acid derivative **66**.

Figure 36 Retrosynthetic analysis of target **D** (*e.g.* **30**)

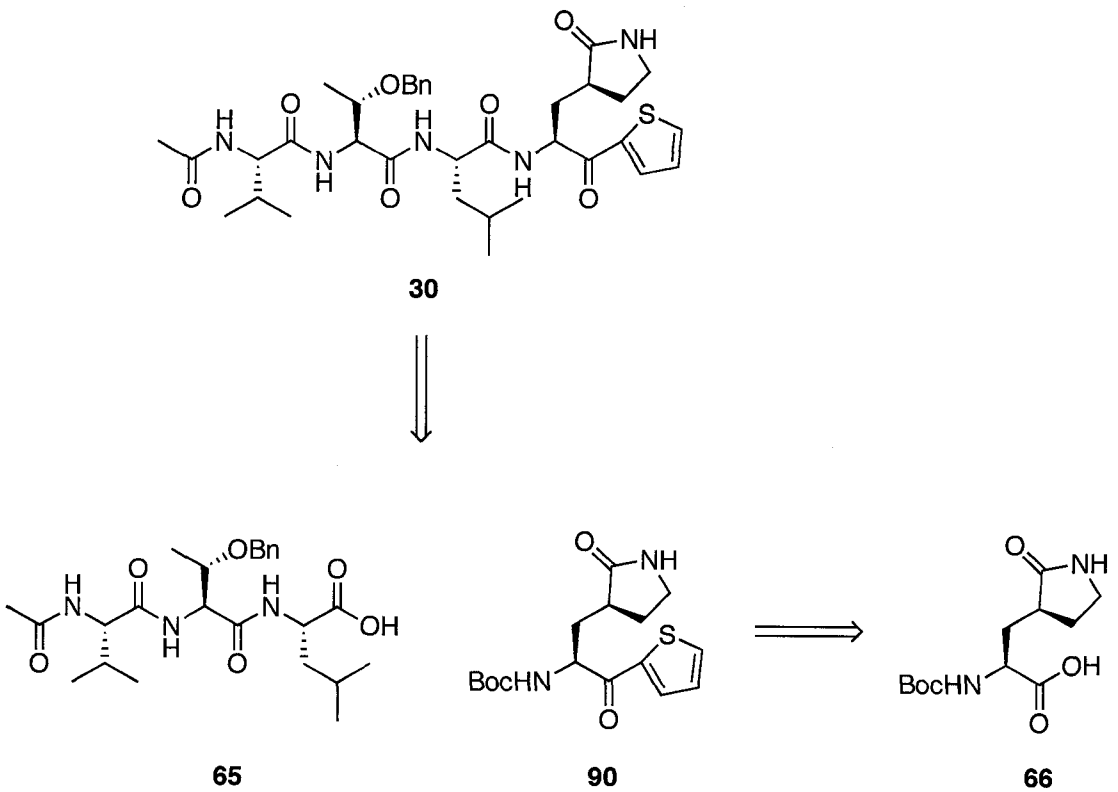

The synthesis starts from the intermediate, cyclic glutamic acid derivative **66** (Scheme 11). Conversion of carboxylic acid **66** to the Weinreb amide[72] **91** proceeds in 66% yield. Isopropyl magnesium bromide is then added to deprotonate the two acidic protons of **91**; this is followed by nucleophilic attack by thiophenyl magnesium bromide to generate compound **90** in 74% yield. Removal of the Boc protective group, followed by coupling with the tripeptide Ac-Val-Thr(OBn)-Leu-OH **65** affords the desired tetrapeptide **30** in 34% yield.

Scheme 11 Synthesis of the cyclic peptidyl keto-glutamine **30**

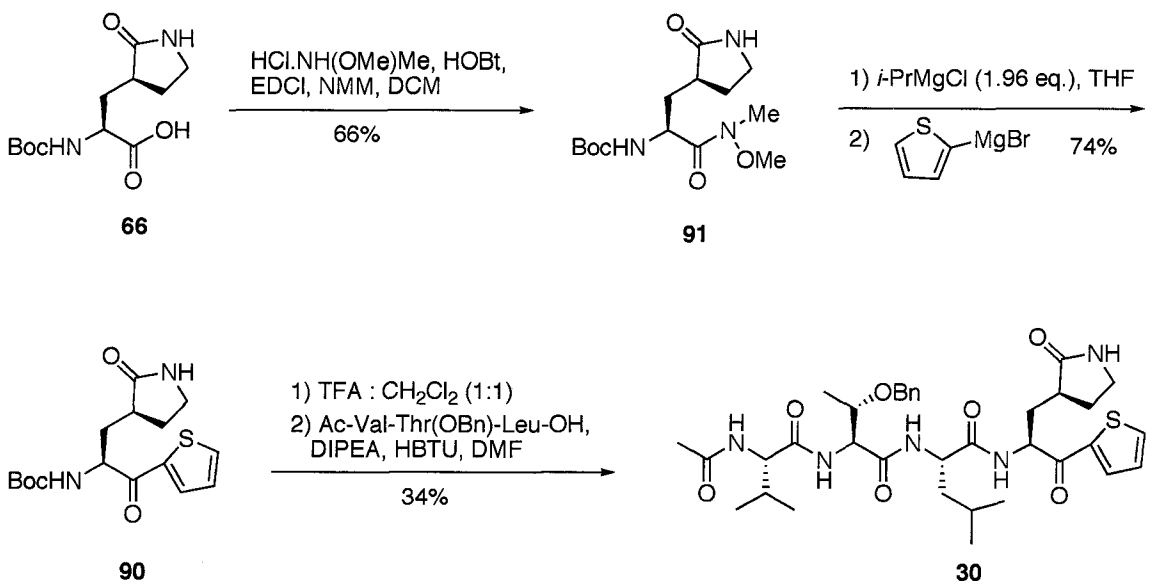

However, attempts to remove the benzyl group of compound **30** to yield compound **31** were not successful, either by palladium-catalyzed hydrogenolysis or by treatment with the Lewis acid TFA/TMSOTf (Scheme 12). We reasoned that the palladium catalyst may be poisoned by the sulfur atom of the thiophenyl functional group, which results in

failure of the debenzylation reaction. The Lewis acid deprotection does remove the benzyl group, and leads to significant epimerization of this tetrapeptide.

Scheme 12 Debenzylation of compound **30** to compound **31**

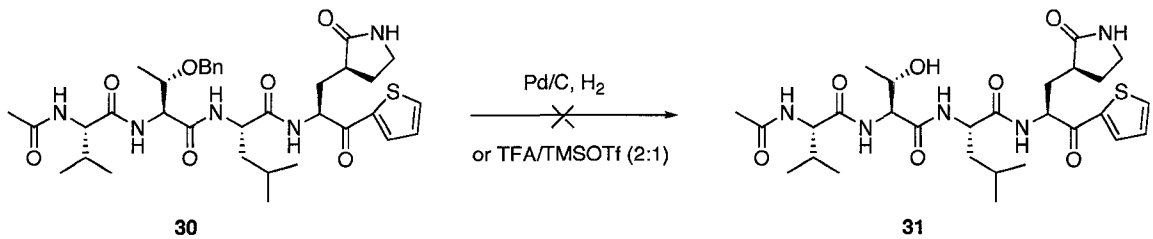

Compound **31** could be obtained in 50% yield by an alternative route, based on the different chemical reactivity of free hydroxyl and amine functional groups. This involves removal of the Boc group of compound **90**, followed by direct coupling with the tripeptide Ac-Val-Thr(OH)-Leu-OH **92** to generate the desired product **31** (Scheme 13).

Scheme 13 Synthesis of cyclic peptidyl keto-glutamine **31**

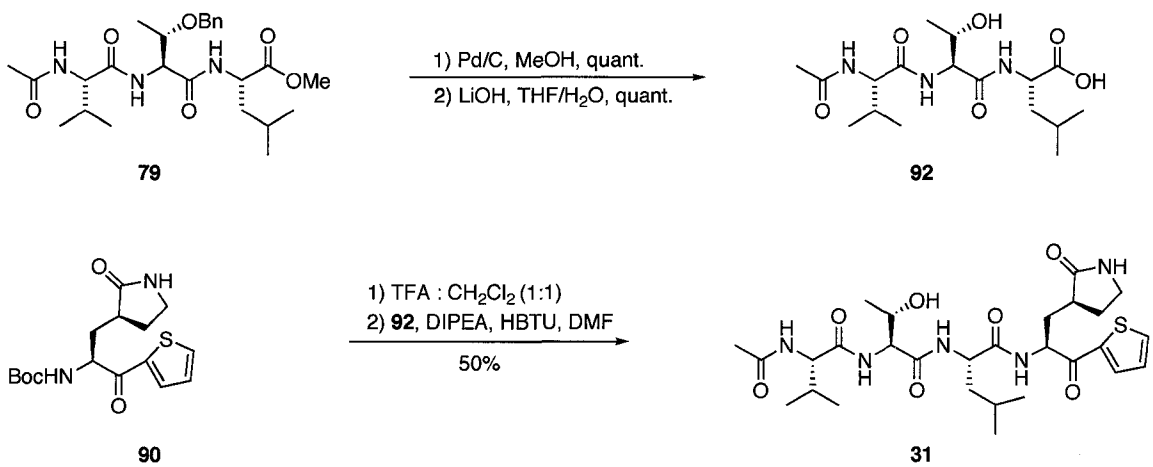

4.3. Evaluation of Target D

Compounds **90**, **30** and **31** were tested as SARS $3CL^{pro}$ inhibitors using a fluorometric assay and 1.0 μM His-tagged protease, as described in the experimental section (Part 5). Compound **90** displays very weak inhibition against $3CL^{pro}$ inhibition (< 10% inhibition at 100 μM concentration). Furthermore, attachment of the recognition tripeptide to the compound **90** does not improve the inhibitory activity much (< 10% inhibition for **30** and 23% inhibition for **31** at 100 μM concentration). These results are consistent with our previous finding that the phthalhydrazide moiety is an important structural feature for this class of tetrapeptide inhibitors.

4.4. Synthesis of Target E (32)

4.4.1. Initial Synthetic Strategy for Target E (32)

The initial synthetic strategy for preparing target **E** (**32**) is described in Figure 37. Target **E** can potentially be synthesized by from the tripeptide **65** and the cyclic keto-glutamine derivative **93**, which can be prepared from the cyclic glutamic acid derivative **66**.

Figure 37 Retrosynthetic analysis of target **E** (**32**)

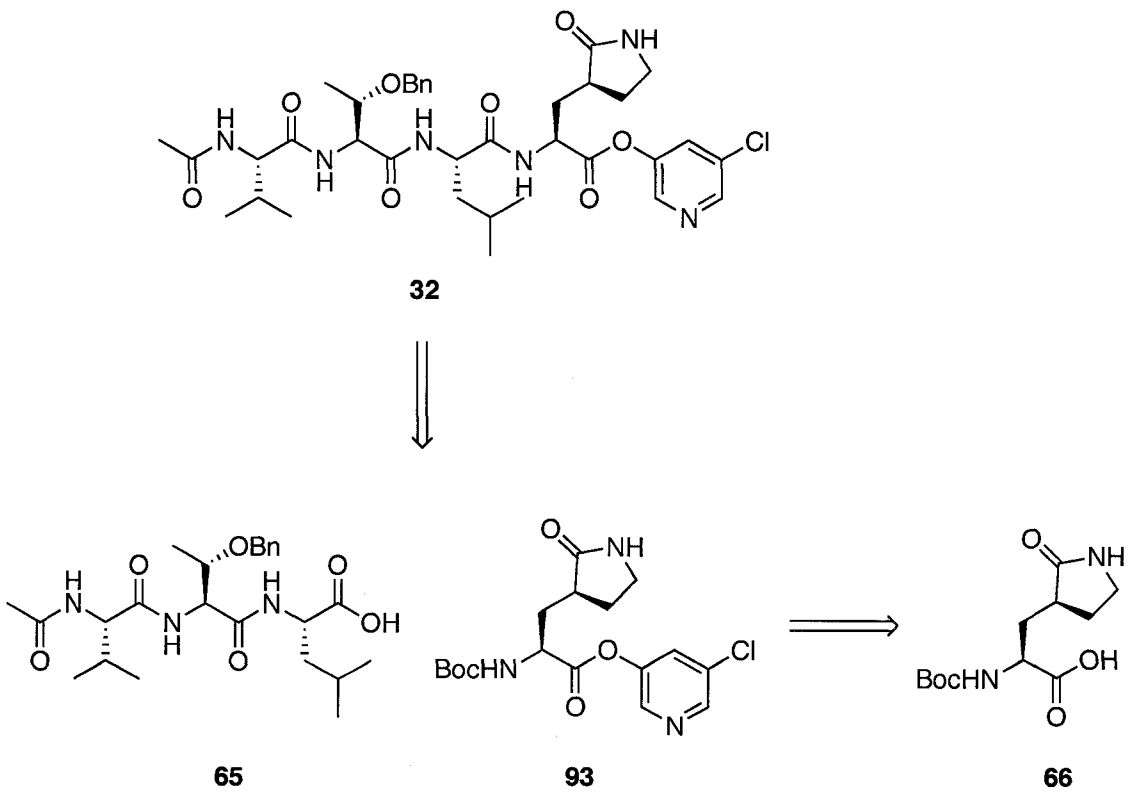

This synthetic strategy was not successful in the case of target **E** (Scheme 14). The cyclic keto-glutamine derivative **93** can be readily prepared by coupling of cyclic glutamic acid derivative **66** with 5-chloro-3-pyridinol (**94**). However, removal of the Boc group followed by coupling with tripepetide **65** does not produce the desired tetrapeptide **32**. Instead, compounds **94** and **95** were collected from HPLC purification and identified by MS and ^{1}H NMR studies (Figure 38).

Scheme 14 An unsuccessful route to the synthesis of tetrapeptide **32**

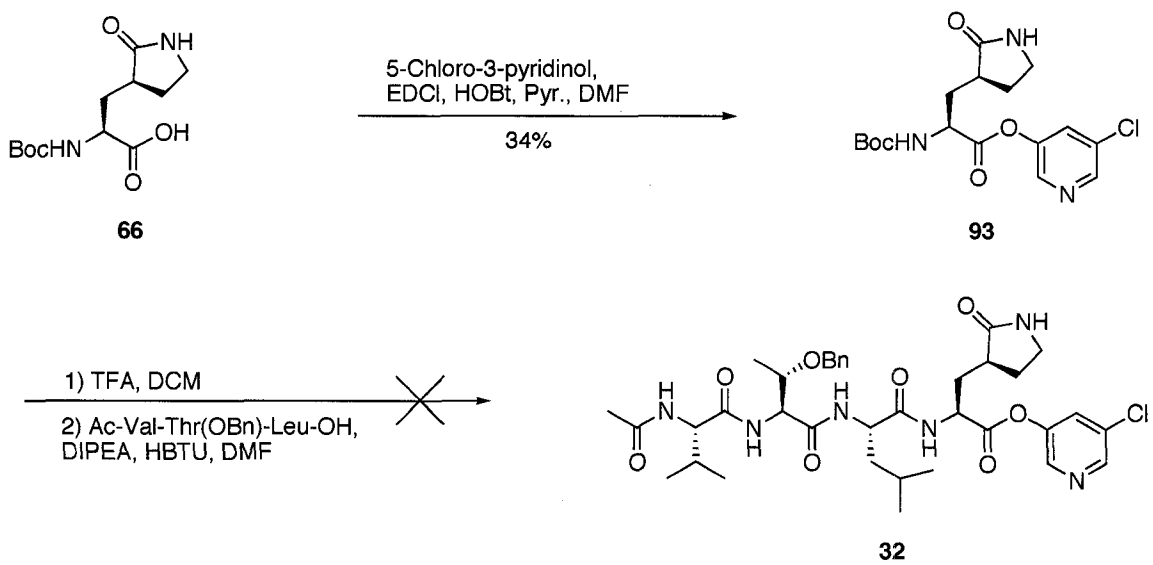

Figure 38 Structures of side products **94** and **95**

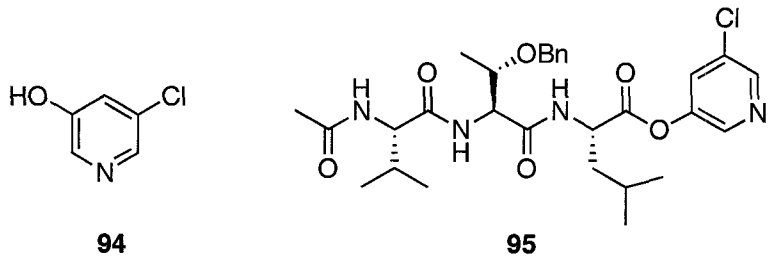

A mechanism is proposed for formation of the undesired products **94** and **95**, as shown in Figure 39. In the first step, the Boc group is removed by TFA and the amine salt **93a** forms. Salt **93a** is then deprotonated by DIPEA to generate the compound **93b** with a free amine functional group. As the pyridinyl moiety is a fairly good leaving group, intermolecular cyclization reaction with **93b** occurs to produce the thermodynamically stable dimer **93c**, and release 5-chloro-3-pyridinol (**94**) in the process. Compound **94** can react with tripeptide **65** in the standard coupling conditions to yield the undesired product **95**.

Figure 39 Proposed mechanism for formation of the undesired product **94** and **95**

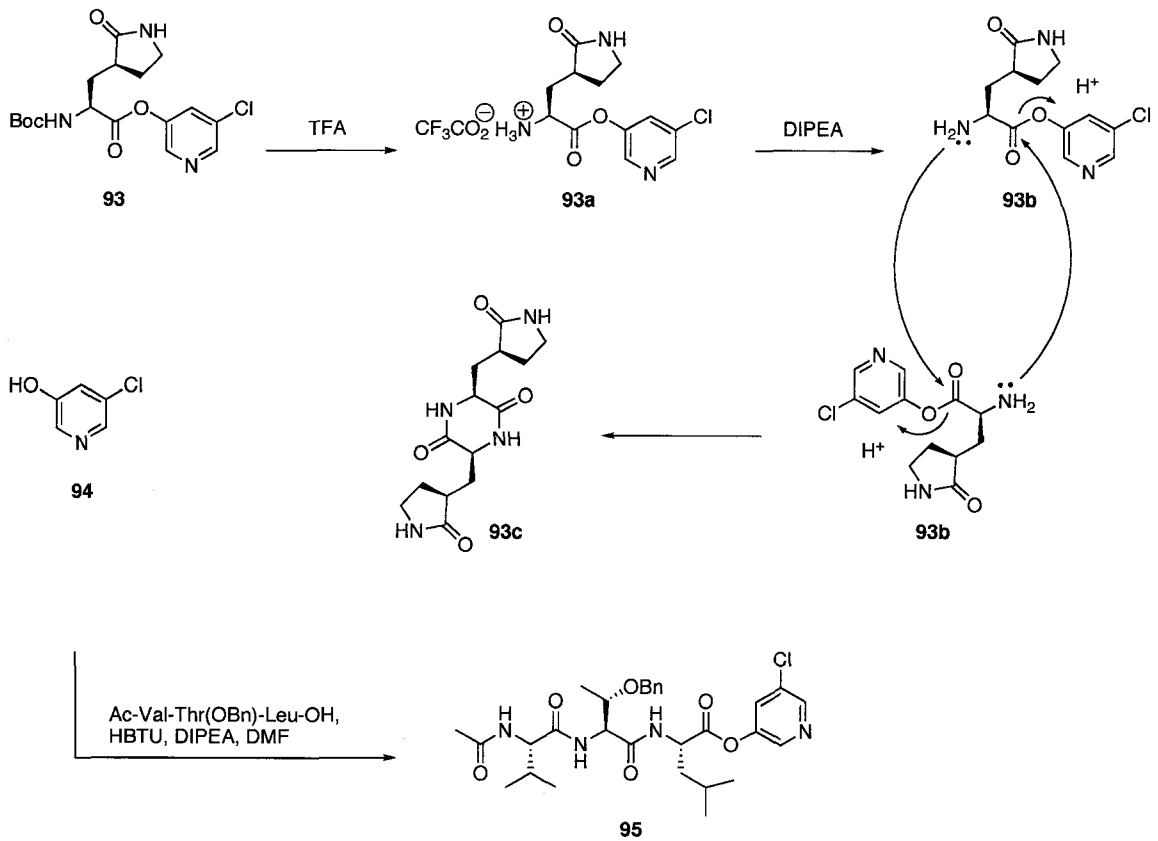

4.4.2. Alternative Strategy for Synthesis of Target E

An alternative route was designed for the synthesis of target **E** (**32**, Figure 40). In this strategy, the pyridinyl moiety is coupled to the tetrapeptide **32** in the last step, which can potentially avoid the problems caused by the relatively unstable pyridinyl ester during the synthetic process.

Figure 40 Retrosynthetic analysis of target **E** (**32**)

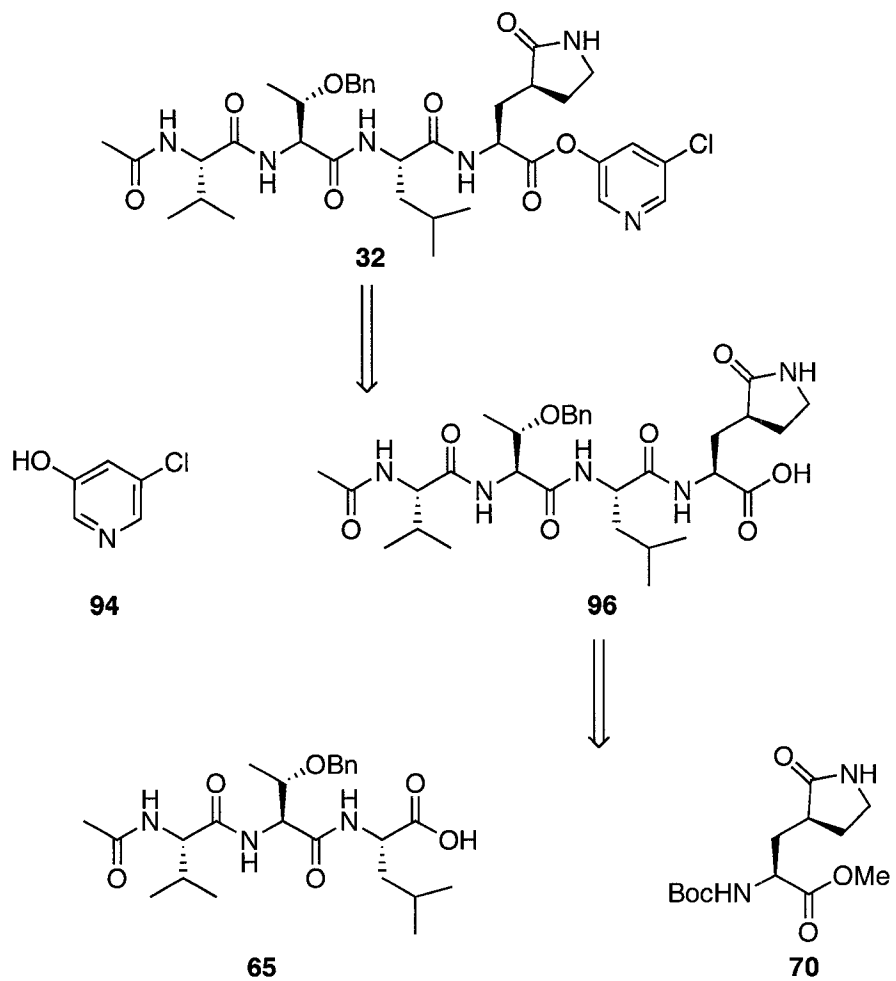

The keto-glutamine tetrapeptide **32** was prepared as described in Scheme 15. Removal of the Boc group of the cyclic methyl ester **70**, followed by coupling with tripeptide Ac-Val-Thr(OBn)-Leu-OH (**65**) provides the tetrapeptide **97** in 65% yield. Hydrolysis of the ester group of **97** yields compound **96** with a carboxylic acid functional group in quantitative yield. Coupling of **96** with 5-chloro-3-pyridinol affords the tetrapeptide **32** as a 1:1 mixture of diastereomers at the glutamine analogue α-carbon. As 5-chloro-3-pyridinol is a poor nucleophile, transient cyclization of the activated carboxyl group with the neighboring amide to an azalactone could compete with the coupling reaction, thereby leading to the observed epimerization.

Scheme 15 Synthesis of the tetrapeptide **32**

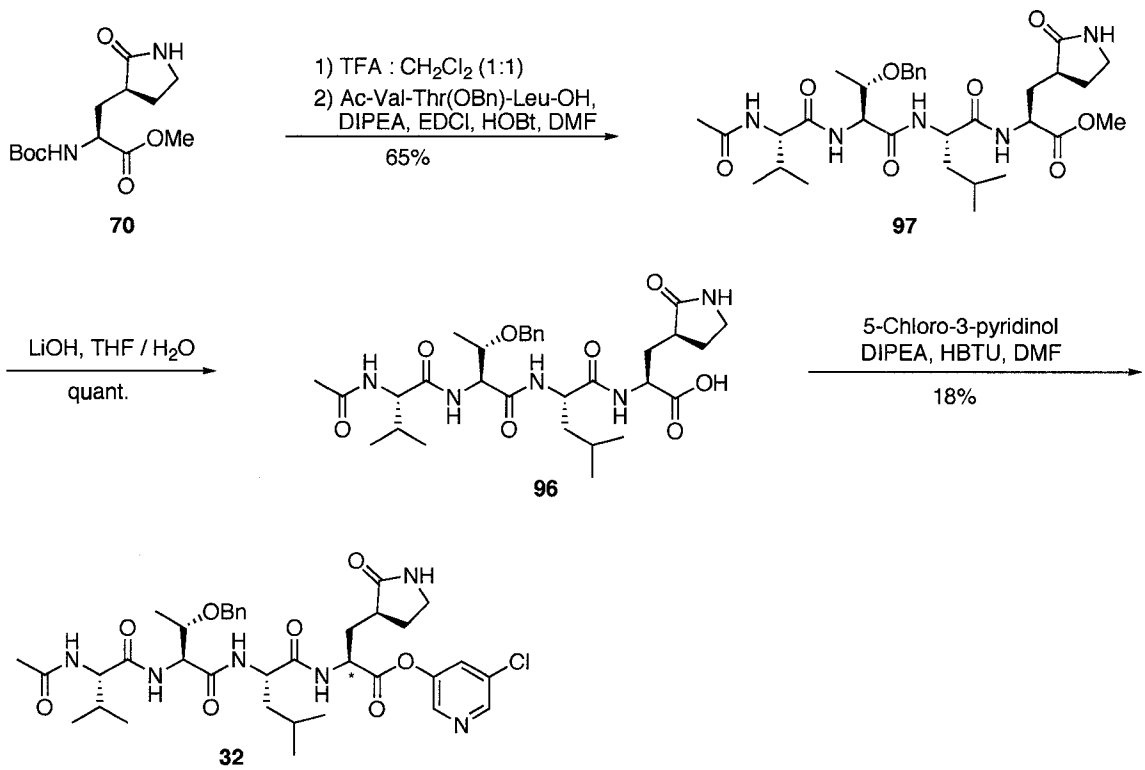

4.5. Evaluation of Target E

Compounds **93** and **32** were tested as SARS $3CL^{pro}$ inhibitors using a fluorometric assay and 1.0 μM His-tagged protease, as described in the experimental section (Part 5). Both display only very weak inhibition against $3CL^{pro}$ (< 10% inhibition at 100 μM concentration), even though **32** would be expected to be a good substrate mimic. The results further confirm that the phthalhydrazide moiety is an important structural feature for the cyclic peptidyl keto-glutamines to be good SARS $3CL^{pro}$ inhibitors.

5. Heteroaromatic Esters – Target F (33-40)

5.1. Design, Synthesis and Evaluation of Target F (33-40)

As described earlier, the heteroaromatic ester **9** is a very potent $3CL^{pro}$ inhibitor (IC_{50} = 0.5 μM) that was identified by high throughput screening of compound libraries.[34] The carbonyl of **9** is suspected to bind at the enzyme active site (*i.e.* at or near the Cys145 nucleophile), because compound **9** displays nearly the equipotent inhibition against both SARS-CoV $3CL^{pro}$ and HAV $3C^{pro}$. It is known that the two proteases can recognize similar substrates in the active site. In addition, both the thiophenyl and pyridinyl moieties are believed to play crucial roles in the strong inhibition of $3CL^{pro}$. Hence, the relatively simple structure of inhibitor **9** encouraged us to make a focused library around this motif in order to examine structure-activity relationships (Figure 41).

Figure 41 Potential structure-activity relationship (SAR) studies of inhibitor **9**

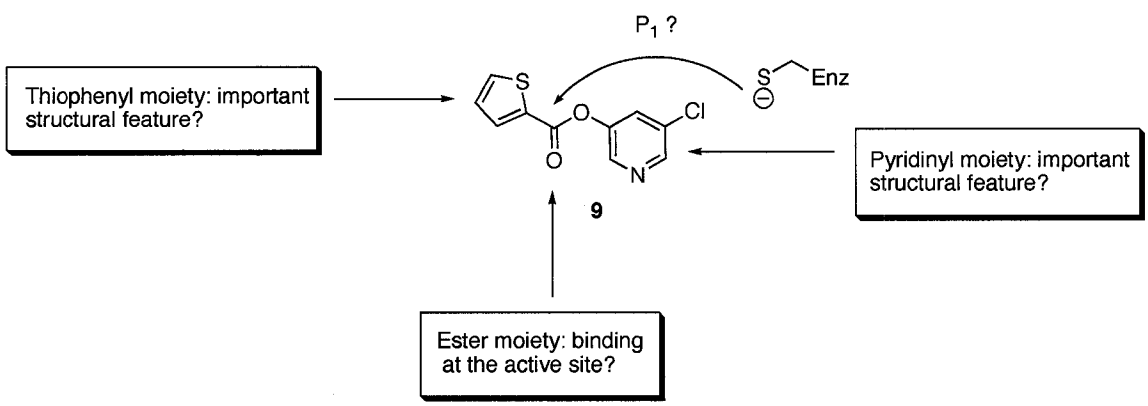

A series of 30 analogues were initially synthesized for preliminary screening (Table 2). The majority of compounds (**98-119**, **122**, **33** and **37**) were prepared by the coupling reaction between the acetyl chlorides derived from commercially available carboxylic acids, and pyridinyl alcohols or amines (Scheme 16). Synthesis of the analogues **120** (Scheme 17), **121** (Scheme 18), **123** (Scheme 19), **34** (Scheme 20), **46** (Scheme 21) are shown below.

Scheme 16 Synthesis of the pyridinyl esters and amides **98-119**, **122**, **33**, **37**

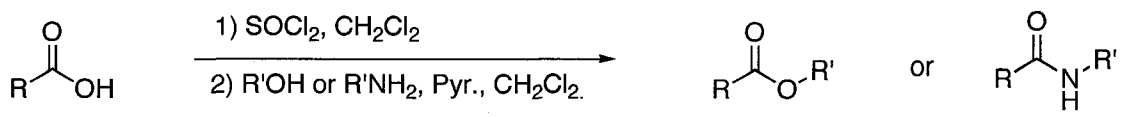

Scheme 17 Synthesis of the ether **120**

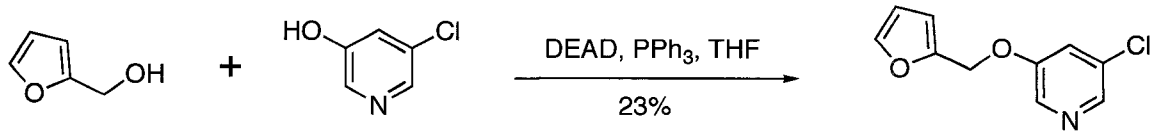

120

Scheme 18 Synthesis of the ester **121**

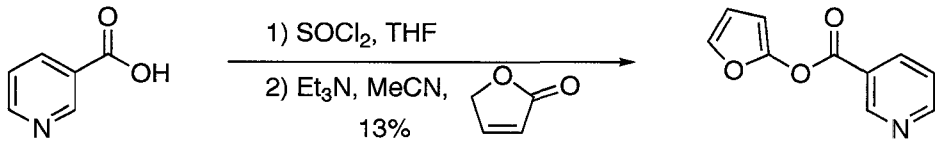

121

Scheme 19 Synthesis of the sulfonamide **123**

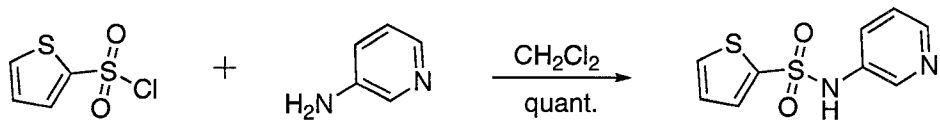

123

Scheme 20 Synthesis of the pyridinyl ester **34**

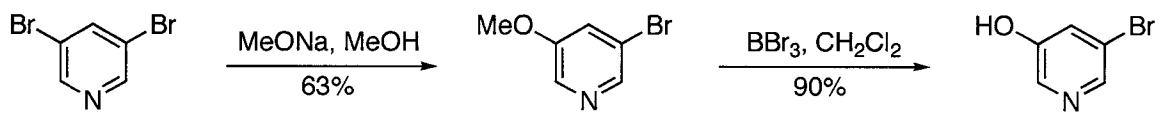

34a **34b** **34c**

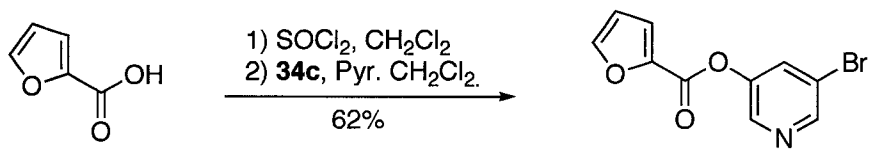

34

Scheme 21 Synthesis of the ketone **46**

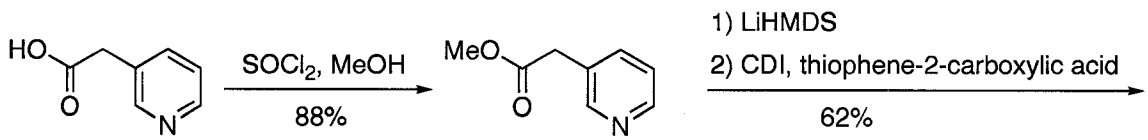

46a **46b**

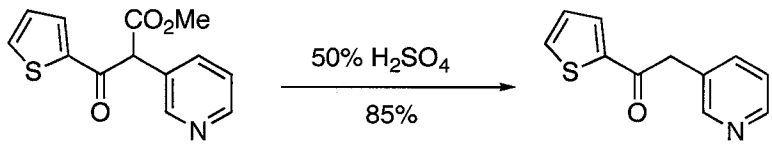

46c **46**

The 30 analogues were tested against $3CL^{pro}$ using the continuous fluorometric assay, as described in the experimental section. The results, which examine only the initial binding, are outlined in Table 2. Due to self-quenching of fluorescence at high substrate concentrations, low concentrations of fluorogenic peptide and consequently low overall conversions (*i.e.* short times) were used. Compared to the ester analogues, the amides (*e.g.* **101**) show almost no inhibition at 100 μM concentration under these conditions. In addition, when the ester groups are at the *ortho* or *para* positions, instead of the *meta* positions, of the pyridinyl rings (*e.g.* **98**, **100**, **109**), poor or no inhibition is observed. Furthermore, if the chlorine substituent is at the 2 or 6 position (*i.e.* **111**, **112**), instead of the 3 position (*i.e.* **9**) of the pyridinyl ring, the inhibition decreases dramatically. However, the analogue with a hydrogen (*i.e.* **99**) instead of a chlorine substituent at the 3 position still displays reasonably good inhibition. From the analysis of compounds (**9**, **99**, **115**, **116**, **117**, **33**, **37**) with moderate to good inhibition, it appears that in addition to the pyridinyl ring, the other aromatic ring (furan or thiophene) is also a key structural feature for potent inhibition. Compound **34** with a bromine substituent at the *meta* position of the pyridinyl ring shows very potent inhibition (98%) against $3CL^{pro}$ even at 1 μM concentration.

Compared to compounds **99** and **34**, the analogues **122** and **118** with one extra carbon inserted between the pyridinyl rings and the oxygen atom exhibit much weaker inhibition. In addition, the amide analogue **102**, the ether **120**, the sulfonamide **123** and the ketone **46** show almost no activity against the enzyme. Compound **121** with a reversed ester linkage also shows decreased inhibition against $3CL^{pro}$ at 100 μM.

Table 2. Preliminary evaluation of selected analogues as SARS 3CL^{pro} inhibitors

Compd No	Structure	% [a]	Compd No	Structure	% [a]
98	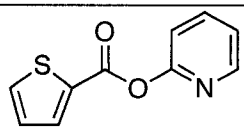	13	**113**	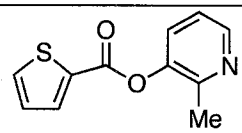	-
99	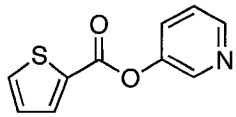	91	**114**	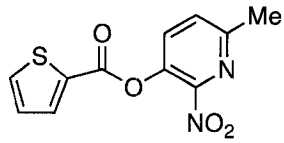	15
100	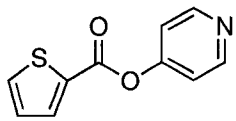	-	**115**	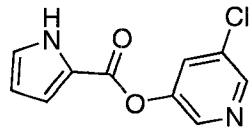	65
101	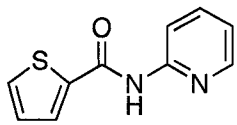	-	**116**	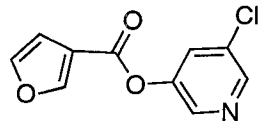	89
102	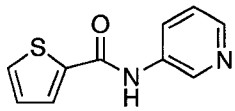	13	**117**	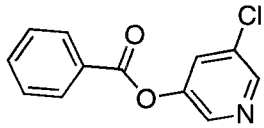	92
103	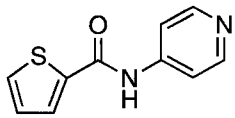	-	**118**	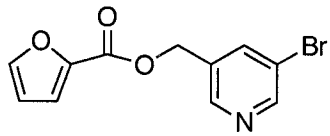	90
104	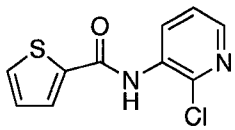	-	**119**	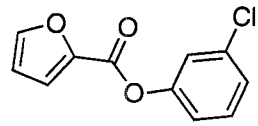	40
105	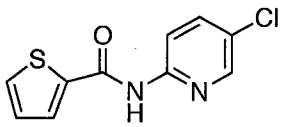	-	**120**	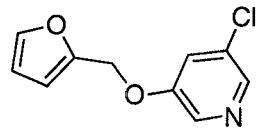	11
106	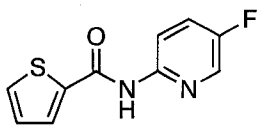	-	**121**	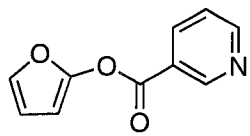	80
107	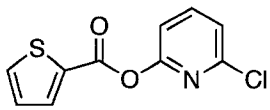	-	**122**	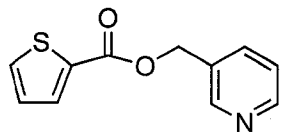	19
108	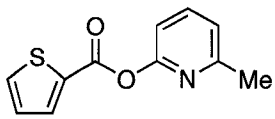	38	**123**	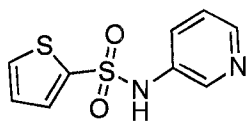	-

109	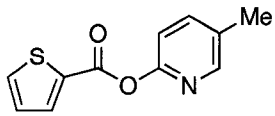	-	**33**	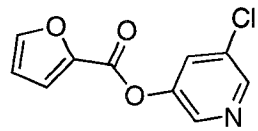	99
110	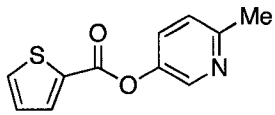	-	**34**	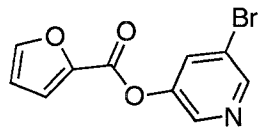	99
111	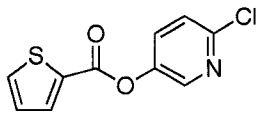	13	**37**	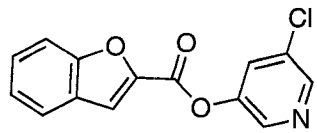	94
112	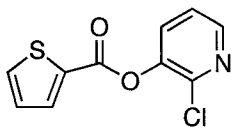	20	**46**	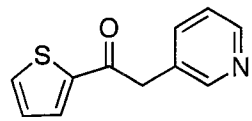	-

a: percentage inhibition at 100 μM; Dash represents < 10% inhibition.

Based on the above screening results, a library of pyridinyl esters were prepared through parallel synthesis, by the coupling reactions (Method **A** or **B**, Scheme 22) between 5-chloro-3-pyridinol and 90 commercially available carboxylic acids, most of which are aromatic carboxylic acids (Figure 42). Of the 90 targets, 18 compounds are relatively unstable to aqueous conditions and were not examined further, but 72 compounds were obtained and purified by automated HPLC-MS analysis. This purification was done by Dr. Eric Pelletier using the Chemistry Department's automated HPLC-MS facility supervised by Professor Dennis Hall. To evaluate the quality of this library of compounds purified by HPLC-MS, a random example (**124**) was picked and then analyzed by comparing the HPLC chromatograms and ^{1}H NMR spectra (Figure 43 and 44, respectively) before and after the purification. The testing results indicate that the sample **124** after HPLC-MS purification has a high purity.

Scheme 22 Synthesis of a library of 3-chloropyridinyl esters by method **A** or **B**

Method **A**:

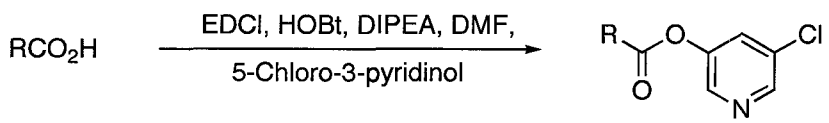

Method **B**:

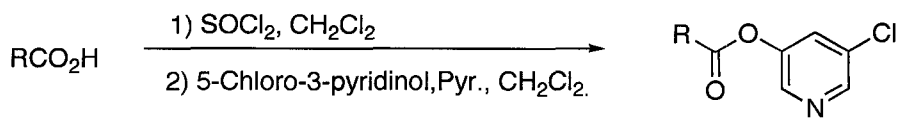

Figure 42 A library of 90 carboxylic acids in the parallel synthesis

Part A: Pyridinyl esters are obtained for the following 72 carboxylic acids

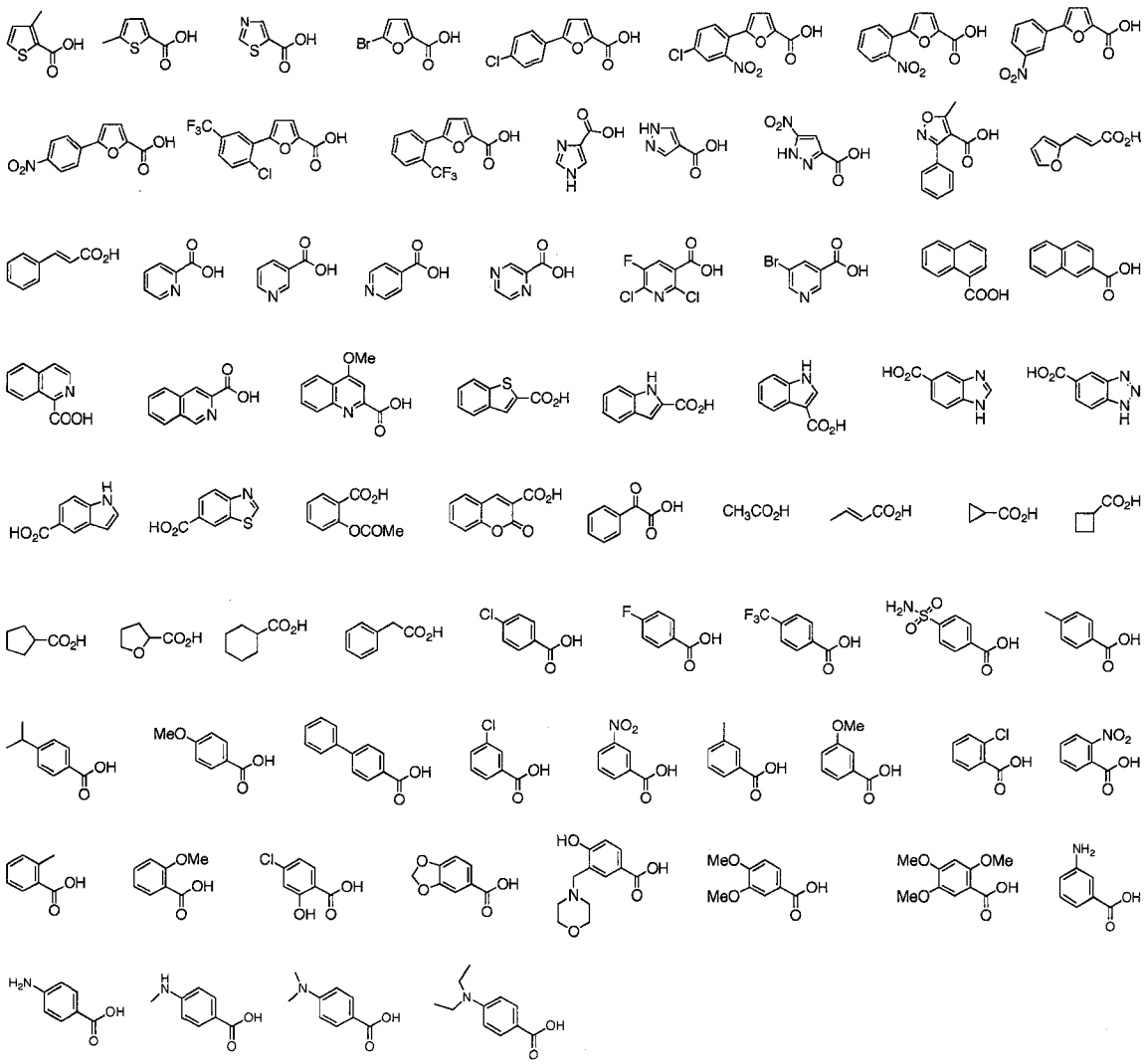

Part B: Pyridinyl esters are not obtained for the following 18 carboxylic acids

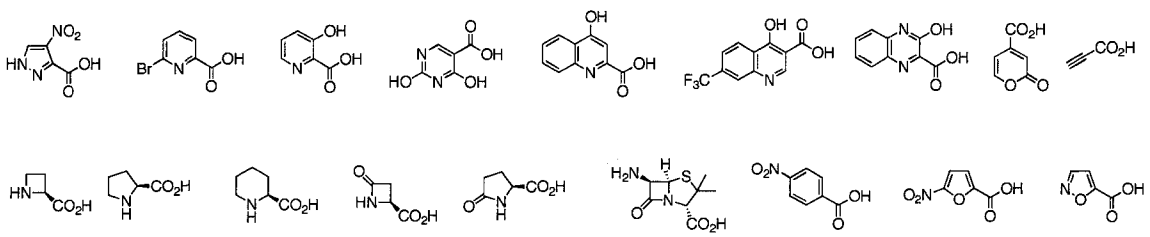

Figure 43 HPLC chromatograms of the crude reaction mixture of **124** (A, Figure 43) and the purified product of **124** (B, Figure 43) by HPLC-MS

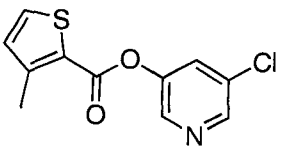

124

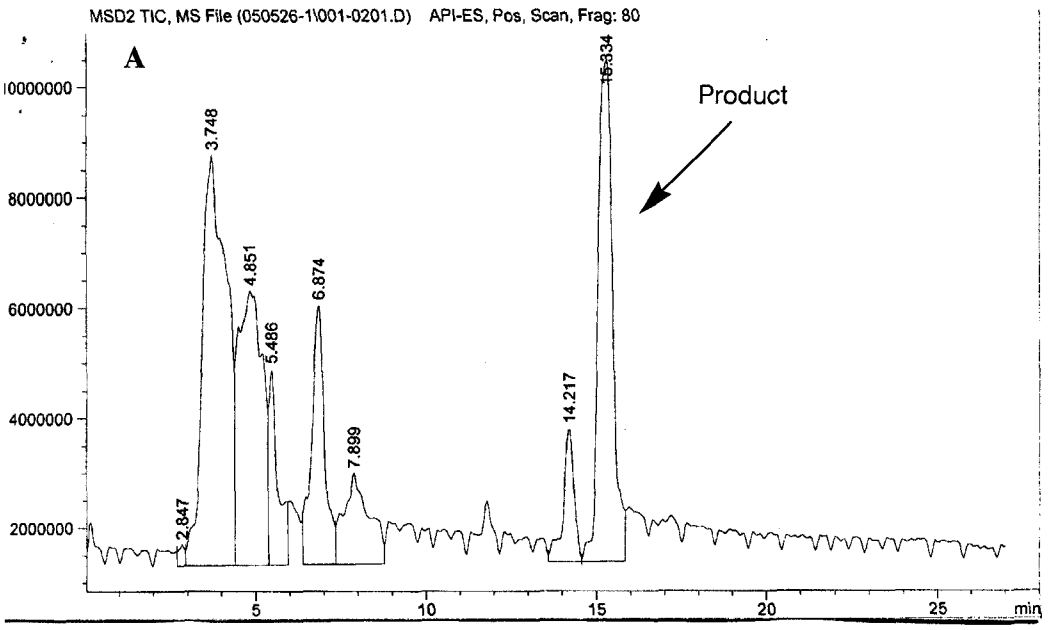

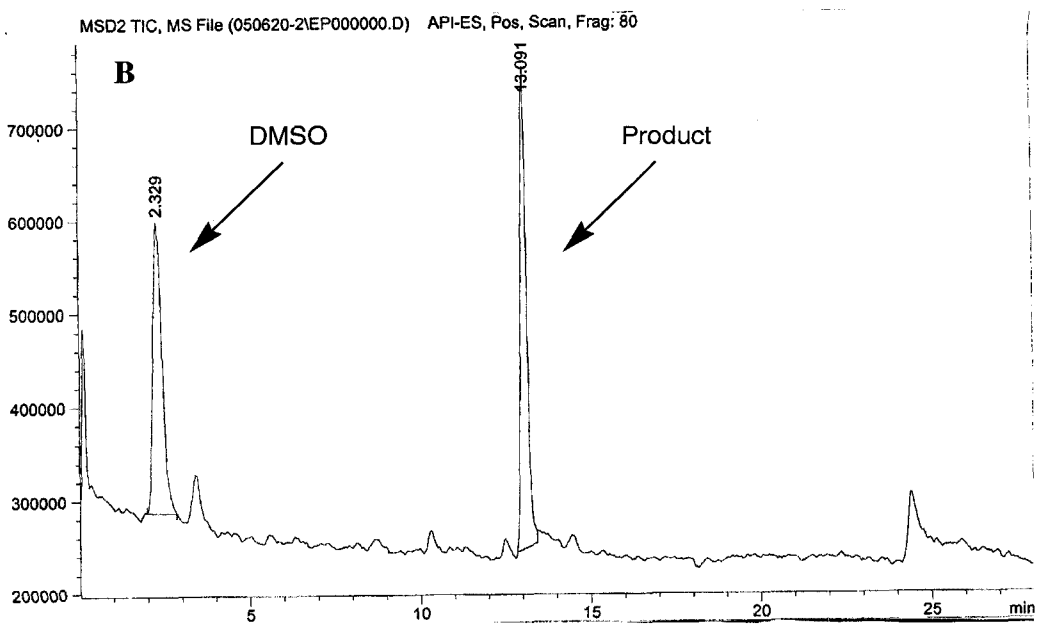

Figure 44 ^{1}H NMR spectra of the crude reaction mixture of **124** (A, Figure 44) and the purified product of **124** (B, Figure 44) by HPLC-MS

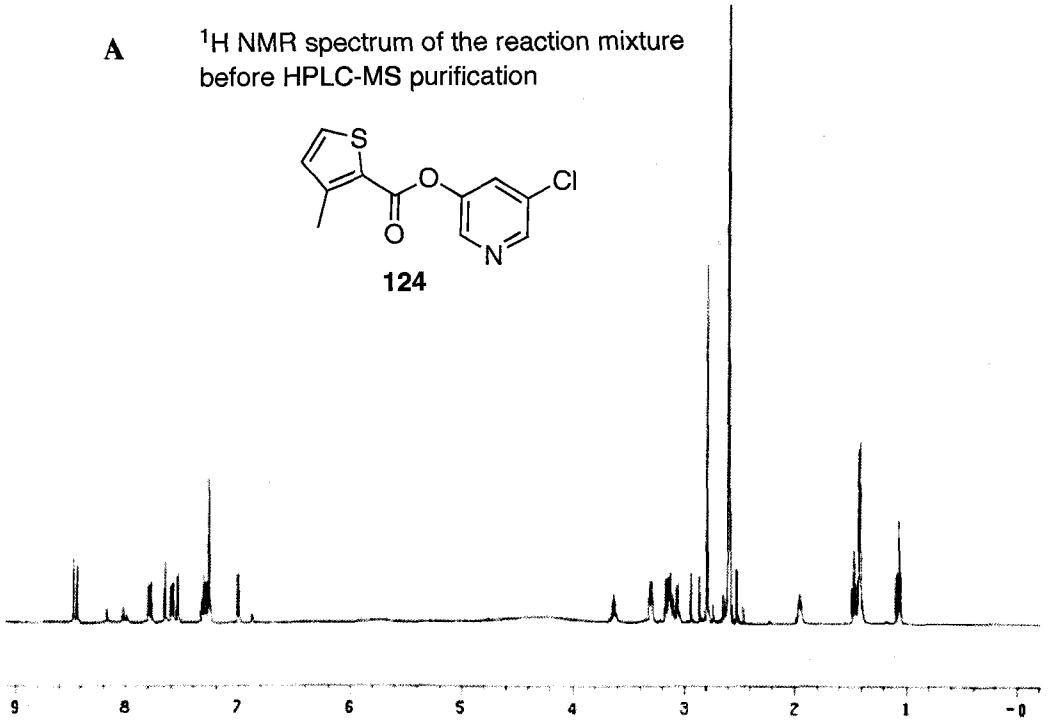

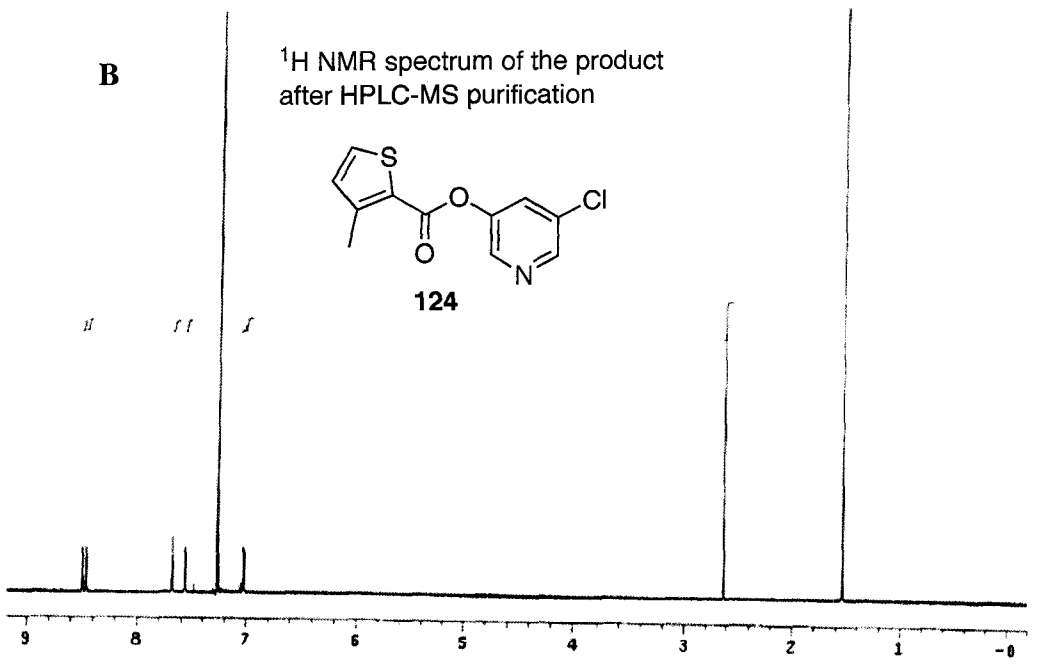

This library of 3-chloropyridinyl esters was tested against 0.4 μM SARS $3CL^{pro}$ using the continuous fluorometric assay. Compounds **35-36** and **38-40** show almost complete inhibition of $3CL^{pro}$ at 1 μM concentration (Figure 45).

Figure 45. SARS $3CL^{pro}$ inhibitors **35-36, 38-40**

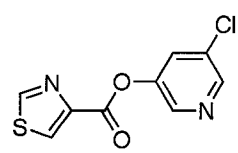

35, 98% inhibition at 1 μM

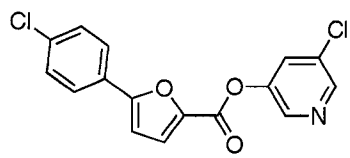

36, 98% inhibition at 1 μM

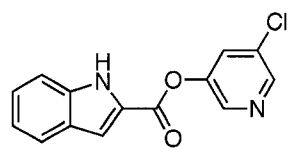

38, 99% inhibition at 1 μM

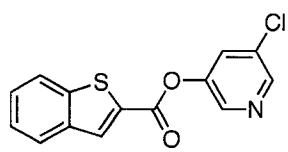

39, 96% inhibition at 1 μM

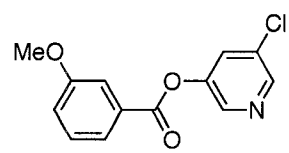

40, 97% inhibition at 1 μM

The activities of selected pyridinyl esters were further investigated using a non-His-tagged protease, which is more stable and has higher activity in the assay. Under the assay conditions, all of the esters are reasonably stable to non-enzymatic hydrolysis as studied by ^1H NMR, and some are extremely potent inhibitors of $3CL^{pro}$, as summarized in Table 3. For example, in an assay containing 100 nM enzyme, compound **34** has an IC_{50} of 50 nM. This corresponds to the lowest IC_{50} theoretically measurable in the assay and, to our knowledge, is one of the lowest IC_{50}'s reported for the SARS $3CL^{pro}$. Further kinetic studies have determined a few kinetic parameters of inhibitor **34**: K_m of 26×10^{-9} M, K_{cat} of 17×10^{-5} s^{-1} and K_{cat}/K_m of 6.5×10^3 M^{-1} s^{-1} (done by Ms. Carly Huitema). Indeed, pyridinyl ester **34** is such an effective inhibitor of $3CL^{pro}$, that it is not possible to

measure k_{inact} and K_i, even in the presence of the fluorogenic substrate. Mixing the enzyme and the inhibitor in a 1:1 molar ratio completely inactivated the enzyme within the dead-time of the assay (~6 s). However, the activity of $3CL^{pro}$ recovered with a $t_{1/2}$ ~4 min. This behavior is consistent with inactivation of the enzyme through rapid acylation of the enzyme by the inhibitor, followed by its reactivation through slow deacylation.

Table 3. Evaluation of pyridinyl esters as SARS $3CL^{pro}$ inhibitors

Compound No	Structure	IC_{50} (nM)	$T_{1/2}$ (h)[a]
33	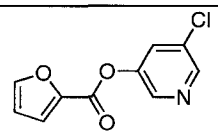	60	12
34	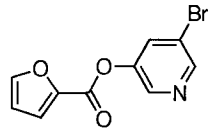	50	119
35	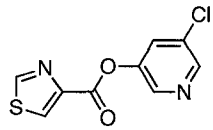	270	125
36	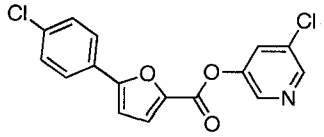	63	41
37	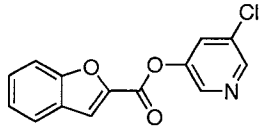	170	28
38	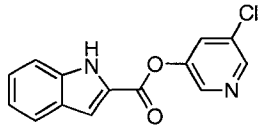	65	42
39	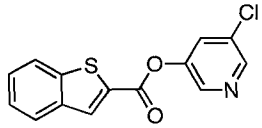	95	32
40	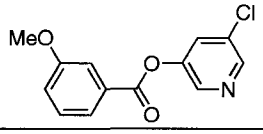	340	53

[a]Half-life for hydrolysis at pH 7.5 in phosphate buffer (no enzyme).

5.2. Inhibition Mechanism Studies of Target F

The inhibition mechanism was also investigated by electrospray mass spectrometry. As shown in Figure 42, the mass of the wild type enzyme is 33,846 Da (A, Figure 46) and the mass of the complex of enzyme and inhibitor **34** is 33,939 Da (B, Figure 46, expected mass 33,940 = 33,845 + 95 Da, ±1 Da). This indicates covalent bond formation via acylation of the enzyme by the furoyl group (MW 95) of inhibitor **34** with departure of the 3-bromo-5-hydroxypyridine leaving group as the likely mechanism of inhibition (Figure 47). The electrospray mass spectra of the complexes of inhibitors **33**, **38** and **40** with the enzyme (Figure 48) have also confirmed an analogous acylation mechanism for these 3-chloropyridinyl esters.

Figure 46 ESI-MS of wild type SARS $3CL^{pro}$ (A, M^+ = 33,846 Da) and mass spectrum of the complex of $3CL^{pro}$ and inhibitor **34** (B, M^+ = 33,939 Da)

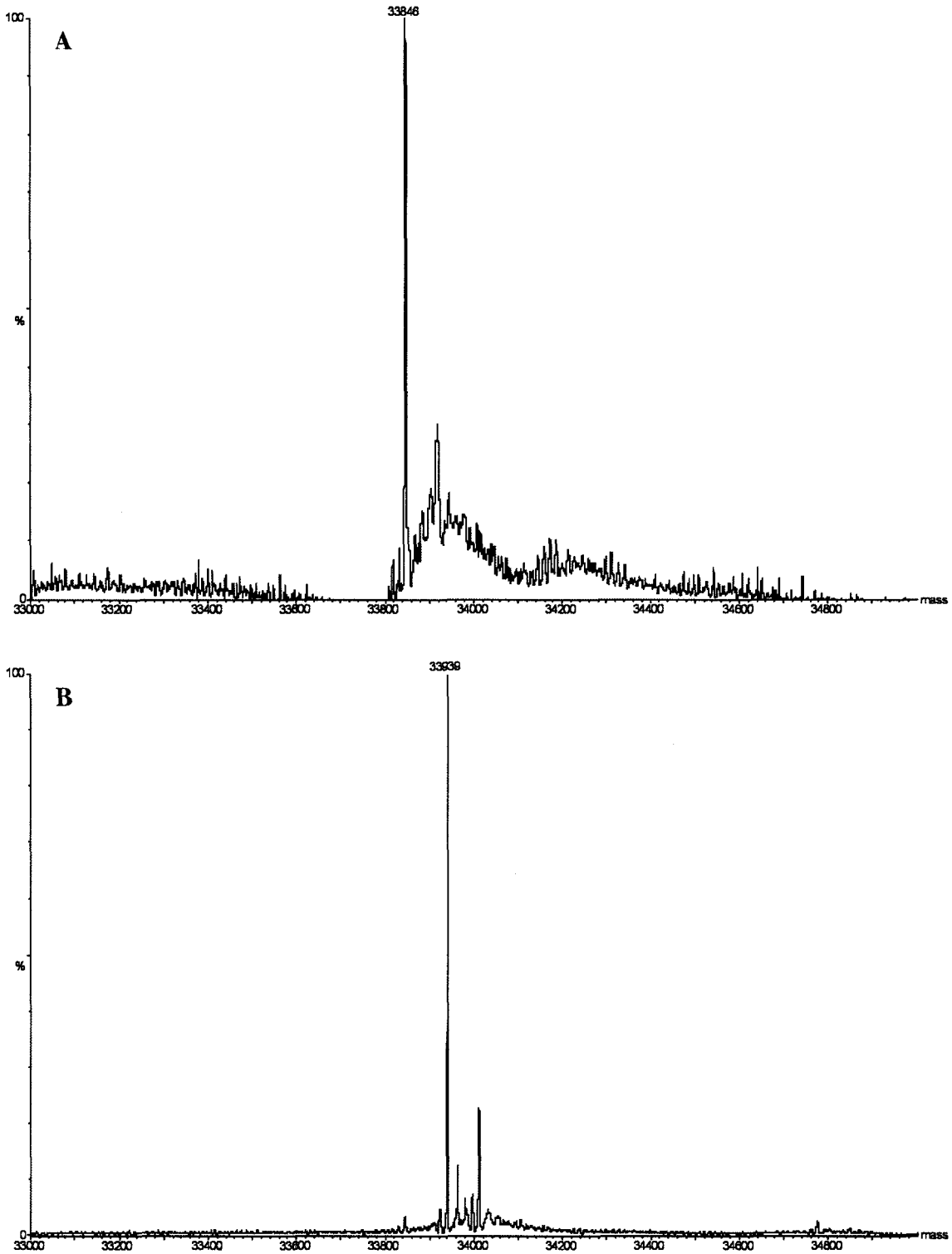

Figure 47 Proposed mechanism of inhibition of SARS 3CL^{pro} by pyridinyl ester inhibitors

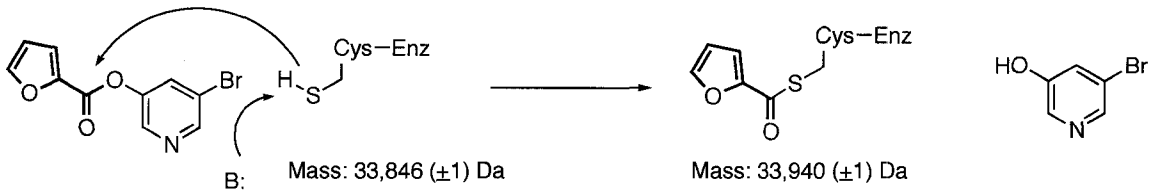

Figure 48 ESI-MS of the complexes of 3CL^{pro} and inhibitors **33** (A, Figure 48), **38** (B, Figure 48), **40** (C, Figure 48)

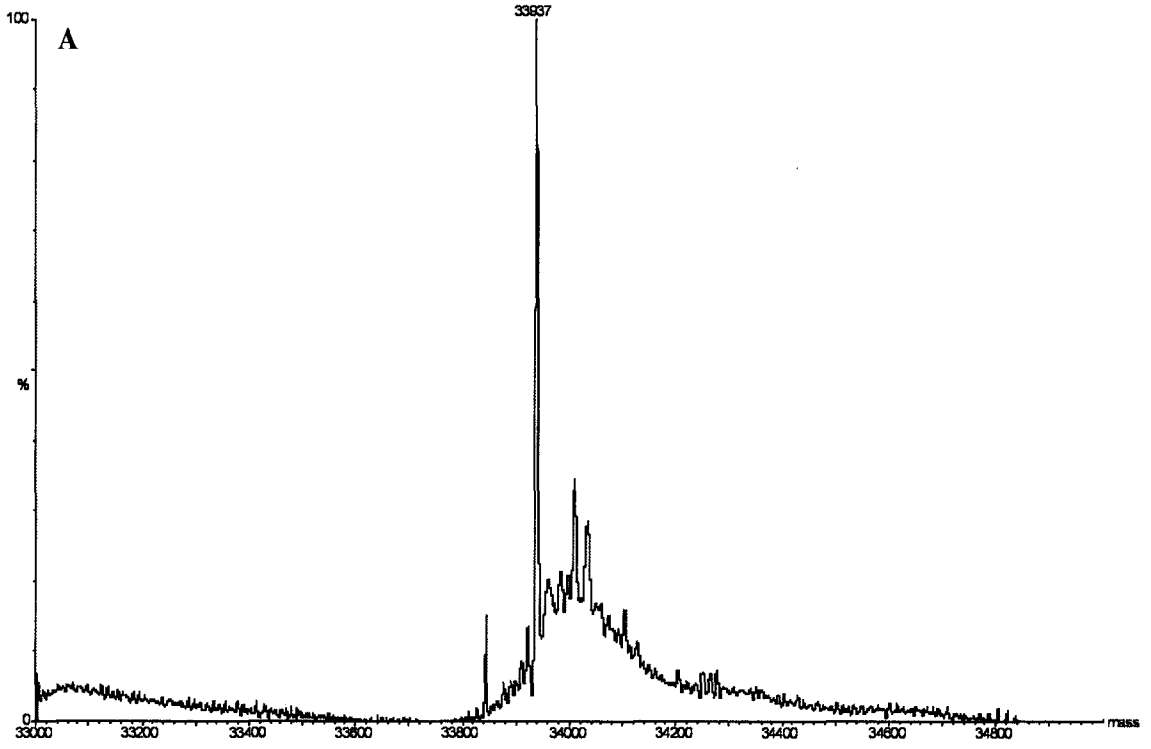

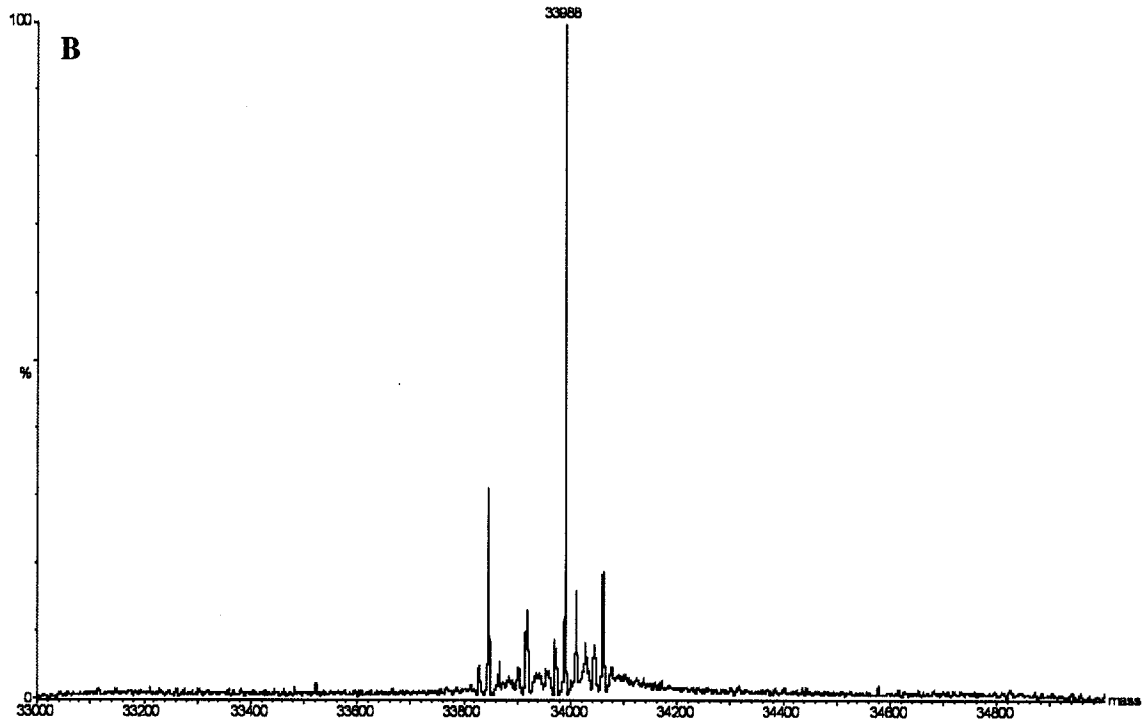

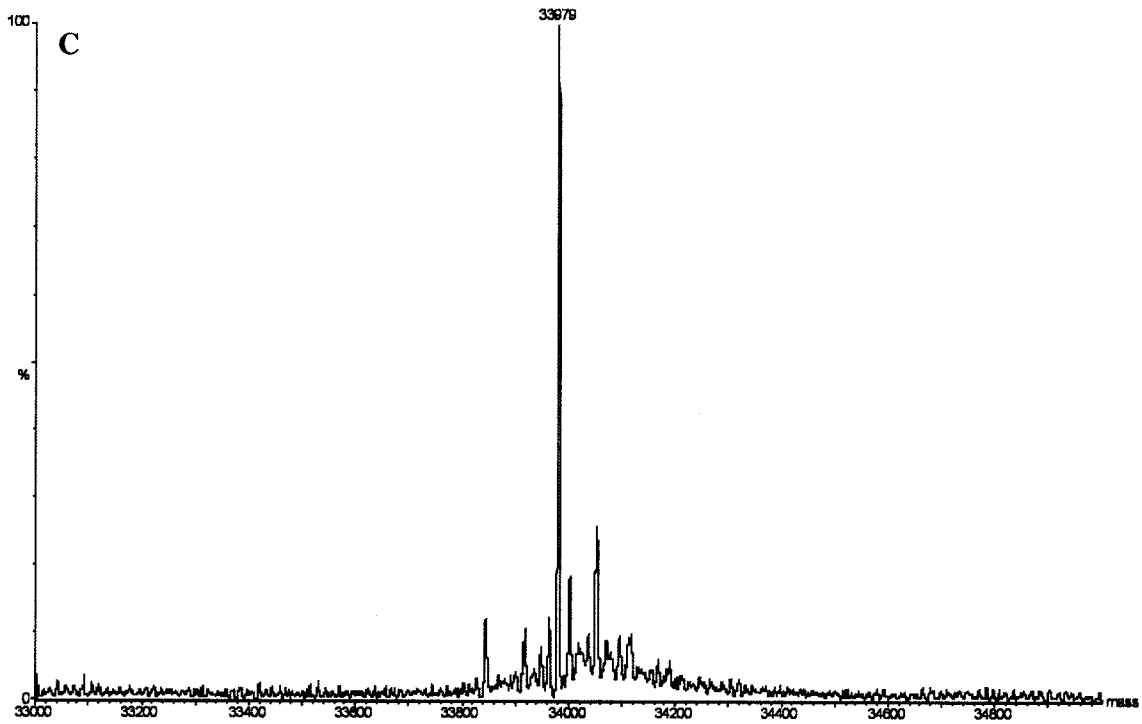

5.3. Modeling Studies of Target F

Modeling studies (Figure 49) of $3CL^{pro}$ with inhibitors **34** and **40** were conducted as described in the experimental section (Part 8), by Dr. Chunying Niu in Prof. Michael James' group at the Department of Biochemistry, University of Alberta. Inhibitors **34** and **40** are modeled into the active site of SARS $3CL^{pro}$ (PDB code: 2A5K)[49a] using the program Autodock 3.0.5 (Figure 49).[73]

Figure 49 The modeling binding conformations of inhibitors **34** and **40** in the active site of SARS $3CL^{pro}$. Inhibitor **34** (yellow) and **40** (white) are shown in the stick mode (oxygen atoms are red; nitrogen atoms are blue; chlorine is green; bromine is orange). The color of the enzyme surface shows the cavity depth from the outside of the protein (blue) to the inside of the protein (yellow) (done by Dr. Chunying Niu).

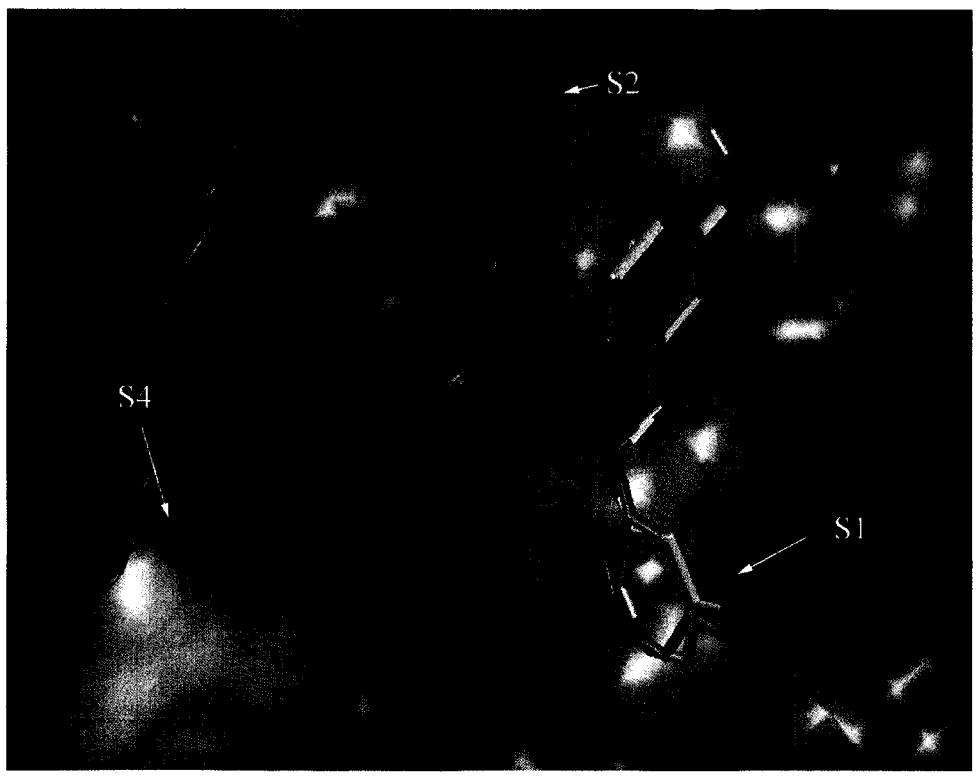

The general trends of the predicted conformations follow the "Cys-S1" binding mode described for a group of compounds having a similar basic design. The halopyridine moieties fit comfortably in the S1 substrate-binding site, where the majority of the interactions with the enzyme are contributed by van der Waals contacts between the pyridine function and the two "walls" of the S1 pocket comprising of residues Phe140, Leu141, Asn142, and residues Glu166, His172, respectively. The halogen atom in either inhibitor does not interact significantly with the enzyme and points out towards the solvent. The pyridine nitrogen atom of inhibitor **34** forms a hydrogen bond with $N^{\varepsilon 2}$ of His163, the P1 specificity-determining residue. The carbonyl oxygen of the central ester function is directed into the oxyanion hole and receives hydrogen bonds from O^{γ} of Ser144 and the main chain N atoms of Gly143, and Cys145. The furan function in inhibitor **34** and anisole function in inhibitor **40** are located near the catalytic residue Cys145, forming mainly hydrophobic contacts. Because the S1 pocket is crucial to substrate recognition, the presence of the halopyridine function in the S1 subsite would effectively block the entry of peptidyl substrates.

Proteases are also known to hydrolyze ester substrates. The inhibition mechanism of the ester-based inhibitors described in this study likely involves covalent attachment of the inhibitors (at the carbonyl carbon) to the nucleophilic sulfur of Cys145. While the central ester bonds of these inhibitors provides the main interaction with the catalytic Cys145, the initial binding of the intact inhibitors into the active site of $3CL^{pro}$ (Figure 49) may critically depend on the derived pyridine moieties as well as the functional groups on the acid side of the ester bond. The docking results indicate that the halopyridine groups of

these inhibitors have a strong propensity to bind inside the S1 pocket of the $3CL^{pro}$ substrate-binding site. In addition, modification on either side of the central ester bond could affect the electrophilicity of the carbonyl function, which in turn, may modify the reactivity of inhibitors to SARS $3CL^{pro}$. The biochemical data presented in this study should be viewed as the consequence of combined effects of inhibitor binding affinity and chemical reactivity with the enzyme.

6. Heteroaromatic Aldehydes – Target G (41-45)

Based on the testing results described earlier for target F (**33-40**), it seems that for this class of pyridinyl esters, both non-covalent protein-inhibitor interactions as well as inherent chemical reactivity (*i.e.* propensity for enzyme acylation) may play important roles in the strong inhibition of $3CL^{pro}$. It is well known that compared to the esters, aldehydes are chemically more reactive towards nucleophiles and are potentially good inhibitors for cysteine enzymes through formation of hemithioacetals.[66] Hence, several aldehydes having part of the structural motif of the most effective inhibitors were designed and synthesized (Figure 50).

Figure 50 Aldehydes as potential SARS $3CL^{pro}$ inhibitors

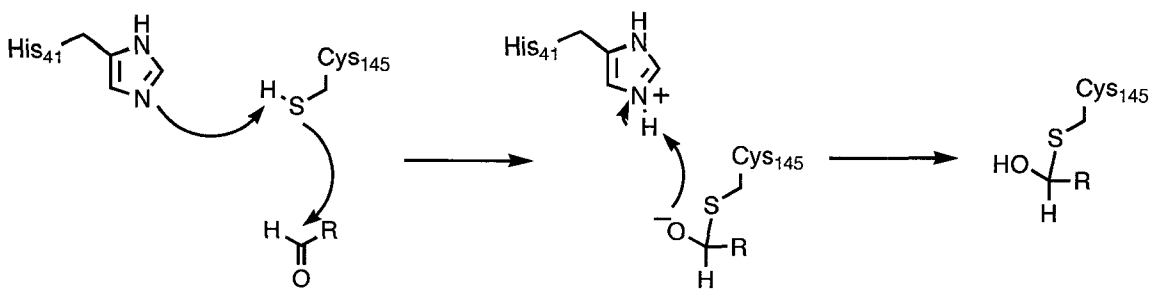

Aldehydes **41-42** are commercially available material, and no synthetic efforts were required for them. Aldehydes **43-45** are prepared using the method described in Scheme 23. Standard coupling of the commercially available carboxylic acids **43-45a** with Weinreb amine[72] generates the amides **43-45b** in 53-79% yields. Reduction of Weinreb amide **43-45b** by $LiAlH_4$ provides the corresponding aldehydes in 9-68% yields.

Scheme 23 Synthesis of aldehydes **43-45**

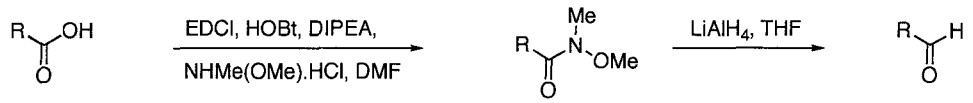

43a: R = thiazole
44a: R = 4-chlorophenylfuran
45a: R = indole

43b: R = thiazole, 70%
44b: R = 4-chlorophenylfuran, 53%
45b: R = indole, 68%

43: R = thiazole, 46%
44: R = 4-chlorophenylfuran, 68%
45: R = indole, 9%

The aldehydes **41-45** were tested against $3CL^{pro}$ using the continuous fluorometric assay, as described in the experimental section (Part 5). However, none of these aldehydes show very potent inhibition against $3CL^{pro}$, which suggests that both the 3-chloropyridinol unit and the other aromatic ring play important roles in strong binding to the enzyme (Table 4).

Table 4. Evaluation of aldehydes **41-45** as SARS $3CL^{pro}$ inhibitors

Compound No	Structure	% Inhibition at 100 μM
41	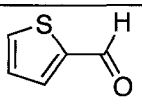	-
42	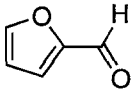	23
43	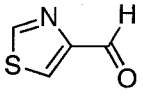	36
44	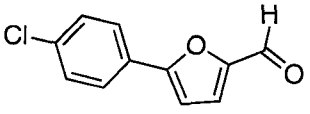	70
45	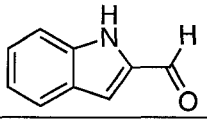	39

Dash represents < 10% inhibition.

7. Methylene Ketones and Fluorinated Methylene Ketones – Target H (46-62)

7.1. Design of Target H (46-62)

In our previous studies, we demonstrated a series of pyridinyl esters as very potent covalent inhibitors of $3CL^{pro}$ with IC_{50} values in the low nanomolar range (Target F, Section 5). Structure-activity relationships indicate that both chemical structure and chemical reactivity play very important roles in the strong inhibition of $3CL^{pro}$. To develop stable and non-covalent inhibitors based on these pyridinyl esters, the ketone **46** was initially investigated as a potential SARS-CoV $3CL^{pro}$ inhibitor. Disappointingly, compared to the pyridinyl ester **99** (91% inhibition at 100 μM concentration, IC_{50} = 7.9 μM), the ketone analogue **46** displays no inhibition at 100 μM concentration. Hence, we decided to examine the fluorinated ketones further; the fluorinated ketones possess the combined features of chemical structures that fit the enzyme active site and an electrophilic carbonyl group (Figure 51). Compared to the corresponding pyridinyl esters, the fluorinated ketones appeared to be more stable and avoid the potential hydrolysis problem that leads to the reactivation of the enzyme. Furthermore, the difluoromethylene moiety is proposed as a mimic of an oxygen atom in biological systems.[67]

Figure 51 Rational design of target **H** based on pyridinyl esters

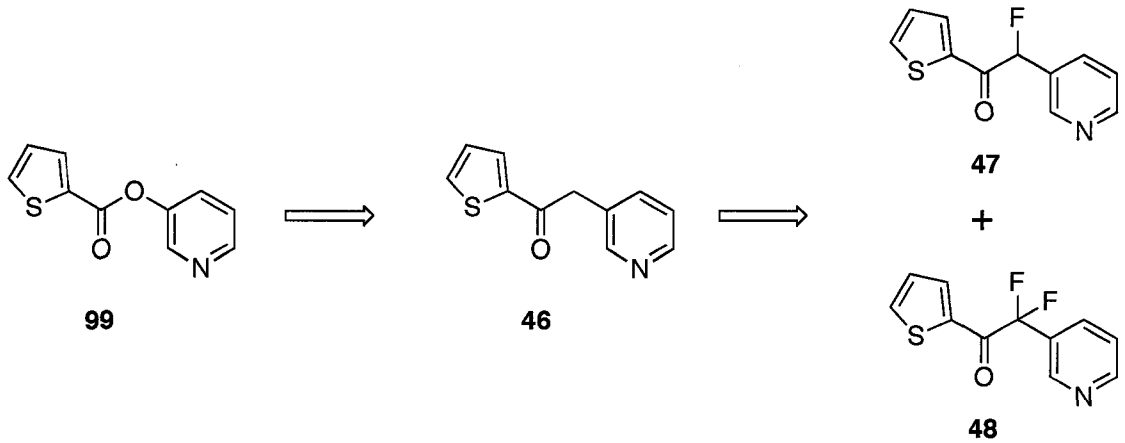

7.2. Synthesis and Evaluation of Target H (46-62)

We started the investigation from fluorinated methylene ketone analogues **47** and **48**, which were prepared as shown in Scheme 24. Deprotonation of the ketone **46** with 1.05 equivalent of LiHMDS, followed by fluorination with 1.1 equivalent of *N*-fluorobenzenesulfonimide (NFSi), provides both the monofluoromethylene ketone **47** and the difluoromethylene ketone **48** in 63% and 6% yields, respectively.

Scheme 24 Synthesis of fluorinated methylene ketones **47** and **48**

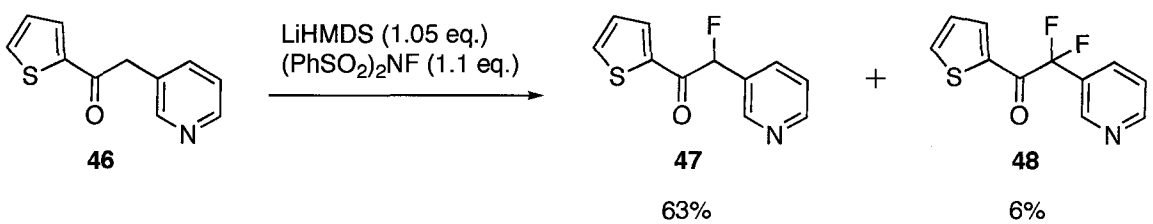

Compounds **47** and **48** were tested against SARS $3CL^{pro}$ using a continuous fluorometric assay, as described in the experimental section. The monofluoromethylene ketone **47** shows weak inhibition against $3CL^{pro}$ (10% at 100 μM concentration), and no improved inhibition was observed after 2 h incubation with the $3CL^{pro}$. However, the difluoromethylene ketone **48** displays stronger inhibition against $3CL^{pro}$ (38% at 100 μM concentration). After incubation of **48** with the $3CL^{pro}$ for 2 h, no improved inhibitory activity was observed. These results suggest that the fluorinated ketones **47** and **48** are non-covalent and reversible inhibitors for SARS $3CL^{pro}$. Interestingly, fluorination leads to substantial improvement in the inhibitory activity against the $3CL^{pro}$. The difluoromethylene ketone **48** (38% inhibition at 100 μM) appears to be a reasonable mimic of the corresponding pyridinyl ester **99** (91% inhibition at 100 μM) with only 2-3 fold less potent inhibition. Given that the pyridinyl ester **99** (IC_{50} = 7.9 μM) is only a moderate inhibitor among the pyridinyl esters (*e.g.* **33** and **34**, IC_{50} = 60 nM and 50 nM, respectively), we believed that the difluoromethylene ketone mimics of the extremely potent esters (*e.g.* **33** and **34**) could display very strong inhibition of SARS $3CL^{pro}$ in a non-covalent and reversible fashion.

Based on this assumption, a series of methylene ketones and fluorinated methylene ketones were synthesized. Synthesis started from halogen-substituted phenyl or pyridinyl acetic acids, most of which are commercially available material except the 5-chloropyridinyl acetic acid **125c** (Scheme 25). Esterification of carboxylic acids **125a-c** yields **126a-c** in 88% to quantitative yields. Treatment of **126a-c** with LiHMDS to generate the anions, followed by the addition of pre-activated CDI/acid solutions,

provides the β-keto esters **127a-d** in 72% to 96% yields. Hydrolytic decarboxylation of the β-keto esters **127a-d** gives the corresponding ketones in 59% to 85% yields.

Scheme 25 Synthesis of methylene ketones **49, 52, 55** and **58**

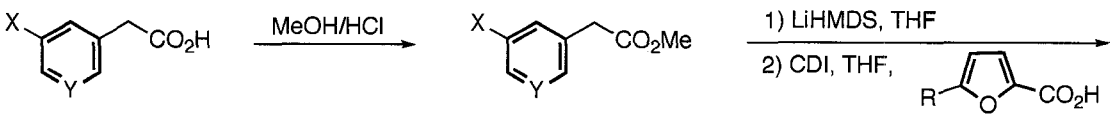

125a: X = Cl, Y = N
125b: X = Cl, Y = C
125c: X = Br, Y = N

126a: X = Cl, Y = N, quant.
126b: X = Cl, Y = C, 88%
126c: X = Br, Y = N, 91%

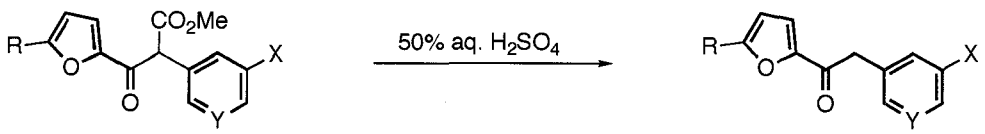

127a: X = Cl, Y = N, R = H, 72%
127b: X = Cl, Y = C, R = H, 75%
127c: X = Br, Y = N, R = H, 96%
127d: X = Br, Y = N, R = 4-Chlorophenyl, 83%

49: X = Cl, Y = N, R = H, 85%
52: X = Cl, Y = C, R = H, 59%
55: X = Br, Y = N, R = H, 68%
58: X = Br, Y = N, R = 4-Chlorophenyl, 85%

The synthesis of fluorinated methylene ketones is described in Scheme 26. Fluorination of the ketones **49, 52, 55, 58** with 1.1 equivalent of LiHMDS and NFSi provides the corresponding monofluoro methylene ketones **50, 53, 56, 59** in 74%, 88%, 74% and 50% yields, respectively. Similarly, fluorination of the ketones **49, 52, 55, 58** with 2.2 equivalent of LiHMDS and NFSi generates the corresponding difluoromethylene ketones **51, 54, 57, 60** in 61%, 57%, 34% and 85% yields, respectively.

Scheme 26 Synthesis of fluorinated methylene ketones **50-51, 53-54, 56-57** and **59-60**

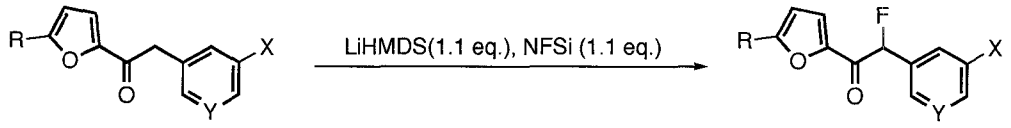

49: X = Cl, Y = N, R = H
52: X = Cl, Y = C, R = H
55: X = Br, Y = N, R = H
58: X = Br, Y = N, R = 4-Chlorophenyl

50: X = Cl, Y = N, R = H, 74%
53: X = Cl, Y = C, R = H, 88%
56: X = Br, Y = N, R = H, 74%
59: X = Br, Y = N, R = 4-Chlorophenyl, 50%

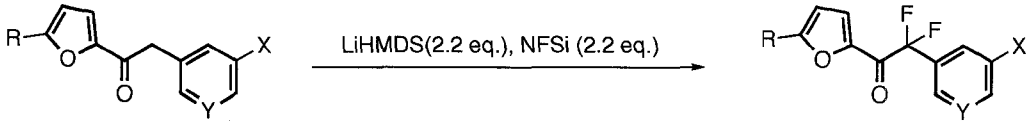

49: X = Cl, Y = N, R = H
52: X = Cl, Y = C, R = H
55: X = Br, Y = N, R = H
58: X = Br, Y = N, R = 4-Chlorophenyl

51: X = Cl, Y = N, R = H, 61%
54: X = Cl, Y = C, R = H, 57%
57: X = Br, Y = N, R = H, 34%
60: X = Br, Y = N, R = 4-Chlorophenyl, 85%

Compound **126a** is not commercially available and was prepared as described in Scheme 27. Esterification of commercially available 5-aminonicotinic acid **128** affords methyl 5-aminonicotinate **129** in 88% yield. Treating the free amine of **129** with sodium nitrite under acidic conditions, followed by the addition of copper (I) chloride and copper (II) chloride yields the methyl 5-chloronicotinate **130** in 79% yield. Hydrolysis of **130** with potassium hydroxide, and then acidic workup generates the acid **131** in 84% yield. Activation of **131** with ethyl chloroformate, followed by lithium aluminum hydride reduction produces the corresponding alcohol, which is readily converted by thionyl chloride to the chloride **132** in 76% yield over 3 steps. Nucleophilic attack of **132** by

potassium cyanide provides compound **133** in 56% yield. Hydrolysis of **133**, followed by esterification gives the desired compound **126a** in quantitative yield.

Scheme 27 Synthesis of methyl 2-(5-chloropyridin-3-yl)acetate **126a**

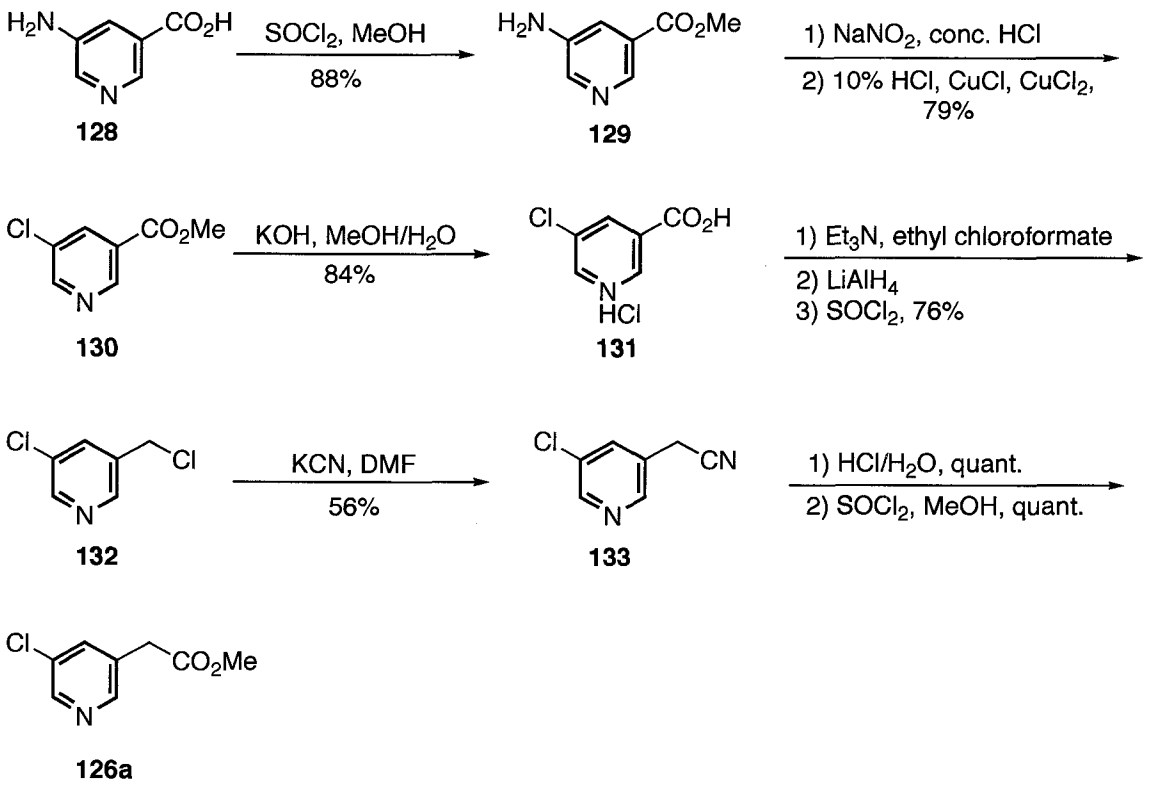

Compounds **49-60** were tested against SARS $3CL^{pro}$ using a continuous fluorometric assay, as described in the experimental section (Part 5). The testing results, which only examine the initial binding affinity, are listed in Table 5. Surprisingly, most of methylene ketones (**49, 52, 55**) as well as their fluorinated methylene ketone analogues (**50, 51, 53, 54, 56, 57**) display poor inhibition against $3CL^{pro}$. However, the methylene ketone **58** and its fluorinated methylene ketone analogues **59, 60** are good inhibitors of $3CL^{pro}$ with IC_{50}

values of 13 to 57 μM. Interestingly, introduction of one fluorine substituent to this class of inhibitors (**58-60**) decreases the inhibitory activity ~2 fold, which stands in contrast to that of inhibitors **46-48**. This suggests that inhibitors **58-60** possessing three aromatic rings may have a totally different binding mode from the inhibitors with two aromatic rings in the structure (**46-57**). After 2 h incubation of 25 μM methylene ketone (**58**) or fluorinated methylene ketones (**59**, **60**) with $3CL^{pro}$, no improved inhibitory activity is observed, suggesting that both the methylene ketone **58** and the fluorinated methylene ketones **59**, **60** are reversible inhibitors for SARS $3CL^{pro}$.

Two additional methylene ketone analogues **61** and **62** were prepared and examined, based on the modification of the ketone **58**. Synthesis of **61** started from commercially available ethyl 2-chloro-2-oxoacetate **134**, as shown in Scheme 28. Nucleophilic reaction of **134** with $TMSCHN_2$ provides the diazo compound **135** in 68% yield. Treating the diazo compound **135** with copper salt generates the carbene intermediate, which readily reacts with 4-chlorobenzonitrile through a [3+2] cyclization to form the ester **136** with the desired oxazole moiety in 14% yield. Hydrolysis of **136** with lithium hydroxide produces the carboxylic acid **137** in 94% yield. Activation of the carboxylic acid **137** with CDI, and then adding this activated solution to the pre-generated anion formed by deprotonation of methyl 2-(5-bromopyridin-3-yl)acetate with LiHMDS, yields the β-keto ester **138** in 23% yield. Hydrolytic decarboxylation of the β-keto ester **138** gives the desired ketone **61** in 58% yield. The ketone **62** was prepared in a similar method as described in Scheme 29.

Scheme 28 Synthesis of ketone **61**

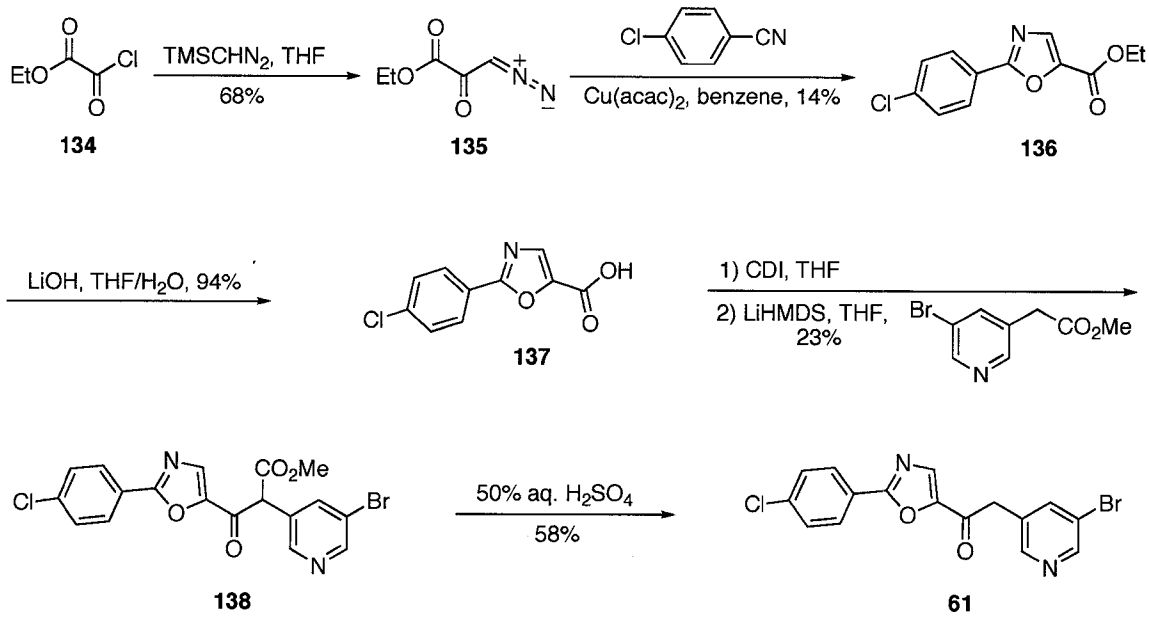

Scheme 29 Synthesis of ketone **62**

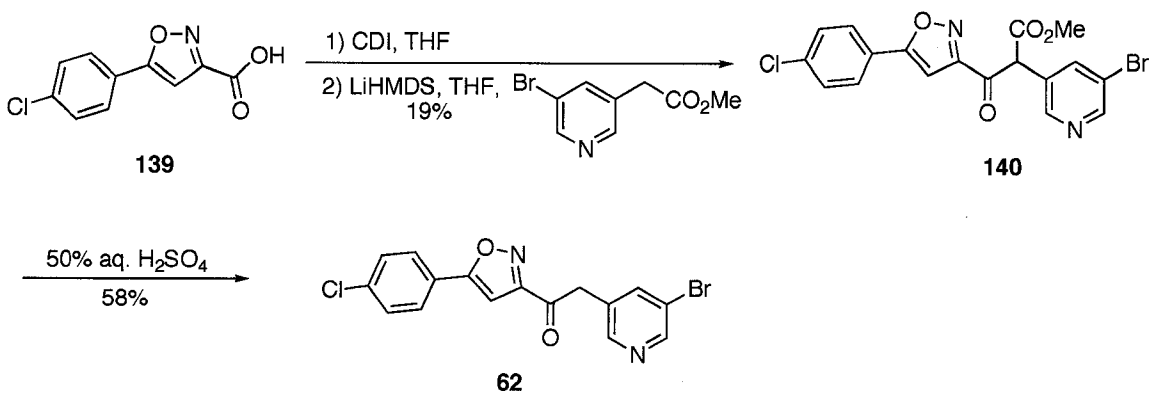

Compounds **61** and **62** were tested against SARS 3CL^{pro} using a continuous fluorometric assay, as described in the experimental section (Part 5). Compounds **61** and **62** display 53% and 35% inhibition at 100 μM against SARS 3CL^{pro}, respectively (Table 5). It is

known that for non-covalent and reversible inhibitors, hydrogen bonds, ionic and van der Waals interactions play crucial roles in binding affinity to the target enzyme. For this class of inhibitors (**58-60**), the oxygen atoms of their furan rings are suspected to have hydrogen bonds with the $3CL^{pro}$. Compared to compounds **58-60**, the oxygen atom of the oxazole ring of **61** and the carbon atom of the isoxazole ring of **62** have low electron density and thus provide weaker binding to the $3CL^{pro}$.

Table 5: Evaluation of methylene ketones and fluorinated methylene ketones **46-62** as SARS $3CL^{pro}$ inhibitors.

Compound No	Inhibition (100 μM)	IC_{50} (μM)
46	-	
47	10%	
48	38%	
49	-	
50	14%	
51	27%	
52	-	
53	15%	
54	13%	
55	-	
56	21%	
57	-	
58		13
59		28
60		57
61	53%	
62	35%	

Dash represents <10% inhibition.

The inhibition mechanism was further investigated through electron spray ionization-mass spectrometry (ESI-MS) studies. After mixing 10 equivalent of inhibitor **58**, **59** or **60** with 1 equivalent of $3CL^{pro}$, and incubating the solution for 24 h, no mass change is

observed in the major mass peak of $3CL^{pro}$. This supports the non-covalent and reversible inhibition nature of compounds **58-60**.

7.3. Modeling Studies of Target H

Modeling studies (Figure 52) of $3CL^{pro}$ with inhibitors **58**, **59** and **60** were conducted as described in the experimental section (part 8), by Dr. Chunying Niu in Prof. Michael James' group at the Department of Biochemistry, University of Alberta.

Figure 52. The modeling binding conformations of **58** (white carbon sticks), **59** (cyan carbon sticks), and **60** (yellow carbon sticks) in the active site of SARS-CoV $3CL^{pro}$ (oxygen atoms are red; nitrogen atoms are blue; chlorine atoms are green; bromine atoms are maroon; and fluorine atoms are purple) (done by Dr. Chunying Niu).

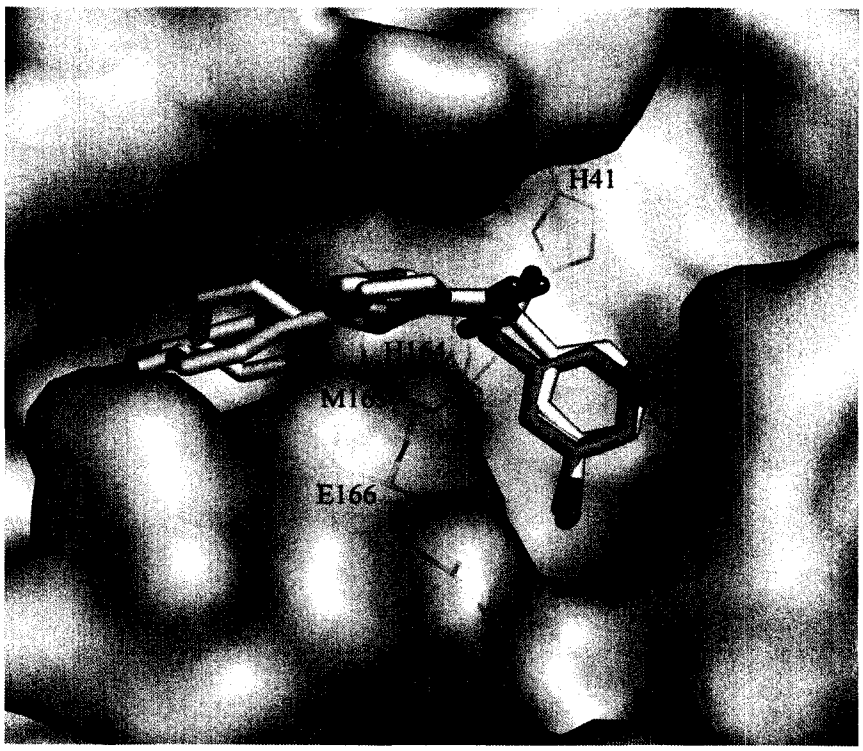

Because the S2 and S4 pockets in the active site of $3CL^{pro}$ are relatively large, the shorter two-aromatic-ring compounds (*e.g.* **55**) can't occupy the maximal volume in these S sites in any docked conformations. However, due to the extended end-to-end length, the three-aromatic-ring compounds can occupy more volume extending from the S2/S4 to the S1 pocket. Therefore, the three-aromatic-ring compounds **58**, **59**, and **60** are more effective in blocking the binding of substrates into the active site, and thus exhibit better inhibition against $3CL^{pro}$ than the two-aromatic-ring ones, as revealed in the enzymatic assay.

Based on our previous modeling studies, the three-aromatic-ring esters show a non-covalent and reversible inhibition mechanism in a S4-S1 binding mode by blocking entry of substrates into the active site of SARS-CoV $3CL^{pro}$. This is supported by a recently reported crystal structure of a three-aromatic-ring thioester with the $3CL^{pro}$.[63] Docking results suggest that these ketone analogues (**58**, **59**, **60**) adopt binding conformations similar to that of the corresponding esters. All three compounds are oriented in an extended conformation from S4 to S1 pocket, with the oxygen atom of their furan ring forming a hydrogen bond with the main chain NH of Glu166, an interaction that was also predicted for the three-aromatic-ring esters. The pyridinyl moiety preferentially binds inside the S1 specificity pocket, which limits the possible spatial orientations of the substituents at the α-position of the central ketone group. The fluorine substituents in both **59** and **60** point towards the main chain carbonyl oxygen of His164 (Figure 52). This slightly pushes **59** and **60** out towards the solvent. Thus, the van der Waals interactions between thee fluorinated compounds and the active site residues of the enzyme are likely to be weaker than those for **58**.

8. Conclusions and Future Work

A series of peptidyl keto-glutamines (targets **A-E**) have been designed, synthesized and evaluated as SARS CoV $3CL^{pro}$ inhibitors. The cyclic peptidyl keto-glutamines (target **A, 21-24**) display very potent inhibition against $3CL^{pro}$ with IC_{50} values ranging from 0.6 to 3.4 μM. Enzyme kinetics studies have demonstrated that the cyclic peptidyl keto-glutamine **21** (IC_{50} = 2.7 μM, K_i = 0.25 μM) initially inhibits the $3CL^{pro}$ in a competitive and reversible fashion in a short time course (15 min or 1 h). However, crystal structure and ESI-MS studies indicate that inhibitor **21** inactivates the $3CL^{pro}$ by the formation of a covalent thioether bond, with departure of the phthalhydrazide moiety in a long time course. Structure-activity relationship studies indicate that the γ-lactam, the phthalhydrazide and the recognition tripeptide are all key structural features for strong inhibition of $3CL^{pro}$ for this class of compounds (Figure 53).

Figure 53 structure-activity relationship studies of peptidyl keto-glutamines

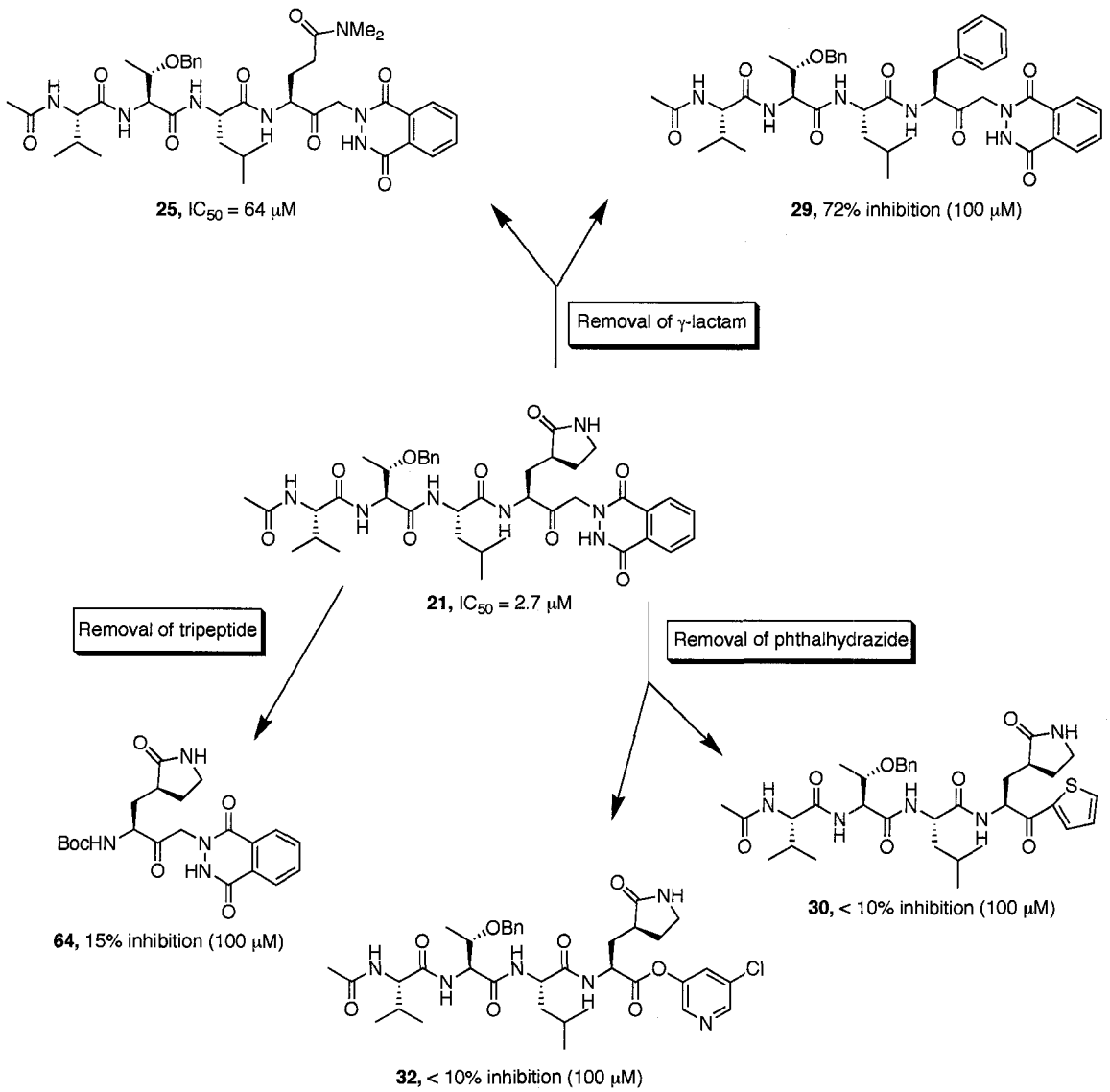

In addition, a series of non-peptidyl heteroaromatic esters and their analogues (target **F**, **33-40**) have been designed, synthesized and evaluated as potential SARS $3CL^{pro}$ inhibitors. Some pyridinyl esters are identified as very potent inhibitors with IC_{50} values in the nanomolar range (50-65 nM). The pyridinyl ester **34** is the most potent inhibitor, with IC_{50} of 50 nM, K_m of 26×10^{-9} M, K_{cat} of 17×10^{-5} s^{-1} and K_{cat}/K_m of 6.5×10^3 M^{-1} s^{-1}. ESI-MS studies suggest a mechanism involving acylation of the active site cysteine thiol. Structure-activity relationship studies indicate that both non-covalent protein-inhibitor interactions as well as inherent chemical reactivity may play important roles in the strong inhibition of $3CL^{pro}$ for this class of inhibitors. This is supported by the observation that the aldehydes (target **G**, **41-45**) possessing part of the structural motif display much weaker inhibition than the corresponding pyridinyl esters.

Based on the structure-activity relationships of targets **F** (**33-40**), and **G** (**41-45**), a series of methylene ketones and fluorinated methylene ketones (target **H**, **46-62**) have also been designed, synthesized and evaluated, in order to develop stable and non-covalent inhibitors. The best compound **58** inhibits the SARS $3CL^{pro}$ in a non-covalent and reversible fashion with IC_{50} of 13 μM.

Currently, work is in progress to obtain the crystal structures of enzyme-inhibitors (targets F and G) complexes, which would assist the understanding of inhibition mechanism and allow further modification for more effective inhibitors of SARS-CoV $3CL^{pro}$.

EXPERIMENTAL SECTION

1. Reagents, Solvents and Solutions

All reactions involving air or moisture-sensitive reactants were done under argon. All reagents employed were of American Chemical Society (ACS) grade or finer and were used without further purification unless otherwise stated. Solvents were dried for anhydrous reactions. Tetrahydrofuran and diethyl ether were distilled over sodium and benzophenone under an atmosphere of dry argon. Acetonitrile, dichloromethane, methanol, pyridine and triethylamine were distilled over calcium hydride. Removal of solvent was performed under reduced pressure below 40 °C using a Büchi rotary evaporator, followed by evacuation (< 0.1 mm Hg) to constant sample weight. Deionized water was obtained from a Milli-Q reagent water system (Millipore Co., Milford, MA). Unless otherwise specified, solutions of NH_4Cl, $NaHCO_3$, HCl, NaOH, and LiOH refer to aqueous solutions. Brine refers to a saturated aqueous solution of NaCl. Ether refers to diethyl ether.

2. Purification Techniques

All reactions and fractions from column chromatography were monitored by thin layer chromatography (TLC) using glass plates with a UV fluorescent indicator (normal SiO_2, Merck 60 F_{254}). One or more of the following methods were used for visualization: UV absorption by fluorescence quenching; iodine staining; phosphomolybdic acid spray

(ceric sulfate:sulfuric acid:H_2O/10 g:1.25 g:12 mL:238 mL). Flash chromatography was performed using Merck type 60, 230-400 mesh silica gel.

High performance liquid chromatography (HPLC) was performed on either a Beckman System Gold instrument equipped with a model 166 variable wavelength UV detector and a Rheodyne 7725i injector with a 20 to 2000 μL sample loop, on a Rainin instrument equipped with a Rainin model UV-1 variable wavelength UV detector and a Rheodyne 7725i injector fitted with a 1 mL sample loop, on a Gilson instrument equipped with a model 152 variable wavelength UV detector and a Rheodyne 7010 injector fitted with a 1 mL sample loop, or on a Varian prostar equipped with a model 325 variable wavelength UV detector and a Rheodyne 7725i injector fitted with a 20 to 2000 μL sample loop. The columns used were Waters Nova-Pak cartridges (reverse phase, 8NVC18, 4 μm C_{18} column, 60 Å, 4 mm, 8 x 100 mm), Waters μBondapak cartridges (reverse phase μBondapak, WAT037684, C_{18} column, 125 Å, 10 mm, 25 x 100 mm), Waters Nova-Pak cartridges (reverse phase, 8NVPH, 4 μm phenyl column, 60 Å, 4 mm, 8 x 100 mm) or Varian C_{18} steel walled column (reverse phase, R0086200C5, microsorb-MV100, 5μm C_{18} column, 5 mm, 4.6 x 250 mm). All HPLC solvents were filtered with a Millipore filtration system under vacuum before use. All GC-MS were performed using a Zebron DB5 column of length (30 m) with a stationary phase thickness of (0.24 μm) using the method (50 °C → 250-290 °C @ 10 °C/min.).

3. Instrumentation for Compound Characterization

Optical rotations were measured on a Perkin Elmer 241 polarimeter with a microcell (10 cm, 1 mL) at ambient temperature and are reported in units of 10^{-1} deg cm^2 g^{-1}. All specific rotations reported were referenced against air and were measured at the sodium D line and values quoted are valid within ± 1°. Infrared spectra (IR) were recorded on a Nicolet Magna 750 or a 20SX FT-IR spectrometer. Cast refers to the evaporation of a solution on a NaCl plate. Mass spectra (MS) were recorded on a Kratos AEIMS-50 high resolution (HRMS), electron impact ionization (EI), and Micromass ZabSpec Hybrid Sector-TOF positive mode electrospray ionization (ES) instruments.

Nuclear magnetic resonance (NMR) spectra were obtained on Inova Varian 300, 400, 500 and 600 MHz spectrometers. ^{1}H NMR chemical shifts are reported in parts per million (ppm) downfield relative to tetramethylsilane (TMS) using the residual proton resonance of solvents as reference: $CDCl_3$ δ 7.26, D_2O δ 4.79, CD_3OD δ 3.30 and DMSO-d_6 δ 2.50. ^{13}C NMR chemical shifts are reported relative to $CDCl_3$ δ 77.0, CD_3OD δ 49.0 and $(CD_3)_2SO$ δ 40.0. Selective homonuclear decoupling, shift correlation spectroscopy (COSY), heteronuclear multiple quantum coherence (HMQC), heteronuclear multiple bond correlation (HMBC) and attached proton test (APT) were used for signal assignments. ^{1}H NMR data are reported in the following order: multiplicity (s, singlet; d, doublet; t, triplet; q, quartet; qn, quintet and m, multiplet), number of protons, coupling constant (*J*) in Hertz (Hz) and assignment. When appropriate, the multiplicity is preceded by br, indicating that the signal was broad. All literature compounds had IR, ^{1}H NMR,

and mass spectra consistent with the assigned structures. More detailed analysis of ^{1}H NMR and ^{13}C NMR spectra was done for all known compounds.

4. Experimental Data for Compounds

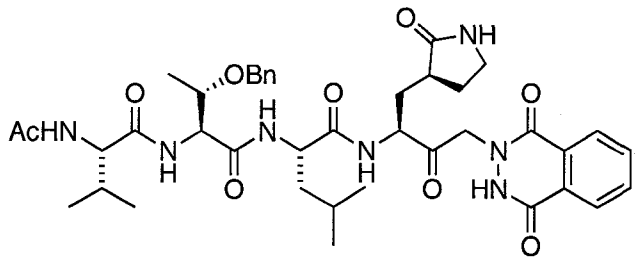

(*S*)-2-((2*S*,3*S*)-2-((*S*)-2-Acetamido-3-methylbutanamido)-3-(benzyloxy)butanamido)-*N*-((*S*)-4-(1,4-dioxo-3,4-dihydrophthalazin-2(1*H*)-yl)-3-oxo-1-((*S*)-2-oxopyrrolidin-3-yl)butan-2-yl)-4-methylpentanamide (21). Compound **64** (30 mg, 0.067 mmol) was stirred with TFA/CH_2Cl_2 (2 mL, 1:1 ratio) at 0 °C for 1.5 h, after which the reaction mixture was concentrated in vacuo and the residue triturated with Et_2O to yield the trifluoroacetate salt. To a solution of Ac-Val-Thr(OBn)-Leu-OH (35 mg, 0.076 mmol) in DMF (2 mL) at ambient temperature was added DIPEA (28 uL, 0.161 mmol) followed by HBTU (30.5 mg, 0.085 mmol). The resulting mixture was treated with a solution of the trifluoroacetate salt in DMF (2 mL). After 6 h of stirring, the solvent was removed in vacuo and the crude product was purified by HPLC (Waters C18 Bondpak 10 μm, 125 Å; 100 x 25 mm, 15 mL/min, 5 min elution of 20% acetonitrile followed by a linear gradient elution over 25 min of 20 to 95% acetonitrile in 0.075% TFA/H_2O, t_R = 20 min) to afford **21** as a white solid after lyophilization (36 mg, 67%). $[\alpha]^{25}_{D}$= -33.41° (*c* 0.09, DMSO); IR (microscope) 3265, 3068, 2958, 2872, 1736, 1654, 1624, 1540, 1494, 1436 cm^{-1}; ^{1}H

NMR (DMSO-d_6, 500 MHz) δ 11.54 (br, 1H, N<u>H</u>), 8.38 (d, 1H, J = 7.2 Hz, Ar<u>H</u>), 8.26-8.22 (m, 1H, N<u>H</u>), 8.04-7.85 (m, 3H, N<u>H</u>), 7.69 (d, 1H, J = 8.0 Hz, Ar<u>H</u>), 7.65 (d, 1H, J = 8.0 Hz, Ar<u>H</u>), 7.51 (d, 1H, J = 7.2 Hz, Ar<u>H</u>), 7.35-7.20 (m, 6H, 1xN<u>H</u> and 5xPh<u>H</u>), 5.19 (d, 1H, J = 17.2 Hz, C<u>H</u>$_2$N), 5.10 (d, 1H, J = 17.2 Hz, C<u>H</u>$_2$N), 4.58-4.46 (m, 3H, 1xNHC<u>H</u>CO(Gln) and 2xOC<u>H</u>$_2$Ph(Thr)), 4.45-4.34 (m, 2H, 1xNHC<u>H</u>CO(Thr) and 1xNHC<u>H</u>CO(Leu)), 4.25-4.16 (m, 1H, NHC<u>H</u>CO(Val)), 4.00-3.92 (m, 1H, CH_3C<u>H</u>OBn(Thr)), 3.21-3.09 (m, 2H, NHC<u>H</u>$_2$CH$_2$(Gln)), 2.35-2.23 (m, 1H, NHCH$_2$C<u>H</u>$_2$(Gln)), 2.21-1.98 (m, 3H, 2xCHC<u>H</u>$_2$CH(Gln) and 1xCHC<u>H</u>$(CH_3)_2$(Val)), 1.88 (s, 3H, COC<u>H</u>$_3$), 1.81-1.61 (m, 3H, 1xNHCH$_2$C<u>H</u>$_2$(Gln), 1xCH$_2$C<u>H</u>CO(Gln) and 1xCHC<u>H</u>$_2$CH(Leu)), 1.56-1.50 (m, 2H, 1xCHC<u>H</u>$_2$CH(Leu) and 1xCH$_2$C<u>H</u>$(CH_3)_2$(Leu)), 1.13 (d, 3H, J = 6.4 Hz, CHC<u>H</u>$_3$(Thr)), 0.92-0.83 (m, 12H, 6xCH(C<u>H</u>$_3)_2$(Val) and 6xCH(C<u>H</u>$_3)_2$(Leu)); ^{13}C NMR (CD_3OD, 125 MHz) δ 203.0, 178.0, 172.0, 171.3, 170.8, 169.3, 159.6, 149.3, 139.3, 134.3, 133.1, 129.3, 128.7, 128.1, 127.8, 126.8, 124.7, 124.0, 74.5, 70.1, 68.3, 57.8, 56.4, 53.6, 50.8, 46.4, 40.4, 30.7, 29.8, 27.0, 23.7, 22.9, 22.1, 21.2, 18.9, 18.0, 16.2, 16.0; HRMS (ES) calcd for $C_{40}H_{53}N_7O_9Na$ ([M+Na]$^+$), 798.3797; found, 798.3800.

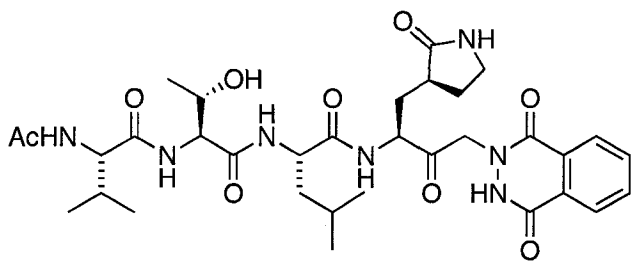

(*S*)-2-((2*S*,3*S*)-2-((*S*)-2-Acetamido-3-methylbutanamido)-3-hydroxybutanamido)-*N*-((*S*)-4-(1,4-dioxo-3,4-dihydrophthalazin-2(1*H*)-yl)-3-oxo-1-((*S*)-2-oxopyrrolidin-3-

yl)butan-2-yl)-4-methylpentanamide (22). To solution of **21** (3 mg) in MeOH (3 mL) was added 10% Pd/C (3 mg) and the reaction mixture was hydrogenated at 1 atm of H_2 at ambient temperature for 8 h. Catalyst was removed by filtration through Celite and the filtrate was concentrated under reduced pressure to obtain **22** (3 mg, quant.) as a white solid. $[\alpha]^{25}_{D}$= -18.57° (*c* 0.15, MeOH); IR (microscope) 3295, 2963, 1669, 1632, 1545, 1493, 1445 cm^{-1}; ^{1}H NMR (CD_3OD, 500 MHz) δ 8.28 (ddd, 1H, *J* = 8.0, 1.4, 0.7 Hz, Ar<u>H</u>), 8.10 (ddd, 1H, *J* = 8.0, 1.4, 0.7 Hz, Ar<u>H</u>), 7.92 (ddd, 1H, *J* = 8.0, 8.0, 1.4 Hz, Ar<u>H</u>), 7.87 (ddd, 1H, *J* = 8.0, 8.0, 1.4 Hz, Ar<u>H</u>), 5.19 (d, 1H, *J* = 16.9 Hz, C<u>H</u>$_2$N), 5.12 (d, 1H, *J* = 16.9 Hz, C<u>H</u>$_2$N), 4.64 (dd, 1H, *J* = 11.5, 3.9 Hz, NHC<u>H</u>CO(Gln)), 4.48-4.40 (m, 1H, NHC<u>H</u>CO(Leu)), 4.32 (d, 1H, *J* = 4.0 Hz, NHC<u>H</u>CO(Thr)), 4.18 (dq, 1H, *J* = 6.3, 4.0 Hz, CH_3C<u>H</u>OH(Thr)), 4.14 (d, 1H, *J* = 6.8 Hz, NHC<u>H</u>CO(Val)), 3.36-3.20 (m, 2H, NHC<u>H</u>$_2$CH$_2$(Gln)), 2.60-2.20 (m, 3H, 1xNHCH$_2$C<u>H</u>$_2$(Gln,) 1xCHC<u>H</u>$_2$CH(Gln) and 1xCHC<u>H</u>$_2$CH(Gln)), 2.14-2.06 (m, 1H, CHC<u>H</u>(CH$_3$)$_2$(Val)), 2.01 (s, 3H, COC<u>H</u>$_3$), 1.92-1.75 (m, 2H, 1xCH$_2$C<u>H</u>CO(Gln) and 1xNHCH$_2$C<u>H</u>$_2$(Gln)), 1.74-1.60 (m, 3H, 2xCHC<u>H</u>$_2$CH(Leu) and 1xCH$_2$C<u>H</u>(CH$_3$)$_2$(Leu)), 1.18 (d, 3H, *J* = 6.4 Hz, CHC<u>H</u>$_3$(Thr)), 0.98 (d, 3H, *J* = 6.8 Hz, CH(C<u>H</u>$_3$)$_2$(Val)), 0.97 (d, 3H, *J* = 6.8 Hz, CH(C<u>H</u>$_3$)$_2$(Val)), 0.95 (d, 3H, *J* = 6.2 Hz, CH(C<u>H</u>$_3$)$_2$(Leu)), 0.90 (d, 3H, *J* = 6.2 Hz, CH(C<u>H</u>$_3$)$_2$(Leu)); ^{13}C NMR (CD_3OD, 125 MHz) δ 204.4, 199.4, 182.0, 175.3, 174.5, 174.1, 172.5, 151.4, 135.0, 133.6, 130.0, 127.4, 126.0, 125.0, 70.0, 68.1, 61.4, 60.0, 55.7, 53.5, 41.5, 41.3, 39.3, 32.5, 31.3, 28.7, 25.9, 23.5, 22.4, 21.7, 20.1, 19.7, 18.6; HRMS (ES) calcd for $C_{33}H_{47}N_7O_9Na$ ($[M+Na]^+$), 708.3327; found, 708.3328.

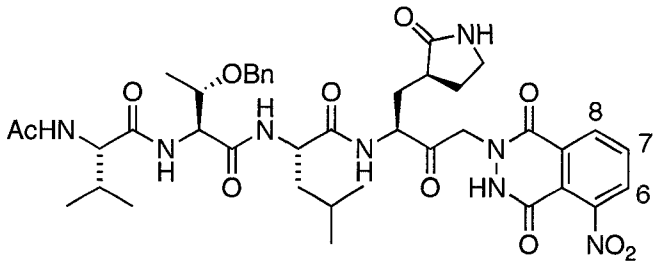

(*S*)-2-((2*S*,3*S*)-2-((*S*)-2-Acetamido-3-methylbutanamido)-3-(benzyloxy)butanamido)-4-methyl-*N*-((*S*)-4-(5-nitro-1,4-dioxo-3,4-dihydrophthalazin-2(1*H*)-yl)-3-oxo-1-((*S*)-2-oxopyrrolidin-3-yl)butan-2-yl)pentanamide (23). This compound was prepared by Dr. Rajendra Jain and Dr. Hanna Pettersson in our group,[74] and was prepared from **74** (68 μmol) as described for **21**. The crude product was purified by HPLC (Waters C18 Bondpak 10 μm, 125 Å; 100 x 25 mm, 15 mL/min, 5 min elution of 40% acetonitrile followed by linear gradient elution over 50 min of 40 to 50% acetonitrile in 0.075% TFA/H_2O, t_R = 15.3 min) to yield **23** (11.7 mg, 21%). ^{1}H NMR (DMSO-d_6, 500 MHz) δ 8.31 (dd, 1H, J = 8.0, 1.0 Hz, H_6), 8.27 (d, 1H, J = 8.0 Hz, N<u>H</u>), 8.22 (d, 1H, J = 6.5 Hz, N<u>H</u>), 8.07 (dd, 1H, J = 8.0, 8.0 Hz, H_7), 7.97 (dd, 1H, J = 8.0, 1.0 Hz, H_8), 7.84 (d, 1H, J = 8.0 Hz, N<u>H</u>), 7.62 (d, 1H, J = 7.0 Hz, N<u>H</u>), 7.23 – 7.31 (m, 5H, Ph<u>H</u>), 5.23 (d, 1H, J = 17.0 Hz, C<u>H</u>$_2$N), 5.16 (d, 1H, J = 17.0 Hz, C<u>H</u>$_2$N), 4.65–4.61 (m, 1H, NHC<u>H</u>CO(Gln)), 4.61 (d, 1H, J = 11.5 Hz, OC<u>H</u>$_2$Ph(Thr)), 4.48–4.46 (m, 1H, NHC<u>H</u>CO(Leu)), 4.44 (d, 1H, J = 11.5 Hz, OC<u>H</u>$_2$Ph(Thr)), 4.38 (dd, 1H, J = 8.0, 3.0 Hz, NHC<u>H</u>CO(Thr)), 4.15 (dd, 1H, J = 6.0, 3.0 Hz, NHC<u>H</u>CO(Val)), 4.13–4.10 (m, 1H, CH_3C<u>H</u>OBn(Thr)), 3.28–3.22 (m, 1H, NHC<u>H</u>$_2$CH$_2$(Gln)), 2.57–2.54 (m, 1H, NHC<u>H</u>$_2$CH$_2$(Gln)), 2.29–2.20 (m, 2H, 1xNHCH$_2$C<u>H</u>$_2$(Gln) and 1xCHC<u>H</u>$_2$CH(Gln)), 2.13–2.07 (m, 1H, CHC<u>H</u>$_2$CH(Gln)), 1.95 (s, 3H, COC<u>H</u>$_3$), 1.88–1.82 (m, 1H, CHC<u>H</u>(CH$_3$)$_2$(Val)), 1.78–1.73 (m, 1H, NHCH$_2$C<u>H</u>$_2$(Gln)), 1.70–1.65 (m, 1H, CH$_2$C<u>H</u>CO(Gln)), 1.63–1.59 (m, 2H,

CHC$\underline{H}_2$CH(Leu)), 1.29–1.28 (m, 1H, $CH_2C\underline{H}(CH_3)_2$(Leu)), 1.26 (d, 3H, J = 6.0 Hz, CHC$\underline{H}_3$(Thr)), 0.99 (d, 6H, J = 7.0 Hz, CH(C$\underline{H}_3$)$_2$(Val)), 0.87 (d, 3H, J = 6.0 Hz, CH(C$\underline{H}_3$)$_2$(Leu)), 0.86 (d, 3H, J = 6.0 Hz, CH(C$\underline{H}_3$)$_2$(Leu)); HRMS (ES) calcd for $C_{40}H_{52}N_8O_{11}Na$ ([M+Na]$^+$), 843.3648; found, 843.3648.

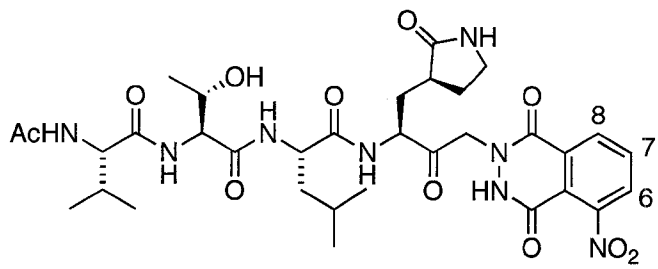

(*S*)-2-((2*S*,3*S*)-2-((*S*)-2-Acetamido-3-methylbutanamido)-3-hydroxybutanamido)-4-methyl-*N*-((*S*)-4-(5-nitro-1,4-dioxo-3,4-dihydrophthalazin-2(1*H*)-yl)-3-oxo-1-((*S*)-2-oxopyrrolidin-3-yl)butan-2-yl)pentanamide (24). This compound was prepared by Dr. Rajendra Jain and Dr. Hanna Pettersson in our group.[74] Trifluoroacetic acid (1.0 mL) was added to the benzyl protected tetrapeptide **23** (6.1 μmol) at 0 °C, followed by trimethylsilyl trifluoroacetate (0.5 mL). The mixture was stirred at 0 °C for 2 h. Saturated $NaHCO_3$ solution was added and the reaction mixture was extracted with EtOAc. The combined organic layers were dried over $MgSO_4$ and the solvent was removed in vacuo. The crude product was purified by HPLC (Waters C18 Bondpak 10 μm, 125 Å; 100 x 25 mm, 15 mL/min, 5 min elution of 30% acetonitrile followed by linear gradient elution over 50 min of 30 to 40% acetonitrile in 0.075% TFA/H_2O, t_R = 9.9 min) to yield **24** (4.4 mg, quant.). ^{1}H NMR (DMSO-d_6, 500 MHz) δ 8.31 (dd, 1H, J = 8.0, 1.0 Hz, H_6), 8.28 (dd, 1H, J = 8.0, 1.0 Hz, N$\underline{H}$), 8.13 (d, 1H, J = 6.5 Hz, N$\underline{H}$), 8.04 (dd, 1H, J = 8.0, 8.0 Hz, H_7), 7.98 (d, 1H, J = 7.0 Hz, N$\underline{H}$), 7.94 (dd, 1H, J = 8.0, 1.0 Hz,

H_8), 7.72 (d, 1H, J = 8.0 Hz, N$\underline{H}$), 5.20 (d, 1H, J = 17.0 Hz, C$\underline{H}_2$N), 5.13 (d, J = 17.0 Hz, 1H, C$\underline{H}_2$N), 4.61 (dd, 1H, J = 14.5, 3.0 Hz, NHC$\underline{H}$CO(Gln)), 4.48–4.46 (m, 1H, NHC$\underline{H}$CO(Leu)), 4.28 (dd, 1H, J = 7.5, 3.5 Hz, NHC$\underline{H}$CO(Thr)), 4.15 (dd, 1H, J = 6.5, 3.5 Hz, NHC$\underline{H}$CO(Val)), 4.12–4.09 (m, 1H, CH_3C$\underline{H}$OH(Thr)), 2.24–2.14 (m, 2H, NHC$\underline{H}_2$$CH_2$(Gln)), 2.08–2.04 (m, 2H, 1xNHCH_2C$\underline{H}_2$(Gln) and 1xCHC$\underline{H}_2$CH(Gln)), 1.98 (s, 3H, COC$\underline{H}_3$), 1.88–1.74 (m, 3H, 1xCHC$\underline{H}_2$CH(Gln), 1xCHC$\underline{H}$$(CH_3)_2$(Val) and 1xNH$CH_2C\underline{H}_2$(Gln)), 1.66–1.60 (m, 4H, 1xCH_2C$\underline{H}$CO(Gln), 2xCHC$\underline{H}_2$CH(Leu), and 1xCH_2C$\underline{H}$$(CH_3)_2$(Leu)), 1.14 (d, 3H, J = 6.5 Hz, CHC$\underline{H}_3$(Thr)), 0.94 (d, 3H, J = 7.0 Hz, CH(C$\underline{H}_3$)$_2$(Val)), 0.93 (d, 3H, J = 6.5 Hz, CH(C$\underline{H}_3$)$_2$(Val)), 0.92 (d, 3H, J = 6.0 Hz, CH(C$\underline{H}_3$)$_2$(Leu)), 0.86 (d, 3H, J = 6.0 Hz, CH(C$\underline{H}_3$)$_2$(Leu)); HRMS (ES) calcd for $C_{40}H_{52}N_8O_{11}Na$ ([M+Na]$^+$), 753.3178; found, 753.3179.

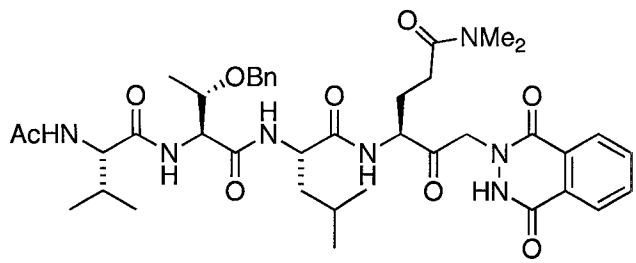

(*S*)-4-((*S*)-2-((2*S*,3*S*)-2-((*S*)-2-Acetamido-3-methylbutanamido)-3-(benzyloxy) butanamido)-4-methylpentanamido)-6-(1,4-dioxo-3,4-dihydrophthalazin-2(1*H*)-yl)-*N*,*N*-dimethyl-5-oxohexanamide (25). Compound **80** (100 mg, 0.23 mmol) was stirred with TFA/CH_2Cl_2 (4 mL, 1:1 ratio) at 0 °C for 1.5 h, after which the reaction mixture was concentrated in vacuo and the residue was triturated with Et_2O to yield the trifluoroacetate salt (106 mg, quant.). To a solution of Ac-Val-Thr(OBn)-Leu-OH (115 mg, 0.25 mmol) in DMF (3 mL) at ambient temperature was added DIPEA (100 uL, 0.57

mmol), followed by HBTU (95 mg, 0.25 mmol). The resulting mixture was treated with a solution of the trifluoroacetate salt (106 mg, 0.23 mmol) in DMF (2 mL). After 24 h of stirring, the solvent was removed in vacuo and the crude product was purified by HPLC (Waters C_{18} Bondpak column; particle size 10 μM, pore size 125 Å, dimensions 25 mm x 100 mm, 15 mL/min linear gradient elution of acetonitrile in 0.1% TFA/H_2O) to afford **25** (63 mg, 33%). $[\alpha]^{25}_{D}$= -33.55° (*c* 0.09, DMSO); IR (microscope) 3275, 3072, 2959, 2931, 1802, 1734, 1632, 1546, 1515, 1448 cm^{-1}; ^1H NMR (DMSO-d_6, 500 MHz, mixture of rotamers) δ 8.29 (d, 1H, *J* = 7.1 Hz, N<u>H</u>), 8.18 (ddd, 1H, *J* = 7.8, 1.4, 0.7 Hz, Ar<u>H</u>), 8.02-7.88 (m, 4H, 2xAr<u>H</u> and 2xN<u>H</u>), 7.90 (d, 1H, *J* = 8.7 Hz, N<u>H</u>), 7.73 (d, 1H, *J* = 7.8 Hz, N<u>H</u>), 7.31-7.22 (m, 5H, 5xPh<u>H</u>), 5.10 (d, 1H, *J* = 17.0 Hz, C<u>H</u>$_2$N), 5.03 (d, 1H, *J* = 17.0 Hz, C<u>H</u>$_2$N), 4.48 (d, 1H, *J* = 11.8 Hz, OC<u>H</u>$_2$Ph (Thr)), 4.39 (d, 1H, *J* = 11.8 Hz, OC<u>H</u>$_2$Ph (Thr)), 4.39-4.31 (m, 3H, 1xNHC<u>H</u>CO(Gln), 1xNHC<u>H</u>CO(Thr)and 1xNHC<u>H</u>CO(Leu)), 4.18 (dd, 1H, *J* = 8.1, 7.1 Hz, NHC<u>H</u>CO(Val)), 3.91 (dd, 1H, *J* = 6.3, 4.5 Hz, CH_3C<u>H</u>OBn(Thr)), 2.86 (s, 3H, N(C<u>H</u>$_3$)$_2$), 2.77 (s, 3H, N(C<u>H</u>$_3$)$_2$), 2.40-2.28 (m, 2H, CH_2C<u>H</u>$_2$CO(Gln)), 2.10-2.02 (m, 1H, CHC<u>H</u>$_2$CH$_2$(Gln)), 1.99-1.91 (m, 1H, CHC<u>H</u>(CH$_3$)$_2$(Val)), 1.84 (s, 3H, COC<u>H</u>$_3$), 1.82-1.71 (m, 1H, CHC<u>H</u>$_2$CH$_2$(Gln)), 1.65-1.54 (m, 1H, CHC<u>H</u>$_2$CH(Leu)), 1.52-1.38 (m, 2H, 1xCHC<u>H</u>$_2$CH(Leu) 1xCH$_2$C<u>H</u>(CH$_3$)$_2$(Leu)), 1.08 (d, 3H, *J* = 6.3 Hz, CHC<u>H</u>$_3$(Thr)), 0.88-0.78 (m, 12H, 6xCH(C<u>H</u>$_3$)$_2$(Val) and 6xCH(C<u>H</u>$_3$)$_2$(Leu)); ^{13}C NMR (CD_3OD, 125 MHz) δ 203.0, 172.1, 171.4, 171.0, 169.5, 169.4, 158.6, 148.4, 138.5, 133.4, 132.3, 128.6, 127.9, 127.3, 127.1, 126.1, 123.9, 123.3, 74.5, 70.2, 68.4, 58.1, 56.7, 55.1, 50.9, 40.5, 36.4, 34.7, 29.9, 28.2, 25.0, 23.9, 22.8, 22.3, 21.3, 19.0, 18.1, 16.3; HRMS (ES) calcd for $C_{40}H_{55}N_7O_9Na$ ($[M+Na]^+$), 800.3954; found, 800.3954.

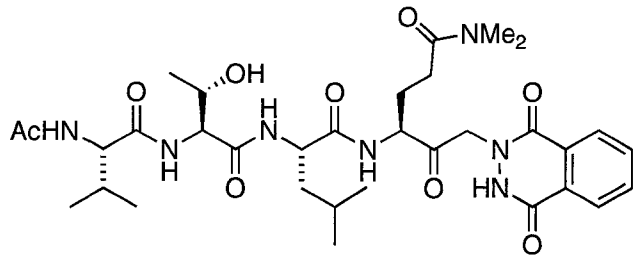

(*S*)-4-((*S*)-2-((2*S*,3*S*)-2-((*S*)-2-Acetamido-3-methylbutanamido)-3-hydroxybutanamido)-4-methylpentanamido)-6-(1,4-dioxo-3,4-dihydrophthalazin-2(1*H*)-yl)-*N*,*N*-dimethyl-5-oxohexanamide (26). To solution of **25** (5 mg) in MeOH/H_2O (3 mL, 1:1 ratio) was added 10% Pd/C (3 mg) and the resulting suspension was hydrogenated at 1 atm of H_2 at ambient temperature for 18 h. Catalyst was removed by filtration through Celite and the filtrate was concentrated under reduced pressure to obtain **26** (4 mg, 80%). $[\alpha]^{25}_{D}$= -26.54° (*c* 0.11, MeOH); IR (microscope) 3275, 3074, 2962, 1737, 1628, 1543 cm^{-1}; ^1H NMR (CD_3OD/D_2O, 500 MHz) δ 8.30 (d, 1H, *J* = 7.5 Hz, Ar<u>H</u>), 8.16 (d, 1H, *J* = 7.5 Hz, Ar<u>H</u>), 8.03-7.94 (m, 2H, Ar<u>H</u>), 5.17 (d, 1H, *J* = 16.5 Hz, C<u>H</u>$_2$N), 5.13 (d, 1H, *J* = 16.5 Hz, C<u>H</u>$_2$N), 4.66-4.63 (m, 1H, NHC<u>H</u>CO(Gln)), 4.44-4.38 (m, 1H, NHC<u>H</u>CO(Leu)), 4.33 (d, 1H, *J* = 4.5 Hz, NHC<u>H</u>CO(Thr)), 4.18-4.14 (m, 1H, CH_3C<u>H</u>OH(Thr)), 4.09 (d, 1H, *J* = 6.5 Hz, NHC<u>H</u>CO(Val)), 3.02 (s, 3H, N(C<u>H</u>$_3$)$_2$), 2.92 (s, 3H, N(C<u>H</u>$_3$)$_2$), 2.52-2.49 (m, 2H, C<u>H</u>$_2$CO(Gln)), 2.34-2.24 (m, 1H, CHC<u>H</u>$_2$CH$_2$(Gln)), 2.03 (s, 3H, COC<u>H</u>$_3$), 1.98-1.90 (m, 1H, CHC<u>H</u>(CH$_3$)$_2$(Val)), 1.69-1.56 (m, 3H, 1xCHC<u>H</u>$_2$CH$_2$(Gln) and 2xCHC<u>H</u>$_2$CH(Leu)), 1.17 (d, 3H, *J* = 6.5 Hz, CHC<u>H</u>$_3$(Thr)), 1.23-1.14 (m, 1H, 1xCH$_2$C<u>H</u>(CH$_3$)$_2$(Leu)), 0.95-0.85 (m, 12H, 6xCH(C<u>H</u>$_3$)$_2$(Val) and 6xCH(C<u>H</u>$_3$)$_2$(Leu)); ^{13}C NMR (CD_3OD, 125 MHz) δ 204.4, 175.2, 174.4, 174.3, 172.5, 151.4, 135.0, 133.6, 133.5, 127.4, 126.0, 125.0, 121.3, 118.0, 70.0,

68.1, 61.5, 60.1, 57.1, 53.4, 41.4, 37.7, 32.6, 29.2, 25.9, 23.5, 22.4, 21.7, 20.2, 19.7, 18.9; HRMS (ES) calcd for $C_{33}H_{49}N_7O_9Na$ ([M+Na]$^+$), 710.3488; found, 710.3484.

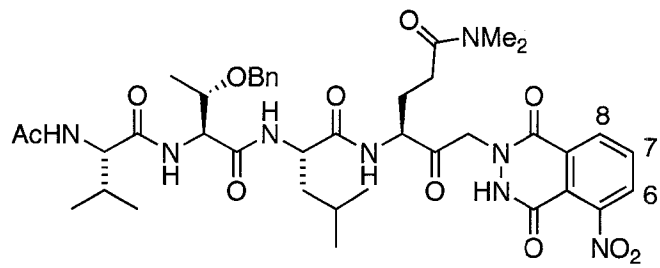

(*S*)-4-((*S*)-2-((2*S*,3*S*)-2-((*S*)-2-Acetamido-3-methylbutanamido)-3-(benzyloxy)butanamido)-4-methylpentanamido)-*N*,*N*-dimethyl-6-(5-nitro-1,4-dioxo-3,4-dihydrophthalazin-2(1*H*)-yl)-5-oxohexanamide (27). This compound was prepared by Dr. Rajendra Jain and Dr. Hanna Pettersson in our group,[74] and was prepared from **86** (34 mg, 68 μmol) as described for **25**. The crude product was purified by HPLC (Waters C_{18} Bondpak column; particle size 10 μM, pore size 125 Å, dimensions 25 mm x 100 mm, 15 mL/min linear gradient elution of 40–50% acetonitrile in 0.075% TFA/H_2O, t_R = 15.3 min) to afford **27** (15.7 mg, 28%). ^{1}H NMR (CD_3OD, 500 MHz) δ 8.31 (d, 1H, J = 8.0, 1.0 Hz, H_6), 8.24 (d, 1H, J = 5.5 Hz, N<u>H</u>), 8.07 (dd, 1H, J = 8.0, 8.0 Hz, H_7), 7.97 (dd, 1H, J = 8.0, 1.5 Hz, H_8), 7.81 (d, 1H, J = 7.5 Hz, N<u>H</u>), 7.60 (d, 1H, J = 7.5 Hz, N<u>H</u>), 7.33–7.25 (m, 5H, Ph<u>H</u>), 5.19 (d, 1H, J = 16.5 Hz, C<u>H</u>$_2$N), 5.15 (d, 1H, J = 17.0 Hz, C<u>H</u>$_2$N), 4.61 (d, 1H, J = 11.5 Hz, OC<u>H</u>$_2$Ph(Thr)), 4.59–4.46 (m, 2H, 1xNHC<u>H</u>CO(Leu) and 1xNHC<u>H</u>CO(Gln)), 4.43 (d, 1H, J = 11.5 Hz, OC<u>H</u>$_2$Ph(Thr)), 4.37 (dq, 1H, J = 8.0, 3.0 Hz, NHC<u>H</u>CO(Thr)), 4.15 (dd, 1H, J = 6.5, 2.5 Hz, NHC<u>H</u>CO(Val)), 4.02–4.00 (m, 1H, CH_3C<u>H</u>OH(Thr)), 2.98 (s, 3H, NC<u>H</u>$_3$), 2.90 (s, 3H, NC<u>H</u>$_3$), 2.49–2.45 (m, 2H, C<u>H</u>$_2$CO(Gln)), 2.11–2.07 (m, 1H, CHC<u>H</u>$_2$CH$_2$(Gln)), 1.97–1.96 (m, 1H,

CHC$\underline{H}$(CH_3)$_2$(Val)), 1.95 (s, 3H, COC$\underline{H}_3$), 1.70–1.64 (m, 1H, CHC$\underline{H}_2$CH$_2$(Gln)), 1.59–1.28 (m, 3H, 2xCHC$\underline{H}_2$CH(Leu) and 1xCH$_2$C$\underline{H}$(CH_3)$_2$(Leu)), 1.25 (d, 3H, J = 6.0 Hz, CHC$\underline{H}_3$(Thr)), 0.99 (d, 3H, J = 7.0 Hz, CH(C$\underline{H}_3$)$_2$(Val)), 0.98 (d, 3H, J = 7.0 Hz, CH(C$\underline{H}_3$)$_2$(Val)), 0.87 (d, 3H, J = 6.0 Hz, CH(C$\underline{H}_3$)$_2$(Leu)), 0.85 (d, 3H, J = 6.0 Hz, CH(C$\underline{H}_3$)$_2$(Leu)); HRMS (ES) calcd for $C_{40}H_{54}N_8O_{11}Na$ ([M+Na]$^+$), 845.3804; found, 845.3805.

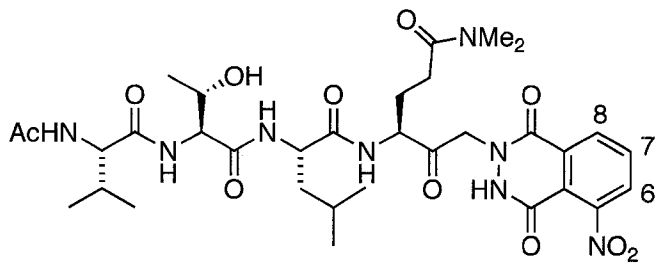

(*S*)-4-((*S*)-2-((2*S*,3*S*)-2-((*S*)-2-Acetamido-3-methylbutanamido)-3-hydroxybutanamido)-4-methylpentanamido)-*N*,*N*-dimethyl-6-(5-nitro-1,4-dioxo-3,4-dihydrophthalazin-2(1*H*)-yl)-5-oxohexanamide (28). This compound was prepared by Dr. Rajendra Jain and Dr. Hanna Pettersson in our group.[74] Trifluoroacetic acid (1.0 mL) was added to the benzyl protected tetrapeptide **27** (6.1 μmol) at 0° C, followed by trimethylsilyl trifluoroacetate (0.5 mL). The mixture was stirred at 0 °C for 2 h. Saturated $NaHCO_3$ solution was added and the mixture was extracted with EtOAc. The combined organic layers were dried over $MgSO_4$ and the solvent was removed in vacuo. The crude product was purified by HPLC (Waters C18 Bondpak 10 μm, 125 Å; 100 x 25 mm, 15 mL/min, 5 min elution of 30% acetonitrile followed by linear gradient elution over 50 min of 30 to 40% acetonitrile in 0.075% TFA/H_2O, t_R = 12 min) to yield **28** (4.5 mg, quant.). ^{1}H NMR (CD_3OD, 500 MHz) δ 8.33 (dd, 1H, J = 1.0, 8.0 Hz, H_6), 8.18 (d,

1H, J = 7.5 Hz, N$\underline{H}$), 8.08 (dd, 1H, J = 7.5, 8.0 Hz, H_7), 7.98 (dd, 1H, J = 1.0, 7.5 Hz, H_8), 7.72 (d, 1H, J = 8.0 Hz, N$\underline{H}$), 5.21 (d, 1H, J = 17.0 Hz, C$\underline{H}_2$N), 5.17 (d, 1H, J = 17.0 Hz, C$\underline{H}_2$N), 4.60 (dd, 1H, J = 8.0, 3.0 Hz, NHC$\underline{H}$CO(Gln)), 4.44–4.40 (m, 2H, 1xNHC$\underline{H}$CO(Leu) and 1xNHC$\underline{H}$CO(Thr)), 4.19 (dd, 1H, J = 6.5, 2.5 Hz, NHC$\underline{H}$CO(Val)), 4.12–4.04 (m, 1H, CH_3C$\underline{H}$OH(Thr)), 3.03 (s, 3H, NC$\underline{H}_3$), 2.93 (s, 3H, NC$\underline{H}_3$), 2.51–2.48 (m, 2H, C$\underline{H}_2$CO(Gln)), 2.33–2.21 (m, 1H, CHC$\underline{H}_2$$CH_2$(Gln)), 2.12–2.04 (m, 1H, CHC$\underline{H}$$(CH_3)_2$(Val)), 2.02 (s, 3H, COC$\underline{H}_3$), 1.99–1.93 (m, 1H, CHC$\underline{H}_2$$CH_2$(Gln)), 1.71–1.63 (m, 3H, 2xCHC$\underline{H}_2$CH(Leu) and 1xCH_2C$\underline{H}$$(CH_3)_2$(Leu)), 1.18 (d, 3H, J = 6.0 Hz, CHC$\underline{H}_3$(Thr)), 0.98 (d, 3H, J = 7.0 Hz, CH(C$\underline{H}_3$)$_2$(Val)), 0.97 (d, 3H, J = 6.5 Hz, CH(C$\underline{H}_3$)$_2$(Val)), 0.95 (d, 3H, J = 6.0 Hz, CH(C$\underline{H}_3$)$_2$(Leu)), 0.90 (d, 3H, J = 6.5 Hz, CH(C$\underline{H}_3$)$_2$(Leu)); HRMS (ES) calcd for $C_{33}H_{48}N_8O_{11}Na$ ([M+Na]$^+$), 755.3334; found, 755.3339.

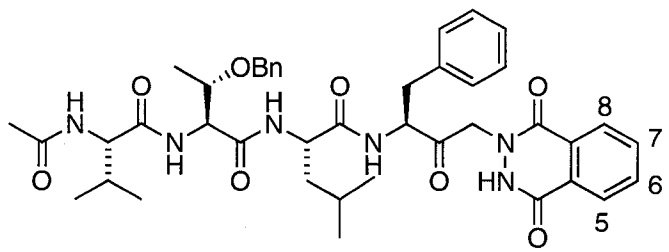

(*S*)-2-((2*S*,3*R*)-2-((*S*)-2-Acetamido-3-methylbutanamido)-3-(benzyloxy)butanamido)-*N*-((*S*)-4-(1,4-dioxo-3,4-dihydrophthalazin-2(1H)-yl)-3-oxo-1-phenylbutan-2-yl)-4-methylpentanamide (29). To a solution of **89** (16.5 mg, 0.045 mmol) was added TFA/DCM (2 mL, 1:1 ratio) at 0 °C. The resulting solution was stirred for 1.5 h, after which the reaction mixture was concentrated in vacuo and the residue was triturated with Et_2O to yield the trifluoroacetate salt. To a solution of trifluoroacetate salt in DMF (4

mL) at rt was added Ac-Val-Thr(OBn)-Leu-OH (30.6 mg, 0.045 mmol), DIPEA (16 mL, 0.090 mmol) and HBTU (17.7 mg, 0.045 mmol). After 4 h of stirring, the solvent was removed in vacuo. The crude product was purified by HPLC (Waters C18 Bondpak 10 μm, 125 Å; 100 x 25 mm, 15 mL/min, 5 min elution of 20% acetonitrile followed by a linear gradient elution over 25 min of 20 to 100% acetonitrile in 0.075% TFA/H_2O, t_R = 26 min) to afford **29** as a white solid (13.6 mg, 45%). $[\alpha]^{25}_D$= -49.4° (*c* 0.05, DMSO); IR (microscope) 3064, 2958, 1740, 1655, 1625, 1535, 1493 cm^{-1}; ^1H NMR (CD_3OD, 500 MHz) δ 8.30 (ddd, 1H, *J* = 7.8, 1.4, 0.7 Hz, H_5 or H_8), 8.10 (ddd, 1H, *J* = 7.8, 1.4, 0.7 Hz, H_5 or H_8), 7.83 (ddd, 1H, *J* = 7.8, 7.8, 1.4 Hz, H_6 or H_7), 7.63 (ddd, 1H, *J* = 7.8, 7.8, 1.4 Hz, H_6 or H_7), 7.36-7.12 (m, 10H, Ph$\underline{H}$), 5.12 (d, 1H, *J* = 17.0 Hz, C$\underline{H}_2$N), 5.04 (d, 1H, *J* = 17.0 Hz, C$\underline{H}_2$N), 4.58 (d, 1H, *J* = 11.3 Hz, OC$\underline{H}_2$Ph), 4.42 (d, 1H, *J* = 11.3 Hz, OC$\underline{H}_2$Ph), 4.40-4.33 (m, 2H, 1xNHC$\underline{H}$CO(Leu) and 1xNHC$\underline{H}$CO(Thr))), 4.13 (dq, 1H, *J* = 6.4, 3.1 Hz, CH_3C$\underline{H}$OBn(Thr)), 4.07 (d, 1H, *J* = 6.4 Hz, NHC$\underline{H}$CO(Val)), 3.48 (dd, 1H, *J* = 14.0, 7.1 Hz, NHC$\underline{H}$CO(Phe)), 3.26-3.18 (m, 1H, C$\underline{H}_2$Ph(Phe)), 2.94 (dd, 1H, *J* = 14.0, 9.7 Hz, C$\underline{H}_2$Ph(Phe)), 2.12 (m, 1H, C$\underline{H}$(CH_3)$_2$(Val)), 1.95 (s, 3H, COC$\underline{H}_3$), 1.57-1.28 (m, 2H, CHC$\underline{H}_2$CH(Leu)), 1.40-1.28 (m, 1H, CH_2C$\underline{H}$(CH_3)$_2$(Leu), 1.22 (d, 3H, *J* = 6.4 Hz, CHC$\underline{H}_3$(Thr)), 0.99 (d, 3H, *J* = 4.2 Hz, CH(C$\underline{H}_3$)$_2$(Val)), 0.98 (d, 3H, *J* = 4.2 Hz, CH(C$\underline{H}_3$)$_2$(Val)), 0.83 (d, 3H, *J* = 6.3 Hz, CH(C$\underline{H}_3$)$_2$(Leu)), 0.79 (d, 3H, *J* = 6.3 Hz, CH(C$\underline{H}_3$)$_2$(Leu)); ^{13}C NMR (DMSO-d_6, 125 MHz) δ 205.4, 174.8, 174.2, 172.3, 172.1, 161.5, 151.2, 142.1, 140.8, 137.0, 135.9, 132.5, 132.1, 131.6, 131.4, 130.8, 130.7, 129.8, 129.6, 127.5, 126.8, 77.4, 73.1, 71.3, 60.9, 59.7, 59.5, 53.6, 42.7, 37.6, 32.8, 26.6, 25.6, 25.1, 24.1, 21.9, 20.9, 19.1; HRMS (ES) calcd for $C_{42}H_{52}N_6O_8Na$ ([M+Na]$^+$), 791.3739; found, 791.3736.

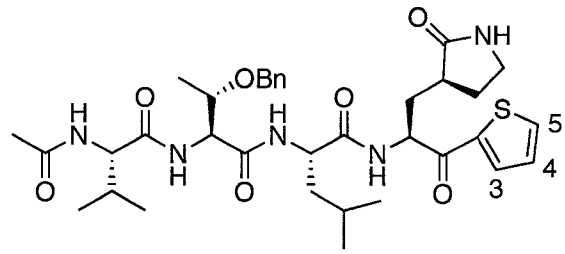

(*S*)-2-((2*S*,3*R*)-2-((*S*)-2-Acetamido-3-methylbutanamido)-3-(benzyloxy)butanamido)-4-methyl-N-((*S*)-1-oxo-3-((*S*)-2-oxopyrrolidin-3-yl)-1-(thiophen-2-yl)propan-2-yl)pentanamide (30). To a solution of **90** (33.8 mg, 0.1 mmol) was added TFA/CH_2Cl_2 (3 mL, 1:1 ratio) at 0 °C. The resulting solution was stirred for 1.5 h, after which the reaction mixture was concentrated in vacuo and the residue triturated with Et_2O to yield the trifluoroacetate salt. To a solution of trifluoroacetate salt in DMF (5 mL) at rt was added Ac-Val-Thr(OBn)-Leu-OH (46.4 mg, 0.1 mmol), DIPEA (35 uL, 0.2 mmol) and HBTU (39.5 mg, 0.1 mmol). After 4 h of stirring, the solvent was removed in vacuo. The crude product was purified by HPLC (Waters C18 Bondpak 10 μm, 125 Å; 100 x 25 mm, 15 mL/min, 10 min elution of 10% acetonitrile followed by linear gradient elution over 45 min of 10 to 100% acetonitrile in 0.075% TFA/H_2O, t_R = 34 min) to afford **30** (23.4 mg, 34%). $[\alpha]^{25}_D$= +2.8° (*c* 0.07, MeOH); IR (microscope) 3280, 3070, 2960, 2873, 1635, 1517, 1438 cm^{-1}; ^1H NMR (CD_3OD, 500 MHz) δ 7.93 (dd, 1H, *J* = 3.8, 1.0 Hz, H_5), 7.83 (dd, 1H, *J* = 4.9, 1.0 Hz, H_3), 7.34-7.26 (m, 5H, Ph<u>H</u>), 7.16 (dd, 1H, *J* = 4.9, 3.8 Hz, H_4), 5.14 (dd, 1H, *J* = 11.0, 4.0 Hz, NHC<u>H</u>CO(Gln)), 4.55 (d, 1H, *J* = 11.5 Hz, OC<u>H_2</u>Ph(Thr)), 4.46 (d, 1H, *J* = 11.5 Hz, OC<u>H_2</u>Ph(Thr)), 4.42-4.38 (m, 2H, 1xNHC<u>H</u>CO(Thr) and 1xNHC<u>H</u>CO(Leu)), 4.23 (d, 1H, *J* = 7.2 Hz, NHC<u>H</u>CO(Val)), 4.03 (dq, 1H, *J* = 6.3, 4.3 Hz, CH_3C<u>H</u>OBn(Thr)), 3.28-3.16 (m, 2H, NHC<u>H_2</u>CH_2(Gln)),

2.32-2.04 (m, 4H, 1xNHCH$_2$C$\underline{H}_2$(Gln), 2xCHC$\underline{H}_2$CH(Gln) and 1xCHC$\underline{H}$(CH$_3$)$_2$(Val)), 2.05 (s, 3H, COC$\underline{H}_3$), 1.86-1.72 (m, 2H, 1xNHCH$_2$C$\underline{H}_2$(Gln) and 1xCH$_2$C$\underline{H}$CO(Gln)), 1.64-1.52 (m, 3H, 2xCHC$\underline{H}_2$CH(Leu) and 1xCH$_2$C$\underline{H}$(CH$_3$)$_2$(Leu)), 1.19 (d, 3H, J = 6.3 Hz, CHC$\underline{H}_3$(Thr)), 0.97 (d, 3H, J = 6.8 Hz, CH(C$\underline{H}_3$)$_2$(Val)), 0.93 (d, 3H, J = 6.8 Hz, CH(C$\underline{H}_3$)$_2$(Val)), 0.87 (d, 3H, J = 6.0 Hz, CH(C$\underline{H}_3$)$_2$(Leu)), 0.85 (d, 3H, J = 6.0 Hz, CH(C$\underline{H}_3$)$_2$(Leu)); ^{13}C NMR (CD$_3$OD, 125 MHz) δ 192.6, 182.1, 174.8, 174.0, 173.9, 171.9, 142.8, 139.8, 136.1, 134.5, 129.6, 129.5, 129.1, 128.8, 75.9, 72.4, 60.5, 59.4, 55.7, 53.2, 41.9, 41.6, 40.0, 33.7, 31.6, 29.3, 25.8, 23.6, 22.5, 21.4, 19.9, 18.6, 16.5; HRMS (ES) calcd for $C_{35}H_{49}N_5O_7SNa$ ([M+Na]$^+$), 706.3245; found, 706.3247.

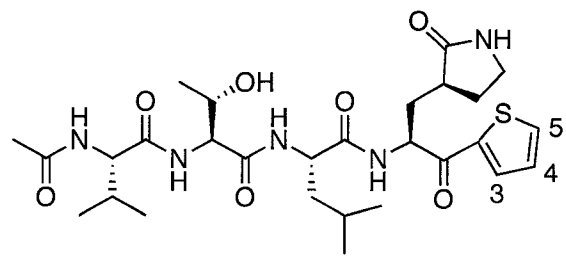

(*S*)-2-((2*S*,3*R*)-2-((*S*)-2-Acetamido-3-methylbutanamido)-3-hydroxybutanamido)-4-methyl-*N*-((*S*)-1-oxo-3-((*S*)-2-oxopyrrolidin-3-yl)-1-(thiophen-2-yl)propan-2-yl)pentanamide (31). To a solution of **30** (9.5 mg, 0.028 mmol) was added TFA/CH$_2$Cl$_2$ (1 mL, 1:1 ratio) at 0 °C. The resulting solution was stirred for 1.5 h, after which the reaction mixture was concentrated in vacuo and the residue triturated with Et$_2$O to yield the trifluoroacetate salt. To a solution of trifluoroacetate salt in DMF (1 mL) at rt was added Ac-Val-Thr(OH)-Leu-OH **92** (10.9 mg, 0.028 mmol), DIPEA (10 uL, 0.056 mmol) and HBTU (11.1 mg, 0.028 mmol). After 4 h of stirring, the solvent was removed in vacuo. The crude product was purified by HPLC (Waters C18 Bondpak 10 μm, 125 Å;

100 x 25 mm, 15 mL/min, 10 min elution of 10% acetonitrile followed by linear gradient elution over 45 min of 10 to 100% acetonitrile in 0.075% TFA/H_2O, t_R = 26 min) to afford **31** (8.3 mg, 48%). $[\alpha]^{25}_D$= -53.1° (*c* 0.11, MeOH); IR (microscope) 3277, 3083, 2962, 1632, 1537, 1438 cm^{-1}; ^1H NMR (CD_3OD, 400 MHz) δ 7.98 (dd, 1H, *J* = 3.9, 1.0 Hz, H_5), 7.88 (dd, 1H, *J* = 5.0, 1.0 Hz, H_3), 7.21 (dd, 1H, *J* = 5.0, 3.9 Hz, H_4), 5.33 (dd, 1H, *J* = 11.4, 4.0 Hz, NHC<u>H</u>CO(Gln)), 4.40 (dd, 1H, *J* = 8.5, 6.2 Hz, NHC<u>H</u>CO(Leu)), 4.36 (d, 1H, *J* = 4.4 Hz, NHC<u>H</u>CO(Thr)), 4.18 (d, 1H, *J* = 7.1 Hz, NHC<u>H</u>CO(Val)), 4.14 (dq, 1H, *J* = 6.4, 4.4 Hz, CH_3C<u>H</u>OH(Thr)), 3.36-3.31 (m, 2H, NHC<u>H_2</u>CH_2(Gln)), 2.64-2.55 (m, 1H, NHCH_2C<u>H_2</u>(Gln)), 2.42-2.32 (m, 1H, CHC<u>H_2</u>CH(Gln)), 2.24 (ddd, 1H, *J* = 14.0, 11.4, 4.0 Hz, CHC<u>H_2</u>CH(Gln)), 2.11-2.01 (m, 1H, CHC<u>H</u>$(CH_3)_2$(Val)), 2.00 (s, 3H, COC<u>H_3</u>), 1.92-1.74 (m, 2H, 1xNHCH_2C<u>H_2</u>(Gln) and 1xCH_2C<u>H</u>CO(Gln)), 1.66-1.54 (m, 3H, 2xCHC<u>H_2</u>CH(Leu) and 1xCH_2C<u>H</u>$(CH_3)_2$(Leu)), 1.16 (d, 3H, *J* = 6.4 Hz, CHC<u>H_3</u>(Thr)), 0.96 (d, 6H, *J* = 6.8 Hz, CH(C<u>H_3</u>)$_2$(Val)), 0.91 (d, 3H, *J* = 6.2 Hz, CH(C<u>H_3</u>)$_2$(Leu)), 0.86 (d, 3H, *J* = 6.2 Hz, CH(C<u>H_3</u>)$_2$(Leu)); ^{13}C NMR (CD_3OD, 125 MHz) δ 192.1, 181.7, 174.5, 173.9, 173.6, 171.9, 142.7, 136.0, 134.4, 129.4, 68.2, 60.7, 59.5, 54.3, 53.1, 41.4, 41.3, 39.4, 34.0, 31.3, 28.8, 25.6, 23.2, 22.2, 21.7, 19.7, 19.5, 18.5; HRMS (ES) calcd for $C_{28}H_{43}N_5O_7SNa$ ([M+Na]$^+$), 616.2775; found, 616.2775.

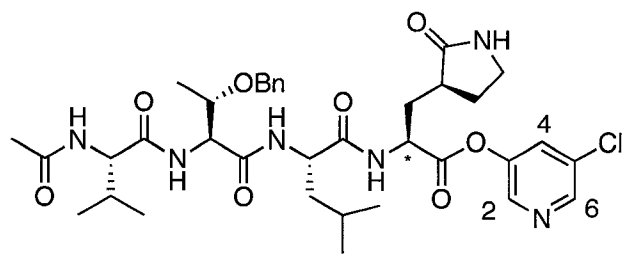

(5*S*,8*S*,11*S*)-5-Chloropyridin-3-yl-8-((*R*)-1-(benzyloxyl)ethyl)-5-isobutyl-11-isopropyl-4,7,10,13-tetraoxo-2-(((*S*)-2-oxopyrrolidin-3-yl)methyl-3,6,9,12-tetraazatetradecan-1-oate (32). To a solution of **96** (26 mg, 0.043 mmol) in DMF (6 mL) at rt was added DIPEA (7.4 uL, 0.043 mmol) and HBTU (16.2 mg, 0.043 mmol) and 3-chloro-5-hydroxy-pyridine (5.5 mg, 0.043 mmol). After 4 h of stirring, the solvent was removed in vacuo. The crude product was purified by HPLC (Waters C18 Bondpak 10 μm, 125 Å; 100 x 25 mm, 15 mL/min, 10 min elution of 10% acetonitrile followed by a linear gradient elution over 45 min of 10 to 100% acetonitrile in 0.075% TFA/H_2O, t_R = 34 min) to afford **32** (5.6 mg, 18%). (Mixture of isomers). IR (microscope) 3286, 3067, 2961, 2873, 2048, 1771, 1631, 1548, 1444 cm^{-1}; ^1H NMR (CD_3OD, 500 MHz) δ 8.50-8.43 (m, 1H, H_2 or H_6), 8.39-8.34 (m, 1H, H_2 or H_6), 7.78 (dd, 0.5H, J = 2.3, 2.3 Hz, H_4), 7.74 (dd, 0.5H, J = 2.3, 2.3 Hz, H_4), 7.32-7.22 (m, 5H, Ph<u>H</u>), 4.58 (d, 0.5H, J = 11.3 Hz, OC<u>H</u>$_2$Ph), 4.56 (d, 0.5H, J = 11.3 Hz, OC<u>H</u>$_2$Ph(Thr)), 4.52-4.42 (m, 4H, 1xNHC<u>H</u>CO(Gln), 1xOC<u>H</u>$_2$Ph(Thr), 1xCH$_3$C<u>H</u>OBn(Thr) and 1xNHC<u>H</u>CO(Thr)), 4.14 (d, 0.5H, J = 6.7 Hz, NHC<u>H</u>CO(Val)), 4.14-4.10 (m, 1H, NHC<u>H</u>CO(Leu)), 4.09 (d, 0.5H, J = 6.7 Hz, NHC<u>H</u>CO(Val)), 3.28-3.16 (m, 2H, NHC<u>H</u>$_2$CH$_2$(Gln)), 2.65-2.45 (m, 1H, NHCH$_2$C<u>H</u>$_2$(Gln)), 2.43-2.32 (m, 2H, CHC<u>H</u>$_2$CH(Gln)), 2.31-2.18 (m, 1H, CHC<u>H</u>(CH$_3$)$_2$(Val)), 2.14-1.96 (m, 2H, 1xCH$_2$C<u>H</u>CO(Gln) and 1xNHCH$_2$C<u>H</u>$_2$(Gln))), 1.95 (s, 1.5H, COC<u>H</u>$_3$), 1.95 (s, 1.5H, COC<u>H</u>$_3$), 1.88-1.56 (m, 3H, 2xCHC<u>H</u>$_2$CH(Leu) and 1xCH$_2$C<u>H</u>(CH$_3$)$_2$(Leu)), 1.23 (d, 1.5H, J = 6.4 Hz, CHC<u>H</u>$_3$(Thr)), 1.22 (d, 1.5H, J = 6.4 Hz, CH(C<u>H</u>$_3$)$_2$(Thr)), 1.00-0.94 (m, 6H, CH(C<u>H</u>$_3$)$_2$(Val)), 0.90-0.84 (m, 6H, CH(C<u>H</u>$_3$)$_2$(Leu)); HRMS (ES) calcd for $C_{36}H_{49}N_6O_8ClNa$ ([M+Na]$^+$), 751.3193; found, 751.3187.

General procedure for the preparation of pyridinyl esters 33-40: To a solution of carboxylic acid (2 mmol, 1.0 equiv.) in DCM (5 mL) at rt was added thionyl chloride (0.4 mL, 1.3 equiv.) and a catalytic amount of DMF (2 drops). After 20 h of stirring, the solvent was removed in vacuo to afford the acyl chloride product. A solution of the acyl chloride in DCM (5 mL) was added dropwise to a solution of pyridinyl alcohol or amine (1.0 equiv.) and pyridine (0.18 mL, 1.1 equiv.) in DCM (5 mL) at 0 °C. After 3 h of stirring, the solvent was removed in vacuo. The residue was diluted with H_2O and extracted with EtOAc. The combined organic layers were washed with brine, dried over $MgSO_4$ and then concentrated in vacuo. Purification of the crude product by flash chromatography on silica gel afforded the product as a solid in 62-87% yield.

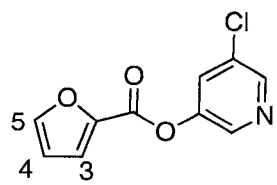

5-Chloropyridin-3-yl furan-2-carboxylate (33). The title compound **33** was obtained following the standard procedure described above. Purification of the crude product by flash chromatography on silica gel (25/75 EtOAc/hexanes) afforded **33** as a white solid (360 mg, 81%). IR ($CHCl_3$ cast) 3131, 3077, 1749, 1564, 1464, 1438 cm^{-1}; ^1H NMR ($CDCl_3$, 500 MHz) δ 8.60 (d, 1H, J = 2.0 Hz, Py<u>H</u>), 8.43 (d, 1H, J = 2.2 Hz, Py<u>H</u>), 7.67 (dd, 1H, J = 1.7, 0.8 Hz, H_5), 7.64 (dd, 1H, J = 2.2, 2.0 Hz, Py<u>H</u>), 7.40 (dd, 1H, J = 3.6, 0.8 Hz, H_3), 6.60 (dd, 1H, J = 3.6, 1.7 Hz, H_4); ^{13}C NMR ($CDCl_3$, 125 MHz) δ 155.8,

147.9, 146.8, 146.1, 142.9, 141.3, 131.8, 129.5, 120.7, 112.5; HRMS (EI) calcd for $C_{10}H_6ClNO_3$ (M^+), 223.0036; found, 223.0035.

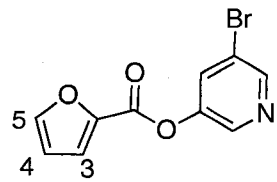

5-Bromopyridin-3-yl furan-2-carboxylate (34). The title compound **34** was obtained following the standard procedure described above. Purification of the crude product by flash chromatography on silica gel (75/25 EtOAc/hexanes) afforded **34** as a white solid (330 mg, 62%). IR ($CHCl_3$ cast) 3131, 3071, 1745, 1559, 1436, 1421 cm^{-1}; ^1H NMR ($CDCl_3$, 400 MHz) δ 8.62-8.58 (m, 1H, Py<u>H</u>), 8.62-8.58 (m, 1H, Py<u>H</u>), 7.79 (dd, 1H, J = 2.0, 2.0 Hz, Py<u>H</u>), 7.72 (dd, 1H, J = 1.7, 0.8 Hz, H_5), 7.44 (dd, 1H, J = 3.5, 0.8 Hz, H_3), 6.63 (dd, 1H, J = 3.5, 1.7 Hz, H_4); ^{13}C NMR ($CDCl_3$, 100 MHz) δ 155.8, 148.2, 147.9, 146.9, 142.9, 141.6, 132.2, 120.7, 120.0, 112.5; HRMS (EI) calcd for $C_{10}H_6BrNO_3$ (M^+), 266.9531; found, 266.9535.

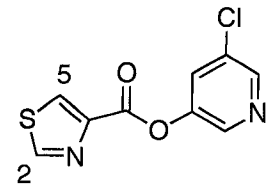

5-Chloropyridin-3-yl thiazole-4-carboxylate (35). The title compound **35** was obtained following the standard procedure described above for the preparation of pyridinyl esters. Purification of the crude product by flash chromatography on silica gel (25/75 EtOAc/hexanes) afforded **35** as a white solid (330 mg, 69%). IR ($CHCl_3$ cast) 3121,

3087, 1745, 1573, 1491, 1419 cm^{-1}; ^1H NMR ($CDCl_3$, 500 MHz) δ 8.93 (d, 1H, J = 2.1 Hz, H_2), 8.49 (d, 1H, J = 2.0 Hz, Py<u>H</u>), 8.47 (d, 1H, J = 2.4 Hz, Py<u>H</u>), 8.46 (d, 1H, J = 2.1 Hz, H_5), 7.68 (dd, 1H, J = 2.4, 2.1 Hz, Py<u>H</u>); ^{13}C NMR ($CDCl_3$, 125 MHz) δ 158.6, 147.1, 146.3, 146.1, 141.3, 131.9, 129.9, 129.5; HRMS (EI) calcd for $C_9H_5ClN_2O_2S$ (M^+), 239.9760; found, 239.9765.

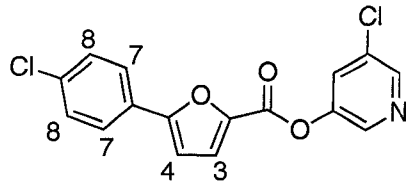

5-Chloropyridin-3-yl 5-(4-chlorophenyl)furan-2-carboxylate (36). The title compound **36** was obtained following the standard procedure described above for the preparation of pyridinyl esters. Purification of the crude product by flash chromatography on silica gel (25/75 EtOAc/hexanes) afforded **36** as a white solid (500 mg, 75%). IR ($CHCl_3$ cast) 3136, 3077, 1736, 1602, 1575, 1565, 1521, 1473, 1438, 1421, 1412 cm^{-1}; ^1H NMR ($CDCl_3$, 500 MHz) δ 8.48 (d, 1H, J = 2.1 Hz, Py<u>H</u>), 8.46 (d, 1H, J = 2.3 Hz, Py<u>H</u>), 7.73 (d, 2H, J = 8.5 Hz, H_7), 7.67 (dd, 1H, J = 2.3, 2.1 Hz, Py<u>H</u>), 7.49 (d, 1H, J = 3.7 Hz, H_3), 7.40 (d, 2H, J = 8.5 Hz, H_8), 6.81 (d, 1H, J = 3.7 Hz, H_4); ^{13}C NMR ($CDCl_3$, 125 MHz) δ 158.1, 155.7, 146.9, 146.1, 141.9, 141.3, 135.5, 131.8, 129.4, 129.3, 127.5, 126.3, 122.7, 107.7; HRMS (EI) calcd for $C_{16}H_9Cl_2NO_3$ (M^+), 332.9959; found, 332.9958.

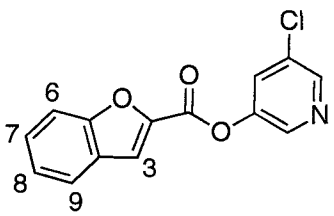

5-Chloropyridin-3-yl benzofuran-2-carboxylate (37). The title compound **37** was obtained following the standard procedure described above. Purification of the crude product by flash chromatography on silica gel (25/75 EtOAc/hexanes) afforded **37** as a white solid (360 mg, 66%). IR ($CHCl_3$ cast) 3034, 1739, 1558, 1443 cm^{-1}; ^1H NMR ($CDCl_3$, 500 MHz) δ 8.55-8.52 (m, 2H, Py<u>H</u>), 7.76 (d, 1H, J = 1.0 Hz, H_3), 7.73 (ddd, 1H, J = 8.0, 1.3, 0.7 Hz, H_6), 7.71 (dd, 1H, J = 2.2, 2.2 Hz, Py<u>H</u>), 7.62 (dddd, 1H, J = 8.5, 1.0, 1.0, 0.7 Hz, H_9), 7.51 (ddd, 1H, J = 8.5, 7.2, 1.3 Hz, H_8), 7.35 (ddd, 1H, J = 8.0, 7.2, 1.0 Hz, H_7); ^{13}C NMR ($CDCl_3$, 125 MHz) δ 156.8, 156.3, 146.8, 146.3, 143.5, 141.2, 131.9, 129.3, 128.7, 126.7, 124.3, 123.2, 116.6, 112.5; HRMS (EI) calcd for $C_{14}H_8ClNO_3$ (M^+), 273.0193; found, 273.0192.

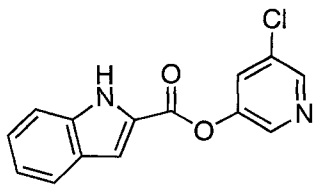

5-Chloropyridin-3-yl 1*H*-indole-2-carboxylate (38). The title compound **38** was obtained following the standard procedure described above for the preparation of pyridinyl esters. Purification of the crude product by flash chromatography on silica gel (25/75 EtOAc/hexanes) afforded **38** as a white solid (460 mg, 85%). IR ($CHCl_3$ cast) 3056, 1729, 1577, 1520, 1421 cm^{-1}; ^1H NMR ($CDCl_3$, 500 MHz) δ 9.05 (br, 1H, N<u>H</u>), 8.52-8.48 (m, 2H, Py<u>H</u>), 7.73 (dd, 1H, J = 8.2, 0.7 Hz, Ar<u>H</u>), 7.70 (dd, 1H, J = 2.2, 2.2 Hz, Py<u>H</u>), 7.50-7.48 (m, 1H, Ar<u>H</u>), 7.47-7.46 (m, 1H, Ar<u>H</u>), 7.38 (ddd, 1H, J = 8.2, 7.0, 1.2 Hz, Ar<u>H</u>), 7.20 (ddd, 1H, J = 8.1, 7.0, 1.0 Hz, Ar<u>H</u>); ^{13}C NMR ($CDCl_3$, 125 MHz) δ

159.3, 147.1, 146.1, 141.3, 137.6, 131.9, 129.5, 127.4, 126.6, 125.0, 123.0, 121.4, 112.0, 111.4; HRMS (EI) calcd for $C_{14}H_9ClN_2O_2$ (M^+), 272.0353; found, 272.0352.

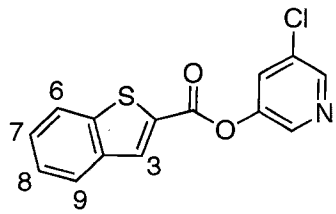

5-Chloropyridin-3-yl benzo[*b*]thiophene-2-carboxylate (39). The title compound **39** was obtained following the standard procedure described above for the preparation of pyridinyl esters. Purification of the crude product by flash chromatography on silica gel (25/75 EtOAc/hexanes) afforded **39** as a white solid (400 mg, 69%). IR ($CHCl_3$ cast) 3097, 1733, 1517, 1458, 1437 cm^{-1}; ^1H NMR ($CDCl_3$, 500 MHz) δ 8.55-8.50 (m, 2H, Py<u>H</u>), 8.26 (d, 1H, J = 0.6 Hz, H_3), 7.97-7.91 (m, 2H, H_6 and H_9), 7.71 (dd, 1H, J = 2.2, 2.2 Hz, Py<u>H</u>), 7.51 (ddd, 1H, J = 8.2, 7.1, 1.3 Hz, H_7 or H_8), 7.45 (ddd, 1H, J = 8.1, 7.1, 1.1 Hz, H_7 or H_8); ^{13}C NMR ($CDCl_3$, 125 MHz) δ 160.3, 147.2, 146.2, 142.9, 141.3, 138.5, 132.9, 131.9, 131.1, 129.5, 127.8, 126.0, 125.4, 122.9; HRMS (EI) calcd for $C_{14}H_8ClNO_2S$ (M^+), 288.9964; found, 288.9956.

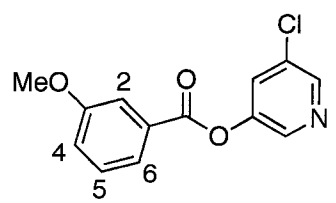

5-Chloropyridin-3-yl 3-methoxybenzoate (40). The title compound **40** was obtained following the standard procedure described above for the preparation of pyridinyl esters.

Purification of the crude product by flash chromatography on silica gel (25/75 EtOAc/hexanes) afforded **40** as a white solid (460 mg, 87%). IR ($CHCl_3$ cast) 3072, 2836, 1744, 1600, 1586, 1488, 1420 cm^{-1}; ^1H NMR ($CDCl_3$, 400 MHz) δ 8.49 (d, 1H, J = 2.1 Hz, Py<u>H</u>), 8.46 (d, 1H, J = 2.3 Hz, Py<u>H</u>), 7.77 (ddd, 1H, J = 7.8, 1.5, 1.0 Hz, H_4), 7.68-7.66 (m, 2H, H_2 and Py<u>H</u>), 7.42 (ddd, 1H, J = 8.2, 7.8, 0.4 Hz, H_5), 7.20 (ddd, 1H, J = 8.3, 2.7, 1.0 Hz, H_6), 3.86 (s, 3H, OC<u>H</u>$_3$); ^{13}C NMR ($CDCl_3$, 125 MHz) δ 164.1, 159.8, 147.5, 146.0, 141.4, 131.8, 129.8, 129.6, 129.5, 122.7, 120.7, 114.7, 55.5; HRMS (EI) calcd for $C_{13}H_{10}ClNO_3$ (M^+), 263.0349; found, 263.0355.

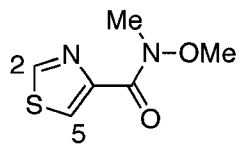

***N*-Methoxy-*N*-methylthiazole-4-carboxamide (43b).** To a solution of thiazole-4-carboxylic acid (194 mg, 1.5 mmol) in DCM (20 mL) at rt was added thionyl chloride (0.4 mL, 5.2 mmol) and a catalytic amount of DMF (2 drops). After 30 h of stirring, the solvent was removed in vacuo to afford the acyl chloride product. A solution of the acyl chloride in DCM (10 mL) was added dropwise to a solution of Weinreb amine (146 mg, 1.5 mmol) and pyridine (0.36 mL, 4.5 mmol) in DCM (10 mL) at 0 °C. After 3 h of stirring, the solvent was removed in vacuo. The residue was treated with saturated $NaHCO_3$ solution and then extracted with EtOAc. The combined organic layers were washed with brine, dried over $MgSO_4$ and then concentrated in vacuo. Purification of the crude product by flash chromatography on silica gel (EtOAc) afforded **43b** as a pale yellow oil (180 mg, 70%). IR ($CHCl_3$ cast) 3078, 2974, 2934, 1641, 1498, 1425 cm^{-1}; ^1H NMR ($CDCl_3$, 500 MHz) δ 8.78 (d, 1H, J = 2.0 Hz, H_2), 8.05 (d, 1H, J = 2.0 Hz, H_5),

3.74 (s, 3H, OC$\underline{H}_3$), 3.40 (s, 3H, NC$\underline{H}_3$); ^{13}C NMR ($CDCl_3$, 125 MHz) δ 162.7, 149.6, 124.8, 124.6, 61.5, 61.4; HRMS (EI) calcd for $C_6H_8N_2O_2S$ (M^+), 172.0307; found, 172.0304.

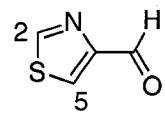

Thiazole-4-carbaldehyde (43). To a solution of **43b** (100 mg, 0.58 mmol) in THF (5 mL) at -30 °C was added $LiAlH_4$ (2.3 mL, 1 M solution in THF, 2.3 mmol) dropwise over 10 min. After 4 h of stirring at -30 °C, the reaction was complete, which was monitored by TLC. The reaction mixture was cooled on ice bath and water was added slowly, followed by DCM extraction. The combined organic layers were dried over $MgSO_4$ and the solvent removed in vacuo to obtain the crude product, which was purified by flash column chromatography on silica gel (EtOAc) to obtain the product **43** (30 mg, 46%) as a light yellow solid. Literature compound.[75] IR ($CHCl_3$ cast) 2905, 1672, 1429 cm^{-1}; ^{1}H NMR ($CDCl_3$, 500 MHz) δ 10.2 (s, 1H, C$\underline{H}$O), 8.92 (d, 1H, J = 2.0 Hz, H_2), 8.26 (d, 1H, J = 2.0 Hz, H_5); HRMS (ES) calcd for C_4H_3NOS (M^+), 112.9935; found, 112.9935.

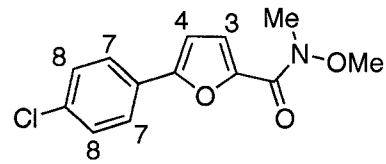

5-(4-Chlorophenyl)-*N*-methoxy-*N*-methylfuran-2-carboxamide (44b). To a solution of 5-(4-chlorophenyl)furan-2-carboxylic acid (334 mg, 2 mmol) in DMF (10 mL) at 0 °C

was added Weinreb amine (147 mg, 2 mmol), EDCI (290 mg, 2 mmol), HOBt (204 mg, 2 mmol) and DIPEA (0.54 mL, 4 mmol). The resulting solution was stirred overnight while warming slowly to rt. The reaction mixture was then diluted with DCM (50 mL) and washed with water and brine. The combined organic layers were dried over $MgSO_4$ and then concentrated in vacuo. Purification of the crude product by flash chromatography on silica gel (50/50 EtOAc/hexanes) afforded **44b** as a white solid (280 mg, 53%). IR ($CHCl_3$ cast) 3109, 2971, 2935, 1640, 1583, 1519, 1477, 1414 cm^{-1}; ^1H NMR ($CDCl_3$, 500 MHz) δ 7.66 (d, 2H, J = 8.5 Hz, H_7), 7.33 (d, 2H, J = 8.5 Hz, H_8), 7.17 (d, 1H, J = 3.6 Hz, H_3), 6.69 (d, 1H, J = 3.6 Hz, H_4), 3.80 (s, 3H, $OC\underline{H}_3$), 3.38 (s, 3H, $NC\underline{H}_3$); ^{13}C NMR ($CDCl_3$, 125 MHz) δ 159.0, 155.1, 145.2, 134.4, 129.1, 128.2, 126.0, 119.6, 107.1, 61.4, 33.3; HRMS (EI) calcd for $C_{13}H_{12}ClNO_3$ (M^+), 265.0506; found, 265.0502.

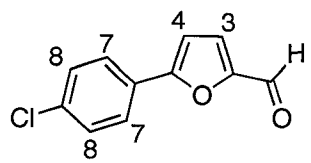

5-(4-Chlorophenyl)furan-2-carbaldehyde (44). To a solution of **44b** (133 mg, 0.5 mmol) in THF (5 mL) at -30 °C was added $LiAlH_4$ (1.5 mL, 1 M solution in THF, 1.5 mmol) dropwise over 10 min. After 4 h of stirring at -30 °C, the reaction was complete. The reaction mixture was cooled on ice bath and water was added slowly, followed by DCM extraction. The combined organic layers were dried over $MgSO_4$ and the solvent removed in vacuo to obtain the crude mixture, which was purified by flash column chromatography on silica gel (50/50 EtOAc/hexanes) to obtain product **44** (70 mg, 68%) as a light yellow solid. Literature compound.[76] IR ($CHCl_3$ cast) 3111, 2855, 1685, 1662, 1478 cm^{-1}; ^1H NMR ($CDCl_3$, 500 MHz) δ 9.61 (s, 1H, $C\underline{H}O$), 7.71 (d, 2H, J = 8.6 Hz,

H_7), 7.38 (d, 2H, J = 8.6 Hz, H_8), 7.28 (d, 1H, J = 3.8 Hz, H_3), 6.80 (d, 1H, J = 3.8 Hz, H_4); HRMS (EI) calcd for $C_{11}H_7ClO_2$ (M^+), 206.0135; found, 206.0134.

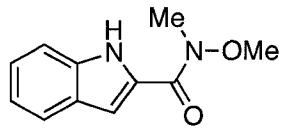

***N*-Methoxy-*N*-methyl-1*H*-indole-2-carboxamide (45b).** The title compound **45b** was obtained from 1*H*-indole-2-carboxylic acid (242 mg, 1.50 mmol) following the procedure described for the preparation of **44b**. The product was obtained as a light yellow solid (210 mg, 68%). Literature compound.[77] IR ($CHCl_3$ cast) 3275, 3080, 2932, 1605, 1564, 1535, 1454, 1411 cm^{-1}; ^1H NMR ($CDCl_3$, 400 MHz) δ 9.91 (s, 1H, N<u>H</u>), 7.73 (d, 1H, J = 8.1 Hz, Ar<u>H</u>), 7.49 (d, 1H, J = 8.4 Hz, Ar<u>H</u>), 7.33 (dd, 1H, J = 8.2, 7.1 Hz, Ar<u>H</u>), 7.28 (s, 1H, Ar<u>H</u>), 7.16 (dd, 1H, J = 8.0, 7.2 Hz, Ar<u>H</u>), 3.86 (s, 3H, OC<u>H</u>$_3$), 3.49 (s, 3H, NC<u>H</u>$_3$); HRMS (EI) calcd for $C_{11}H_{12}N_2O_2$ (M^+), 204.0899; found, 204.0895.

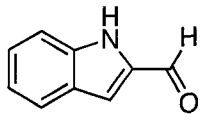

1*H*-indole-2-carbaldehyde (45). The title compound **45** was obtained from **45b** (100 mg, 0.49 mmol) following the procedure described for the preparation of **44**. The product was obtained as a white solid (6.4 mg, 9%). Literature compound.[77] IR ($CHCl_3$ cast) 3180, 3115, 3080, 3056, 2992, 2925, 2853, 2752, 2676, 1684, 1651, 1620, 1528, 1448, 1429 cm^{-1}; ^1H NMR ($CDCl_3$, 400 MHz) δ 9.87 (s, 1H, C<u>H</u>O), 9.06 (br, 1H, N<u>H</u>), 7.77 (ddd, 1H, J = 8.1, 1.8, 1.0 Hz, Ar<u>H</u>), 7.47 (ddd, 1H, J = 8.4, 2.0, 1.0 Hz, Ar<u>H</u>), 7.42 (ddd, 1H, J =

8.4, 6.1, 1.1 Hz, Ar<u>H</u>), 7.30 (dd, 1H, J = 2.1, 1.0 Hz, Ar<u>H</u>), 7.20 (ddd, 1H, J = 8.0, 6.7, 1.1 Hz, Ar<u>H</u>); HRMS (EI) calcd for C_9H_7NO (M^+), 145.0528; found, 145.0526.

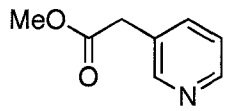

Methyl 2-(pyridin-3-yl)acetate (46b). To a solution of 3-pyridinylacetic acid (0.45 g, 2.60 mmol) in CH_2Cl_2 (20 mL) was added $SOCl_2$ (0.70 mL, 4.55 mmol) and 2 drops of DMF as a catalyst. The reaction mixture was stirred overnight, and the solvent was removed under reduced pressure. The resulting acetyl chloride was treated with MeOH (20 mL) at 0 °C, and then refluxed for 2 h. The solvent was again removed in vacuo, and the residue was diluted with saturated $NaHCO_3$ solution (20 mL), and extracted with EtOAc (3 x 20 mL). The combined organic layers were washed with brine (20 mL), dried over $MgSO_4$ and concentrated in vacuo. Purification of the crude product by flash chromatography on silica gel (EtOAc) afforded the product **46b** as a pale yellow liquid (0.31 g, 79%). Literature compound.[78] IR (microscope) 3403, 3033, 3002, 2954, 1739, 1595, 1578, 1428 cm^{-1}; ^1H NMR ($CDCl_3$, 400 MHz) δ 8.42-8.40 (m, 1H, Py<u>H</u>), 8.40 (d, 1H, J = 1.5 Hz, Py<u>H</u>), 7.53 (m, 1H, Py<u>H</u>), 7.15 (ddd, 1H, J = 7.8, 4.8, 0.9 Hz, Py<u>H</u>), 3.58 (s, 3H, $CO_2C\underline{H}_3$), 3.52 (s, 2H, $C\underline{H}_2CO_2CH_3$); HRMS (EI) calcd for $C_8H_9NO_2$ (M^+),
151.0633, found, 151.0632. (s, 3H, $CO_2C\underline{H}_3$), 3.52 (s, 2H, $C\underline{H}_2CO_2CH_3$); HRMS (EI) calcd for $C_8H_9NO_2$ (M^+),

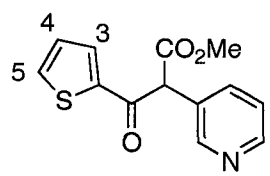

Methyl 3-oxo-2-(pyridin-3-yl)-3-(thiophen-2-yl)propanoate (46c). To a solution of 2-thiophenecarboxylic acid (0.79 g, 6.17 mmol) in THF (20 mL) was added CDI (1.11 g, 6.8 mmol). The resulting solution was stirred at rt for 1 h. In a separate flask, to a solution of methyl 2-(pyridin-3-yl)acetate **46b** (1.96 g, 13.0 mmol) in THF (45 mL) at -78 °C was added LiHMDS (14.2 mL, 1.0 M solution in THF, 14.2 mmol) dropwise. After stirring for 1.5 h at -78 °C, the thiophenyl carboxylic acid/CDI solution prepared above was added dropwise to the lithium enolate solution. The resulting mixture was stirred for another 2.5 h at -78 °C and then quenched with 1.0 M aqueous HCl (20 mL). The pH of the solution was adjusted to around 9 by saturated $NaHCO_3$ and the solution was extracted with EtOAc (3 x 50 mL). The combined organic layers were washed with brine (30 mL), dried over $MgSO_4$ and concentrated in vacuo. Purification of the crude product by flash chromatography on silica gel (EtOAc) afforded **46c** as a yellow liquid with ~10% impurities (1.00 g, 62%), and recovered starting material **46b** (0.71 g). IR ($CHCl_3$ cast): 3090, 2952, 2843, 1744, 1660, 1591, 1577, 1551, 1517, 1480, 1427, 1412 cm^{-1}; ^1H NMR ($CDCl_3$, 500 MHz) δ 8.68-8.56 (m, 2H, Py<u>H</u>), 7.75 (dd, 1H, J = 3.8, 1.1 Hz, H_5), 7.71 (dd, 1H, J = 4.9, 1.1 Hz, H_3), 7.39 (m, 2H, Py<u>H</u>), 7.13 (dd, 1H, J = 4.9, 3.8 Hz, H_4), 5.45 (s, 1H, COC<u>H</u>CO_2), 3.78 (s, 3H, $CO_2C\underline{H}_3$); ^{13}C NMR ($CDCl_3$, 125 MHz) δ 170.5, 165.9, 147.8, 145.9, 139.3, 134.3, 133.8, 132.7, 130.9, 127.8, 124.2, 52.3, 37.9; HRMS (EI) calcd for $C_{13}H_{11}NO_3S$ (M^+), 261.0460; found, 261.0453.

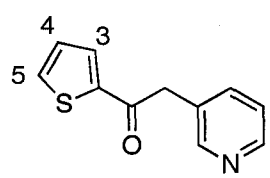

2-(Pyridin-3-yl)-1-(thiophen-2-yl)ethanone (46). A solution of **46c** (1.00 g, 3.83 mmol) in 50% H_2SO_4 (15 mL) was refluxed at 100 °C overnight. NaOH (30 mL, 6.6 M) and saturated $NaHCO_3$ solution (25 mL) were added to adjust the pH of the solution to 7. The solution was extracted with EtOAc (3 x 50 mL). The combined organic layers were washed with H_2O (20 mL), brine (20 mL), dried over $MgSO_4$ and concentrated in vacuo. Purification of the crude product by flash chromatography on silica gel (EtOAc) afforded the product **46** as a light yellow solid (0.66 g, 85%). Literature compound.[79] IR ($CHCl_3$ cast): 3087, 3030, 2901, 1660, 1593, 1576, 1518, 1480, 1413 cm^{-1}; ^1H NMR ($CDCl_3$, 500 MHz) δ 8.56-8.47 (m, 2H, Py<u>H</u>), 7.76 (dd, 1H, J = 3.8, 0.9 Hz, H_5), 7.62 (dd, 1H, J = 5.0, 0.9 Hz, H_3), 7.59 (d, 1H, J = 7.8 Hz, Py<u>H</u>), 7.21 (dd, 1H, J = 7.6, 5.0 Hz, Py<u>H</u>), 7.10 (dd, 1H, J = 4.8, 3.8 Hz, H_4), 4.19 (s, 2H, COC<u>H</u>$_2$); HRMS (EI) calcd for $C_{11}H_9NOS$ (M^+), 203.0405; found, 203.0405.

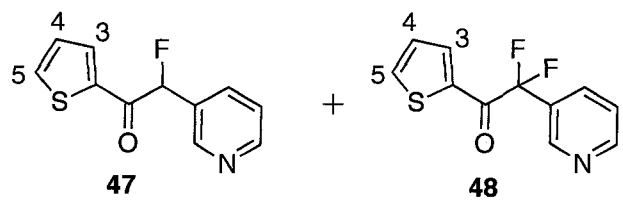

2-Fluoro-2-(pyridin-3-yl)-1-(thiophen-2-yl)ethanone (47) and 2,2-difluoro-2-(pyridin-3-yl)-1-(thiophen-2-yl)ethanone (48). To a solution of **46** (0.14 g, 0.70 mmol) in dry THF (25 mL) at -78 °C was added LiHMDS (0.84 mL, 1.0 M solution in THF, 0.84 mmol) dropwise over 15 min. After 1.5 h of stirring at -78 °C, a solution of NFSi (0.24 g, 0.77 mmol) in THF (5 mL) was added slowly. The reaction mixture was stirred at -78 °C for 6 h and then quenched with 1 M aqueous HCl (1 mL). Saturated $NaHCO_3$ was added to adjust the pH to 9 and the resulting solution was extracted with $CHCl_3$ (3 x 50 mL).

The combined organic layers were washed with brine (20 mL), dried over $MgSO_4$ and concentrated in vacuo. Purification of the crude product by flash chromatography on silica gel (EtOAc) afforded **47** as a brown solid (97.5 mg, 63%) and **48** as a brown solid (9.7 mg, 6%).

Data for **47**. IR ($CHCl_3$ cast): 3093, 1673, 1592, 1577, 1515, 1479, 1428, 1412 cm^{-1}; ^1H NMR ($CDCl_3$, 500 MHz) 8.81-8.77 (m, 1H, Py<u>H</u>), 8.66-8.62 (m, 1H, Py<u>H</u>), 7.99-7.95 (m, 1H, Py<u>H</u>), 7.79 (d, 1H, J = 7.6 Hz, Py<u>H</u>), 7.72 (d, 1H, J = 4.9 Hz, H_5), 7.31 (dd, 1H, J = 7.3, 5.0 Hz, H_3), 7.14 (dd, 1H, J = 4.8, 4.0 Hz, H_4), 6.28 (d, 1H, $J_{H\text{-}F}$ = 47.9 Hz, COC<u>H</u>F); ^{13}C NMR ($CDCl_3$, 125 MHz) δ 187.0 (d, $J_{C\text{-}F}$ = 23.8 Hz), 150.7 (d, $J_{C\text{-}F}$ = 2.0 Hz), 148.1 (d, $J_{C\text{-}F}$ = 7.3 Hz), 139.5 (d, $J_{C\text{-}F}$ = 3.0 Hz), 135.9 (d, $J_{C\text{-}F}$ = 1.6 Hz), 134.6 (d, $J_{C\text{-}F}$ = 7.3 Hz), 134.4 (d, $J_{C\text{-}F}$ = 5.8 Hz), 130.5(d, $J_{C\text{-}F}$ = 20.6 Hz), 128.6, 123.7, 93.0 (d, $J_{C\text{-}F}$ = 189.4 Hz); HRMS (EI) calcd for $C_{11}H_8FNOS$ (M^+), 221.0311; found, 221.0311.

Data for **48**. IR ($CHCl_3$ cast): 3105, 1677, 1650, 1632, 1593, 1514, 1502, 1480, 1424, 1410 cm^{-1}; ^1H NMR ($CDCl_3$, 500 MHz) 8.92-8.88 (m, 1H, Py<u>H</u>), 8.77-8.73 (m, 1H, Py<u>H</u>), 8.07-8.04 (m, 1H, Py<u>H</u>), 7.91 (d, 1H, J = 8.0 Hz, Py<u>H</u>), 7.80 (d, 1H, J = 5.0 Hz, H_5), 7.38 (dd, 1H, J = 7.9, 4.9 Hz, H_3), 7.19 (dd, 1H, J = 4.9 Hz, H_4); ^{13}C NMR ($CDCl_3$, 125 MHz) δ 181.8 (t, $J_{C\text{-}F}$ = 33.0 Hz), 152.1, 147.2 (t, $J_{C\text{-}F}$ = 6.7 Hz), 137.7, 137.0, 136.2 (t, $J_{C\text{-}F}$ = 5.2 Hz), 133.9 (t, $J_{C\text{-}F}$ = 5.7 Hz), 128.9, 128.8 (t, $J_{C\text{-}F}$ = 25.8 Hz), 123.3, 115.9 (t, $J_{C\text{-}F}$ = 255.0 Hz); HRMS (EI) calcd for $C_{11}H_7F_2NOS$ (M^+), 239.0216; found, 239.0216.

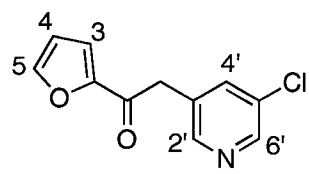

2-(5-Chloropyridin-3-yl)-1-(furan-2-yl)ethanone (49). A solution of **127a** (70 mg, 0.25 mmol) in 50% H_2SO_4 (5 mL) was refluxed at 100 °C for 8 h. NaOH (6.25 M, 10 mL) and saturated $NaHCO_3$ (9 mL) were then added to neutralize the solution to pH 7. The resulting solution was extracted with EtOAc (3 x 20 mL). The combined organic layers were washed with brine (15 mL), dried over anhydrous $MgSO_4$, and concentrated in vacuo. The crude product was purified by column chromatography (EtOAc) to yield **49** as a white solid (47 mg, 85%). IR ($CHCl_3$ cast): 3132, 3042, 2910, 1675, 1569, 1467, 1443, 1425 cm^{-1}; ^1H NMR ($CDCl_3$, 400 MHz) δ 8.48 (d, 1H, J = 2.2 Hz, $H_{2'}$ or $H_{6'}$), 8.42 (d, 1H, J = 1.7 Hz, $H_{2'}$ or $H_{6'}$), 7.66 (dd, 1H, J = 2.2, 1.7 Hz, $H_{4'}$), 7.63 (dd, 1H, J = 1.8, 0.8 Hz, H_5), 7.29 (dd, 1H, J = 3.7, 0.8 Hz, H_3), 6.59 (dd, 1H, J = 3.7, 1.8 Hz, H_4); 4.14 (s, 2H, $COC\underline{H}_2$); ^{13}C NMR ($CDCl_3$, 100 MHz) δ 184.7, 152.0, 148.4, 147.5, 146.9, 136.9, 131.9, 130.8, 118.1, 112.8, 41.6; HRMS (EI) calcd for $C_{11}H_8ClNO_2$ (M^+), 221.0244; found, 221.0243.

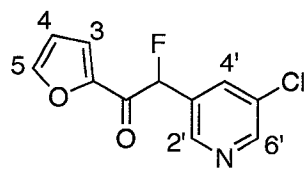

2-(5-Chloropyridin-3-yl)-2-fluoro-1-(furan-2-yl)ethanone (50). To a solution of **49** (20 mg, 0.09 mmol) in dry THF (5 mL) was added LiHMDS (0.1 mL, 1.0 M solution in THF, 0.1 mmol) over 5 min. The reaction mixture was stirred for 1 h at -78 °C. A solution of NFSi (32 mg, 0.1 mmol) in dry THF (3 mL) was added dropwise to the reaction mixture over 10 min. The resulting mixture was stirred for another 2 h at -78 °C. Saturated $NaHCO_3$ (5 mL) was added to adjust pH to 9, and the solution was extracted with EtOAc (3 x 15 mL). The combined organic layers were washed with brine (10 mL), dried over

$MgSO_4$ and concentrated in vacuo. The crude product was purified by column chromatography (50/50 EtOAc/hexanes) to yield **50** as a light yellow solid (16 mg, 74%). IR ($CHCl_3$ cast): 3136, 3059, 1690, 1584, 1569, 1464, 1425 cm^{-1}; ^1H NMR ($CDCl_3$, 400 MHz) 8.67 (dd, 1H, J = 1.9, 1.7 Hz, $H_{2'}$ or $H_{6'}$), 8.60 (d, 1H, J = 1.9 Hz, $H_{2'}$ or $H_{6'}$), 7.89-7.87 (m, 1H, $H_{4'}$), 7.69 (dd, 1H, J = 1.7, 0.7 Hz, H_5), 7.48 (ddd, 1H, J = 3.7, 2.1, 0.7 Hz, H_3), 6.62 (dd, 1H, J = 3.7, 1.7 Hz, H_4), 6.37 (d, 1H, J = 47.2 Hz, COC<u>H</u>F); ^{13}C NMR ($CDCl_3$, 125 MHz) δ 182.2 (d, $J_{C\text{-}F}$ = 23.5 Hz), 150.2 (d, $J_{C\text{-}F}$ = 1.7 Hz), 150.1 (d, $J_{C\text{-}F}$ = 1.7 Hz), 149.0, 146.2 (d, $J_{C\text{-}F}$ = 7.0 Hz), 135.3 (d, $J_{C\text{-}F}$ = 6.2 Hz), 133.4, 132.3 (d, $J_{C\text{-}F}$ = 21.0 Hz), 122.0 (d, $J_{C\text{-}F}$ = 7.4 Hz), 113.6 (d, $J_{C\text{-}F}$ = 1.2 Hz), 91.0 (d, $J_{C\text{-}F}$ = 189.2 Hz); ^{19}F NMR ($CDCl_3$, 376 MHz) -186.6 (d, $J_{H\text{-}F}$ = 47.2 Hz); HRMS (EI) calcd for $C_{11}H_7ClFNO_2$ (M^+), 239.0149; found, 239.0145.

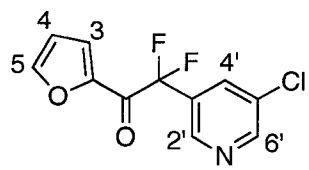

2-(5-Chloropyridin-3-yl)-2,2-difluoro-1-(furan-2-yl)ethanone (51). To a solution of **49** (10 mg, 0.045 mmol) in dry THF (5 mL) was added LiHMDS (0.1 mL, 1.0 M solution in THF, 0.100 mmol) over a period of 5 min. The reaction mixture was stirred for 1 h at -78 °C and a solution of NFSi (32 mg, 0.100 mmol) in dry THF (3 mL) was added dropwise over 10 min. The reaction mixture was stirred for another 2 h at -78 °C. Saturated $NaHCO_3$ (5 mL) was added to adjust pH to 9, and the solution was extracted with EtOAc (3 x 15 mL). The combined organic layers were washed with brine (10 mL), dried over $MgSO_4$ and concentrated in vacuo. The crude product was purified by column chromatography (50/50 EtOAc/hexanes) to yield **51** as a light yellow solid (7.1 mg,

61%). IR ($CHCl_3$ cast): 3142, 3068, 2933, 1687, 1563, 1460, 1424 cm^{-1}; ^1H NMR ($CDCl_3$, 500 MHz) 8.72 (d, 1H, J = 1.9 Hz, $H_{2'}$ or $H_{6'}$), 8.67 (d, 1H, J = 2.2 Hz, $H_{2'}$ or $H_{6'}$), 7.90 (dd, 1H, J = 2.2, 1.9 Hz, $H_{4'}$), 7.74 (dd, 1H, J = 1.7, 0.6 Hz, H_5), 7.58 (ddt, 1H, J = 3.7, 1.9, 0.7 Hz, H_3), 6.63 (dd, 1H, J = 3.8, 1.7 Hz, H_4); ^{13}C NMR ($CDCl_3$, 125 MHz) δ 175.8 (t, $J_{C\text{-}F}$ = 33.0 Hz), 151.5, 149.8, 148.1, 145.3 (t, $J_{C\text{-}F}$ = 6.2 Hz), 140.0 (t, $J_{C\text{-}F}$ = 6.2 Hz), 132.5, 130.0 (t, $J_{C\text{-}F}$ = 25.8 Hz), 124.0 (t, $J_{C\text{-}F}$ = 5.2 Hz), 114.9 (t, $J_{C\text{-}F}$ = 255.5 Hz), 113.3; ^{19}F NMR ($CDCl_3$, 376 MHz) -102.1; HRMS (EI) calcd for $C_{11}H_6ClF_2NO_2$ (M^+), 257.0055; found, 257.0055.

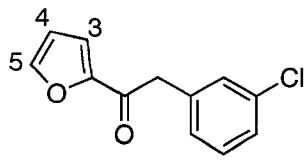

2-(3-Chlorophenyl)-1-(furan-2-yl)ethanone (52). The title compound **52** was obtained from **127b** (160 mg, 0.58 mmol) following the standard procedure described above for the preparation of **49**. Purification of the crude product by flash chromatography on silica gel (25/75 EtOAc/hexanes) afforded **52** as a yellow oil (75 mg, 59%), which solidified in the fridge. Literature compound.[80] IR ($CHCl_3$ cast): 3135, 1732, 1673, 1598, 1570, 1466, 1432 cm^{-1}; ^1H NMR ($CDCl_3$, 500 MHz) δ 7.59 (dd, 1H, J = 1.7, 0.7 Hz, H_5), 7.28-7.18 (m, 5H, H_3 and Ph<u>H</u>), 6.53 (dd, 1H, J = 3.6, 1.7 Hz, H_4), 4.10 (s, 2H, COC<u>H_2</u>); HRMS (EI) calcd for $C_{12}H_9ClO_2$ (M^+), 220.0291; found, 220.0291.

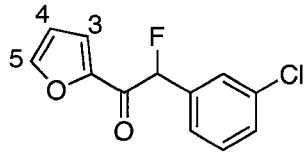

2-(3-Chlorophenyl)-2-fluoro-1-(furan-2-yl)ethanone (53). The title compound **53** was obtained from **52** (40 mg, 0.181 mmol) following the standard procedure described above for the preparation of **50**. Purification of the crude product by flash chromatography on silica gel (25/75 EtOAc/hexanes) afforded **53** as a yellow oil (38 mg, 88%), which solidified in the fridge. IR ($CHCl_3$ cast): 3140, 1689, 1597, 1569, 1464, 1433 cm^{-1}; ^1H NMR ($CDCl_3$, 500 MHz) δ 7.63 (dd, 1H, J = 1.7, 0.7 Hz, H_5), 7.53-7.51 (m, 1H, Ph<u>H</u>), 7.40 (ddd, 1H, J = 3.7, 2.0, 0.7 Hz, H_3), 7.42-7.31 (m, 3H, Ph<u>H</u>), 6.56 (dd, 1H, J = 3.7, 1.7 Hz, H_4), 6.24 (d, 1H, J = 47.6 Hz, COC<u>H</u>F); ^{13}C NMR ($CDCl_3$, 125 MHz) δ 183.2 (d, $J_{C\text{-}F}$ = 24.3 Hz), 149.9, 148.1, 136.3 (d, $J_{C\text{-}F}$ = 20.7 Hz), 135.2, 130.4, 130.0 (d, $J_{C\text{-}F}$ = 2.1 Hz), 127.2 (d, $J_{C\text{-}F}$ = 6.7 Hz), 125.2 (d, $J_{C\text{-}F}$ = 6.2 Hz), 121.1 (d, $J_{C\text{-}F}$ = 7.2 Hz), 113.0, 93.0 (d, $J_{C\text{-}F}$ = 187.9 Hz); ^{19}F NMR ($CDCl_3$, 376 MHz) -183.4 (d, $J_{H\text{-}F}$ = 47.5 Hz); HRMS (EI) calcd for $C_{12}H_8ClFO_2$ (M^+), 238.0197; found, 238.0120.

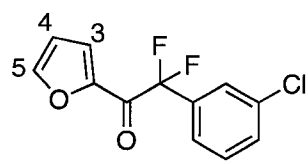

2-(3-Chlorophenyl)-2,2-difluoro-1-(furan-2-yl)ethanone (54). The title compound **54** was obtained from **52** (36 mg, 0.163 mmol) following the standard procedure described above for the preparation of **51**. Purification of the crude product by flash chromatography on silica gel (25/75 EtOAc/hexanes) afforded **54** as a yellow oil (24 mg, 57%), which solidified in the fridge. IR ($CHCl_3$ cast): 1687, 1578, 1560, 1477, 1461, 1427, 1394 cm^{-1}; ^1H NMR ($CDCl_3$, 500 MHz) δ 7.71 (dd, 1H, J = 1.7, 0.7 Hz, H_5), 7.61 (dd, 1H, J = 1.9, 1.7 Hz, Ph<u>H</u>), 7.53-7.45 (m, 3H, H_3 and 2xPh<u>H</u>), 7.37 (dd, 1H, J = 7.9, 7.5 Hz, Ph<u>H</u>), 6.59 (dd, 1H, J = 3.8, 1.7 Hz, H_4); ^{13}C NMR ($CDCl_3$, 125 MHz) δ 177.1 (t,

$J_{C\text{-}F}$ = 33.0 Hz), 149.4, 148.3, 135.2, 134.7 (t, $J_{C\text{-}F}$ = 25.4 Hz), 131.5, 130.4, 126.3 (t, $J_{C\text{-}F}$ = 6.2 Hz), 124.3 (t, $J_{C\text{-}F}$ = 6.2 Hz), 123.5 (t, $J_{C\text{-}F}$ = 5.0 Hz), 115.6 (t, $J_{C\text{-}F}$ = 254.5 Hz), 113.1; ^{19}F NMR ($CDCl_3$, 376 MHz) -102.0; HRMS (EI) calcd for $C_{12}H_7ClF_2O_2$ (M^+), 256.0103; found, 256.0106.

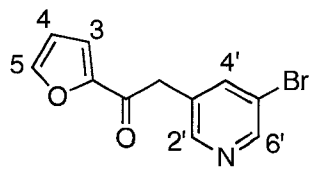

2-(5-Bromopyridin-3-yl)-1-(furan-2-yl)ethanone (55). The title compound **55** was obtained from **127c** (0.52 g, 1.59 mmol) following the standard procedure described for the preparation of **49**. Purification of the crude product by flash chromatography on silica gel (EtOAc) afforded **55** as a brown solid (0.30 g, 68%), which sublimes under vacuum. IR ($CHCl_3$ cast): 3130, 3039, 2926, 1703, 1677, 1650, 1631, 1568, 1555, 1466, 1439, 1424, 1392, 1334 cm^{-1}; ^{1}H NMR ($CDCl_3$, 500 MHz) δ 8.57 (s, 1H, $H_{2'}$ or $H_{6'}$), 8.45 (s, 1H, $H_{2'}$ or $H_{6'}$), 7.81 (s, 1H, $H_{4'}$), 7.63 (m, 1H, H_5), 7.28 (d, 1H, J = 1.6 Hz, H_3), 6.57 (m, 1H, H_4), 4.10 (s, 2H, COC$\underline{H}_2$); ^{13}C NMR ($CDCl_3$, 125 MHz) δ 184.7, 152.0, 149.5, 148.7, 147.0, 139.7, 131.3, 120.6, 118.1, 112.8, 41.5; HRMS (EI) calcd for $C_{11}H_8BrNO_2$ (M^+), 264.9738; found, 264.9739.

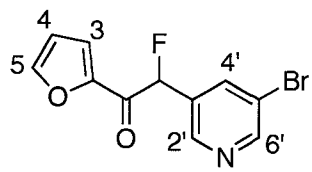

2-(5-Bromopyridin-3-yl)-2,2-difluoro-1-(furan-2-yl)ethanone (56). The title compound **56** was obtained from **55** (53 mg, 0.20 mmol) following the standard procedure described

for the preparation of **50**. Purification of the crude product by flash chromatography on silica gel (EtOAc) afforded **56** as a yellow oil (42 mg, 74%), which solidified in the fridge. IR ($CHCl_3$ cast): 3136, 2960, 2924, 2850, 1732, 1690, 1569, 1463, 1425, 1394, 1261 cm^{-1}; ^1H NMR ($CDCl_3$, 500 MHz) 8.86 (m, 2H, $H_{2'}$ and $H_{6'}$), 7.95 (dd, 1H, J = 2.2, 2.0 Hz, $H_{4'}$), 7.65 (d, 1H, J = 1.6 Hz, H_5), 7.44 (dd, 1H, J = 3.7, 2.0 Hz, H_3), 6.58 (dd, 1H, J = 3.8, 1.7 Hz, H_4), 6.32 (d, 1H, J = 47.2 Hz, COC<u>H</u>F); ^{13}C NMR ($CDCl_3$, 125 MHz) δ 181.8 (d, $J_{C\text{-}F}$ = 23.2 Hz), 152.3 (d, $J_{C\text{-}F}$ = 2.1 Hz), 149.8, 148.5, 146.7 (d, $J_{C\text{-}F}$ = 7.2 Hz), 137.2 (d, $J_{C\text{-}F}$ = 6.2 Hz), 131.8 (d, $J_{C\text{-}F}$ = 21.2 Hz), 121.5 (d, $J_{C\text{-}F}$ = 7.2 Hz), 121.2, 113.3, 90.8 (d, $J_{C\text{-}F}$ = 188.9 Hz); ^{19}F NMR ($CDCl_3$, 376 MHz) -186.1 (d, $J_{H\text{-}F}$ = 46.9 Hz); HRMS (EI) calcd for $C_{11}H_7BrFNO_2$ (M^+), 282.9644; found, 282.9647.

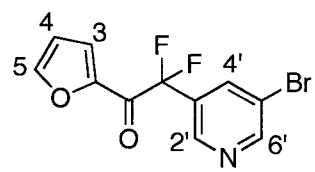

2-(5-Bromopyridin-3-yl)-2-fluoro-1-(furan-2-yl)ethanone (57). The title compound **57** was obtained from **55** (114 mg, 0.39 mmol) following the standard procedure described above for the preparation of **51**. Purification of the crude product by flash chromatography on silica gel (50/50 EtOAc/hexanes) afforded **57** as a brown solid (60 mg, 51%). IR ($CHCl_3$ cast): 3139, 3126, 3033, 1691, 1653, 1559, 1467, 1437, 1424, 1395, 1308, 1261 cm^{-1}; ^1H NMR ($CDCl_3$, 400 MHz) 8.82-8.78 (m, 2H, $H_{2'}$ and $H_{6'}$), 8.08 (dd, 1H, J = 2.1, 2.1 Hz, $H_{4'}$), 7.78 (dd, 1H, J = 1.6, 0.7 Hz, H_5), 7.59-7.56 (m, 1H, H_3), 6.66 (dd, 1H, J = 3.7, 1.6 Hz, H_4); ^{13}C NMR ($CDCl_3$, 125 MHz) δ 176.9 (t, $J_{C\text{-}F}$ = 32.6 Hz), 154.2, 150.5, 148.7, 146.2 (t, $J_{C\text{-}F}$ = 6.6 Hz), 137.3 (t, $J_{C\text{-}F}$ = 6.2 Hz), 130.9 (t, $J_{C\text{-}F}$ = 26.0 Hz), 124.5 (t, $J_{C\text{-}F}$ = 5.0 Hz), 121.4, 115.3 (t, $J_{C\text{-}F}$ = 255.7 Hz), 113.8; ^{19}F NMR

($CDCl_3$, 376 MHz) -102.1; HRMS (EI) calcd for $C_{11}H_6BrF_2NO_2$ (M^+), 300.9550; found, 300.9555.

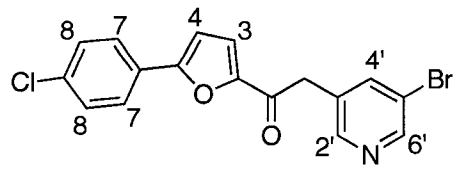

2-(5-Bromopyridin-3-yl)-1-(5-(4-chlorophenyl)furan-2-yl)ethanone (58). The title compound **58** was obtained from **127d** (1.22 g, 2.81 mmol) following the standard procedure described above for the preparation of **49**. Purification of the crude product by flash chromatography on silica gel (EtOAc) afforded **58** as a yellow solid (0.90 g, 85%). IR ($CHCl_3$ cast): 3127, 3030, 2914, 1675, 1665, 1518, 1469, 1436, 1410, 1402 cm^{-1}; ^1H NMR ($CDCl_3$, 300 MHz) 8.60 (d, 1H, J = 2.2 Hz, $H_{2'}$ or $H_{6'}$), 8.51 (d, 1H, J = 1.9 Hz, $H_{2'}$ or $H_{6'}$), 7.86 (dd, 1H, J = 2.2, 1.9 Hz, $H_{4'}$), 7.72 (d, 2H, J = 8.7 Hz, H_7), 7.44 (d, 2H, J = 8.5 Hz, H_8), 7.36 (d, 1H, J = 3.7 Hz, H_3), 6.81 (d, 1H, J = 3.7 Hz, H_4), 4.18 (s, 2H, $COC\underline{H}_2$); ^{13}C NMR ($CDCl_3$, 125 MHz) δ 184.1, 157.2, 151.1, 149.6, 148.7, 139.7, 135.5, 131.4, 129.3, 127.6, 126.2, 120.7, 120.4, 108.2, 41.7; HRMS (EI) calcd for $C_{17}H_{11}BrClNO_2$ (M^+), 374.9662; found, 376.9642.

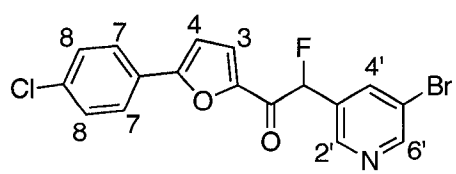

2-(5-Bromopyridin-3-yl)-1-(5-(4-chlorophenyl)furan-2-yl)-2-fluoroethanone (59). The title compound **59** was obtained from **58** (57 mg, 0.15 mmol) following the standard procedure described above for the preparation of **50**. Purification of the crude product by

flash chromatography on silica gel (25/75 EtOAc/hexanes) afforded **59** as a yellow oil (30 mg, 50%), which solidified in the fridge. IR ($CHCl_3$ cast): 3309, 3146, 3087, 3067, 2925, 1656, 1626, 1588, 1513, 1467, 1446, 1425, 1411 cm^{-1}; ^1H NMR ($CDCl_3$, 500 MHz) 8.70 (m, 1H, $H_{2'}$ or $H_{6'}$), 8.68 (d, 1H, J = 1.6 Hz, $H_{2'}$ or $H_{6'}$), 7.99 (dd, 1H, J = 1.8, 1.6 Hz, $H_{4'}$), 7.68 (d, 2H, J = 8.7 Hz, H_7), 7.53 (dd, 1H, J = 3.8, 2.3 Hz, H_3), 7.41 (d, 2H, J = 8.7 Hz, H_8), 6.80 (d, 1H, J = 3.9 Hz, H_4), 6.31 (d, 1H, J = 47.3 Hz, COC<u>H</u>F); ^{13}C NMR ($CDCl_3$, 125 MHz) δ 181.2 (d, $J_{C\text{-}F}$ = 23.2 Hz), 158.9, 152.3 (d, $J_{C\text{-}F}$ = 2.1 Hz), 148.8, 146.5 (d, $J_{C\text{-}F}$ = 7.2 Hz), 137.1 (d, $J_{C\text{-}F}$ = 6.2 Hz), 136.4, 132.1 (d, $J_{C\text{-}F}$ = 21.2 Hz), 129.7, 127.4, 126.8, 124.0 (d, $J_{C\text{-}F}$ = 8.3 Hz), 121.3, 108.6, 91.3 (d, $J_{C\text{-}F}$ = 190.0 Hz); ^{19}F NMR ($CDCl_3$, 376 MHz) -185.9 (d, $J_{H\text{-}F}$ = 47.5 Hz); HRMS (EI) calcd for $C_{17}H_{10}BrClFNO_2$ (M^+), 394.9538; found, 394.9531.

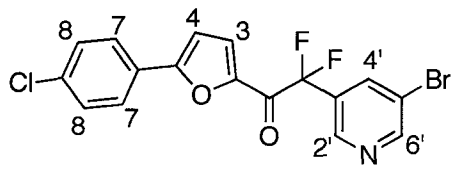

2-(5-Bromopyridin-3-yl)-1-(5-(4-chlorophenyl)furan-2-yl)-2,2-difluoroethanone (60). The title compound **60** was obtained from **58** (57 mg, 0.15 mmol) following the standard procedure described for the preparation of **51**. Purification of the crude product by flash chromatography on silica gel (50/50 EtOAc/hexanes) afforded **60** as a yellow solid (53 mg, 85%). IR ($CHCl_3$ cast): 3369, 3175, 3036, 1691, 1582, 1522, 1472, 1424, 1412 cm^{-1}; ^1H NMR ($CDCl_3$, 500 MHz) 8.78 (m, 2H, $H_{2'}$ and $H_{6'}$), 8.08 (dd, 1H, J = 2.2, 1.9 Hz, $H_{4'}$), 7.71 (d, 2H, J = 8.8 Hz, H_7), 7.61 (dt, 1H, J = 3.8, 1.8 Hz, H_3), 7.41 (d, 2H, J = 8.8 Hz, H_8), 6.83 (d, 1H, J = 3.9 Hz, H_4); ^{13}C NMR ($CDCl_3$, 125 MHz) δ 175.5 (t, $J_{C\text{-}F}$ = 32.5 Hz), 160.1, 153.6, 147.3, 145.6 (t, $J_{C\text{-}F}$ = 6.7 Hz), 136.8, 136.7, 130.6 (t, $J_{C\text{-}F}$ = 26.0 Hz), 129.2,

127.2, 127.0, 126.2 (t, $J_{C\text{-}F}$ = 5.2 Hz), 121.0, 115.0 (t, $J_{C\text{-}F}$ = 256.0 Hz), 108.7; ^{19}F NMR ($CDCl_3$, 376 MHz) -101.9; HRMS (EI) calcd for $C_{17}H_9BrClF_2NO_2$ (M^+), 412.9453; found, 412.9452.

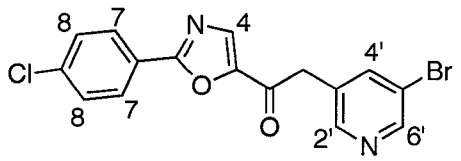

2-(5-Bromopyridin-3-yl)-1-(2-(4-chlorophenyl)oxazol-5-yl)ethanone (61). The title compound **61** was obtained from **138** (26 mg, 0.060 mmol) following the standard procedure described for the preparation of **49**. Purification of the crude product by flash chromatography on silica gel (EtOAc) afforded **61** as a white solid (13 mg, 58%). IR ($CHCl_3$ cast): 3039, 2926, 1680, 1603, 1580, 1556, 1526, 1472, 1408 cm^{-1}; ^{1}H NMR ($CDCl_3$, 400 MHz) δ 8.65-8.61 (m, 1H, $H_{2'}$ or $H_{6'}$), 8.52-8.48 (m, 1H, $H_{2'}$ or $H_{6'}$), 8.10 (d, 2H, J = 8.7 Hz, H_7), 7.97 (s, 1H, H_4), 7.85 (dd, 1H, J = 2.1, 1.8 Hz, $H_{4'}$), 7.52 (d, 2H, J = 8.7 Hz, H_8), 4.16 (s, 2H, COC$\underline{H}_2$); ^{13}C NMR ($CDCl_3$, 100 MHz) δ 183.3, 163.8, 149.9, 148.7, 148.5, 139.6, 138.5, 136.0, 130.3, 129.4, 128.6, 124.3, 120.7, 42.3; HRMS (EI) calcd for $C_{16}H_{10}BrClN_2O_2$ (M^+), 377.9594; found, 377.9608.

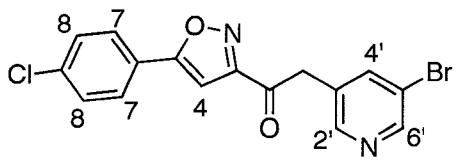

2-(5-Bromopyridin-3-yl)-1-(5-(4-chlorophenyl)isoxazol-3-yl)ethanone (62). The title compound **62** was obtained from **140** (60 mg, 0.138 mmol) following the standard procedure described for the preparation of **49**. Purification of the crude product by flash

chromatography on silica gel (50/50 EtOAc/hexanes) afforded **62** as a white solid (30 mg, 58%). IR ($CHCl_3$ cast): 3217, 3090, 3045, 2894, 1709, 1608, 1589, 1560, 1492, 1440 cm^{-1}; ^1H NMR ($CDCl_3$, 500 MHz) δ 8.59 (s, 1H, $H_{2'}$ or $H_{6'}$), 8.49 (s, 1H, $H_{2'}$ or $H_{6'}$), 7.82 (dd, 1H, J = 2.0, 2.0 Hz, $H_{4'}$), 7.72 (d, 2H, J = 8.8 Hz, H_7), 7.46 (d, 2H, J = 8.8 Hz, H_8), 6.90 (s, 1H, H_4), 4.39 (s, 2H, $COC\underline{H}_2$); ^{13}C NMR ($CDCl_3$, 125 MHz) δ 190.0, 171.0, 161.8, 149.8, 149.0, 139.9, 137.2, 130.4, 129.6, 127.2, 124.9, 120.7, 89.3, 24.8; HRMS (EI) calcd for $C_{16}H_{10}BrClN_2O_2$ (M^+), 377.9594; found, 377.9604.

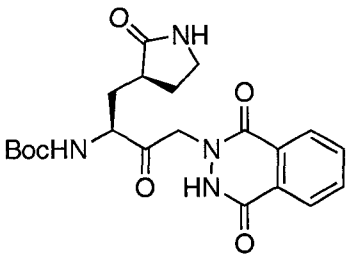

***tert*-Butyl (*S*)-4-(1,4-dioxo-3,4-dihydrophthalazin-2(1*H*)-yl)-3-oxo-1-((*S*)-2-oxopyrrolidin-3-yl)butan-2-ylcarbamate (64).** To a solution of phthalhydrazide (2.00 g, 12.3 mmol) in DMF (60 mL) was added NaH (0.34 g, 13.6 mmol) and the mixture was stirred at rt for 2 h, after which it was filtered and washed with anhydrous Et_2O to yield sodium phthalhydrazide as a white solid (2.37 g, quantitative). To a suspension of sodium phthalhydrazide (57 mg, 0.31 mmol) in DMF (2 mL) was added a solution of the bromoketone **72** (100 mg, 0.28 mmol) in DMF (4 mL) dropwise over 1 h. After stirring for 8 h at rt, the solvent was removed in vacuo and the residue was diluted with H_2O (15 mL) and extracted with EtOAc (3 x 15 mL). The combined organic layers were dried over $MgSO_4$ and the solvent was removed in vacuo to obtain the crude product, which was purified by flash column chromatography on silica gel (95/5 EtOAc/MeOH) to

obtain **64** (39 mg, 32%) as a white foam. $[\alpha]^{25}_{D}$= +15.2° (*c* 0.5, $CHCl_3$); IR ($CHCl_3$ cast) 3253, 2977, 1687, 1600 cm^{-1}; ^1H NMR ($CDCl_3$, 500 MHz) δ 10.11 (br, 1H, N<u>H</u>), 8.36 (d, 1H, *J* = 7.5 Hz, Ar<u>H</u>), 8.05 (d, 1H, *J* = 7.5 Hz, Ar<u>H</u>), 7.81 (dd, 1H, *J* = 7.5, 7.5 Hz, Ar<u>H</u>), 7.77 (dd, 1H, *J* = 7.5, 7.5 Hz, Ar<u>H</u>), 6.19 (br, 1H, N<u>H</u>), 6.01 (d, 1H, *J* = 7.5 Hz, N<u>H</u>), 5.15 (d, 1H, *J* = 17.0 Hz, C<u>H</u>$_2$N) 5.07 (d, 1H, *J* = 17.0 Hz, C<u>H</u>$_2$N), 4.56-4.48 (m, 1H, NHC<u>H</u>CH$_2$), 3.37-3.30 (m, 2H, NHC<u>H</u>$_2$CH$_2$), 2.46-2.32 (m, 3H, 1xCH$_2$C<u>H</u>CO and 2xNHCH$_2$C<u>H</u>$_2$), 2.04-1.98 (m, 1H, CHC<u>H</u>$_2$CH), 1.89-1.80 (m, 1H, CHC<u>H</u>$_2$CH), 1.44 (s, 9H, (C<u>H</u>$_3$)$_3$); ^{13}C NMR ($CDCl_3$, 125 MHz) δ 204.0, 180.3, 160.1, 155.9, 149.5, 133.3, 132.0, 128.9, 126.7, 124.5, 123.7, 80.1, 68.4, 56.5, 40.6, 37.9, 32.3, 28.5, 28.3; HRMS (ES) calcd for $C_{21}H_{26}N_4O_6Na$ ([M+Na]$^+$), 453.1744; found, 453.1745.

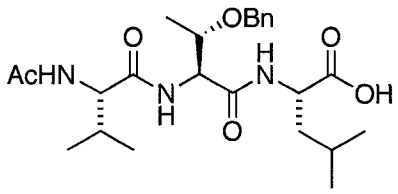

(*S*)-2-((2*S*,3*S*)-2-((*S*)-2-Acetamido-3-methylbutanamido)-3-(benzyloxy)butanamido)-4-methylpentanoic acid (65). The tripeptide **78** (3.76 g, 6.73 mmol) was stirred with TFA/CH_2Cl_2 (100 mL, 1:1 ratio) at 0 °C for 2 h, after which the reaction mixture was concentrated in vacuo and the residue was triturated with Et_2O to yield the trifluoroacetate salt. To a solution of the trifluoroacetate salt in CH_2Cl_2 (50 mL) was added Et_3N (50 mL) and Ac_2O (50 mL). The solvent was removed in vacuo after 24 h stirring. The residue was diluted with H_2O (50 mL) and extracted with EtOAc (3 x 50 mL). The combined organic layers were washed with brine, dried over $MgSO_4$ and then concentrated in vacuo to afford the *N*-acetyl tripeptide product, which was used in the

next reaction without any further purification. To a solution of *N*-acetyl tripeptide in THF/H_2O (120 mL, 1:1 ratio) at 0 °C was added LiOH (426 mg, 10.12 mmol). The resulting solution was stirred for 3 h until complete consumption of the starting material was confirmed by TLC. The reaction mixture was quenched with AcOH and then the solvent was removed in vacuo. The solution was treated with H_2O (40 mL) and citric acid until pH = 3, and then extracted with EtOAc (3 x 40 mL). The combined organic layers were washed with brine (30 mL) and dried over $MgSO_4$. The solvent was removed under reduced pressure to afford the product **65** as a white solid (3.20 g, quant.). $[\alpha]^{25}_{D}$= -23.02° (*c* 0.086, MeOH); IR (microscope) 3291, 3089, 2961, 2873, 1725, 1642, 1546, 1469, 1454 cm^{-1}; ^1H NMR (CD_3OD, 500 MHz) δ 7.34-7.22 (m, 5H, Ph<u>H</u>), 4.56 (d, 1H, *J* = 11.2 Hz, OC<u>H</u>$_2$Ph), 4.50 (d, 1H, *J* = 3.9 Hz, NHC<u>H</u>CO(Thr)), 4.46 (d, 1H, *J* = 11.2 Hz, OC<u>H</u>$_2$Ph), 4.50-4.43 (m, 1H, NHC<u>H</u>CO(Leu)), 4.19 (d, 1H, *J* = 7.1 Hz, NHC<u>H</u>CO(Val)), 4.06 (dq, 1H, *J* = 6.3, 4.1 Hz, CH_3C<u>H</u>OBn(Thr)), 2.08 (m, 1H, CHC<u>H</u>(CH_3)$_2$(Val)), 1.95 (s, 3H, COC<u>H</u>$_3$), 1.70-1.58 (m, 3H, 2xCHC<u>H</u>$_2$CH(Leu) and 1xCH_2C<u>H</u>(CH_3)$_2$(Leu)), 1.22 (d, 3H, *J* = 6.3 Hz, CHC<u>H</u>$_3$(Thr)), 0.95 (d, 3H, *J* = 6.8 Hz, CH(C<u>H</u>$_3$)$_2$(Val)), 0.94 (d, 3H, *J* = 6.8 Hz, CH(C<u>H</u>$_3$)$_2$(Val)), 0.89 (d, 3H, *J* = 6.3 Hz, CH(C<u>H</u>$_3$)$_2$(Leu)), 0.87 (d, 3H, *J* = 6.2 Hz, CH(C<u>H</u>$_3$)$_2$(Leu)); ^{13}C NMR (CD_3OD, 125 MHz) δ 187.0, 175.4, 173.9, 171.9, 139.7, 129.3, 129.0, 128.7, 76.4, 72.6, 60.8, 58.6, 52.1, 41.8, 31.5, 25.9, 23.4, 22.4, 21.9, 19.8, 18.7, 16.8; HRMS (ES) calcd for $C_{24}H_{37}N_3O_6Na$ ([M+Na]$^+$), 486.2575; found, 486.2571.

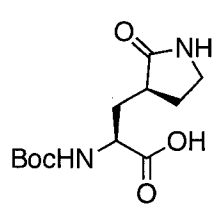

(*R*)-2-(*tert*-Butoxycarbonylamino)-3-((*S*)-2-oxopyrrolidin-3-yl) propanoic acid (66). The title compound was prepared by a modified literature procedure of Tian.[68] To a solution of the methyl ester **70** (127 mg, 0.44 mmol) in THF/H_2O (5 mL/5 mL) at 0 °C was added LiOH (24 mg, 0.57 mmol). The resulting reaction mixture was stirred for 1 h until complete consumption of the starting material was confirmed by TLC. The mixture was quenched with AcOH (0.1 g) and the solvent was removed under reduced pressure. The solution was treated with H_2O (10 mL) and citric acid until pH = 3, and extracted with EtOAc (3 x 10 mL). The combined organic layers were washed with brine (10 mL) and dried over $MgSO_4$. The solvent was removed to afford the product **66** as a white foam (130 mg, quant.). Literature compound.[68] IR (microscope) 3320, 2979, 2565, 1709, 1523, 1444 cm^{-1}; ^1H NMR ($CDCl_3$, 300 MHz) δ 6.58 (br, 1H, N<u>H</u>), 5.78-5.68 (br, 1H, N<u>H</u>), 4.48-4.32 (m, 1H, NHC<u>H</u>CO), 3.52-3.35 (m, 2H, NHC<u>H</u>$_2$CH$_2$), 2.65 (m, 1H, CHC<u>H</u>$_2$CH), 2.52-2.38 (m, 1H, NHCH$_2$C<u>H</u>$_2$), 2.21 (m, 1H, CHC<u>H</u>$_2$CH), 1.98-1.82 (m, 2H, 1xNHCH$_2$C<u>H</u>$_2$ and 1xCH$_2$C<u>H</u>CO), 1.45 (s, 9H, C(C<u>H</u>$_3$)$_3$); HRMS (ES) calcd for $C_{12}H_{20}N_2O_5Na$ ([M+Na]$^+$), 295.1264; found, 295.1265.

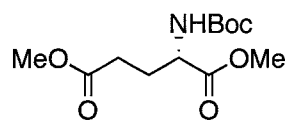

(*S*)-Dimethyl 2-(*tert*-butoxycarbonylamino)pentanedioate (68). The title compound was prepared by a literature procedure of Kikotos.[81] To a stirred solution of L-glutamic acid (8.8 g, 60 mmol) in MeOH (156 mL) was added TMSCl (33.6 mL, 264 mmol) at 0 °C. The temperature was allowed to warm to rt and the reaction mixture was stirred overnight. Then Et_3N (54 mL, 390 mmol) and Boc_2O (14.4 g, 66 mmol) were added and

the resulting mixture was stirred until the evolution of gas stopped. The solvent was removed under reduced pressure, and the residue was triturated and washed with Et_2O. The combined filtrates were concentrated to provide a crude product, which was purified by flash chromatography on silica gel (50/50 EtOAc/hexanes) to afford **68** as a colorless oil (16.0 g, 90%). Literature compound.[81] IR (microscope) 3370, 2978, 2956, 1715, 1717, 1518, 1438 cm^{-1}; ^1H NMR ($CDCl_3$, 400 MHz) δ 5.12 (br, 1H, N<u>H</u>), 4.38-4.20 (m, 1H, NHC<u>H</u>CO_2), 3.71 (s, 3H, $CO_2C\underline{H}_3$), 3.65 (s, 3H, $CO_2C\underline{H}_3$), 2.38 (dd, 2H, J = 16.6, 8.1 Hz, $C\underline{H}_2CO_2CH_3$), 2.15 (ddt, 1H, J = 13.5, 7.5, 5.9 Hz, $CH_2C\underline{H}_2CH$), 1.92 (ddt, 1H, J = 14.2, 8.1, 6.7 Hz, $CH_2C\underline{H}_2CH$), 1.41 (s, 9H, $C(C\underline{H}_3)_3$); HRMS (ES) calcd for $C_{12}H_{21}NO_6Na$ ($[M+Na]^+$), 298.1261; found, 298.1264.

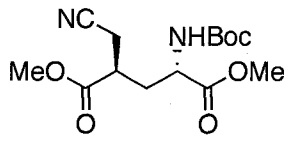

(2*S*,4*R*)-Dimethyl 2-(*tert*-butoxycarbonylamino)-4-(cyanomethyl)pentanedioate (69). The title compound was prepared by a literature procedure of Tian.[68] To a solution of *N*-Boc-L-glutamic acid dimethyl ester **68** (11.5 g, 41.8 mmol) in THF (120 mL) was added dropwise a solution of LiHMDS in THF (90 mL, 90.0 mmol) at -78 °C under argon. The resulting dark mixture was stirred at -78 °C for 1 h. Then bromoacetonitrile (3.0 mL, 44.7 mmol) was added dropwise to the dianion solution over a period of 1 h while maintaining the temperature below -70 °C. The reaction mixture was stirred at -78 °C for an additional 2 h until disappearance of the starting material was confirmed by TLC, and then quenched by adding 1 M HCl (60 mL) at -78 °C. The solution was warmed to the rt, and extracted with EtOAc (3 x 50 mL). The combined organic layers were washed with brine

(50 mL) and dried over $MgSO_4$. The solvent was removed under reduced pressure. Purification of the crude product by flash chromatography on silica gel (50/50 EtOAc/hexanes) afforded **69** as a brown oil (12.0 g, 85%). Literature compound.[68] IR (microscope) 3371, 2979, 2250, 1740, 1713, 1517, 1440 cm^{-1}; ^1H NMR ($CDCl_3$, 400 MHz) δ 5.11 (br, 1H, N<u>H</u>), 4.46-4.32 (m, 1H, NHC<u>H</u>CO_2), 3.77 (s, 3H, $CO_2C\underline{H}_3$), 3.76 (s, 3H, $CO_2C\underline{H}_3$), 2.90-2.74 (m, 3H, 1xC<u>H</u>CH_2CN and 2xCHC<u>H</u>$_2$CN), 2.24-2.08 (m, 2H, $CH_2C\underline{H}_2CH$), 1.45 (s, 9H, $C(C\underline{H}_3)_3$); HRMS (ES) calcd for $C_{14}H_{22}N_2O_6Na$ ($[M+Na]^+$), 337.1370; found, 337.1369.

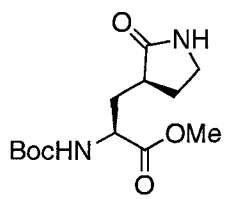

(*R*)-Methyl 2-(*tert*-butoxycarbonylamino)-3-((*S*)-2-oxopyrrolidin-3-yl)propanoate (70). The title compound was prepared by a modified literature procedure of Tian.[68] To a solution of the nitrile **69** (5.43 g, 16.1 mmol) in MeOH (120 mL) and $CHCl_3$ (30 mL) was added PtO_2 (0.54 g, 10% w/w). The resulting suspension was shaken under a 50 Psi hydrogen atmosphere for 3 days. Filtration through celite, followed by removal of solvent afforded the amine salt product as a light yellow foam (5.62 g, quant.), which was used for the next reaction without any further purification. To the solution of the amine salt in CH_2Cl_2 (40 mL) was added saturated $NaHCO_3$ solution (40 mL). The resulting reaction mixture was stirred at rt overnight. The two layers were then separated and the aqueous layer was extracted with EtOAc (3 x 40 mL). The combined organic layers were washed with brine (40 mL) and dried over $MgSO_4$. The solvent was removed under reduced

pressure. Purification of the crude product by flash chromatography on silica gel (EtOAc) afforded **70** as a white foam (3.43 g, 69%). Literature compound.[68] IR (microscope) 3292, 2977, 1744, 1698, 1524, 1440 cm^{-1}; ^1H NMR ($CDCl_3$, 400 MHz) δ 7.02 (br, 1H, N<u>H</u>), 5.64 (d, 1H, J = 8.1 Hz, N<u>H</u>), 4.30-4.20 (m, 1H, NHC<u>H</u>CO), 3.68 (s, 3H, $CO_2C\underline{H}_3$), 3.34-3.24 (m, 2H, $NHC\underline{H}_2CH_2$), 2.50-2.32 (m, 2H, 1x$NHCH_2C\underline{H}_2$ and 1x$CHC\underline{H}_2CH$), 2.08 (m, 1H, $CHC\underline{H}_2CH$), 1.84-1.70 (m, 2H, 1x$NHCH_2C\underline{H}_2$ and 1x$CH_2C\underline{H}CO$), 1.39 (s, 9H, $C(C\underline{H}_3)_3$); HRMS (ES) calcd for $C_{13}H_{22}N_2O_5Na$ ($[M+Na]^+$), 309.1421; found, 309.1421.

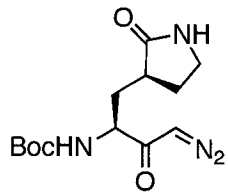

***tert*-Butyl (*R*)-4-diazo-3-oxo-1-((*S*)-2-oxopyrrolidin-3-yl)butan-2-ylcarbamate (71).** To a solution of carboxylic acid **66** (1.07 g, 3.94 mmol) in THF (40 mL) was added Et_3N (0.55 mL, 3.94 mmol), followed by ethyl chloroformate (0.41 mL, 4.28 mmol). The resulting solution was stirred at -30 °C for 1 h and then transferred into excess ethereal diazomethane solution (approx. 10 mmol) maintained at 0 °C. The reaction mixture was slowly warmed to rt and stirred for a further 2 h. Solvent was removed under reduced pressure to obtain the crude product, which was purified by flash chromatography on silica gel (EtOAc) to afford the diazoketone **71** as a yellow-orange oil (1.09 g, 85%). $[\alpha]^{25}_D$= -8.1° (c 1.00, $CHCl_3$); IR ($CHCl_3$ cast) 3304, 2978, 2107, 1694, 1643 cm^{-1}; ^1H NMR ($CDCl_3$, 300 MHz) δ 6.04 (br, 2H, N<u>H</u>), 5.59 (br, 1H, $C\underline{H}N_2$), 4.20 (m, 1H, NHC<u>H</u>CO), 3.37-3.26 (m, 2H, $NHC\underline{H}_2CH_2$), 2.47-2.33 (m, 2H, 1x$NHCH_2C\underline{H}_2$ and

1xCHC$\underline{H}_2$CH), 2.05-1.93 (m, 1H, CHC$\underline{H}_2$CH), 1.89-1.77 (m, 2H, 1xNHCH$_2$C$\underline{H}_2$ and 1xCH$_2$C$\underline{H}$CO), 1.41 (s, 9H, C(C$\underline{H}_3$)$_3$); ^{13}C NMR ($CDCl_3$, 125 MHz) δ 195.0, 180.4, 156.0, 79.8, 57.1, 53.5, 40.7, 38.5, 33.4, 28.4, 28.3; HRMS (ES) calcd for $C_{13}H_{20}N_4O_4Na$ ([M+Na]$^+$), 319.1376; found, 319.1377.

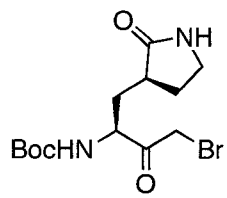

***tert*-Butyl (*R*)-4-bromo-3-oxo-1-((*S*)-2-oxopyrrolidin-3-yl)butan-2-ylcarbamate (72).** To a solution of the diazoketone **71** (0.8 g, 2.7 mmol) in THF (20 mL) at 0 °C was added aq. 48% HBr (0.45 mL, 2.7 mmol) dropwise over 15 min (the pH and progress of reaction were carefully monitored by TLC). The reaction mixture was stirred at 0 °C for an additional 15 min, quenched with saturated $NaHCO_3$ solution (5 mL) and the solvent was concentrated in vacuo. The residue was diluted with H_2O (30 mL) and extracted with EtOAc (3 x 30 mL). The combined organic layers were dried over $MgSO_4$ and then concentrated in vacuo. Purification of the crude product by flash chromatography on silica gel (EtOAc) afforded **72** as a yellow oil (838 mg, 89%). $[\alpha]^{25}_D$= +8.57° (*c* 0.133, $CHCl_3$); IR (CH_2Cl_2 cast) 3291, 2977, 2933, 1693, 1515, 1457, 1439 cm^{-1}; ^{1}H NMR ($CDCl_3$, 300 MHz) δ 6.52 (br, 1 H, N$\underline{H}$), 6.25 (br, 1H, N$\underline{H}$), 4.50 (m, 1 H, NHC$\underline{H}$CO), 4.19 (d, 1H, *J* = 14.0 Hz, C$\underline{H}_2$Br), 4.12 (d, 1H, *J* = 14.0 Hz, C$\underline{H}_2$Br), 3.41-3.31 (m, 2 H, NHC$\underline{H}_2$CH$_2$), 2.47–2.38 (m, 2 H, 1xNHCH$_2$C$\underline{H}_2$ and 1xCHC$\underline{H}_2$CH), 2.13-2.03 (m, 1 H, CHC$\underline{H}_2$CH), 1.99-1.81 (m, 2 H, 1xNHCH$_2$C$\underline{H}_2$ and 1xCH$_2$C$\underline{H}$CO), 1.44 (s, 9 H, C(C$\underline{H}_3$)$_3$); ^{13}C NMR ($CDCl_3$, 125 MHz) δ 201.3, 179.9, 156.3, 155.9, 80.2, 57.0, 40.6,

38.1, 32.5, 28.5, 28.3; HRMS (ES) calcd for $C_{13}H_{21}N_2O_4BrNa$ ([M+Na]$^+$), 371.0582; found, 371.0583.

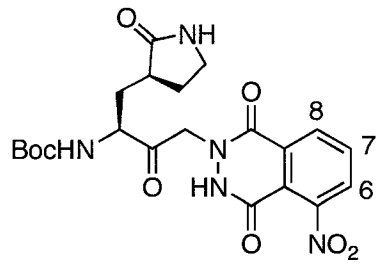

***tert*-Butyl (*S*)-4-(5-nitro-1,4-dioxo-3,4-dihydrophthalazin-2(1*H*)-yl)-3-oxo-1-((*S*)-2-oxopyrrolidin-3-yl)butan-2-ylcarbamate (74).** The title compound was prepared from the bromoketone **72** (50 mg, 0.14 mmol) as described for **64**. The product was obtained as a white foam (25 mg, 34%). $[\alpha]^{25}_D$= -2.5° (*c* 0.7, $CHCl_3$); IR ($CHCl_3$ cast) 3235, 2977, 2930, 1738, 1682, 1622, 1601, 1545 cm^{-1}; ^{1}H NMR ($CDCl_3$, 500 MHz) δ 8.25 (dd, 1H, *J* = 1.0, 8.0 Hz, H_6), 7.92 (dd, 1H, *J* = 8.0, 8.0 Hz, H_7), 7.73 (d, 1H, *J* = 8.0 Hz, H_8), 6.69 (br, 1H, N<u>H</u>), 6.12 (d, 1H, *J* = 7.0 Hz, N<u>H</u>), 5.21 (d, 1H, *J* = 16.5 Hz, C<u>H</u>$_2$N), 5.17 (d, 1H, *J* = 16.5 Hz, C<u>H</u>$_2$N), 4.51-4.46 (m, 1H, NHC<u>H</u>CO), 3.42-3.33 (m, 2H, NHC<u>H</u>$_2$CH$_2$), 2.52-2.41 (m, 2H, 1xNHCH$_2$C<u>H</u>$_2$ and 1xCHC<u>H</u>$_2$CH), 2.37-2.29 (m, 1H, CHC<u>H</u>$_2$CH), 2.04-1.83 (m, 2H, 1xNHCH$_2$C<u>H</u>$_2$ and 1xCH$_2$C<u>H</u>CO), 1.46 (s, 9H, C(C<u>H</u>$_3$)$_3$); ^{13}C NMR ($CDCl_3$, 125 MHz) δ 203.4, 180.4, 155.9, 148.9, 148.2, 133.8, 126.5, 126.0, 125.4, 119.8, 80.3, 68.7, 56.6, 40.7, 37.8, 32.1, 28.5, 28.3; HRMS (ES) calcd for $C_{21}H_{25}N_5O_8Na$ ([M+Na]$^+$), 498.1595; found, 498.1588.

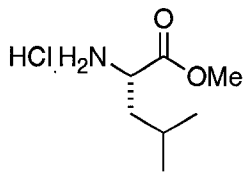

(*S*)-Methyl 2-amino-4-methylpentanoate hydrochloride salt (76). The title compound was prepared by a literature procedure of Eisenbarth.[82] $SOCl_2$ (10 mL) was added dropwise to L-leucine (5.0 g, 38.1 mmol) in MeOH (60 mL) at -10 °C. The solution was allowed to warm to rt, and then stirred overnight. The reaction mixture was refluxed for 2 more hours, cooled and the solvent was removed in vacuo. The resulting solid was suspended in Et_2O, filtered, and then washed several times to afford the product **76** as a white solid (6.4 g, quant.). Literature compound.[82] IR (microscope) 3465, 2957, 2921, 2872, 2630, 2584, 2022, 1740, 1588, 1505, 1468, 1452 cm^{-1}; ^1H NMR (CD_3OD, 400 MHz) δ 8.82 (br, 2H, N$\underline{H}_2$), 4.12-4.05 (m, 1H, NHC$\underline{H}$CO$_2$), 3.80 (s, 3H, CO$_2$C$\underline{H}_3$), 2.04-1.94 (m, 2H, CHC$\underline{H}_2$CH), 1.90-1.80 (m, 1H, C$\underline{H}$(CH$_3$)$_2$), 0.99 (d, 6H, J = 6.0 Hz, CH(C$\underline{H}_3$)$_2$); HRMS (ES) calcd for $C_7H_{16}NO_2$ ([M+H]$^+$), 146.1176; found, 146.1176.

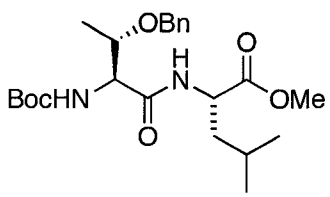

(*S*)-Methyl 2-((2*S*,3*S*)-3-(benzyloxy)-2-(*tert*-butoxycarbonylamino)butanamido)-4-methylpentanoate (77). To a solution of Boc-Thr(OBn)-OH (2.00 g, 6.46 mmol) in CH_2Cl_2 (30 mL) was added Et_3N (1.89 mL, 13.57 mmol) followed by ethyl chloroformate (0.65 mL, 6.78 mmol), and the resulting solution was stirred at 0 °C for 30 min. The precipitated Et_3N•HCl was filtered out, and the filtrate was treated with **76** (1.17 g, 6.46

mmol) and DMAP (0.079 g, 0.65 mmol) at 0 °C. The resulting solution was slowly warmed to rt and stirred further for 3 h. The solvent was removed under reduced pressure to obtain the crude product, which was purified by flash chromatography on silica gel (EtOAc) to afford the dipeptide product **77** as a white solid (2.37 g, 84%). Literature compound.[83] IR (microscope) 3320, 2959, 2871, 1749, 1686, 1651, 1530, 1454 cm^{-1}; ^1H NMR ($CDCl_3$, 500 MHz) δ 7.37-7.27 (m, 5H, Ph<u>H</u>), 7.03 (br, 1H, N<u>H</u>), 5.49 (br, 1H, N<u>H</u>), 4.65 (d, 1H, J = 11.2 Hz, OC<u>H</u>$_2$Ph), 4.56 (d, 1H, J = 11.2 Hz, OC<u>H</u>$_2$Ph), 4.58-4.46 (m, 1H, NHC<u>H</u>CO(Thr)), 4.36-4.32 (m, 1H, NHC<u>H</u>CO(Leu)), 4.14 (dq, 1H, J = 6.4, 3.1 Hz, CH_3C<u>H</u>OBn (Thr)), 3.70 (s, 3H, CO_2C<u>H</u>$_3$), 1.62-1.43 (m, 3H, 2xCHC<u>H</u>$_2$CH(Leu) and 1xCH_2C<u>H</u>(CH_3)$_2$(Leu)), 1.44 (s, 9H, C(C<u>H</u>$_3$)$_3$), 1.23 (d, 3H, J = 6.3 Hz, CHC<u>H</u>$_3$(Thr)), 0.87 (d, 3H, J = 6.3 Hz, CH(C<u>H</u>$_3$)$_2$(Leu)), 0.84 (d, 3H, J = 6.4 Hz, CH(C<u>H</u>$_3$)$_2$(Leu)); HRMS (ES) calcd for $C_{23}H_{36}N_2O_6Na$ ([M+Na]$^+$), 459.2466; found, 459.2465.

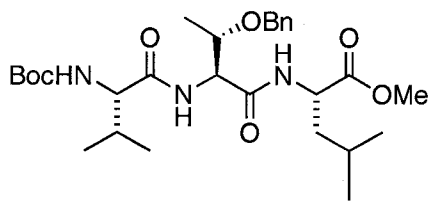

(6*S*,9*S*,12*S*)-Methyl 9-((*S*)-1-(benzyloxy)ethyl)-6-isopropyl-2,2,14-trimethyl-4,7,10-trioxo-3-oxa-5,8,11-triazapentadecane-12-carboxylate (78). The dipeptide **77** (5.13 g, 11.75 mmol) was stirred with TFA/CH_2Cl_2 (60 mL, 1:1 ratio) at 0 °C for 1.5 h, after which the reaction mixture was concentrated in vacuo and the residue triturated with Et_2O to yield the trifluoroacetate salt. To a solution of Boc-Val-OH (2.56 g, 11.75 mmol) in DMF (80 mL) at ambient temperature was added Et_3N (3.28 mL, 23.47 mmol), EDCI (2.25 g, 11.75 mmol) and HOBt (1.59 g, 11.75 mmol). The resulting mixture was treated

with a solution of the trifluoroacetate salt in DMF (20 mL). After 24 h stirring, the solvent was removed in vacuo. The residue was diluted with H_2O (60 mL) and extracted with EtOAc (3 x 60 mL). The combined organic layers were washed with brine, dried over $MgSO_4$ and then concentrated in vacuo. Purification of the crude product by flash chromatography on silica gel (gradient column, 25/75 EtOAc/hexanes to 100% EtOAc) afforded **78** as a white solid (4.15 g, 66%). $[\alpha]^{25}_{D}$= -12.45° (*c* 0.408, $CHCl_3$); IR (microscope) 3291, 3087, 2960, 2871, 1751, 1690, 1643, 1520, 1454 cm^{-1}; ^1H NMR (CD_3OD, 500 MHz) δ 7.35-7.23 (m, 5H, Ph<u>H</u>), 4.60 (d, 1H, *J* = 11.3 Hz, OC<u>H</u>$_2$Ph), 4.52-4.48 (m, 2H, NHC<u>H</u>CO(Thr) and NHC<u>H</u>CO(Leu)), 4.49 (d, 1H, *J* = 10.8 Hz, OC<u>H</u>$_2$Ph), 4.13-4.05 (m, 1H, CH_3C<u>H</u>OBn(Thr)), 3.92 (d, 1H, *J* = 6.5 Hz, NHC<u>H</u>CO(Val)), 3.66 (s, 3H, CO_2C<u>H</u>$_3$), 2.26-2.16 (m, 1H, CHC<u>H</u>$_2$CH(Val)), 1.68-1.57 (m, 3H, 2xCHC<u>H</u>$_2$CH(Leu) and 1xCH_2C<u>H</u>$(CH_3)_2$(Leu)), 1.41 (s, 9H, C(C<u>H</u>$_3)_3$), 1.24 (d, 3H, *J* = 6.3 Hz, CHC<u>H</u>$_3$(Thr)), 0.96 (d, 3H, *J* = 6.8 Hz, CH(C<u>H</u>$_3)_2$(Val)), 0.92 (d, 3H, *J* = 6.9 Hz, CH(C<u>H</u>$_3)_2$(Val)), 0.89 (t, 6H, *J* = 5.7 Hz, CH(C<u>H</u>$_3)_2$(Leu)); ^{13}C NMR (CD_3OD, 125 MHz) δ 172.8, 171.6, 169.3, 137.9, 128.4, 127.8, 127.7, 80.2, 76.7, 74.1, 71.6, 60.2, 56.0, 52.1, 51.1, 41.0, 30.7, 28.3, 24.7, 22.7, 21.7, 19.3, 17.5; HRMS (ES) calcd for $C_{28}H_{45}N_3O_7Na$ ([M+Na]$^+$), 558.3150; found, 558.3152.

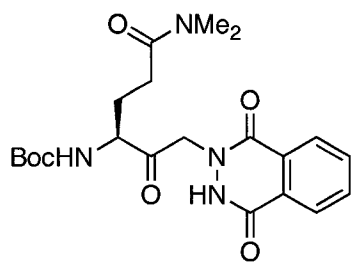

(*R*)-*tert*-Butyl 6-(dimethylamino)-1-(1,4-dioxo-3,4-dihydrophthalazin-2(1*H*)-yl)-2,6-dioxohexan-3-ylcarbamate (80). The title compound was prepared by a literature procedure of Yeeman[65b] from the bromoketone **85** (100 mg, 0.27 mmol) as described for **64**. The product was obtained as a white solid (50 mg, 41%). Literature compound.[65b] IR (microscope) 3397, 3233, 3164, 2986, 2865, 1735, 1696, 1653, 1617, 1602, 1498, 1448 cm^{-1}; ^1H NMR ($CDCl_3$, 500 MHz) δ 10.41 (br, 1H, N<u>H</u>), 8.39 (ddd, 1H, J = 7.8, 1.5, 0.6 Hz, Ar<u>H</u>), 8.08 (ddd, 1H, J = 7.8, 1.5, 0.6 Hz, Ar<u>H</u>), 7.86-7.75 (m, 2H, Ar<u>H</u>), 5.78-5.73 (m, 1H, N<u>H</u>), 5.19 (d, 1H, J = 16.6 Hz, C<u>H</u>$_2$N), 5.07 (d, 1H, J = 16.7 Hz, C<u>H</u>$_2$N), 4.56-4.49 (m, 1H, NHC<u>H</u>CO), 3.00 (s, 3H, N(C<u>H</u>$_3$)$_2$), 2.95 (s, 3H, N(C<u>H</u>$_3$)$_2$), 2.56-2.33 (m, 3H, 1xCHC<u>H</u>$_2$CH$_2$ and 2xCH$_2$C<u>H</u>$_2$CO), 2.17-2.09 (m, 1H, CHC<u>H</u>$_2$CH$_2$), 1.45 (s, 9H, (C<u>H</u>$_3$)$_3$); HRMS (ES) calcd for $C_{21}H_{28}N_4O_6Na$ ([M+Na]$^+$), 455.1901; found, 455.1899.

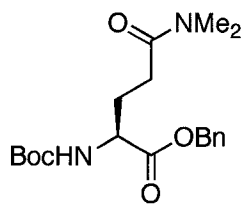

(*S*)-Benzyl 2-(*tert*-butoxycarbonylamino)-5-(dimethylamino)-5-oxopentanoate (82). The title compound was prepared by a literature procedure of Yeeman.[65b] To a stirred solution of Boc-Glu(OBn)-OH (5.00 g, 14.8 mmol) in CH_2Cl_2 (70 mL) at 0 °C was added Et_3N (2.3 mL, 16.3 mmol) and EtOCOCl (1.5 mL, 15.6 mmol). After stirring for 30 min at 0 °C, $NHMe_2$•HCl (1.33 g, 16.8 mmol) and Et_3N (2.60 mL, 18.5 mmol) were added to the reaction mixture. The resulting mixture was stirred overnight at rt. The solvent was removed and the residue was diluted with H_2O (60 mL) and extracted with EtOAc (3 x 60 mL). The combined organic layers were washed with 1 N HCl (20 mL), brine (20 mL)

and dried over $MgSO_4$. The solvent was removed under reduced pressure and the crude product was recrystallized from CH_2Cl_2/hexanes to afford the product as a white crystalline solid (4.80 g, 89%). Literature compound.[65b] IR (microscope) 3304, 3034, 2977, 2935, 1744, 1711, 1638, 1501, 1456 cm^{-1}; ^1H NMR ($CDCl_3$, 400 MHz) δ 7.36-7.26 (m, 5H, Ph<u>H</u>), 5.48-5.40 (br, 1H, N<u>H</u>), 5.20 (d, 1H, J = 12.3 Hz, OC<u>H</u>$_2$Ph), 5.12 (d, 1H, J = 12.3 Hz, OC<u>H</u>$_2$Ph), 4.36-4.26 (m, 1H, NHC<u>H</u>CH$_2$), 2.90 (s, 3H, N(C<u>H</u>$_3$)$_2$), 2.88 (s, 3H, N(C<u>H</u>$_3$)$_2$), 2.40-2.25 (m, 2H, CH$_2$C<u>H</u>$_2$CO), 2.23-2.13 (m, 1H, CHC<u>H</u>$_2$CH$_2$), 2.01 (m, 1H, J = 14.4, CHC<u>H</u>$_2$CH$_2$), 1.41 (s, 9H, (C<u>H</u>$_3$)$_3$); HRMS (ES) calcd for $C_{19}H_{28}N_2O_5Na$ ([M+Na]$^+$), 387.1890; found, 387.1894.

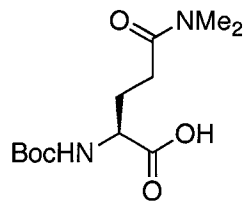

(*R*)-2-(*tert*-Butoxycarbonylamino)-5-(dimethylamino)-5-oxopentanoic acid (83). The title compound was prepared by a literature procedure of Yeeman.[65b] To a solution of **82** (3.70 g, 9.6 mmol) in MeOH (35 mL) was added Pd/C (0.37 g, 10% w/w). The resulting suspension was stirred under a hydrogen atmosphere for 3 days. Filtration through celite, followed by removal of solvent afforded the crude product, which was recrystallized from CH_2Cl_2/hexanes to afford the product as a white crystalline solid (2.50 g, 86%). Literature compound.[65b] IR (microscope) 3322, 2979, 2935, 2591, 1711, 1631, 1509, 1454, 1405 cm^{-1}; ^1H NMR ($CDCl_3$, 400 MHz) δ 5.70-5.65 (br, 1H, N<u>H</u>), 4.25-4.19 (m, 1H, NHC<u>H</u>CH$_2$), 3.03 (s, 3H, N(C<u>H</u>$_3$)$_2$), 2.97 (s, 3H, N(C<u>H</u>$_3$)$_2$), 2.80-2.67 (m, 1H, CH$_2$C<u>H</u>$_2$CO), 2.51-2.35 (m, 1H, CH$_2$C<u>H</u>$_2$CO), 2.30-2.13 (m, 1H, CHC<u>H</u>$_2$CH$_2$), 1.99 (m,

1H, CHC$\underline{H}_2$CH$_2$), 1.42 (s, 9H, (C$\underline{H}_3$)$_3$); HRMS (ES) calcd for $C_{12}H_{22}N_2O_5Na$ ([M+Na]$^+$), 297.1421; found, 297.1424.

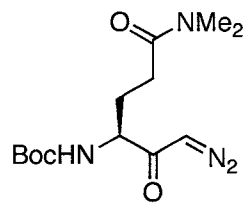

(*S*)-*tert*-Butyl 1-diazo-6-(dimethylamino)-2,6-dioxohexan-3-ylcarbamate (84). The title compound was prepared by a literature procedure of Yeeman[65b] from the carboxylic acid **83** (4.1 g, 13.8 mmol) as described for **71**. The product was obtained as a white solid (3.8 g, 85%). Literature compound.[65b] IR (microscope) 3302, 2978, 2934, 2108, 1710, 1634, 1513, 1454 cm^{-1}; ^{1}H NMR ($CDCl_3$, 400 MHz) δ 5.78-5.68 (br, 1H, N$\underline{H}$), 5.62 (s, 1H, C$\underline{H}$N$_2$), 4.20-4.10 (m, 1H, NHC$\underline{H}$CH$_2$), 2.96 (s, 3H, N(C$\underline{H}_3$)$_2$), 2.92 (s, 3H, N(C$\underline{H}_3$)$_2$), 2.52-2.28 (m, 2H, CH$_2$C$\underline{H}_2$CO), 2.20-2.08 (m, 1H, CHC$\underline{H}_2$CH$_2$), 1.85 (ddt, 1H, J = 14.2, 8.7, 6.3 Hz, CHC$\underline{H}_2$CH$_2$), 1.40 (s, 9H, (C$\underline{H}_3$)$_3$); HRMS (ES) calcd for $C_{13}H_{22}N_4O_4Na$ ([M+Na]$^+$), 321.1533; found, 321.1532.

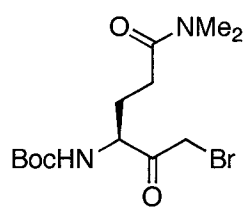

(*R*)-*tert*-Butyl 1-bromo-6-(dimethylamino)-2,6-dioxohexan-3-ylcarbamate (85). The title compound was prepared by a literature procedure of Yeeman[65b] from the diazoketone **84** (3.4 g, 10.6 mmol) as described for **72.** The product was obtained as a yellow solid (3.0 g, 74%). Literature compound.[65b] IR (microscope) 3230, 3013, 2983, 2936, 1735,

1699, 1614, 1526, 1457 cm^{-1}; ^1H NMR ($CDCl_3$, 500 MHz) δ 5.76-5.64 (br, 1H, N<u>H</u>), 4.56-4.48 (m, 1H, NHC<u>H</u>CH_2), 4.22 (d, 1H, J = 13.5 Hz, C<u>H</u>$_2$Br), 4.20 (d, 1H, J = 13.5 Hz, C<u>H</u>$_2$Br), 3.00 (s, 3H, N(C<u>H</u>$_3$)$_2$), 2.95 (s, 3H, N(C<u>H</u>$_3$)$_2$), 2.53-2.33 (m, 2H, CH_2C<u>H</u>$_2$CO), 2.26-2.18 (m, 1H, CHC<u>H</u>$_2$$CH_2$), 2.05-1.95 (m, 1H, CHC<u>H</u>$_2$$CH_2$), 1.45 (s, 9H, (C<u>H</u>$_3$)$_3$); HRMS (ES) calcd for $C_{13}H_{23}N_2O_4BrNa$ 373.0733, found 373.0729.

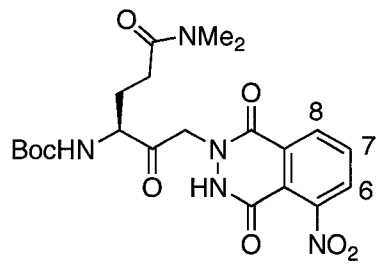

(*R*)-*tert*-Butyl 6-(dimethylamino)-1-(5-nitro-1,4-dioxo-3,4-dihydrophthalazin-2(1*H*)-yl)-2,6-dioxohexan-3-ylcarbamate (86). The title compound was prepared by a literature procedure of Yeeman[65b] from the bromoketone **85** (200 mg, 0.54 mmol) as described for **64**. The product was obtained as a white solid (138 mg, 34%). Literature compound.[65b] IR (microscope) 3289, 2978, 2934, 1709, 1628, 1603, 1546, 1507, 1454 cm^{-1}; ^1H NMR ($CDCl_3$, 500 MHz) δ 8.23 (dd, 1H, J = 8.0, 1.0 Hz, H_6), 7.91 (dd, 1H, J = 8.0, 8.0 Hz, H_7), 7.71 (dd, 1H, J = 8.0, 1.0 Hz, H_8), 5.92 (d, 1H, J = 6.9 Hz, N<u>H</u>), 5.45 (d, 1H, J = 7.8 Hz, N<u>H</u>), 5.21 (d, 1H, J = 16.8 Hz, C<u>H</u>$_2$N), 5.09 (d, 1H, J = 16.8 Hz, C<u>H</u>$_2$N), 4.46-4.38 (m, 1H, NHC<u>H</u>CH_2), 2.97 (s, 3H, N(C<u>H</u>$_3$)$_2$), 2.92 (s, 3H, N(C<u>H</u>$_3$)$_2$), 2.60-2.22 (m, 3H, 2xCH_2C<u>H</u>$_2$CO, 1xCHC<u>H</u>$_2$$CH_2$), 2.10-2.00 (m, 1H, CHC<u>H</u>$_2$$CH_2$), 1.41 (s, 9H, (C<u>H</u>$_3$)$_3$); HRMS (ES) calcd for $C_{21}H_{27}N_5O_8Na$ ([M+Na]$^+$), 500.1752; found, 500.1756.

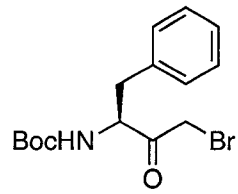

(*R*)-*tert*-Butyl 4-bromo-3-oxo-1-phenylbutan-2-ylcarbamate (88). To a solution of N-Boc-phenylalanine (1 g, 3.77 mmol) in THF (30 mL) at 0 °C was added triethylamine (0.58 mL, 4.15 mmol) followed by ethyl chloroformate (0.39 mL, 4.02 mmol). The resulting solution was stirred at 0 °C for half an hour. The formed salt was filtered quickly by gravity filtration, and the filtrate was transferred into an excess ethereal diazomethane solution (approx. 12 mmol) and the temperature was maintained at 0 °C. The reaction mixture was slowly warmed to rt and stirred for another hour. The solvent was removed under reduced pressure to obtain the crude diazo product (1.08 g, quant.), which was used in the following step without any purification. To the solution of the diazo-ketone compound in THF (30 mL) at 0 °C was added aq. 48% HBr (0.67 mL, 4.00 mmol) dropwise over 15 min. The reaction mixture was stirred for an additional 15 min, quenched with saturated aq. $NaHCO_3$ (10 mL) and the solvent was removed in vacuo. The residue was diluted with H_2O and extracted with CH_2Cl_2. The combined organic layers were dried over $MgSO_4$ and then concentrated in vacuo. Purification of the crude product by flash chromatography on silica gel (EtOAc) afforded **88** as a white solid (0.98 g, 76%). $[\alpha]^{25}_{D}$= +6.1° (*c* 0.18, $CHCl_3$); IR ($CHCl_3$ cast) 3364, 3029, 2985, 2936, 1733, 1679, 1515, 1456 cm^{-1}; ^1H NMR ($CDCl_3$, 500 MHz) δ 7.12-7.33 (m, 5 H, Ph<u>H</u>), 5.05-5.12 (br, 1 H, N<u>H</u>), 4.64-4.74 (m, 1 H, NHC<u>H</u>CO), 3.95 (d, 1H, *J* = 13.7 Hz, C<u>H</u>$_2$Br), 3.83 (d, 1H, *J* = 13.7 Hz, C<u>H</u>$_2$Br), 3.04–3.13 (m, 1 H, C<u>H</u>$_2$Ph), 2.94–3.04 (m, 1 H, C<u>H</u>$_2$Ph), 1.40 (s, 9 H, C(C<u>H</u>$_3$)$_3$); ^{13}C NMR (125 MHz, $CDCl_3$) δ 200.8, 155.2, 135.8, 129.2, 128.9,

127.3, 80.5, 58.5, 37.8, 33.2, 28.3; HRMS (ES) calcd for $C_{15}H_{20}NO_3BrNa$ ([M+Na]$^+$), 364.0519; found, 364.0516.

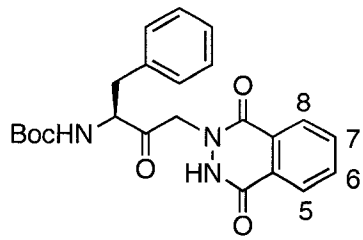

(*S*)-*tert*-Butyl 4-(1,4-dioxo-3,4-dihydrophthalazin-2(1H)-yl)-3-oxo-1-phenylbutan-2-ylcarbamate (89). To a solution of phthalhydrazide (1.00 g, 6.15 mmol) in DMF (30 mL) was added NaH (0.17 g, 6.8 mmol) and the mixture was stirred at rt for 2 h after which it was filtered and washed with anhydrous Et_2O to yield sodium phthalhydrazide as a white solid (1.18 g, quant.). To a suspension of sodium phthalhydrazide (117 mg, 0.64 mmol) in DMF (4 mL) was added a solution of bromoketone **88** (200 mg, 0.58 mmol) in DMF (8 mL) dropwise over 1 h. After stirring for 6 h at rt, the solvent was removed in vacuo and the residue diluted with H_2O and extracted with EtOAc. The combined organic layers were dried over $MgSO_4$ and the solvent removed in vacuo to obtain the crude product, which was purified by flash column chromatography on silica gel (50/50 EtOAc/hexanes) to obtain **89** (83 mg, 34%) as a white solid. $[\alpha]^{25}_D$= -20.4° (*c* 0.09, MeOH); IR (microscope) 3359, 3167, 3012, 2921, 1751, 1738, 1687, 1656, 1601, 1523, 1494 cm^{-1}; ^{1}H NMR (CD_3OD, 500 MHz) δ 8.28 (d, 1H, *J* = 7.6 Hz, H_5 or H_8), 8.11 (d, 1H, *J* = 8.0 Hz, H_5 or H_8), 7.91 (dd, 1H, *J* = 7.6, 7.3 Hz, H_6 or H_7), 7.86 (dd, 1H, *J* = 8.0, 7.3 Hz, H_6 or H_7), 7.15-7.28 (m, 5H, Ph<u>H</u>), 5.12 (s, 2H, C<u>H</u>$_2$N), 4.56 (dd, 1H, *J* = 9.8, 5.0 Hz, NHC<u>H</u>CO), 3.21 (dd, 1H, *J* = 14.0, 5.0 Hz, C<u>H</u>$_2$Ph), 2.83 (dd, 1H, *J* = 14.0, 9.8 Hz, C<u>H</u>$_2$Ph), 1.36 (s, 9H, C(C<u>H</u>$_3$)$_3$); ^{13}C NMR (CD_3OD, 125 MHz) δ 205.4, 161.7, 157.8,

151.4, 138.6, 135.0, 133.6, 130.5, 129.9, 129.5, 127.7, 127.4, 126.0, 125.0, 80.8, 70.2, 60.0, 37.5, 28.6; HRMS (ES) calcd for $C_{23}H_{25}N_3O_5Na$ ([M+Na]$^+$), 446.1686; found, 446.1683.

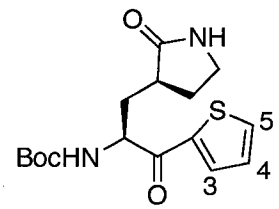

(*S*)-*tert*-Butyl 1-oxo-3-((*S*)-2-oxopyrrolidin-3-yl)-1-(thiophen-2-yl)propan-2-ylcarbamate (90). To a solution of **91** (120 mg, 0.38 mmol) in THF (2 mL) at -15 °C was charged *i*-PrMgCl (0.37 mL, 2 M solution in THF, 0.74 mmol) dropwise to afford a clear solution. After stirring for 10 min, thiophen-2-yl-magnesium bromide (1.2 mL, 1.0 M solution in THF, 1.2 mmol) was added slowly and the temperature was maintained lower than -5 °C. The cooling bath was removed and the mixture was allowed to warm to rt over 30 min. After 4 h stirring at rt, the reaction was complete. The reaction mixture was cooled on an ice bath and 1.0 N HCl (2 mL) was added slowly, followed by EtOAc extraction. The combined organic layers were dried over $MgSO_4$ and the solvent was removed in vacuo to obtain the crude mixture, which was purified by flash column chromatography on silica gel (EtOAc) to obtain product **90** (81 mg, 63%) as a white foam and recovered starting material **91** (18 mg, 15%). $[\alpha]^{25}_D$= +33.7° (*c* 0.25, $CHCl_3$); IR ($CHCl_3$ cast) 3283, 2977, 1663, 1515, 1440 cm^{-1}; ^{1}H NMR ($CDCl_3$, 500 MHz) δ 7.84 (d, 1H, *J* = 3.8 Hz, H_5), 7.66 (d, 1H, *J* = 4.8 Hz, H_3), 7.12 (dd, 1H, *J* = 4.8, 3.8 Hz, H_4), 6.29 (br, 1H, N<u>H</u>), 5.68 (br, 1H, N<u>H</u>), 5.10 (dd, 1H, *J* = 6.5, 0.6 Hz, NHC<u>H</u>CO), 3.38-3.30 (m, 2H, NHC<u>H</u>$_2$CH$_2$), 2.58-2.46 (m, 2H, 1xNHCH$_2$C<u>H</u>$_2$ and 1xCHC<u>H</u>$_2$CH), 2.22-2.14 (m, 1H,

CHC$\underline{H}_2$CH), 1.94-1.84 (m, 2H, 1xNHCH$_2$C$\underline{H}_2$ and 1xCH$_2$C$\underline{H}$CO), 1.42 (s, 9H, C(C$\underline{H}_3$)$_3$); ^{13}C NMR (CDCl$_3$, 125 MHz) δ 191.5, 179.5, 155.6, 141.2, 134.8, 133.2, 128.4, 79.9, 54.9, 40.3, 38.2, 35.3, 35.2, 28.3; HRMS (ES) calcd for $C_{16}H_{22}N_2O_4SNa$ ([M+Na]$^+$), 361.1193; found, 361.1190.

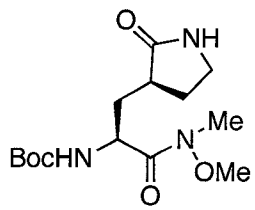

(*S*)-*tert*-Butyl 1-(methoxy(methyl)amino)-1-oxo-3-((*S*)-2-oxopyrrolidin-3-yl)propan-2-ylcarbamate (91). To a solution of cyclic glutamic acid **66** (200 mg, 0.73 mmol) in DCM (5 mL) at 0 °C was added Weinreb amine (71 mg, 0.73 mmol), EDCI (141 mg, 0.73 mmol), HOBt (99 mg, 0.73 mmol) and NMM (0.16 mL, 1.46 mmol). The resulting solution was stirred overnight while warming slowly to rt. Then the reaction mixture was diluted with DCM (50 mL) and washed with water and brine. The combined organic layers were dried over $MgSO_4$ and then concentrated in vacuo. Purification of the crude product by flash chromatography on silica gel (90/10, EtOAc/MeOH) afforded **91** as a white foam (151 mg, 66%). $[\alpha]^{25}_D$= -0.22° (*c* 0.27, CHCl$_3$); IR (CHCl$_3$ cast) 3293, 2976, 1693 cm^{-1}; ^{1}H NMR (CDCl$_3$, 500 MHz) δ 6.85 (br, 1H, N$\underline{H}$), 5.45 (br, 1H, N$\underline{H}$), 4.60 (dd, 1H, *J* = 8.0, 8.0 Hz, NHC$\underline{H}$CO), 3.77 (s, 3H, OC$\underline{H}_3$), 3.33 (dd, 2H, *J* = 8.7, 4.0 Hz, NHC$\underline{H}_2$CH$_2$), 3.20 (s, 3H, NC$\underline{H}_3$), 2.54-2.42 (m, 2H, 1xNHCH$_2$C$\underline{H}_2$ and 1xCHC$\underline{H}_2$CH), 2.15-2.02 (m, 1H, CHC$\underline{H}_2$CH), 1.89-1.77 (m, 1H, NHCH$_2$C$\underline{H}_2$), 1.72-1.62 (m, 1H, CH$_2$C$\underline{H}$CO), 1.42 (s, 9H, C(C$\underline{H}_3$)$_3$); ^{13}C NMR (CDCl$_3$, 125 MHz) δ 179.6, 172.6, 155.8,

79.6, 61.6, 49.3, 40.3, 38.0, 34.4, 32.1, 28.3, 28.0; HRMS (ES) calcd for $C_{14}H_{25}N_3O_5Na$ ($[M+Na]^+$), 338.1686; found, 338.1688.

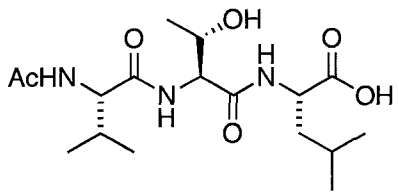

(*S*)-2-((2*S*,3*S*)-2-((*S*)-2-Acetamido-3-methylbutanamido)-3-hydroxybutanamido)-4-methylpentanoic acid (92). The tripeptide **78** (3.76 g, 6.73 mmol) was stirred with TFA/CH_2Cl_2 (100 mL, 1:1 ratio) at 0 °C for 2 h, after which the reaction mixture was concentrated in vacuo and the residue was triturated with Et_2O to yield the trifluoroacetate salt. To a solution of the trifluoroacetate salt in CH_2Cl_2 (50 mL) was added Et_3N (50 mL) and Ac_2O (50 mL). The solvent was removed in vacuo after 24 h stirring. The residue was diluted with H_2O (50 mL) and extracted with EtOAc (3 x 50 mL). The combined organic layers were washed with brine, dried over $MgSO_4$ and then concentrated in vacuo to afford the *N*-acetyl tripeptide product, which was used for next reaction without any further purification. To a solution of the *N*-acetyl tripeptide product (0.48 g, 1.00 mmol) in MeOH (15 mL) was added Pd/C (48 mg, 10% w/w). The resulting suspension was stirred under a hydrogen atmosphere overnight. Filtration through celite, followed by removal of solvent afforded the deprotected tripeptide as a white solid (0.39 g, quant.), which was used for next reaction without any further purification. To a solution of the deprotected tripeptide (0.20 g, 0.52 mmol) in THF/H_2O (5 mL/5 mL) was added LiOH (28.4 mg, 0.68 mmol) at 0 °C. The resulting mixture was stirred for further 2 h until complete consumption of the starting material was confirmed by TLC. The

solution was quenched with AcOH (0.12 g) and then the solvent was removed in vacuo. The residue was treated with H_2O (20 mL) and citric acid (150 mg) until pH = 3, and then extracted with EtOAc (3 x 30 mL). The combined organic layers were washed with brine (30 mL) and dried over $MgSO_4$. The solvent was removed to afford the product **92** as a white solid (0.21 g, quant.). $[\alpha]^{25}_{D}$= -53.11° (*c* 0.189, MeOH); IR (microscope) 3282, 3083, 2959, 2872, 1726, 1638, 1545, 1456 cm^{-1}; ^1H NMR (CD_3OD, 400 MHz) δ 4.45 (dd, 1H, *J* = 8.6, 6.1 Hz, NHC<u>H</u>CO(Leu)), 4.36 (d, 1H, *J* = 5.0 Hz, NHC<u>H</u>CO(Thr)), 4.21 (d, 1H, *J* = 7.2 Hz, NHC<u>H</u>CO(Val)), 4.11 (dq, 1H, *J* = 11.5, 5.1 Hz, CH_3C<u>H</u>OBn(Thr)), 2.09 (m, 1H, CHC<u>H</u>$(CH_3)_2$(Val)), 2.00 (s, 3H, COC<u>H</u>$_3$), 1.77-1.67 (m, 2H, CHC<u>H</u>$_2$CH(Leu)), 1.67-1.62 (m, 1H, CH_2C<u>H</u>$(CH_3)_2$(Leu)), 1.20 (d, 3H, *J* = 6.4 Hz, CHC<u>H</u>$_3$(Thr)), 0.96 (d, 6H, *J* = 6.7 Hz, CH(C<u>H</u>$_3)_2$(Val)), 0.95 (d, 3H, *J* = 6.4 Hz, CH(C<u>H</u>$_3)_2$(Leu)), 0.90 (d, 3H, *J* = 6.4 Hz, CH(C<u>H</u>$_3)_2$(Leu)); ^{13}C NMR (CD_3OD, 125 MHz) δ 175.7, 173.9, 173.6, 172.3, 68.5, 60.7, 60.0, 52.1, 41.7, 31.7, 25.9, 23.4, 22.4, 21.8, 19.9, 19.7, 18.7; HRMS (ES) calcd for $C_{17}H_{31}N_3O_6Na$ ([M+Na]$^+$), 396.2105; found, 396.2107.

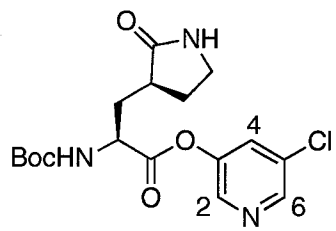

(*S*)-5-Chloropyridin-3-yl 2-(*tert*-butoxycarbonylamino)-3-((*S*)-2-oxopyrrolidin-3-yl)propanoate (93). To a solution of the cyclic glutamic acid **66** (150 mg, 0.55 mmol) in DMF (2 mL) at ambient temperature was added pyridine (45 μL, 0.55 mmol), EDCI (106 mg, 0.55 mmol), HOBt (74 mg, 0.55 mmol) and 5-chloropyridinol (71 mg, 0.55 mmol). The reaction mixture was stirred at rt overnight, and then the solvent was removed in

vacuo. The residue was diluted with H_2O (15 mL) and extracted with EtOAc (3 x 15 mL). The combined organic layers were dried over $MgSO_4$ and then concentrated in vacuo. Purification of the crude product by flash chromatography on silica gel (EtOAc) afforded the product **93** as a white foam (83 mg, 39%). $[\alpha]^{25}_{D}$= +16.83° (*c* 0.24, $CHCl_3$); IR (microscope) 3267, 2978, 1774, 1695, 1569, 1522, 1441, 1423 cm^{-1}; ^1H NMR ($CDCl_3$, 400 MHz) δ 8.48 (d, 1H, *J* = 1.9 Hz, H_2 or H_6), 8.37 (d, 1H, *J* = 2.1 Hz, H_2 or H_6), 7.60 (dd, 1H, *J* = 2.1, 2.2 Hz, H_4), 6.18-6.12 (br, 1H, N<u>H</u>), 6.10-6.02 (br, 1H, N<u>H</u>), 4.59-4.50 (m, 1H, NHC<u>H</u>CO), 3.46-3.35 (m, 2H, NHC<u>H</u>$_2$CH$_2$), 2.62-2.44 (m, 2H, 1xNHCH$_2$C<u>H</u>$_2$ and 1xCHC<u>H</u>$_2$CH), 2.33-2.25 (m, 1H, CHC<u>H</u>$_2$CH), 2.18-2.04 (m, 1H, NHCH$_2$C<u>H</u>$_2$), 1.98-1.80 (m, 1H, CH$_2$C<u>H</u>CO), 1.47 (s, 9H, C(C<u>H</u>$_3$)$_3$); ^{13}C NMR ($CDCl_3$, 125 MHz) δ 179.3, 170.5, 155.9, 147.2, 146.2, 141.1, 131.8, 129.4, 80.4, 61.5, 53.0, 40.4, 38.0, 28.5, 28.3; HRMS (ES) calcd for $C_{17}H_{22}N_3O_5ClNa$ ([M+Na]$^+$), 406.1140; found, 406.1142.

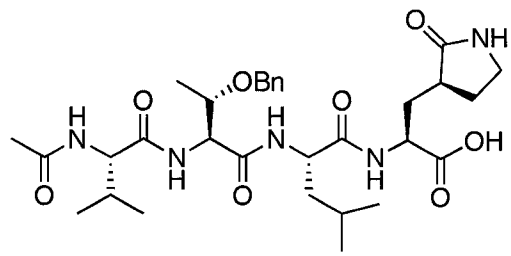

(2*S*,5*S*,8*S*,11*S*)-8-((*R*)-1-(Benzyloxyl)ethyl)-5-isobutyl-11-isopropyl-4,7,10,13-tetraoxo-2-(((*S*)-2-oxopyrrolidin-3-yl)methyl-3,6,9,12-tetraazatetradecan-1-oic acid (96). To a solution of **97** (45 mg, 0.071mmol) in THF/H_2O (10 mL, 1:1 ratio) at 0 °C was added LiOH (4.0 mg, 0.092 mmol). After 2 h of stirring, the solvent was removed in vacuo. Water (10 mL) and citric acid was added to adjust the pH of the solution to 3. The mixture was extracted with EtOAc, washed with water and brine. The combined organic

layers were dried over $MgSO_4$ and then the solvent was removed in vacuo to afford the product **96** (42 mg, quant.) as a white foam. $[\alpha]^{25}_{D}$= -22.9° (*c* 0.30, MeOH); IR (microscope) 3276, 3089, 2961, 2873, 1633, 1545, 1438, 1404 cm^{-1}; ^{1}H NMR (CD_3OD, 400 MHz) δ 7.38-7.20 (m, 5H, Ph<u>H</u>), 4.59 (d, 1H, *J* = 11.1 Hz, OC<u>H</u>$_2$Ph), 4.47 (d, 1H, *J* = 11.1 Hz, OC<u>H</u>$_2$Ph), 4.49-4.45 (m, 3H, 1xNHC<u>H</u>CO(Gln), 1x NHC<u>H</u>CO(Leu) and 1xNHC<u>H</u>CO(Thr)), 4.18 (d, 1H, *J* = 6.8 Hz, NHC<u>H</u>CO(Val)), 4.16-4.06 (m, 1H, CH_3C<u>H</u>OBn(Thr)), 3.28-3.10 (m, 2H, NHC<u>H</u>$_2$CH$_2$(Gln)), 2.54-2.42 (m, 1H, NHCH$_2$C<u>H</u>$_2$(Gln)), 2.28-2.04 (m, 3H, 1xNHCH$_2$C<u>H</u>$_2$(Gln), 1xCH$_2$C<u>H</u>CO(Gln) and 1xCHC<u>H</u>(CH$_3$)$_2$(Val)), 1.95 (s, 3H, COC<u>H</u>$_3$), 1.84-1.70 (m, 2H, CHC<u>H</u>$_2$CH(Gln)), 1.68-1.54 (m, 3H, 2xCHC<u>H</u>$_2$CH(Leu) and 1xCH$_2$C<u>H</u>(CH$_3$)$_2$(Leu)), 1.22 (d, 3H, *J* = 6.4 Hz, CH(C<u>H</u>$_3$)$_2$(Thr)), 0.98 (d, 3H, *J* = 6.8 Hz, CHC<u>H</u>$_3$(Val)), 0.96 (d, 3H, *J* = 6.8 Hz, CH(C<u>H</u>$_3$)$_2$(Val)), 0.90-0.85 (m, 6H, CH(C<u>H</u>$_3$)$_2$(Leu)); ^{13}C NMR (CD_3OD, 125 MHz) δ 174.7, 174.5, 174.2, 173.9, 171.9, 171.8, 139.6, 129.4, 128.9, 128.7, 76.0, 72.5, 61.2, 58.9, 53.2, 52.0, 42.0, 41.4, 39.6, 34.3, 31.3, 28.7, 25.7, 23.5, 22.4, 22.0, 19.7, 18.7, 16.9; HRMS (ES) calcd for $C_{31}H_{47}N_5O_8Na$ ([M+Na]$^+$), 640.3317; found, 640.3320.

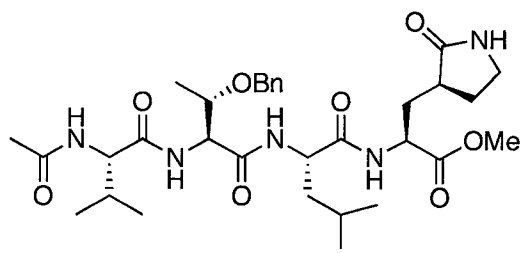

(2*S*,5*S*,8*S*,11*S*)-Methyl 8-((*S*)-1-(benzyloxy)ethyl)-5-isobutyl-11-isopropyl-4,7,10,13-tetraoxo-2-(((*S*)-2-oxopyrrolidin-3-yl)methyl)-3,6,9,12-tetraazatetradecan-1-oate (97). Compound **70** (35 mg, 0.12 mmol) was stirred with TFA/CH_2Cl_2 (2 mL, 1:1 ratio) at

0 °C for 1.5 h, after which the reaction mixture was concentrated in vacuo and the residue triturated with Et_2O to yield the trifluoroacetate salt. To a solution of Ac-Val-Thr(OBn)-Leu-OH (57 mg, 0.12 mmol) in DMF (3 mL) at ambient temperature was added Et_3N (41 μM, 0.29 mmol), EDCI (29 mg, 0.15 mmol), HOBt (20 mg, 0.15 mmol) and the trifluoroacetate salt in DMF (2 mL). The reaction mixture was stirred at 0 °C for 30 min, and then allowed to warm to rt overnight. The solvent was removed in vacuo and the crude product was purified by HPLC (Waters C_{18} Bondpak column; particle size 10 μM, pore size 125 Å, dimensions 25 mm x 100 mm, linear gradient elution of over 45 min of 10 to 100% acetonitrile in 0.075% TFA/H_2O, t_R = 31 min) to afford the product **97** (50 mg, 65%). $[\alpha]^{25}_D$= -20.24° (*c* 0.165, $CHCl_3$); IR (microscope) 3287, 3087, 2960, 2932, 2873, 2469, 2408, 1745, 1696, 1632, 1545, 1454 cm^{-1}; ^1H NMR (CD_3OD, 500 MHz) δ 7.34-7.24 (m, 5H, Ph<u>H</u>), 4.59 (d, 1H, *J* = 11.5 Hz, OC<u>H</u>$_2$Ph), 4.49-4.42 (m, 4H, 1xOC<u>H</u>$_2$Ph, 1xNHC<u>H</u>CO(Gln), 1x NHC<u>H</u>CO(Leu) and 1xNHC<u>H</u>CO(Thr)), 4.17 (d, 1H, *J* = 6.5 Hz, NHC<u>H</u>CO(Val)), 4.11-4.06 (m, 1H, CH_3C<u>H</u>OBn(Thr)), 3.69 (s, 3H, CO_2C<u>H</u>$_3$), 3.26-3.11 (m, 2H, NHC<u>H</u>$_2$CH$_2$(Gln)), 2.53-2.46 (m, 1H, NHCH$_2$C<u>H</u>$_2$(Gln)), 2.22-2.06 (m, 3H, 1xNHCH$_2$C<u>H</u>$_2$(Gln), 1xCHC<u>H</u>$_2$CH(Gln) and 1xCHC<u>H</u>(CH$_3$)$_2$(Val)), 1.95 (s, 3H, COC<u>H</u>$_3$), 1.79-1.57 (m, 5H, 1xCHC<u>H</u>$_2$CH(Gln), 1xCH$_2$C<u>H</u>CO(Gln), 2xCHC<u>H</u>$_2$CH(Leu) and 1xCH$_2$C<u>H</u>(CH$_3$)$_2$(Leu)), 1.22 (d, 3H, *J* = 6.5 Hz, CHC<u>H</u>$_3$(Thr)), 0.97 (d, 3H, *J* = 7.0 Hz, CH(C<u>H</u>$_3$)$_2$(Val)), 0.96 (d, 3H, *J* = 6.5 Hz, CH(C<u>H</u>$_3$)$_2$(Val)), 0.90 (d, 3H, *J* = 6.5 Hz, CH(C<u>H</u>$_3$)$_2$(Leu)), 0.88 (d, 3H, *J* = 6.5 Hz, CH(C<u>H</u>$_3$)$_2$(Leu)); ^{13}C NMR (CD_3OD, 125 MHz) δ 174.7, 174.3, 174.0, 171.9, 139.6, 129.5, 129.0, 128.8, 76.0, 72.5, 61.2, 58.9, 53.2, 52.8, 51.8, 41.9, 41.4, 39.4, 33.8, 28.6, 25.7, 22.4, 22.0, 19.7, 16.9; HRMS (ES) calcd for $C_{32}H_{49}N_5O_8Na$ ([M+Na]$^+$), 654.3473; found, 654.3473.

General procedure for the preparation of pyridinyl esters or amides 98-119 and 122. To a solution of carboxylic acid (2 mmol, 1.0 equiv.) in DCM (5 mL) at rt was added thionyl chloride (0.4 mL, 1.3 equiv.) and a catalytic amount of DMF (2 drops). After 20 h of stirring, the solvent was removed in vacuo to afford the acyl chloride product. A solution of the acyl chloride in DCM (5 mL) was added dropwise to a solution of pyridinyl alcohol or amine (1.0 equiv.) and pyridine (0.18 mL, 1.1 equiv.) in DCM (5 mL) at 0 °C. After 3 h of stirring, the solvent was removed in vacuo. The residue was diluted with H_2O and extracted with EtOAc. The combined organic layers were washed with brine, dried over $MgSO_4$ and then concentrated in vacuo. Purification of the crude product by flash chromatography on silica gel afforded the product as a solid in 43-90% yield.

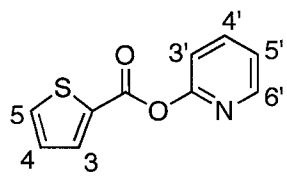

Pyridin-2-yl thiophene-2-carboxylate (98). The title compound **98** was obtained following the standard procedure described above. Purification of the crude product by flash chromatography on silica gel (25/75 EtOAc/hexanes) afforded **98** as a white solid (270 mg, 66%). Literature compound.[84] IR (microscope) 3097, 1731, 1593, 1523, 1469, 1433, 1414 cm^{-1}; ^1H NMR ($CDCl_3$, 300 MHz) δ 8.45 (ddd, 1H, J = 4.9, 2.0, 0.8 Hz, $H_{6'}$), 8.02 (dd, 1H, J = 3.8, 1.3 Hz, H_5), 7.84 (ddd, 1H, J = 8.1, 7.4, 2.0 Hz, $H_{4'}$), 7.69 (dd, 1H, J = 4.9, 1.3 Hz, H_3), 7.27 (ddd, 1H, J = 7.4, 4.9, 0.8 Hz, $H_{5'}$), 7.22 (ddd, 1H, J = 8.1, 0.8,

0.8 Hz, $H_{3'}$), 7.18 (dd, 1H, J = 5.0, 3.8 Hz, H_4); HRMS (EI) calcd for $C_{10}H_7NO_2S$ (M^+), 205.0197; found 205.0195.

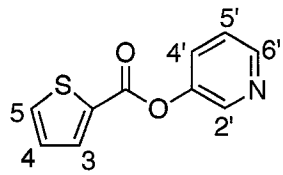

Pyridin-3-yl thiophene-2-carboxylate (99). The title compound **99** was obtained following the standard procedure described above. Purification of the crude product by flash chromatography on silica gel (50/50 EtOAc/hexanes) afforded **99** as a white solid (320 mg, 78%). IR ($CHCl_3$ cast) 3093, 1731, 1572, 1413 cm^{-1}; ^1H NMR ($CDCl_3$, 500 MHz) δ 8.54-8.50 (m, 1H, $H_{2'}$), 8.48 (dd, 1H, J = 4.6, 1.0 Hz, $H_{6'}$), 7.96 (dd, 1H, J = 3.8, 1.3 Hz, H_5), 7.65 (dd, 1H, J = 5.0, 1.3 Hz, H_3), 7.57 (ddd, 1H, J = 8.3, 2.8, 1.0 Hz, $H_{4'}$), 7.33 (ddd, 1H, J = 8.3, 4.6, 0.5 Hz, $H_{5'}$), 7.15 (dd, 1H, J = 5.0, 3.8 Hz, H_4); ^{13}C NMR ($CDCl_3$, 125 MHz) δ 160.0, 147.3, 147.1, 143.5, 135.2, 134.2, 131.9, 129.3, 128.2, 123.9; HRMS (EI) calcd for $C_{10}H_7NO_2S$ (M^+), 205.0197; found, 205.0197.

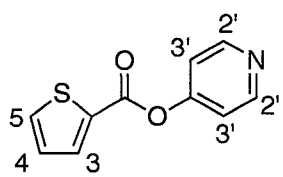

Pyridin-4-yl thiophene-2-carboxylate (100). The title compound **100** was obtained following the standard procedure described above. Purification of the crude product by flash chromatography on silica gel (50/50 EtOAc/hexanes) afforded **100** as a white solid (300 mg, 73%). IR (microscope) 3426, 3109, 3090, 3076, 3066, 3025, 2981, 2458, 1941, 1842, 1772, 1722, 1682, 1579, 1520, 1496, 1478, 1410 cm^{-1}; ^1H NMR ($CDCl_3$, 300 MHz)

δ 8.67 (d, 2H, J = 6.1 Hz, $H_{2'}$), 8.01 (dd, 1H, J = 3.8, 1.2 Hz, H_5), 7.72 (dd, 1H, J = 5.0, 1.3 Hz, H_3), 7.26 (d, 2H, J = 6.1 Hz, $H_{3'}$), 7.21 (dd, 1H, J = 5.0, 3.8 Hz, H_4); ^{13}C NMR ($CDCl_3$, 125 MHz) δ 159.2, 157.4, 151.5, 135.4, 134.4, 131.9, 128.2, 116.9; HRMS (EI) calcd for $C_{10}H_7NO_2S$ (M^+), 205.0197; found, 205.0199.

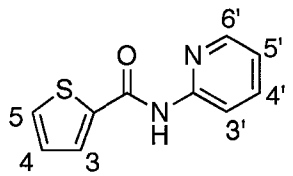

***N*-(Pyridin-2-yl)thiophene-2-carboxamide (101).** The title compound **101** was obtained following the standard procedure described above. Purification of the crude product by flash chromatography on silica gel (50/50 EtOAc/hexanes) afforded **101** as a white solid (280 mg, 69%). Literature compound.[85] IR (microscope) 3296, 3103, 1662, 1576, 1530, 1514, 1467, 1433, 1416 cm^{-1}; ^{1}H NMR (CD_3OD, 300 MHz) δ 8.33 (ddd, 1H, J = 5.0, 1.9, 1.0 Hz, $H_{6'}$), 8.13 (ddd, 1H, J = 8.1, 7.5, 1.9 Hz, $H_{4'}$), 7.92 (dd, 1H, J = 3.8, 1.2 Hz, H_5), 7.80 (ddd, 1H, J = 8.1, 1.0, 1.0 Hz, $H_{3'}$), 7.75 (dd, 1H, J = 5.0, 1.2 Hz, H_3), 7.18 (dd, 1H, J = 5.0, 3.8 Hz, H_4), 7.14 (ddd, 1H, J = 7.5, 5.0, 1.0 Hz, $H_{5'}$); HRMS (EI) calcd for $C_{10}H_8NO_2S$ (M^+), 204.0357; found, 204.0357.

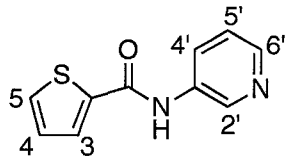

***N*-(Pyridin-3-yl)thiophene-2-carboxamide (102).** The title compound **102** was obtained following the standard procedure described above. Purification of the crude product by flash chromatography on silica gel (EtOAc) afforded **102** as a light yellow solid (230 mg,

57%). Literature compound.[86] IR ($CHCl_3$ cast) 3327, 3073, 2966, 1660, 1645, 1599, 1531, 1480 cm^{-1}; ^1H NMR ($CDCl_3$, 500 MHz) δ 9.09 (br, 1H, N<u>H</u>), 8.64 (m, 1H, $H_{2'}$), 8.26 (dd, 1H, J = 4.7, 1.3 Hz, $H_{6'}$), 8.18 (ddd, 1H, J = 8.4, 2.5, 1.3 Hz, $H_{4'}$), 7.72 (dd, 1H, J = 3.8, 1.1 Hz, H_5), 7.48 (dd, 1H, J = 5.0, 1.1 Hz, H_3), 7.21 (dd, 1H, J = 8.3, 4.7 Hz, $H_{5'}$), 7.01 (dd, 1H, J = 5.0, 3.8 Hz, H_4); HRMS (EI) calcd for $C_{10}H_8N_2OS$ (M^+), 206.0357; found, 206.03253.

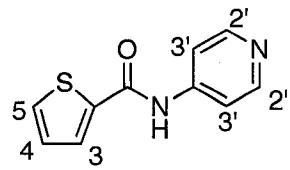

***N*-(Pyridin-4-yl)thiophene-2-carboxamide (103).** The title compound **103** was obtained following the standard procedure described above. Purification of the crude product by flash chromatography on silica gel (5/95 MeOH/EtOAc) afforded **103** as a brown solid (190 mg, 47%). Literature compound.[87] IR (microscope) 3144, 3047, 2982, 1657, 1595, 1513, 1491, 1421 cm^{-1}; ^1H NMR (CD_3OD, 300 MHz) δ 8.41 (dd, 2H, J = 5.0, 1.6 Hz, $H_{2'}$), 7.94 (dd, 1H, J = 3.8, 1.2 Hz, H_5), 7.79 (dd, 2H, J = 4.9, 1.6 Hz, $H_{3'}$), 7.77 (dd, 1H, J = 5.0, 1.1 Hz, H_3), 7.19 (dd, 1H, J = 5.0, 3.8 Hz, H_4); HRMS (EI) calcd for $C_{10}H_8N_2OS$ (M^+), 204.0357; found, 204.0358.

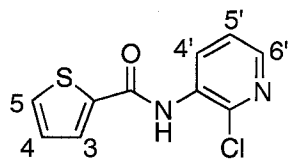

***N*-(2-Chloropyridin-3-yl)thiophene-2-carboxamide (104).** The title compound **104** was obtained following the standard procedure described above. Purification of the crude

product by flash chromatography on silica gel (50/50 EtOAc/hexanes) afforded **104** as a white solid (400 mg, 84%). Literature compound.[88] IR (microscope) 3424, 3328, 3114, 3084, 3052, 1645, 1584, 1571, 1534, 1510, 1452, 1421 cm^{-1}; ^1H NMR ($CDCl_3$, 300 MHz) δ 8.85 (dd, 1H, J = 8.2, 1.6 Hz, $H_{6'}$), 8.29 (br, 1H, N<u>H</u>), 8.15 (dd, 1H, J = 4.6, 1.6 Hz, $H_{4'}$), 7.70 (dd, 1H, J = 3.8, 1.1 Hz, H_5), 7.63 (dd, 1H, J = 5.0, 1.1 Hz, H_3), 7.32 (dd, 1H, J = 8.2, 4.6 Hz, $H_{5'}$), 7.19 (dd, 1H, J = 5.0, 3.8 Hz, H_4); HRMS (EI) calcd for $C_{10}H_7ClN_2OS$ (M^+), 237.9968; found, 237.9968.

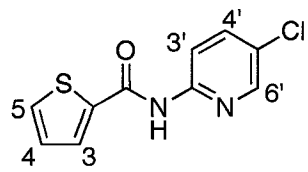

***N*-(5-Chloropyridin-2-yl)thiophene-2-carboxamide (105).** The title compound **105** was obtained following the standard procedure described above. Purification of the crude product by flash chromatography on silica gel (50/50 EtOAc/hexanes) afforded **105** as a white solid (430 mg, 90%). Literature compound.[89] IR (microscope) 3222, 3100, 3083, 3017, 2799, 1666, 1577, 1540, 1516, 1459, 1414 cm^{-1}; ^1H NMR ($CDCl_3$, 300 MHz) δ 8.41 (br, 1H, N<u>H</u>), 8.31 (d, 1H, J = 8.9 Hz, $H_{3'}$), 8.26 (d, 1H, J = 2.5 Hz, $H_{6'}$), 7.71 (dd, 1H, J = 8.9, 2.5 Hz, $H_{4'}$), 7.67 (dd, 1H, J = 3.8, 1.1 Hz, H_5), 7.61 (dd, 1H, J = 5.0, 1.1 Hz, H_3), 7.16 (dd, 1H, J = 5.0, 3.8 Hz, H_4); HRMS (EI) calcd for $C_{10}H_7ClN_2OS$ (M^+), 237.9968; found, 237.9966.

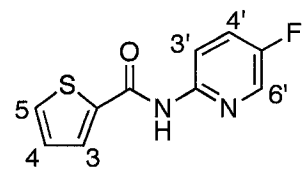

***N*-(5-Fluoropyridin-2-yl)thiophene-2-carboxamide (106).** The title compound **106** was obtained following the standard procedure described above. Purification of the crude product by flash chromatography on silica gel (50/50 EtOAc/hexanes) afforded **106** as a yellow solid (350 mg, 79%). IR (microscope) 3295, 3105, 1663, 1596, 1531, 1512, 1472, 1417 cm^{-1}; ^1H NMR ($CDCl_3$, 300 MHz) δ 8.45 (br, 1H, N<u>H</u>), 8.35 (dd, 1H, J = 9.1, 4.0 Hz, $H_{6'}$), 8.18-8.12 (m, 1H, $H_{3'}$), 7.67 (dd, 1H, J = 3.8, 1.2 Hz, H_5), 7.60 (dd, 1H, J = 5.0, 1.2 Hz, H_3), 7.49 (ddd, 1H, J = 9.2, 7.7, 3.0 Hz, $H_{4'}$), 7.15 (dd, 1H, J = 5.0, 3.8 Hz, H_4); ^{13}C NMR ($CDCl_3$, 125 MHz) δ 159.9, 157.5, 155.5, 147.6, 138.6, 136.1 (d, $J_{C\text{-}F}$ = 25.8 Hz), 132.4, 129.2 (d, $J_{C\text{-}F}$ = 132.5 Hz), 126.1 (d, $J_{C\text{-}F}$ = 19.1 Hz), 115.8 (d, $J_{C\text{-}F}$ = 4.6 Hz); HRMS (EI) calcd for $C_{10}H_7FN_2OS$ (M^+), 222.0263; found, 222.0264.

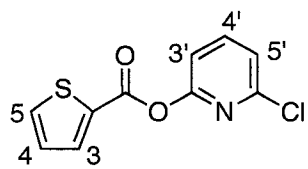

6-Chloropyridin-2-yl thiophene-2-carboxylate (107). The title compound **107** was obtained following the standard procedure described above. Purification of the crude product by flash chromatography on silica gel (50/50 EtOAc/hexanes) afforded **107** as a white solid (390 mg, 88%). IR (microscope) 3096, 1736, 1587, 1522, 1431, 1413 cm^{-1}; ^1H NMR ($CDCl_3$, 300 MHz) δ 8.02 (dd, 1H, J = 4.9, 1.3 Hz, H_5), 7.80 (dd, 1H, J = 7.9, 7.9 Hz, $H_{4'}$), 7.71 (dd, 1H, J = 5.0, 1.3 Hz, H_3), 7.33 (d, 1H, J = 7.9 Hz, $H_{3'}$ or $H_{5'}$), 7.19 (d, 1H, J = 7.7 Hz, $H_{3'}$ or $H_{5'}$), 7.19 (dd, 1H, J = 4.2, 3.0 Hz, H_4); ^{13}C NMR ($CDCl_3$, 125 MHz) δ 159.5, 156.8, 149.6, 141.6, 135.5, 134.5, 131.8, 128.2, 122.6, 115.0; HRMS (EI) calcd for $C_{10}H_6ClNO_2S$ (M^+), 238.9808; found, 238.9812.

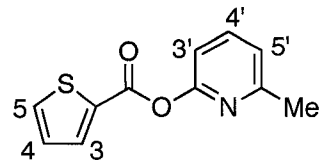

6-Methylpyridin-2-yl thiophene-2-carboxylate (108). The title compound **108** was obtained following the standard procedure described above. Purification of the crude product by flash chromatography on silica gel (50/50 EtOAc/hexanes) afforded **108** as a white solid (370 mg, 84%). IR (microscope) 3096, 2924, 1730, 1604, 1576, 1523, 1453, 1413 cm^{-1}; ^1H NMR ($CDCl_3$, 300 MHz) δ 8.01 (dd, 1H, J = 3.8, 1.3 Hz, H_5), 7.71 (dd, 1H, J = 8.0, 7.5 Hz, $H_{4'}$), 7.67 (dd, 1H, J = 4.9, 1.3 Hz, H_3), 7.17 (dd, 1H, J = 5.0, 3.8 Hz, H_4), 7.12 (dd, 1H, J = 7.5, 0.5 Hz, $H_{3'}$), 7.01 (dd, 1H, J = 8.0, 0.5 Hz, $H_{5'}$), 2.56 (s, 3H, $C\underline{H}_3$); ^{13}C NMR ($CDCl_3$, 125 MHz) δ 160.3, 158.2, 157.0, 139.7, 135.1, 133.9, 132.6, 128.0, 121.7, 113.3, 24.1; HRMS (EI) calcd for $C_{11}H_9NO_2S$ (M^+), 219.0354; found, 219.0355.

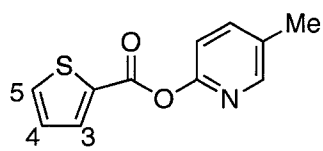

5-Methylpyridin-2-yl thiophene-2-carboxylate (109). The title compound **109** was obtained following the standard procedure described above. Purification of the crude product by flash chromatography on silica gel (50/50 EtOAc/hexanes) afforded **109** as a white solid (320 mg, 73%). IR (microscope) 3097, 1727, 1609, 1562, 1522, 1483, 1445, 1415, 1401 cm^{-1}; ^1H NMR ($CDCl_3$, 300 MHz) δ 8.29 (dd, 1H, J = 5.1, 0.3 Hz, Py$\underline{H}$), 8.00 (dd, 1H, J = 3.8, 1.3 Hz, H_5), 7.68 (dd, 1H, J = 5.0, 1.4 Hz, H_3), 7.18 (dd, 1H, J = 5.0, 3.8

Hz, H_4), 7.10-7.08 (m, 1H, Py<u>H</u>), 7.08-7.06 (m, 1H, Py<u>H</u>), 2.40 (s, 3H, C<u>H</u>$_3$); ^{13}C NMR ($CDCl_3$, 125 MHz) δ 160.2, 158.0, 151.3, 148.1, 135.0, 134.0, 132.6, 128.1, 123.4, 117.0, 21.0; HRMS (EI) calcd for $C_{11}H_9NO_2S$ (M^+), 219.0354; found, 219.0354.

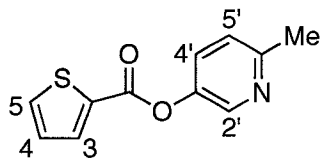

6-Methylpyridin-3-yl thiophene-2-carboxylate (110). The title compound **110** was obtained following the standard procedure described above. Purification of the crude product by flash chromatography on silica gel (50/50 EtOAc/hexanes) afforded **110** as a white solid (390 mg, 89%). IR (microscope) 3094, 1731, 1598, 1580, 1523, 1485, 1415 cm^{-1}; ^{1}H NMR ($CDCl_3$, 300 MHz) δ 8.43 (d, 1H, J = 2.8 Hz, $H_{2'}$), 8.00 (dd, 1H, J = 3.8, 1.2 Hz, H_5), 7.70 (dd, 1H, J = 5.0, 1.3 Hz, H_3), 7.49 (dd, 1H, J = 8.5, 2.8 Hz, $H_{4'}$), 7.24-7.18 (m, 2H, H_4 and $H_{5'}$), 2.60 (s, 3H, C<u>H</u>$_3$); ^{13}C NMR ($CDCl_3$, 125 MHz) δ 160.3, 156.0, 145.2, 142.4, 135.1, 134.0, 132.1, 129.5, 128.1, 123.5, 23.9; HRMS (EI) calcd for $C_{11}H_9NO_2S$ (M^+), 219.0354; found, 219.0352.

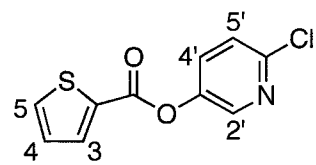

6-Chloropyridin-3-yl thiophene-2-carboxylate (111). The title compound **111** was obtained following the standard procedure described above. Purification of the crude product by flash chromatography on silica gel (50/50 EtOAc/hexanes) afforded **111** as a white solid (380 mg, 79%). IR (microscope) 3297, 3092, 1642, 1593, 1531, 1513, 1464,

1417 cm^{-1}; ^1H NMR ($CDCl_3$, 300 MHz) δ 8.40 (d, 1H, J = 2.6 Hz, $H_{2'}$), 8.03 (dd, 1H, J = 3.8, 1.2 Hz, H_5), 7.80 (dd, 1H, J = 8.6, 2.6 Hz, $H_{4'}$), 7.71 (dd, 1H, J = 4.9, 1.2 Hz, H_3), 7.22 (d, 1H, J = 8.6 Hz, $H_{5'}$), 7.19 (dd, 1H, J = 4.9, 3.8 Hz, H_4); ^{13}C NMR ($CDCl_3$, 125 MHz) δ 160.1, 146.4, 140.8, 137.9, 133.6, 131.7, 130.4, 129.2, 128.1, 124.4; HRMS (EI) calcd for $C_{10}H_6ClNO_2S$ (M^+), 238.9808; found, 238.9808.

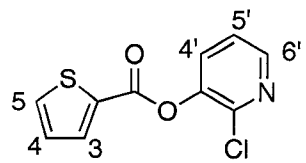

2-Chloropyridin-3-yl thiophene-2-carboxylate (112). The title compound **112** was obtained following the standard procedure described above. Purification of the crude product by flash chromatography on silica gel (50/50 EtOAc/hexanes) afforded **112** as a white solid (410 mg, 85%). IR (microscope) 3112, 3099, 3081, 1733, 1580, 1522, 1460, 1414 cm^{-1}; ^1H NMR ($CDCl_3$, 300 MHz) δ 8.34 (dd, 1H, J = 4.7, 1.7 Hz, $H_{6'}$), 8.06 (dd, 1H, J = 3.8, 1.2 Hz, H_5), 7.74 (dd, 1H, J = 5.0, 1.3 Hz, H_3), 7.69 (dd, 1H, J = 8.0, 1.7 Hz, $H_{4'}$), 7.34 (dd, 1H, J = 8.0, 4.7 Hz, $H_{5'}$), 7.22 (dd, 1H, J = 5.0, 3.8 Hz, H_4); ^{13}C NMR ($CDCl_3$, 125 MHz) δ 159.8, 156.0, 147.3, 139.2, 135.4, 134.4, 132.0, 130.0, 128.2, 117.4; HRMS (EI) calcd for $C_{10}H_6ClNO_2S$ (M^+), 238.9808; found, 238.9806.

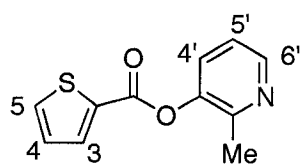

2-Methylpyridin-3-yl thiophene-2-carboxylate (113). The title compound **113** was obtained following the standard procedure described above. Purification of the crude

product by flash chromatography on silica gel (EtOAc) afforded **113** as a white solid (380 mg, 87%). IR (microscope) 3068, 1731, 1596, 1523, 1450, 1414 cm^{-1}; ^1H NMR ($CDCl_3$, 300 MHz) δ 8.48 (dd, 1H, J = 4.8, 1.5 Hz, $H_{6'}$), 8.02 (dd, 1H, J = 3.8, 1.3 Hz, H_5), 7.71 (dd, 1H, J = 5.0, 1.3 Hz, H_3), 7.52 (dd, 1H, J = 8.1, 1.5 Hz, $H_{4'}$), 7.25-7.19 (m, 2H, H_4 and $H_{5'}$), 2.50 (s, 3H, $C\underline{H}_3$); ^{13}C NMR ($CDCl_3$, 125 MHz) δ 159.8, 151.5, 146.7, 145.6, 135.1, 134.0, 132.0, 129.6, 128.2, 121.9, 19.5; HRMS (EI) calcd for $C_{11}H_9NO_2S$ (M^+), 219.0354; found, 219.0354.

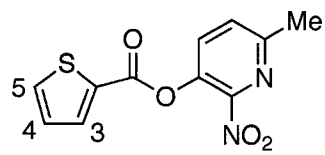

6-Methyl-2-nitropyridin-3-yl thiophene-2-carboxylate (114). The title compound **114** was obtained following the standard procedure described above. Purification of the crude product by flash chromatography on silica gel (EtOAc) afforded **114** as a white solid (460 mg, 87%). IR (microscope) 3098, 1736, 1547, 1522, 1474, 1413, 1360, 1258, 1232 cm^{-1}; ^1H NMR ($CDCl_3$, 300 MHz) δ 8.01 (dd, 1H, J = 3.8, 1.3 Hz, H_5), 7.78 (d, 1H, J = 8.3 Hz, Py$\underline{H}$), 7.75 (dd, 1H, J = 5.0, 1.0 Hz, H_3), 7.53 (d, 1H, J = 8.3 Hz, Py$\underline{H}$), 7.21 (dd, 1H, J = 5.0, 3.8 Hz, H_4), 2.68 (s, 3H, $C\underline{H}_3$); ^{13}C NMR ($CDCl_3$, 125 MHz) δ 159.1, 155.9, 149.3, 137.3, 136.1, 135.1, 135.0, 130.7, 129.2, 128.4, 23.6; HRMS (EI) calcd for $C_{11}H_8N_2O_4S$ (M^+), 264.0205; found, 264.0206.

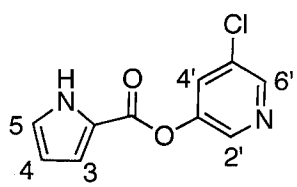

5-Chloropyridin-3-yl 1*H*-pyrrole-2-carboxylate (115). The title compound **115** was obtained following the standard procedure described above. Purification of the crude product by flash chromatography on silica gel (25/75 EtOAc/hexanes) afforded **115** as a white solid (320 mg, 72%). IR (microscope) 3148, 3126, 3109, 3072, 3057, 2973, 2872, 2792, 2714, 1716, 1582, 1445, 1426, 1401 cm^{-1}; ^1H NMR ($CDCl_3$, 300 MHz) δ 9.40-9.20 (br, 1H, N<u>H</u>), 8.49 (d, 1H, J = 2.3 Hz, $H_{2'}$ or $H_{6'}$), 8.45 (d, 1H, J = 2.3 Hz, $H_{2'}$ or $H_{6'}$), 7.66 (dd, 1H, J = 2.3, 2.3 Hz, $H_{4'}$), 7.17 (ddd, 1H, J = 3.9, 2.5, 1.4 Hz, H_5), 7.11 (ddd, 1H, J = 2.8, 2.8, 1.4 Hz, H_3), 6.38 (ddd, 1H, J = 3.9, 2.8, 2.8 Hz, H_4); ^{13}C NMR ($CDCl_3$, 125 MHz) δ 158.3, 147.2, 145.7, 141.5, 131.8, 129.6, 125.1, 120.7, 117.9, 111.3; HRMS (EI) calcd for $C_{10}H_7N_2O_2Cl$ (M^+), 222.0196; found, 222.0198.

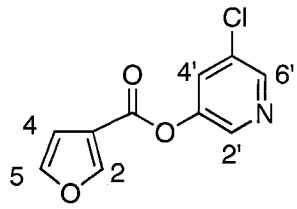

5-Chloropyridin-3-yl furan-3-carboxylate (116). The title compound **116** was obtained following the standard procedure described above. Purification of the crude product by flash chromatography on silica gel (25/75 EtOAc/hexanes) afforded **116** as a white solid (400 mg, 90%). IR (microscope) 3136, 1749, 1566, 1509, 1440, 1421 cm^{-1}; ^1H NMR ($CDCl_3$, 300 MHz) δ 8.50 (d, 1H, J = 2.1 Hz, $H_{2'}$ or $H_{6'}$), 8.44 (d, 1H, J = 2.3 Hz, $H_{2'}$ or $H_{6'}$), 8.23 (dd, 1H, J = 1.5, 0.8 Hz, H_5), 7.65 (dd, 1H, J = 2.3, 2.1 Hz, $H_{4'}$), 7.53 (dd, 1H, J = 1.9, 1.5 Hz, H_2), 6.87 (dd, 1H, J = 1.9, 0.8 Hz, H_4); ^{13}C NMR ($CDCl_3$, 125 MHz) δ 160.3, 149.2, 147.0, 146.0, 144.4, 141.4, 131.7, 129.5, 117.8, 109.9; HRMS (EI) calcd for $C_{10}H_6ClNO_3$ (M^+), 223.0036; found, 223.0035.

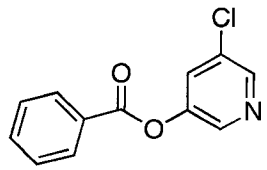

5-Chloropyridin-3-yl benzoate (117). The title compound **117** was obtained following the standard procedure described above. Purification of the crude product by flash chromatography on silica gel (25/75 EtOAc/hexanes) afforded **117** as a white solid (270 mg, 90%). IR (microscope) 1747, 1577, 1452, 1421 cm^{-1}; ^1H NMR ($CDCl_3$, 300 MHz) δ 8.51 (d, 1H, J = 2.1 Hz, Py<u>H</u>), 8.48 (d, 1H, J = 2.3 Hz, Py<u>H</u>), 8.21 (m, 1H, Py<u>H</u>), 8.18 (m, 1H, Ph<u>H</u>), 7.72-7.65 (m, 2H, Ph<u>H</u>), 7.58-7.50 (m, 2H, Ph<u>H</u>); ^{13}C NMR ($CDCl_3$, 125 MHz) δ 164.3, 147.5, 146.0, 141.5, 134.3, 131.8, 130.3, 129.6, 128.8, 128.3; HRMS (EI) calcd for $C_{12}H_8ClNO_2$ (M^+), 233.0244; found, 233.0242.

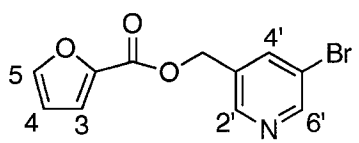

(5-Bromopyridin-3-yl)methyl furan-2-carboxylate (118). The title compound **118** was obtained following the standard procedure described above. Purification of the crude product by flash chromatography on silica gel (50/50 EtOAc/hexanes) afforded **118** as a white solid (310 mg, 58%). IR ($CHCl_3$ cast) 3139, 1725, 1580, 1473, 1424 cm^{-1}; ^1H NMR ($CDCl_3$, 500 MHz) δ 8.73-8.60 (m, 2H, $H_{2'}$ and $H_{6'}$), 7.98-7.96 (m, 1H, $H_{4'}$), 7.59 (d, 1H, J = 1.7 Hz, H_5), 7.22 (d, 1H, J = 3.5 Hz, H_3), 6.52 (dd, 1H, J = 3.5, 1.7 Hz, H_4), 5.32 (s, 2H, $OC\underline{H}_2$); ^{13}C NMR ($CDCl_3$, 125 MHz) δ 158.1, 150.4, 147.2, 146.9, 143.9, 139.1,

133.2, 119.0, 118.9, 112.1, 63.0; HRMS (EI) calcd for $C_{11}H_8BrNO_3$ (M^+), 282.9759; found, 282.9763.

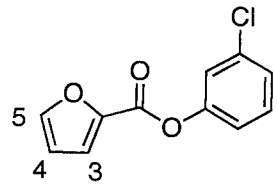

3-Chlorophenyl furan-2-carboxylate (119). The title compound **119** was obtained following the standard procedure described above. Purification of the crude product by flash chromatography on silica gel (25/75 EtOAc/hexanes) afforded **119** as a white solid (370 mg, 84%). IR ($CHCl_3$ cast) 3141, 1743, 1593, 1574, 1468 cm^{-1}; ^1H NMR ($CDCl_3$, 125 MHz) δ 7.65 (dd, 1H, J = 1.6, 0.7 Hz, H_5), 7.36 (dd, 1H, J = 3.5, 0.7 Hz, H_3), 7.36-7.32 (m, 1H, Ph<u>H</u>), 7.24 (m, 1H, Ph<u>H</u>), 7.22 (dd, 1H, J = 1.9, 1.0 Hz, Ph<u>H</u>), 7.15-7.12 (m, 1H, Ph<u>H</u>), 6.57 (dd, 1H, J = 3.5, 1.6 Hz, H_4); ^{13}C NMR ($CDCl_3$, 125 MHz) δ 156.4, 150.7, 147.4, 143.6, 134.8, 130.2, 126.4, 122.3, 120.0, 119.9, 112.3; HRMS (EI) calcd for $C_{11}H_7ClO_3$ (M^+), 222.0084; found, 220.0083.

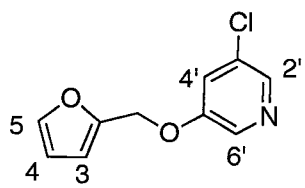

3-Chloro-5-furan-(2-ylmethoxy)pyridine (120). To a solution of PPh_3 (1.24 g, 4.74 mmol) in THF (20 mL) at rt was added DEAD (0.75 mL, 4.74 mmol) dropwise. After 30 min of stirring at rt, furfuryl alcohol (0.31 mg, 3.16 mmol) and 3-chloro pyridinol (0.61 g, 4.74 mmol) were added to the reaction mixture. The resulting solution was stirred

overnight at rt and then the solvent was removed in vacuo. The residue was diluted with DCM, washed with water, 1 N HCl, saturated $NaHCO_3$ solution, brine, dried over $MgSO_4$ and then concentrated in vacuo. Purification of the crude product by flash chromatography on silica gel (gradient column, 25/75 EtOAc/hexanes to 50/50 EtOAc/hexanes) afforded **120** as a yellow liquid (150 mg, 23%), which solidified in the fridge. IR ($CHCl_3$ cast) 3048, 2932, 1575, 1449, 1422 cm^{-1}; ^1H NMR ($CDCl_3$, 500 MHz) δ 8.22 (d, 1H, J = 2.6 Hz, $H_{2'}$ or $H_{6'}$), 8.14 (d, 1H, J = 1.9 Hz, $H_{2'}$ or $H_{6'}$), 7.41 (dd, 1H, J = 1.8, 0.8 Hz, H_5), 7.27 (dd, 1H, J = 2.6, 1.9 Hz, $H_{4'}$), 6.43 (dd, 1H, J = 2.2, 0.8 Hz, H_3), 6.35 (dd, 1H, J = 2.2, 1.8 Hz, H_4), 5.00 (s, 2H); ^{13}C NMR ($CDCl_3$, 125 MHz) δ 154.7, 148.8, 143.6, 141.2, 136.3, 132.0, 122.0, 110.9, 110.7, 62.9; HRMS (EI) calcd for $C_{10}H_8ClNO_2$ (M^+), 209.0244; found 209.0244.

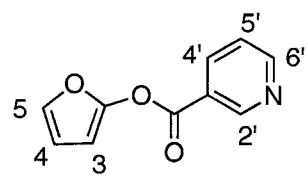

Furan-2-yl nicotinate (121). The title compound **121** was prepared by a modified literature procedure.[90] To a solution of nicotinic acid (500 mg, 4 mmol) in THF (5 mL) at rt was added thionyl chloride (2 mL, 26 mmol). After several hours of stirring, the solvent was removed in vacuo to afford the acyl chloride product. A solution of the acyl chloride in MeCN (5 mL) was added dropwise to a solution of 2(5H)-furanone (0.25 mL, 3.5 mmol) and triethylamine (1.6 mL, 12 mmol) in MeCN (5 mL) at 0 °C. The ice bath was replaced with an oil bath, and the reaction mixture was heated at 50 °C for 4 h. After cooling, the solvent was removed in vacuo. The residue was diluted with EtOAc and then

washed with saturated $NaHCO_3$ solution. The combined organic layers were washed with brine, dried over $MgSO_4$ and then concentrated in vacuo. Purification of the crude product by flash chromatography on silica gel (50/50 EtOAc/hexanes) afforded **121** as a pale yellow oil (88 mg, 13%). IR ($CHCl_3$ cast) 3127, 1765, 1590, 1511, 1422 cm^{-1}; ^1H NMR ($CDCl_3$, 500 MHz) δ 9.35 (dd, 1H, J = 2.1, 0.8 Hz, $H_{2'}$), 8.85 (dd, 1H, J = 5.0, 1.7 Hz, $H_{6'}$), 8.41 (ddd, 1H, J = 8.0, 2.1, 1.7 Hz, $H_{4'}$), 7.46 (ddd, 1H, J = 8.0, 5.0, 0.9 Hz, $H_{5'}$), 7.11 (dd, 1H, J = 2.1, 1.1 Hz, H_5), 6.41 (dd, 1H, J = 3.4, 2.1 Hz, H_4), 6.05 (dd, 1H, J = 3.4, 1.1 Hz, H_3); ^{13}C NMR ($CDCl_3$, 125 MHz) δ 161.2, 154.3, 151.4, 150.7, 137.8, 135.7, 124.4, 123.6, 111.3, 92.9; HRMS (EI) calcd for $C_{10}H_7NO_3$ (M^+), 189.0426; found, 189.0424.

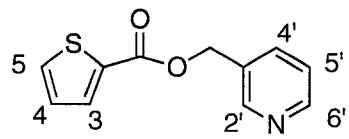

Pyridin-3-ylmethyl thiophene-2-carboxylate (122). The title compound **122** was obtained following the standard procedure described above for the preparation of pyridinyl esters. Purification of the crude product by flash chromatography on silica gel (50/50 EtOAc/hexanes) afforded **122** as a white solid (190 mg, 43%). IR ($CHCl_3$ cast) 3019, 2926, 2852, 1711, 1525, 1417 cm^{-1}; ^1H NMR ($CDCl_3$, 500 MHz) δ 8.64 (d, 1H, J = 1.7 Hz, $H_{2'}$), 8.53 (dd, 1H, J = 5.0, 2.2 Hz, $H_{6'}$), 7.94 (ddd, 1H, J = 7.9, 2.2, 1.7 Hz, $H_{4'}$), 7.84 (dd, 1H, J = 3.8, 1.3 Hz, H_5), 7.77 (dd, 1H, J = 5.0, 1.3 Hz, H_3), 7.47 (dd, 1H, J = 7.9, 5.0 Hz, $H_{5'}$), 7.16 (dd, 1H, J = 5.0, 3.8 Hz, H_4), 5.39 (s, 2H, $OC\underline{H}_2$); ^{13}C NMR ($CDCl_3$, 125 MHz) δ 161.8, 149.7, 149.6, 135.9, 133.8, 133.1, 132.9, 131.4, 127.8, 123.4, 64.1; HRMS (EI) calcd for $C_{11}H_9NO_2S$ (M^+) 219.0354; found, 219.0354.

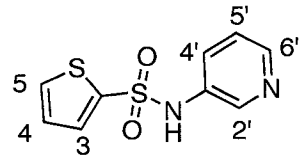

***N*-(Pyridin-3-yl)thiophene-2-sulfonamide (123).** To a solution of thiophene-2-sulfonyl chloride (36.6 mg, 0.2 mmol) in THF (3 mL) at rt was added 3-aminopyridine (18.8 mg, 0.2 mmol). After several hours of stirring, the solvent was removed to yield the crude product, which was purified by flash chromatography on silica gel (EtOAc) to afford **123** as a white solid (48 mg, quant.). Literature compound.[91] IR (microscope) 3128, 3091, 3067, 3006, 2937, 2620, 1584, 1518, 1475 cm^{-1}; ^1H NMR (CD_3OD, 500 MHz) δ 8.25 (d, 1H, J = 1.5 Hz, $H_{2'}$), 8.24 (m, 1H, $H_{6'}$), 7.72 (dd, 1H, J = 4.9, 1.4 Hz, H_5), 7.67 (ddd, 1H, J = 8.3, 2.6, 1.5 Hz, $H_{4'}$), 7.51 (dd, 1H, J = 3.8, 1.4 Hz, H_3), 7.35 (ddd, 1H, J = 8.3, 5.0, 0.6 Hz, $H_{5'}$), 7.05 (dd, 1H, J = 5.0, 3.8 Hz, H_4); HRMS (EI) calcd for $C_9H_8N_2O_2S_2$ (M^+), 240.0027; found, 240.0026.

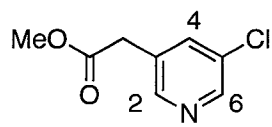

Methyl 2-(5-chloropyridin-3-yl)acetate (126a). To a solution of **133** (0.32 g, 2.10 mmol) in H_2O (5 mL) was added conc. HCl (5 mL) and the reaction mixture was refluxed at 100 °C overnight. The solvent was removed in vacuo to afford the product 5-chloro-3-pyridinylacetic acid, which was used for next reaction without any further purification. A solution of 5-chloro-3-pyridinylacetic acid in MeOH (5 mL) was treated with a solution of MeOH (3 mL) and CH_3COCl (1 mL). The resulting mixture was refluxed overnight,

and then the solvent was removed in vacuo. The residue was diluted with saturated $NaHCO_3$, and the solution was extracted with EtOAc (3 x 20 mL). The combined organic layers were washed with brine (15 mL), dried over $MgSO_4$, and concentrated in vacuo. The crude product was purified by column chromatography (EtOAc) to yield **126a** as a pale yellow liquid (0.28 g, 72% over two steps). IR ($CHCl_3$ cast): 3043, 3003, 2954, 1740, 1584, 1560, 1436, 1424 cm^{-1}; ^1H NMR ($CDCl_3$, 400 MHz) δ 8.46 (d, 1H, J = 2.3 Hz, H_6), 8.36 (d, 1H, J = 1.8 Hz, H_2), 7.63 (dd, 1H, J = 2.3, 1.9 Hz, H_4), 3.70 (s, 3H, $CO_2C\underline{H}_3$), 3.61 (s, 2H, $C\underline{H}_2CO_2$); ^{13}C NMR ($CDCl_3$, 100 MHz) δ 170.4, 148.1, 147.5, 136.6, 131.9, 130.8, 52.4, 37.6; HRMS (EI) calcd for $C_8H_8ClNO_2$ (M^+), 185.0244; found, 185.0241.

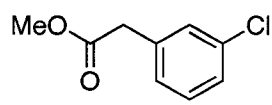

Methyl 2-(3-chlorophenyl)acetate (126b). The title compound **126b** was obtained from 5-chloro-phenylacetic acid **125b** (1.71 g, 10 mmol) following the standard procedure described above for the preparation of **126a**. Purification of the crude product by flash chromatography on silica gel (10/90 EtOAc/hexanes) afforded **126b** as a pale yellow liquid (1.63 g, 88%). Literature compound.[92] IR ($CHCl_3$ cast): 3000, 2953, 2843, 1741, 1599, 1576, 1477, 1434 cm^{-1}; ^1H NMR ($CDCl_3$, 400 MHz) δ 7.31-7.14 (m, 4H, Ph$\underline{H}$), 3.71 (s, 2H, $C\underline{H}_2CO_2$), 3.61 (s, 3H, $CO_2C\underline{H}_3$); HRMS (EI) calcd for $C_9H_9ClO_2$ (M^+), 184.0291; found, 184.0290.

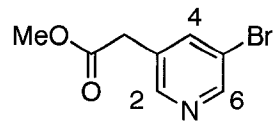

Methyl 2-(5-bromopyridin-3-yl)acetate (126c). The title compound **126c** was obtained from 5-bromo-3-pyridinylacetic acid **125c** (1.04 g, 4.80 mmol) following the standard procedure described above for the preparation of **126a**. Purification of the crude product by flash chromatography on silica gel (EtOAc) afforded **126c** as a yellow-orange liquid (1.00 g, 91%). Literature compound.[93] IR ($CHCl_3$ cast): 3040, 2953, 1740, 1583, 1558, 1436, 1425 cm^{-1}; ^1H NMR ($CDCl_3$, 400 MHz) δ 8.56 (d, 1H, J = 1.8 Hz, H_6), 8.40 (s, 1H, H_2), 7.78 (dd, 1H, J = 1.8, 1.8 Hz, H_4), 3.69 (s, 2H, $C\underline{H}_2CO_2$), 3.59 (s, 3H, $CO_2C\underline{H}_3$); HRMS (EI) calcd for $C_8H_8BrNO_2$ (M^+), 230.9769; found, 230.9786.

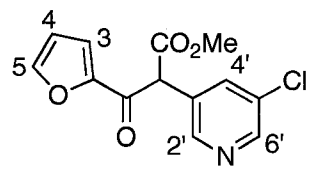

Methyl 2-(5-chloropyridin-3-yl)-3-(furan-2-yl)-3-oxopropanoate (127a). To a solution of **126a** (175 mg, 0.94 mmol) in THF (5 mL) at -78 °C was added LiHMDS (1.0 mL of 1.0 M solution in THF, 1.0 mmol) dropwise over 15 min. The solution was stirred for 1 h at -78 °C. To this solution was added dropwise over 15 min. 2-furoic acid (50 mg, 0.45 mmol) and CDI (80 mg, 0.49 mmol) in anhydrous THF (5 mL), which had been previously stirred for 1 h for activation at rt. The reaction mixture was stirred for 4 h at -78 °C, and quenched with 1.0 M aqueous HCl (10 mL). The pH was adjusted to between 7 and 9 by adding saturated aqueous $NaHCO_3$ and the solution was extracted with EtOAc (3 x 25 mL). The combined organic layers were washed with brine (15 mL), dried over

anhydrous $MgSO_4$, and concentrated in vacuo. The crude product was purified by column chromatography (50/50 EtOAc/hexanes) to yield **127a** as a yellow liquid (90 mg, 72%). IR ($CHCl_3$ cast): 3134, 3043, 2955, 1747, 1677, 1567, 1464, 1427 cm^{-1}; ^1H NMR ($CDCl_3$, 400 MHz) δ 8.53 (d, 1H, J = 2.4 Hz, $H_{2'}$ or $H_{6'}$), 8.50 (d, 1H, J = 2.0 Hz, $H_{2'}$ or $H_{6'}$), 7.92 (dd, 1H, J = 2.4, 2.0 Hz, $H_{4'}$), 7.63 (dd, 1H, J = 1.7, 0.7 Hz, H_5), 7.34 (dd, 1H, J = 3.7, 0.7 Hz, H_3), 6.59 (dd, 1H, J = 3.7, 1.7 Hz, H_4); 5.51 (s, 1H, $COC\underline{H}CO_2$), 3.79 (s, 3H, $CO_2C\underline{H}_3$); ^{13}C NMR ($CDCl_3$, 100 MHz) δ 180.2, 167.6, 151.1, 148.6, 148.3, 137.1, 132.1, 131.2, 129.5, 119.4, 113.2, 56.5, 53.2; HRMS (EI) calcd for $C_{13}H_{10}ClNO_4$ (M^+), 279.0298; found, 279.0298.

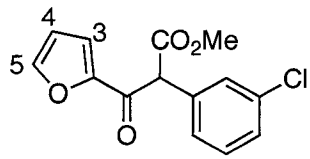

Methyl 2-(3-chlorophenyl)-3-(furan-2-yl)-3-oxopropanoate (127b). The title compound **127b** was obtained from **126b** (550 mg, 3 mmol) following the standard procedure described above for the preparation of **127a**. Purification of the crude product by flash chromatography on silica gel (10/90 EtOAc/hexanes) afforded **127b** as a pale yellow liquid (300 mg, 75%). IR ($CHCl_3$ cast): 3135, 3006, 2954, 1748, 1676, 1597, 1568, 1464, 1434 cm^{-1}; ^1H NMR ($CDCl_3$, 500 MHz) δ 7.57 (dd, 1H, J = 1.7, 0.7 Hz, H_5), 7.42 (dd, 1H, J = 1.8, 1.8 Hz, Ph$\underline{H}$), 7.38-7.01 (m, 4H, H_3 and 3xPh$\underline{H}$), 6.53 (dd, 1H, J = 3.6, 1.7 Hz, H_4), 5.44 (s, 1H, $COC\underline{H}CO_2$), 3.77 (s, 3H, $CO_2C\underline{H}_3$); ^{13}C NMR ($CDCl_3$, 100 MHz) δ 181.2, 168.3, 151.4, 147.2, 134.5, 134.1, 129.8, 128.5, 127.9, 119.0, 112.9, 59.4, 52.9; HRMS (EI) calcd for $C_{14}H_{11}ClO_4$ (M^+), 278.0346; found, 278.0345.

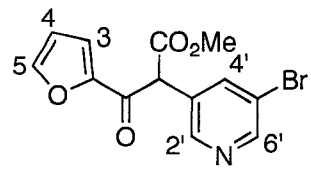

Methyl 2-(5-bromopyridin-3-yl)-3-(furan-2-yl)-3-oxopropanoate (127c). The title compound **127c** was obtained from **126c** (0.91 g, 3.95 mmol) following the standard procedure described above for the preparation of **127a**. Purification of the crude product by flash chromatography on silica gel (50/50 EtOAc/hexanes) afforded **127c** as a yellow liquid (0.59 g, 96%). IR ($CHCl_3$ cast): 3134, 2954, 1746, 1676, 1567, 1464, 1426, 1393 cm^{-1}; ^1H NMR ($CDCl_3$, 500 MHz) δ 8.61 (d, 1H, J = 2.0 Hz, $H_{2'}$ or $H_{6'}$), 8.52 (d, 1H, J = 1.6 Hz, $H_{2'}$ or $H_{6'}$), 8.05 (dd, 1H, J = 2.0, 1.6 Hz, $H_{4'}$), 7.62 (d, 1H, J = 1.6 Hz, H_5), 7.23 (d, 1H, J = 3.7 Hz, H_3), 6.57 (dd, 1H, J = 3.7, 1.6 Hz, H_4), 5.49 (s, 1H, $COC\underline{H}CO_2$), 3.76 (s, 3H, $CO_2C\underline{H}_3$); ^{13}C NMR ($CDCl_3$, 125 MHz) δ 180.2, 167.6, 151.0, 148.6, 147.5, 140.0, 120.7, 119.5, 130.0, 120.7, 119.5, 113.2, 56.4, 53.2; HRMS (EI) calcd for $C_{13}H_{10}BrNO_4$ (M^+), 322.9793; found, 322.9793.

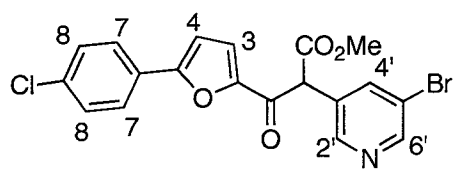

Methyl 2-(5-bromopyridin-3-yl)-3-(5-(4-chlorophenyl)furan-2-yl)-3-oxopropanoate (127d). The title compound **127d** was obtained from **126c** (1.81 g, 7.86 mmol) following the standard procedure described above for the preparation of **127a**. Purification of the crude product by flash chromatography on silica gel (33/67 EtOAc/$CHCl_3$) afforded **127d** as a yellow oil (1.35 g, 83%). IR ($CHCl_3$ cast): 3129, 3035, 2953, 1748, 1670, 1603, 1581, 1561, 1516, 1471, 1442, 1426, 1412 cm^{-1}; ^1H NMR ($CDCl_3$, 500 MHz) δ 8.61 (d,

1H, J = 2.1 Hz, $H_{2'}$ or $H_{6'}$), 8.55 (d, 1H, J = 1.7 Hz, $H_{2'}$ or $H_{6'}$), 8.06 (dd, 1H, J = 2.1, 1.7 Hz, $H_{4'}$), 7.64 (d, 2H, J = 8.5 Hz, H_7), 7.40 (d, 2H, J = 8.5 Hz, H_8), 7.38 (d, 1H, J = 3.8 Hz, H_4), 6.78 (d, 1H, J = 3.8 Hz, H_3), 5.46 (s, 1H, COC<u>H</u>CO_2), 3.78 (s, 3H, $CO_2C\underline{H}_3$); ^{13}C NMR ($CDCl_3$, 100 MHz) δ 179.5, 167.7, 157.8, 150.8, 150.1, 148.6, 139.9, 135.8, 130.0, 129.4, 127.3, 126.3, 121.7, 120.8, 108.6, 56.9, 53.3; HRMS (EI) calcd for $C_{19}H_{13}BrClNO_4$ (M^+), 434.9696; found, 434.9693.

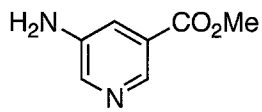

Methyl 5-aminonicotinate (129). Acetyl chloride (30 mL) was slowly added to dry MeOH (30 mL) at 0 °C to generate HCl and MeOAc. This solution was stirred for 10 minutes at 0° C, and then was added to a solution of 5-aminonicotinic acid (9.89 g, 71.57 mmol) in MeOH (120 mL) at 0 °C. The reaction mixture was refluxed over 18 h and then the solvent was removed in vacuo. The residue was treated with saturated $NaHCO_3$ until pH of the solution was ~7, and the resulting solution was extracted with EtOAc (3 x 80 mL). The combined organic layers were dried over anhydrous $MgSO_4$ and concentrated in vacuo. The crude product was purified by column chromatography (EtOAc) and yield **129** as a white solid (8.58 g, 79%). Literature compound.[94] IR ($CHCl_3$ cast): 3316, 3135, 2993, 2962, 1726, 1646, 1581, 1473, 1446, 1435 cm^{-1}; ^1H NMR ($CDCl_3$, 300 MHz) δ 8.62 (d, 1H, J = 1.8 Hz, Py<u>H</u>), 8.27 (d, 1H, J = 2.8 Hz, Py<u>H</u>), 7.58 (dd, 1H, J = 2.8, 1.8 Hz, Py<u>H</u>), 4.05-3.70 (br, 2H, N$\underline{H}_2$), 3.93 (s, 3H, $CO_2C\underline{H}_3$); HRMS (EI) calcd for $C_7H_8N_2O_2$ (M^+), 152.0586; found, 152.0585.

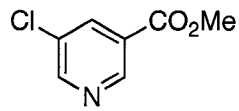

Methyl 5-chloronicotinate (130). A solution of $NaNO_2$ (3.26 g, 47.2 mmol) in H_2O (21 mL) was added over 30 min to a solution of **129** (5.91 g, 38.9 mmol) in conc. aqueous HCl (42 mL) and H_2O (21 mL) at 0 °C. The resulting mixture was stirred for another 30 min at 0 °C. To the reaction mixture was added HCl solution (10% w/w, 50 mL), and then a solution of $CuCl_2$ (8.82 g) and CuCl (42 mg) in HCl solution (10% w/w, 30 mL). The reaction mixture was stirred for 4 h at 0 °C and then allowed to warm to rt slowly. NaOH solution and saturated $NaHCO_3$ were added to neutralize the solution until the pH of ~7. The aqueous layer (250 mL) was extracted with EtOAc (3 x 80 mL). The combined organic layers were dried over anhydrous $MgSO_4$ and concentrated in vacuo. The crude product was purified by column chromatography (50/50 EtOAc/ hexanes) to yield **130** as a white solid (4.74 g, 71%). Literature compound.[95] IR ($CHCl_3$ cast): 3056, 1725, 1579, 1444, 1425 cm^{-1}; ^1H NMR ($CDCl_3$, 500 MHz) δ 9.06 (s, 1H, Py<u>H</u>), 8.71 (d, 1H, J = 2.0 Hz, Py<u>H</u>), 8.25 (d, 1H, J = 1.7 Hz, Py<u>H</u>), 4.00 (s, 3H, $CO_2C\underline{H}_3$); HRMS (EI) calcd for $C_7H_6ClNO_2$ (M^+), 171.0087; found, 171.0088.

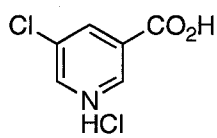

5-Chloronicotinic acid hydrogen chloride salt (131). To a solution of **130** (0.51 g, 2.96 mmol) in MeOH (5 mL) and H_2O (5 mL) was added KOH solution (0.24 g, 10% w/w) to pH between 10 and 11. The reaction mixture was stirred for 24 h at rt. A white precipitate appeared upon acidifying the reaction mixture to pH 1 with 1 N HCl (5 mL). This solid

was collected and then washed several times with H_2O. The filtrate was concentrated in vacuo and then dissolved in dry MeOH. The insoluble impurities were removed by gravity filtration, and the filtrate was concentrated in vacuo to afford the product **131** as a white solid (0.48 g, 84%). Literature compound.[96] IR (microscope): 3351 (broad), 3055, 1853, 1632, 1585, 1540, 1431 cm^{-1}. ^1H NMR (CD_3OD, 500 MHz) δ 9.05 (s, 1H, Py<u>H</u>), 8.78 (s, 1H, Py<u>H</u>), 8.31 (d, 1H, J = 1.4 Hz, Py<u>H</u>); HRMS (EI) calcd for $C_6H_4ClNO_2$ (M^+), 156.9931; found, 156.9930.

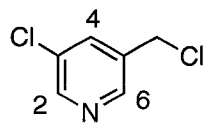

3-Chloro-5-(chloromethyl)pyridine (132). To a solution of **131** (0.49 g, 2.54 mmol) in THF (20 mL) at 0 °C was added dry Et_3N (0.78 mL, 5.60 mmol), followed by ethyl chloroformate (0.29 mL, 3.05 mmol). The reaction mixture was stirred for 1.5 h at 0 °C and then the precipitate, $Et_3N{\cdot}HCl$, was removed by gravity filtration. To the filtrate at -78 °C was added $LiAlH_4$ (3.05 mL of 1.0 M solution in THF, 3.05 mmol) over a period of 15 min. The reaction mixture was stirred at -78 °C for another 4 h, and then quenched with 5 % NaOH (8 mL). The solvent was removed in vacuo and the residue was diluted with H_2O (20 mL). Saturated NH_4Cl was added to adjust pH of the solution to around 8. The resulting mixture was stirred for another 1 h and then EtOAc (30 mL) was added. The solution was filtered through celite, and then the two layers were separated. The aqueous layer was extracted with EtOAc (3 x 50 mL). The combined organic layers were dried over anhydrous $MgSO_4$ and the solvent was removed to yield the product (5-chloropyridin-3-yl)methanol as a yellow oil (0.3793 g), which was used for next reaction

without any further purification. To a solution of the above alcohol (0.38 g, 2.65 mmol) in DCM (15 mL) at rt was added $SOCl_2$ (0.98 mL, 16.0 mmol). The reaction mixture was stirred for 42 h at rt. The solvent was removed in vacuo and the residue was treated with saturated $NaHCO_3$ (25 mL) until pH to around 8. The solution was then extracted with EtOAc (3 x 40 mL). The combined organic layers were dried over anhydrous $MgSO_4$ and concentrated in vacuo. The crude product was purified by column chromatography (50/50 EtOAc/hexanes) to yield **132** as a white solid (0.32 g, 76% over three steps). IR ($CHCl_3$ cast): 3046, 2964, 1584, 1563, 1556, 1461, 1442, 1423 cm^{-1}; ^1H NMR (CD_3OD, 400 MHz) δ 8.53 (d, 1H, J = 2.3 Hz, H_2 or H_6), 8.52 (d, 1H, J = 1.9 Hz, H_2 or H_6), 7.96 (dd, 1H, J = 2.3, 1.9 Hz, H_4), 4.70 (s, 2H, $C\underline{H}_2Cl$); ^{13}C NMR (CD_3OD, 100 MHz) δ 148.8, 148.2, 137.7, 137.2, 133.3, 42.5; HRMS (EI) calcd for $C_6H_5Cl_2N$ (M^+), 160.9799; found, 160.9803.

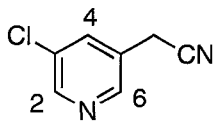

(5-Chloropyridin-3-yl)acetonitrile (133). A solution of **132** (0.10 g, 0.62 mmol) and KCN (0.10 g, 1.54 mmol) in dry DMF (3 mL) was stirred for 48 h at rt. The solvent was removed in vacuo and the residue was treated with K_2CO_3 solution (15 mL, 10% w/w). The solution was then extracted with EtOAc (3 x 15 mL). The combined organic layers were dried over $MgSO_4$ and concentrated in vacuo. The crude product was purified by column chromatography (EtOAc) to yield **133** as a light yellow crystalline solid (52.9 mg, 56%). IR ($CHCl_3$ cast): 3048, 3031, 2928, 2251, 2231, 1583, 1566, 1447, 1413 cm^{-1}; ^1H NMR ($CDCl_3$, 400 MHz) δ 8.57 (d, 1H, J = 2.3 Hz, H_2 or H_6), 8.47 (d, 1H, J = 2.0 Hz,

H_2 or H_6), 7.72 (dd, 1H, J = 2.3, 2.0 Hz, H_4), 3.78 (s, 2H, C$\underline{H}_2$CN); ^{13}C NMR ($CDCl_3$, 100 MHz) δ 148.5, 146.7, 135.2, 132.4, 127.2, 116.1, 20.7; HRMS (EI) calcd for $C_7H_5ClN_2$ (M^+), 152.0141; found, 152.0138.

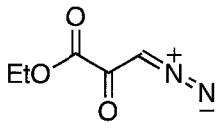

Ethyl 3-diazo-2-oxopropanoate (135). The title compound was prepared by a literature procedure of Müller.[97] To a solution of ethyl chlorooxoacetate (1.6 mL, 14 mmol) in THF (20 mL) was added $TMSCHN_2$ (21 mL, 2 M solution in hexane, 42 mmol) dropwise. After 3 h of stirring at rt, the solvent was removed in vacuo and the crude product was purified by column chromatography on silica gel (25/75 EtOAc/hexanes) to yield **135** as a yellow solid (1.35 g, 68%). Literature compound.[97] IR ($CHCl_3$ cast): 3458, 3241, 3080, 2994, 2971, 2943, 2909, 2869, 2432, 2159, 2109, 1734, 1697, 1641, 1530, 1476, 1459, 1442 cm^{-1}; ^{1}H NMR ($CDCl_3$, 400 MHz) δ 6.15 (s, 1H, COC$\underline{H}N_2$), 4.27 (q, 2H, J = 7.1 Hz, OC$\underline{H}_2$CH$_3$), 1.74 (t, 3H, J = 7.1 Hz, OCH$_2$C$\underline{H}_3$); HRMS (ES) calcd for $C_5H_6N_2O_3Na$ ([M+Na]$^+$), 165.0271; found, 165.0273.

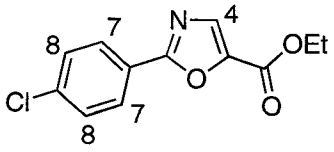

Ethyl 2-(4-chlorophenyl)oxazole-5-carboxylate (136). To a stirred suspension of bis-copper acetylacetonate (5.2 mg) in benzene (5 mL) and 4-chloro-benzonitrile (1.80 g, 13.1 mmol) at reflux temperature was added ethyl diazopyruvate **135** (1.00 g, 6.06 mmol) in benzene (14 mL) during a period of 3 h. The reaction mixture was heated for several

hours until the complete consumption of the starting material was confirmed by TLC. The solvent was removed in vacuo, and the residue was diluted with saturated $NaHCO_3$ solution (30 mL). The solution was then extracted with EtOAc (3 x 30 mL). The combined organic layers were washed with brine (20 mL), dried over $MgSO_4$ and then concentrated in vacuo. The crude residue was purified by column chromatography on silica gel (25/75 EtOAc/hexanes) to afford **136** as a white solid (0.24 g, 14%). Literature compound.[98] IR ($CHCl_3$ cast): 3089, 2983, 1735, 1606, 1587, 1574, 1534, 1475, 1408 cm^{-1}; ^1H NMR ($CDCl_3$, 300 MHz) δ 8.08 (d, 2H, J = 8.6 Hz, H_7), 7.83 (s, 1H, H_4), 7.47 (d, 2H, J = 8.6 Hz, H_8), 4.42 (q, 2H, J = 7.1 Hz, $OC\underline{H}_2CH_3$), 1.41 (t, 3H, J = 7.1 Hz, $OCH_2C\underline{H}_3$); HRMS (EI) calcd for $C_{12}H_{10}ClNO_3$ (M^+), 253.0349; found, 253.0347.

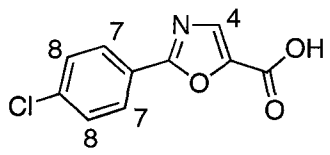

2-(4-Chlorophenyl)oxazole-5-carboxylic acid (137). To a solution of **136** (180 mg, 0.72 mmol) in THF/H_2O (8 mL/8 mL) at 0 °C was added LiOH (39 mg, 0.93 mmol). The resulting solution was stirred for 2 h until complete consumption of the starting material was confirmed by TLC. The solution was quenched with 1 N HCl until pH to around 3, and solvent was removed in vacuo. The residue was diluted with H_2O (20 mL) and then extracted with EtOAc (3 x 20 mL). The combined organic layers were washed with brine (10 mL) and dried over $MgSO_4$. The solvent was removed in vacuo to afford **137** as a white solid (150 mg, 94%). IR ($CHCl_3$ cast): 2917, 2849, 2633, 2528, 1739, 1603, 1569, 1530, 1475, 1411 cm^{-1}; ^1H NMR (CD_3OD, 400 MHz) δ 8.07 (d, 2H, J = 8.5 Hz, H_7), 7.86 (s, 1H, H_4), 7.54 (d, 2H, J = 8.5 Hz, H_8); ^{13}C NMR (CD_3OD, 100 MHz) δ 164.1, 161.3,

145.8, 138.9, 135.2, 130.5, 129.6, 126.5; HRMS (EI) calcd for $C_{10}H_6ClNO_3$ (M^+), 223.0036; found, 223.0040.

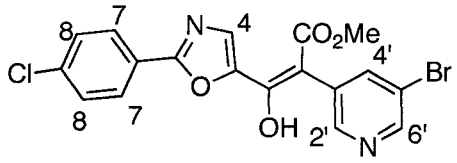

isomer **A**

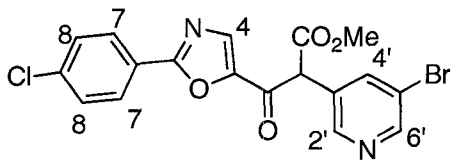

isomer **B**

Methyl 2-(5-bromopyridin-3-yl)-3-(2-(4-chlorophenyl)oxazol-5-yl)-3-oxopropanoate (138). The title compound **138** was obtained from **137** (112 mg, 0.5 mmol) following the standard procedure described above for the preparation of **127a**. Purification of the crude product by flash chromatography on silica gel (25/75 EtOAc/hexanes) afforded **138** as a white solid (50 mg, 23%). (Mixture of isomers A and B, 3:2 ratio). IR ($CHCl_3$ cast): 2954, 1744, 1683, 1650, 1603, 1580, 1556, 1526, 1473, 1443, 1408 cm^{-1}; ^1H NMR ($CDCl_3$, 300 MHz) (isomer A) δ 8.75 (d, 1H, J = 2.2 Hz, $H_{6'}$), 8.44 (d, 1H, J = 1.9 Hz, $H_{2'}$), 7.80 (dd, 1H, J = 2.2, 1.9 Hz, $H_{4'}$), 7.49 (d, 2H, J = 8.8 Hz, H_7), 7.43 (s, 1H, H_4), 7.37 (d, 1H, J = 8.8 Hz, H_8), 3.81 (s, 3H, $CO_2C\underline{H}_3$); ^1H NMR ($CDCl_3$, 300 MHz) (isomer B) δ 8.68 (d, 1H, J = 2.2 Hz, $H_{6'}$), 8.57 (d, 1H, J = 1.9 Hz, $H_{2'}$), 8.08 (dd, 1H, J = 2.2, 1.9 Hz, $H_{4'}$), 8.06 (d, 2H, J = 8.8 Hz, H_7), 7.99 (s, 1H, H_4), 7.52 (d, 2H, J = 8.8 Hz, H_8), 5.35 (s, 1H, $COC\underline{H}CO_2$), 3.82 (s, 3H, $CO_2C\underline{H}_3$); ^{13}C NMR ($CDCl_3$, 100 MHz) (mixture of isomers A and B) δ 176.6, 169.9, 164.5, 161.7, 160.1, 156.2, 148.6, 147.7, 147.2, 145.9, 145.5, 142.8, 138.8, 137.3, 137.0, 136.4, 135.2, 134.7, 131.6, 129.1, 127.1, 126.7, 126.2, 125.4, 122.0, 121.7, 118.4, 117.7, 96.3, 55.1, 51.0, 50.3; HRMS (EI) calcd for $C_{18}H_{12}BrClN_2O_4$ (M^+), 435.9640; found, 435.9642.

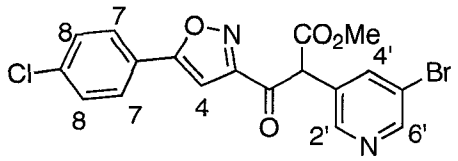

Methyl 2-(5-bromopyridin-3-yl)-3-(5-(4-chlorophenyl)isoxazol-3-yl)-3-oxopropanoate (140). The title compound **140** was obtained from 5-(4-chlorophenyl)isoxazole-3-carboxylic acid **139** (630 mg, 2.82 mmol) following the standard procedure described above for the preparation of **127a**. Purification of the crude product by flash chromatography on silica gel (50/50 EtOAc/hexanes) afforded **140** as a white solid (230 mg, 19%). IR ($CHCl_3$ cast): 3217, 3031, 2953, 1739, 1719, 1653, 1607, 1576, 1559, 1490, 1436 cm^{-1}; ^1H NMR ($CDCl_3$, 300 MHz) δ 8.67 (d, 1H, J = 2.1 Hz, $H_{6'}$), 8.59 (d, 1H, J = 1.9 Hz, $H_{2'}$), 8.03 (dd, 1H, J = 2.1, 1.9 Hz, $H_{4'}$), 7.74 (d, 2H, J = 8.9 Hz, H_7), 7.49 (d, 2H, J = 8.9 Hz, H_8), 6.92 (s, 1H, H_4), 5.84 (s, 1H. COC<u>H</u>CO_2), 3.81 (s, 3H, $CO_2C\underline{H}_3$); ^{13}C NMR ($CDCl_3$, 100 MHz) δ 183.2, 168.9, 164.9, 158.6, 148.4, 146.4, 137.3, 134.8, 127.1, 126.7, 124.7, 122.2, 118.2, 96.0, 54.9, 50.9; HRMS (EI) calcd for $C_{18}H_{12}BrClN_2O_4$ (M^+), 435.9648; found, 435.9651.

5. Enzyme assays. SARS-CoV $3CL^{pro}$ activity was measured by a quenched fluorescence resonance energy transfer (FRET) assay with the peptide substrate (Abz-SVTLQSG-Tyr(NO_2)R, 93% purity).[34] The rate of enzyme activity was determined by the increase in fluorescence (λ_{ex} 340 nm, λ_{em} 415 nm) upon continuous monitoring of reactions using a Shimadzu RF5301 spectrofluorimeter. The IC_{50} value of individual inhibitor was measured at 22 °C in a reaction mixture (700 mL) containing 100 mM KH_2PO_4/K_2HPO_4 at pH 7.5, 2 mM EDTA, 10 μM fluorogenic substrate, 1 μM His-tagged, or 20 mM Bis-Tris buffer at pH 7.0, 2 mM DTT, 10 μM fluorogenic substrate, 0.2 μM non-His-tagged

protease, and 1% inhibitor solution without any preincubation. The initial 3 or 5 min of the reaction were used for calculation purposes. Initial stock solutions were prepared at 10 mM in DMSO and serial dilutions made in DMSO. The protease activity in the presence of the specified inhibitor was expressed as a percentage of that obtained from the respective control samples. For inhibitors displaying dose-dependent inhibition of the protease activity, IC_{50} values were determined from plots of the relative protease activity *versus* the log of inhibitor concentration. IC_{50} values were not determined for compounds showing weak inhibition.

6. HPLC-MS purification. The samples were purified on a 1100 HPLC coupling with a ES-MSD Agilent 1956B with positive ion detection: Semi-prep column, Zorbax RX-C8, 9.4 x 250 mm, 5 μM with guard column; flow rate 3 mL/min, a linear gradient elution over 20 min of 35 to 100% acetonitrile in 0.05% formic acid/H_2O, then holding 2 min at 100% acetonitrile in 0.05% formic acid/H_2O, followed by return to 35% acetonitrile in 0.05% formic acid/H_2O over 0.5 min. The quality of some purified samples were confirmed by re-injection of purified samples to analytic column: Zorbax RX-C18, 4.6 x 150 mm, 5 μM; flow rate 0.7 mL/min, the same linear gradient elution as described above.

7. Mass spectrometry of enzyme-inhibitor complexes. The wild-type enzyme (~ 0.2 mM) was mixed with 10 equivalents of inhibitor at 22 °C without any preincubation. In addition, a control parallel experiment was preformed on the enzyme alone without any inhibitor. The samples were purified by C4 Ziptip (Millipore, MA, USA) and eluted by

50% acetonitrile in 0.1% formic acid. Mass spectrometric analysis was performed on the Waters (Micromass) Q-TOF Premier using infusion at a flow rate of 0.5-1 mL/min.

8. Molecular docking for SARS 3CL^{pro} inhibitors. Modeling studies of 3CL^{pro} with inhibitors **21-24** were carried out based on the previously solved structures of a 3CL^{pro}/inhibitor complex (PDB code 1UK4),[23] a rhinovirus 3C protease/inhibitor complex (PDB code 1CQQ),[30] and a glutamic acid specific serine protease/inhibitor complex (PDB code 1HPG).[99] Graphical manipulations were carried out using XtalView[100] and energy minimizations using CNS v1.1.[101] Additional forcefield parameters for the inhibitor were derived from the Cambridge Structural Database.[102] Graphics were produced using MolMol[103] and POV-Ray v3.5.

Modeling studies of 3CL^{pro} with inhibitors **34**, **40**, **58-60**: The crystal structure of SARS 3CL protease in complex with an aza-peptide epoxide (APE) (PDB code: 2A5K)[49a] was selected to construct the predictive model after deleting the coordinates of the epoxide inhibitor from the pdb file. The 3-dimensional (3D) coordinates of 3CL enzyme (experimental) and those of the inhibitors (calculated) were processed in Sybyl 7.1.[104] The essential hydrogen atoms were added to the protein molecule and the Kollman united atom charges were applied; the 3D structures of inhibitors were constructed and energy-minimized using the Tripos force field in Sybyl 7.1; hydrogen atoms and Gasteiger-Marsili charges were added to inhibitors.[105] Autodock 3.0.5[73] was used to perform the automated molecular docking. The grid map with 60×60×60 points spaced at 0.375 Å was generated using the AUTOGRID program to evaluate the binding energies. The

docked complexes of 3CL protease with inhibitors were evaluated according to the predicted binding energy and the geometric ideality of the docked inhibitors.

REFERENCES

(1) (a) Byrd, C. M.; Hruby, D. E. Viral proteinases: targets of opportunity. *Drug Dev. Res.* **2006**, *67*, 501-510. (b) Yoshimura, K.; Kato, R.; Kavlick, M. F.; Nguyen, A.; Maroun, V.; Maeda, K.; Hussain, K. A.; Ghosh, A. K.; Gulnik, S. V.; Erickson, J. W.; Mitsuya, H. A potent human immunodeficiency virus type 1 protease inhibitor, UIC-94003 (TMC-126), and selection of a novel (A28S) mutation in the protease active site. *J. Virol.* **2002**, *76*, 1349-1358.

(2) Patick, A. K.; Potts, K. E. Protease inhibitors as antiviral agents. *Clin. Microbiol. Rev.* **1998**, *11*, 614-627.

(3) Leung, D.; Abbenante, G.; Fairlie, D. P. Protease inhibitors: current status and future prospects. *J. Med. Chem.* **2000**, *43*, 305-341.

(4) Mills, J. S. Viral protease inhibitors – what next after HIV. *Antiviral Chem. Chemother.* **1996**, *7*, 281-293.

(5) Oxford, J. S. Influenza A pandemics of the 20th century with special reference to 1918: virology, pathology and epidemiology. *Rev. Med. Virol.* **2000**, *10*, 119-133.

(6) Drosten, C.; Günther, S.; Preiser, W.; van der Werf, S.; Brodt, H. -R.; Becker, S.; Rabenau, H.; Panning, M.; Kolesnikova, L.; Fouchier, R. A. M.; Berger, A.; Burguière, A.-M.; Cinatl, J.; Eickmann, M.; Escriou, N.; Grywna, K.; Kramme, S.; Manuguerra, J.-C.; Müller, S.; Rickerts, V.; Stürmer, M.; Vieth, S.; Klenk, H.-D.; Osterhaus, A. D. M. E.; Schmitz, H.; Doerr, H. W. Identification of a novel

coronavirus in patients with severe acute respiratory syndrome. *New Engl. J. Med.* **2003**, *348*, 1967-1976.

(7) Ksiazek, T. G.; Erdman, D.; Goldsmith, C. S.; Zaki, S. R.; Peret, T.; Emery, S.; Tong, S.; Urbani, C.; Comer, J. A.; Lim, W.; Rollin, P. E.; Dowell, S. F.; Ling, A. -E.; Humphrey, C. D.; Shieh, W.-J.; Guarner, J.; Paddock, C. D.; Roca, P.; Fields, B.; DeRisi, J.; Yang, J.-Y.; Cox, N.; Hughes, J. M.; LeDuc, J. W.; Bellini, W. J.; Anderson, L. J. A novel coronavirus associated with severe acute respiratory syndrome. *New Engl. J. Med.* **2003**, *348*, 1953-1966.

(8) Lee, N.; Hui, D.; Wu, A.; Chan, P.; Cameron, P.; Joynt, G. M.; Ahuja, A.; Yung, M. Y.; Leung, C. B.; To, K. F.; Lui, S. F.; Szeto, C. C.; Chung, S. and Sung, Joseph J. Y. A major outbreak of severe acute respiratory syndrome in Hong Kong. *New Engl. J. Med.* **2003**, *348*, 1986-1994.

(9) (a) World Health Organization (15 August 2003). http://www.who.int/csr/sars/country/2003 08 15/en/. (b) World Health Organization (31 January 2004). http://www.who.int/csr/sars/country/2003 01 31/en/. (c) World Health Organization (30 April 2004). http://www.who.int/csr/sars/country/2003 01 31/en/.

(10) Anand, K.; Ziebuhr, J.; Wadhwani, P.; Mesturs, J. R.; Hilgenfeld, R. Coronavirus main proteinase ($3CL^{pro}$) structure: basis for design of anti-SARS drugs. *Science* **2003**, *300*, 1763–1767.

(11) Rota, P. A.; Oberste, M. S.; Nix, W. A.; Campagnoli, R.; Icenogle, J. P.; Peñaranda, S.; Bankamp, B.; Maher, K.; Chen, M. -H.; Tong, S.; Tamin, A.;

Lowe, L.; Frace, M.; DeRisi, J. L.; Chen, Q.; Wang, D.; Erdman, D. D.; Peret, T. C. T.; Burns, C.; Ksiazek, T. G.; Rollin, P. E.; Sanchez, A.; Liffick, S.; Holloway, B.; Limor, J.; McCaustland, K.; Olsen-Rasmussen, M.; Fouchier, R.; Günther, S.; Osterhaus, A. D. H. E.; Drosten, C.; Pallansch, M. A.; Anderson, L. J.; Bellini, W. J. Characterization of a novel coronavirus associated with severe acute respiratory syndrome. *Science* **2003**, *300*, 1394–1399.

(12) Marra, M. A.; Jones, S. J. M.; Astell, C. R.; Holt, R. A.; Brooks-Wilson, A.; Butterfield, Y. S. N.; Khattra, J.; Asano, J. K.; Barber, S. A.; Chan, S. Y.; Cloutier, A.; Coughlin, S. M.; Freeman, D.; Girn, N.; Griffith, O. L.; Leach, S. R.; Mayo, M.; McDonald, H.; Montgomery, S. B.; Pandoh, P. K.; Petrescu, A. S.; Robertson, A. G.; Schein, J. E.; Siddiqui, A.; Smailus, D. E.; Stott, J. M.; Yang, G. S.; Plummer, F.; Andonov, A.; Artsob, H.; Bastien, N.; Bernard, K.; Booth, T. F.; Bowness, D.; Czub, M.; Drebot, M.; Fernando, L.; Flick, R.; Garbutt, M.; Gray, M.; Grolla, A.; Jones, S.; Feldmann, H.; Meyers, A.; Kabani, A.; Li, Y.; Normand, S.; Stroher, U.; Tipples, G. A.; Tyler, S.; Vogrig, R.; Ward, D.; Watson, B.; Brunham, R. C.; Krajden, M.; Petric, M.; Skowronski, D. M.; Upton, C.; Roper, R. L. The genome sequence of the SARS-associated coronavirus. *Science* **2003**, *300,* 1399–1404.

(13) Oxford, J. S.; Bossuyt, S.; Lambkin, R. A new infectious disease challenge: urbani severe acute respiratory syndrome (SARS) associated coronavirus. *Immunology* **2003**, *109*, 326–328.

(14) Myint, S. H. in *The Coronaviridae*, Ed.; Siddell, S. G. Plenum Press: New York, 1995; p. 389-401.

(15) Li, W.; Moore, M. J.; Vasilieva, N.; Sui, J.; Wong, S. K.; Berne, M. A.; Somasundaran, M.; Sullivan, J. L.; Luzuriaga, K.; Greenough, T. C.; Choe, H.; Farzan, M. Angiotensin-converting enzyme 2 is a functional receptor for the SARS coronavirus. *Nature* **2003**, *426*, 450–454.

(16) Thiel, V.; Ivanov, K. A.; Putics, Á.; Hertzig, T.; Schelle, B.; Bayer, S.; Weißbrich, B.; Snijder, E. J.; Rabenau, H.; Doerr, H. W.; Ziebuhr, J. Mechanisms and enzymes involved in SARS coronavirus genome expression. *J. Gen. Virol.* **2003**, *84*, 2305-2315.

(17) Ng, M. L.; Tan, S. H.; See, E. E.; Ooi, E. E.; Ling, A. E. Early events of SARS coronavirus infection in Vero cells. *J. Med. Virol.* **2003**, *71*, 323-331.

(18) Ng, M. L.; Tan, S. H.; See, E. E.; Ooi, E. E.; Ling, A. E. Proliferative growth of SARS coronavirus in Vero E6 cells. *J. Gen. Virol.* **2003**, *84*, 3291-3303.

(19) Holmes, K. V. SARS coronavirus: a new challenge for prevention and therapy. *J. Clin. Invest.* **2003**, *111*, 1605-1609.

(20) Kliger, Y.; Levanon, E. Y.; Gerber, D. From genome to antivirals: SARS as a test tube. *Drug Discov. Today* **2005**, *10*, 345-352.

(21) Hofmann, H.; Pohlmann, S. Cellular entry of the SARS coronavirus. *Trends Microbiol.* **2004**, *12*, 466-472.

(22) Kao, R. Y.; Tsui, W. H. W.; Lee, T. S. W.; Tanner, J. A.; Watt, R. M.; Huang, J. D.; Hu, L.; Chen, G.; Chen, Z.; Zhang, L.; He, T.; Chan, K. H.; Tse, H.; To, A. P. C.; Ng, L. W. Y.; Wong, B. C. W.; Tsoi, H. W.; Yang, D.; Ho, D. D.; Yuen, K. Y. Identification of novel small-molecule inhibitors of severe acute respiratory syndrome-associated coronavirus by chemical genetics. *Chem. Biol.* **2004**, *11*, 1293-1299.

(23) Yang, H.; Yang, M.; Ding, Y.; Liu, Y.; Lou, Z.; Zhou, Z.; Sun, L.; Mo, L.; Ye, S.; Pang, H.; Gao, G.; Anand, K.; Bartlam, M.; Hilgenfeld, R.; Rao, Z. The crystal structures of SARS virus main protease M^{pro} and its complex with an inhibitor. *Proc. Natl. Acad. Sci. U. S. A.* **2003**, *100*, 13190-13195.

(24) Huang, C.; Wei, P.; Fan, K.; Liu, Y.; Lai, Y. 3C-like proteinase from SARS coronavirus catalyzes substrate hydrolysis by a general base mechanism. *Biochemistry* **2004**, *43*, 4568-4574.

(25) Allaire, M.; Chernaia, M. M.; Malcolm, B. A.; James, M. N. G. Picornaviral 3C cysteine proteinases have a fold similar to chymotrypsin-like serine proteinases. *Nature* **1994**, *369*, 72-76.

(26) (a) Fan, K.; Wei, P.; Feng, Q.; Chen, S.; Huang, C.; Ma, L.; Lai, B.; Pei, J.; Liu, Y.; Chen, J.; Lai, L. Biosynthesis, purification, and substrate specificity of severe acute respiratory syndrome coronavirus 3C-like proteinase. *J. Biol. Chem.* **2004**, *279*, 1637-1642. (b) Shi, J.; Wei, Z.; Feng, Q.; Song, J. Dissection study on the SARS 3C-like protease reveals the critical role of the extra domain in

dimerization of the enzyme: defining the extra domain as a new target for design of highly-specific protease inhibitors. *J. Biol. Chem.* **2004**, *279*, 24765-24773.

(27) Bonanno, J. B.; Fowler, R.; Gupta, S.; Hendle, J.; Lorimer, D.; Romero, R.; Sauder, M.; Wei, C. L.; Liu, E. T.; Burley, S. K.; Harris, T. X-ray crystal structure of the SARS coronavirus main protease. http://www.rscb.org (PDB code: 1Q2W).

(28) Hegyi, A.; Ziebuhr, J. Conservation of substrate specificities among coronavirus main proteases. *J. Gen. Virol.* **2002**, *83*, 595-599.

(29) Schechter, I.; Berger, A. On the size of the active site in proteases. I. Papain. *Biochem. Biophys. Res. Commun.* **1967**, *27*, 157-162.

(30) Matthews, D.; Dragovich, P. S.; Webber, S. E.; Fuhrman, S. A.; Patick, A. K.; Zalman, L. S.; Hendrickson, T. F.; Love, R. A.; Prins, T. J.; Marakovits, J. T.; Zhou, R.; Tikhe, J.; Ford, C. E.; Meador, J. W.; Ferre, R. A.; Brown, E. L.; Binford, S. L.; Brothers, M. A.; Delisle, D. M.; Worland, S. T. Structure-assisted design of mechanism-based irreversible inhibitors of human rhinovirus 3C protease with potent antiviral activity against multiple rhinovirus serotypes. *Proc. Natl. Acad. Sci. USA,* **1999**, *96*, 11000-11007.

(31) Wu, C. -Y.; Jan, J. -T.; Ma, S. -H.; Kuo, C. -J.; Juan, H. -F.; Cheng, Y. -S. E.; Hsu, H. -H.; Huang, H. -C.; Wu, D.; Brik, A.; Liang, F. -S.; Liu, R. -S.; Fang, J. -M.; Chen, S. -T.; Liang, P. -H.; Wong, C. -H. Small molecules targeting severe acute respiratory syndrome human coronavirus. *Proc. Natl. Acad. Sci. USA.* **2004**, *101*, 10012-10017.

(32) Hsu, J. T. A.; Kuo, C. J.; Hsieh, H. P.; Wang, Y. C.; Huang, K. K.; Lin, C. P.; Lin, C. P.; Huang, P. F.; Chen, X.; Liang, P. H. Evaluation of metal-conjugated compounds as inhibitors of 3CL protease of SARS-CoV. *FEBS Lett.* **2004**, *574*, 116-120.

(33) Bacha, U.; Barrila, J.; Velazquez-Campoy, A.; Leavitt, S. A.; Freire, E. Identification of novel inhibitors of the SARS coronavirus main protease $3CL^{pro}$. *Biochemistry* **2004**, *43*, 4906-4912.

(34) Blanchard J. E.; Elowe, N. H.; Fortin, P. D.; Huitema, C.; Cechetto, J. D.; Eltis, L. D.; Brown E. D. High-throughput screening identifies inhibitors of the SARS coronavirus main proteinase. *Chem. Biol.* **2004**, *11*, 1445-1453.

(35) Ghosh, A. K.; Xi, K.; Ratia, K.; Santarsiero, B. D.; Fu, W.; Harcourt, B. H.; Rota, P. A.; Baker, S. C.; Johnson, M. E.; Mesecar, A. D. Design and synthesis of peptidomimetic severe acute respiratory syndrome chymotrypsin-like protease inhibitors. *J. Med. Chem.* **2005**, *48*, 6767-6771.

(36) Shie, J. J.; Fang, J. M.; Kuo, T. H.; Kuo, C. J.; Liang, P. H.; Huang, H. J.; Wu, Y. T.; Jan, J. T.; Cheng, Y. S. E.; Wong, C. H. Inhibition of the severe acute respiratory syndrome 3CL protease by peptidomimetic α,β-unsaturated esters. *Bioorg. Med. Chem.* **2005**, *13*, 5240-5252.

(37) Shie, J. -J.; Fang, J. -M.; Kuo, C. -J.; Kuo, T. -H.; Liang, P. -H.; Huang, H. -J.; Yang, W. -B.; Lin, C. -H.; Chen, J. -L.; Wu, Y. -T.; Wong, C. -H. Discovery of potent anilide inhibitors against the severe acute respiratory syndrome 3CL protease. *J. Med. Chem.* **2004**, *48*, 4469-4473.

(38) Chen, L. R.; Wang, Y. C.; Lin, Y. W.; Chou, S. Y.; Chen, S. F.; Liu, L. T.; Wu, Y. T.; Kuo, C. J.; Chen, T. S. S.; Juang, S. H. Synthesis and evaluation of isatin derivatives as effective SARS coronavirus 3CL protease inhibitors. *Bioorg. Med. Chem.* **2005**, *15*, 3058-3062.

(39) Zhou, L.; Liu, Y.; Zhang, W.; Wei, P.; Huang, C.; Pei, J.; Yuan, Y.; Lai, L. Isatin compounds as noncovalent SARS coronavirus 3C-like protease inhibitors. *J. Med. Chem.* **2006**, *49*, 3440-3443.

(40) Wu, C. Y.; King, K. -Y.; Kuo, C. -J.; Fang, J. -M.; Wu, Y. -T.; Ho, M. -Y.; Liao, C. -L.; Shie, J. -J.; Liang, P. -H.; Wong, C. -H. Stable benzotriazole esters as mechanism-based inactivators of the severe acute respiratory syndrome 3CL protease. *Chem. Biol.* **2006**, *13*, 261-268.

(41) Liang, P. H. Characterization and inhibition of SARS-coronavirus main protease. *Curr. Topics Med. Chem.* **2006**, *6*, 361-376.

(42) Lai, L.; Han, X.; Chen, H.; Wei, P.; Huang, C.; Liu, S.; Fan, K.; Zhou, L.; Liu, Z.; Pei, J.; Liu, Y. Quaternary structure, substrate selectivity and inhibitor design for SARS 3C-like proteinase. *Curr. Pharm. Des.* **2006**, *12*, 4555-4564.

(43) Yang, H.; Bartlam, M.; Rao, Z. Drug design targeting the main protease, the Achilles' heel of coronavirus. *Curr. Pharm. Des.* **2006**, *12*, 4573-4599.

(44) Webber, S. E.; Tikhe, J.; Worland, S. T.; Fuhrman, S. A.; Hendrickson, T. F.; Matthews, D. A.; Love, R. A.; Patick, A. K.; Meador, J. W.; Ferre, R. A.; Brown, E. L.; DeLisle, D. M.; Ford, C. E.; Binford, S. L. Design, synthesis, and

evaluation of nonpeptidic inhibitors of human rhinovirus 3C protease. *J. Med. Chem.* **1996**, *39*, 5072-5082.

(45) Yang, H.; Xie, W.; Xue, X.; Yang, K.; Ma, J.; Liang, W.; Zhao, Q.; Zhou, Z.; Pei, D.; Ziebuhr, J.; Hilgenfeld, R.; Yuen, K. Y.; Wong, L.; Gao, G.; Chen, S.; Chen, Z.; Ma, D.; Bartlam, M.; Rao, Z. Design of wide-spectrum inhibitors targeting coronavirus main proteases. *PLoS. Biol.* **2005**, *3*, e324.

(46) Asgian, J. L.; James, K. E.; Li, Z. Z.; Carter, W.; Barrett, A. J.; Mikolajczyk, J.; Salvesen, G. S.; Powers, J. C. Aza-peptide epoxides: A new class of inhibitors selective for clan CD cysteine proteases. *J. Med. Chem.* **2002**, *45*, 4958-4960.

(47) Barrett, A. J.; Rawlings, N. D. Evolutionary lines of cysteine peptidases. *Biol. Chem.* **2001**, *382*, 727-733.

(48) (a) James, K. E.; Gotz, M. G.; Caffrey, C. R.; Hansell, E.; Carter, W.; Barrett, A. J.; Mckerrow, J. H.; Powers, J. C. Aza-peptide epoxides: potent and selective inhibitors of *Schistosoma mansoni* and pig kidney legumains (asparaginyl endopeptidases). *Biol. Chem.* **2003**, *384*, 1613-1618. (b) James, K. E.; Asgian, J. L.; Li, Z. Z.; Ekici, O. D.; Rubin, J. R.; Mikolajczyk, J.; Salvesen, G. S.; Powers, J. C. Design, synthesis, and evaluation of aza-peptide epoxides as selective and potent inhibitors of Caspases-1, -3, -6, and -8. *J. Med. Chem.* **2002**, *47*, 1553-1573.

(49) (a) Lee, T. W.; Cherney, M. M.; Huitema, C.; Liu, J.; James, K. E.; Powers, J. C.; Eltis, L. D.; James, M. N. Crystal structures of the main peptidase from the SARS coronavirus inhibited by a substrate-like aza-peptide epoxide. *J. Mol. Biol.* **2005**,

353, 1137-1151. (b) Lee, T. W.; Cherney, M. M.; Liu, J.; James, K. E.; Powers, J. C.; Eltis, L. D.; James, M. N. Crystal structures reveal an induced-fit binding of a substrate-like aza-peptide epoxide to SARS coronavirus main peptidase. *J. Mol. Biol.* **2007**, *366*, 916-932.

(50) Demuth, H. U. J. Recent developments in inhibiting cysteine and serine proteases. *Enzyme Inhib.* **1990**, *3*, 249-278.

(51) Angliker, H.; Wikstrom, P.; Rauber, P.; Stone, S.; Shaw, E. Synthesis and properties of peptidyl derivatives of arginylfluoromethanes. *Biochem. J.* **1987**, *241*, 871-875.

(52) Mittl, P. R. E.; Marco, S. D.; Krebs, J. F.; Bai, X.; Karanewsky, D. S.; Priestle, J. P.; Tomaselli, K. J.; Grütter, M. G. Structure of recombinant human CPP32 in complex with the tetrapeptide Acetyl-Asp-Val-Ala-Asp fluoromethyl ketone. *J. Biol. Chem.* **1997**, *272*, 6539-6547.

(53) Kreutter, K.; Steinmetz, A. C. U.; Liang, T. C.; Prorok, M.; Abeles, R. H. and Ringe, D. Three-dimensional structure of chymotrypsin inactivated with (2*S*)-N-acetyl-L-alanyl-L-phenylalanyl alpha-chloroethane: implications for the mechanism of inactivation of serine proteases by chloroketones. *Biochemistry* **1994**, *33*, 13792-13800.

(54) Zhang, H. Z.; Zhang, H.; Kemnitzer, W.; Tseng, B.; Cinatl, J., Jr.; Michaelis, M.; Doerr, H. W.; Cai, S. X. Design and synthesis of dipeptidyl glutaminyl fluoromethyl ketones as potent severe acute respiratory syndrome coronavirus (SARS-CoV) inhibitors. *J. Med. Chem.* **2006**, *49*, 1198-1201.

(55) Smith, R. A.; Copp, L. J.; Donnelly, S. L.; Spencer, R. W.; Krantz, A. Inhibition of cathepsin B by peptidyl aldehydes and ketones: slow-binding behavior of a trifluoromethyl ketone. *Biochemistry* **1988**, *27*, 6568-6573.

(56) Gelb, M. H.; Svaren, J. P.; Abeles, R. H. Fluoro ketone inhibitors of hydrolytic enzymes. *Biochemistry* **1985**, *24*, 1813-1817.

(57) Bégué, J. P. and Bonnet-Delpon, D. Preparation of trifluoromethyl ketones and related fluorinated ketones. *Tetrahedron* **1991**, *47*, 3207-3258.

(58) Sydnes, M. O.; Hayashi, Y.; Sharma, V. K.; Hamada, T.; Bacha, U.; Barrila, J.; Freire, E. and Kiso, Y. Synthesis of glutamic acid and glutamine peptides possessing a trifluoromethyl ketone group as SARS-CoV 3CL protease inhibitors. *Tetrahedron* **2006**, *62*, 8601-8609.

(59) Liu, B.; Zhou, J. SARS-CoV protease inhibitors design using virtual screening method from natural products libraries. *J. Comput. Chem.* **2005**, *26*, 484-490.

(60) Liu, Z.; Huang, C.; Fan, K.; Wei, P.; Chen, H.; Liu, S.; Pei, J.; Shi, L.; Li, B.; Yang, K.; Liu, Y.; Lai, L. Virtual screening of novel noncovalent inhibitors for SARS-CoV 3C-like proteinase. *J. Chem. Inf. Model.* **2005**, *45*, 10-17.

(61) Kaeppler, U.; Stiefl, N.; Schiller, M.; Vicik, R.; Breuning, A.; Schmitz, W.; Rupprecht, D.; Schmuck, C.; Baumann, K.; Ziebuhr, J.; Schirmeister, T. A new lead for nonpeptidic active-site-directed inhibitors of the severe acute respiratory syndrome coronavirus main protease discovered by a combination of screening and docking methods. *J. Med. Chem.* **2005**, *48*, 6832-6842.

(62) Tsai, K.-C.; Chen, S.-Y.; Liang, P.-H.; Lu, I-L.; Mahindroo, N.; Hsieh, H.-P.; Chao, Y.-S.; Liu, L.; Liu, D.; Lien, W.; Lin, T.-H.; Wu, S.-Y. Discovery of a novel family of SARS-CoV protease inhibitors by virtual screening and 3D-QSAR studies. *J. Med. Chem.* **2006**, *49*, 3485-3495.

(63) Lu, I.-L.; Mahindroo, N.; Liang, P.-H.; Peng, Y.-H.; Kuo, C.-J.; Tsai, K.-C.; Hsieh, H.-P.; Chao, Y.-S.; Wu, S.-Y. Structure-based drug design and structural biology study of novel nonpeptide inhibitors of severe acute respiratory syndrome coronavirus main protease. *J. Med. Chem.* **2006**, *49*, 5154-5161.

(64) Chen, L.; Chen, S.; Gui, C.; Shen, J.; Shen, X. and Jiang, H. Discovering severe acute respiratory syndrome coronavirus 3CL protease inhibitors: virtual screening, surface plasmon resonance, and fluorescence resonance energy transfer assays. *J. Biomol. Screen.* **2006**, *11*, 915-921.

(65) (a) Jain, R. P.; Vederas, J. C. Structural variations in keto-glutamines for improved inhibition against hepatitis A virus 3C proteinase. *Bioorg. Med. Chem. Lett.* **2004**, *14*, 3655-3658. (b) Ramtohul, Y. K.; James, M. N. G.; Vederas, J. C. Synthesis and evaluation of keto-glutamine analogues as inhibitors of hepatitis A virus 3C proteinase. *J. Org. Chem.* **2002**, *67*, 3169-3178. (c) Ramtohul, Y. K.; Martin, N. I.; Silkin, L.; James, M. N. G.; Vederas, J. C. Synthesis of pseudoxazolones and their inhibition of the 3C cysteine proteinases from hepatitis A virus and human rhinovirus-14. *J. Chem. Soc., Perkin Trans. 1* **2002**, 1351-1359. (d) Lall, M. S.; Ramtohul, Y. K.; James, M. N. G.; Vederas, J. C. Serine and threonine beta-Lactones: a new class of hepatitis A virus 3C cysteine

proteinase inhibitors. *J. Org. Chem.* **2002**, *67*, 1536-1547. (e) Ramtohul, Y. K.; Martin, N. I.; Silkin, L.; James, M. N. G.; Vederas, J. C. Pseudoxazolones, a new class of inhibitors for cysteine proteinases: inhibition of hepatitis A virus and human rhinovirus 3C proteinases. *J. Chem. Soc. Chem. Commun.* **2001**, 2740-2741.

(66) Dufour, E.; Storer, A. C.; Menard, R. Peptide aldehydes and nitriles as transition state analog inhibitors of cysteine proteases. *Biochemistry* **1995**, *34*, 9136-9143.

(67) Silva, A. M.; Cachau, R. E.; Sham, H. L.; Erickson, J. W. Inhibition and catalytic mechanism of HIV-1 aspartic protease. *J. Mol. Biol.* **1996**, *255*, 321-334.

(68) Tian, Q.; Nayyar, N. K.; Babu, S.; Chen, L.; Tao, J.; Lee, S.; Tibbetts, A.; Moran, T.; Liou, J.; Guo, M.; Kennedy, T. P. An efficient synthesis of a key intermediate for the preparation of the rhinovirus protease inhibitor AG7088 via asymmetric dianionic cyanomethylation of *N*-Boc-(+)-glutamic acid dimethyl ester. *Tetrahedron Lett.* **2001**, *42*, 6807-6809.

(69) (a) Yin, J.; Niu, C.; Cherney, M. M.; Zhang, J.; Huitema, C.; Eltis, L. D.; Vederas, J. C.; James, M. N. G. A mechanistic view of enzyme inhibition and peptide hydrolysis in the active site of SARS-CoV 3C-like peptidase. *J. Mol. Biol.* **2007**, in press. (b) Yin, J.; Cherney, M. M.; Bergmann, E. M.; Zhang, J.; Huitema, C.; Pettersson, H. I.; Eltis, L. D.; Vederas, J. C.; James, M. N. G. An episulfide cation (thiiranium ring) trapped in the active site of HAV 3C proteinase inactivated by peptide-based ketone inhibitors. *J. Mol. Biol.* **2006**, *361*, 673-686.

(70) Malcolm, B. A.; Lowe, C.; Shechosky, S.; McKay, R. T.; Yang, C. C.; Shah, V. J.; Simon, R. J.; Vederas, J. C.; Smith. D. V. Peptide aldehyde inhibitors of hepatitis A virus 3C proteinase. *Biochemistry* **1995**, *34*, 8172-8179.

(71) Morris, T. S.; Frormann, S.; Shechosky, S.; Lowe, C.; Lall, M. S.; Gauss-Müller, V.; Purcell, R. H.; Emerson, S. U.; Vederas, J. C.; Malcolm, B. A. In vitro and ex vivo inhibition of hepatitis A virus 3C proteinase by a peptidyl monofluoromethyl ketone. *Bioorg. Med. Chem.* **1997**, *5*, 797-807.

(72) Nahm, S.; Weinreb, S. M. *N*-methoxy-*N*-methylamides as effective acylating agents. *Tetrahedron Lett.* **1981**, *22*, 3815-3818.

(73) Morris, G. M.; Goodsell, D. S.; Halliday, R. S.; Huey, R.; Hart, W. E.; Belew, R. K.; Olson, A. J. Automated docking using Lamarckian genetic algorithm and empirical binding free energy function. *J. Comput. Chem.* **1998**, *19*, 1639-1662.

(74) Jain, R. P.; Pettersson, H. I.; Zhang, J.; Aull, K. D.; Fortin, P. D.; Huitema, C.; Eltis, L. D.; Parrish, J. C.; James, M. N. G.; Wishart, D. S.; Vederas, J. C. Synthesis and evaluation of keto-glutamine analogues as potent inhibitors of severe acute respiratory syndrome $3CL^{pro}$. *J. Med. Chem.* **2004**, *47*, 6113-6116.

(75) Dondoni, A.; Fantin, G.; Fogagnolo, M.; Medici, A.; Pedrini, P. Synthesis of (trimethylsilyl)thiazoles and reactions with carbonyl compounds. Selectivity aspects and synthetic utility. *J. Org. Chem.* **1988**, *53*, 1748-1761.

(76) Du, X.; Guo, C.; Hansell, E.; Doyle, P. S.; Caffrey, C. R.; Holler, T. P.; McKerrow, J. H.; Cohen, F. E. Synthesis and structure-activity relationship study

of potent trypanocidal thiol semicarbazone inhibitors of the trypanosomal cysteine protease cruzain. *J. Med. Chem.* **2002**, *45*, 2695-2707.

(77) Kolhatkar, R. B.; Ghorai, S. K.; George, C.; Reith, M. E. A.; Dutta, A. K. Interaction of *cis*-(6-benzhydrylpiperidin-3-yl)benzylamine analogues with monoamine transporters: structure-activity relationship study of structurally constrained 3,6-disubstituted piperidine analogues of (2,2-diphenylethyl)-[1-(4-fluorobenzyl)piperidin-4-ylmethyl]amine. *J. Med. Chem.* **2003**, *46*, 2205-2215.

(78) Horikawa, M.; Hashimoto, K.; Shirahama, H. Efficient syntheses of acromelic acids B and E, which are potent neuroexcitatory amino acids. *Tetrahedron Lett.* **1993**, *34*, 331-334.

(79) Miller, A. D.; Osuch, C.; Goldberg, N. N.; Levine, R. The synthesis of nitrogen-containing ketones *vs* the direct acylation of 3-picoline. *J. Am. Chem. Soc.* **1956**, *78*, 674-676.

(80) Borredon, M. E.; Delmas, M.; Gaset, A. Epoxydation en milieu heterogene solide-liquide faiblement hydrate: etude de la reaction autour de la structure du sel de sulfonium. *Tetrahedron* **1987**, *43*, 3945-3954.

(81) Kokotos, G.; Padron, J. M.; Martin, T.; Gibbons, W. A.; Martin, V. S. A general approach to the asymmetric synthesis of unsaturated lipidic α-amino acids. The first synthesis of α-aminoarachidonic acid. *J. Org. Chem.* **1998**, *63*, 3741-3744.

(82) Eisenbarth, S. and Steffan, B. Structure and biosynthesis of chrysophysarin A, a plasmodial pigment from the slime mould *Physarum polycephalum* (Myxomycetes). *Tetrahedron* **2000**, *56*, 363-365.

(83) Aydin, M.; Lucht, N.; Konig, W. A.; Lupp, R.; Jung, G.; Winkelmann, G. Structure elucidation of the peptide antibiotics Herbicolin A and B. *Liebigs Ann. Chem.* **1985**, *11*, 2285-2300.

(84) Rayabarapu, D. K.; Majumdar, K. K.; Sambaiah, T.; Cheng, C.-H. Unusual 1,4-addition of 2-pyridyl carboxylates to benzynes: a convenient route to 1-(2-acylphenyl)-2-pyridones. *J. Org. Chem.* **2001**, *66*, 3646-3649.

(85) Kanaoka, Y.; San-nohe, K.; Hatanaka, Y.; Itoh, K.; Machida, M.; Terashima, M. Syntheses of thieno[2,3-*c*]-, pyrrolo[2,3-*c*]- and indolo[2,3-*c*]diazanaphthalenes by photocyclization of acylaminopyridines. *Heterocycles.* **1977**, *6*, 29-32.

(86) Couture, A.; Grandclaudon, P. 2-Aryl-oxazolo- and thiazolopyridines. Synthesis *via* cyclization of *N*-(2-chloro-3-pyridinyl)arylamides and thioamides. *Heterocycles.* **1984**, *22*, 1383-1385.

(87) Kim, K.; Le, K. Two efficient *N*-acylation methods mediated by solid-supported reagents for weakly nucleophilic heterocyclic amines. *Synlett.* **1999**, *12*, 1957-1959.

(88) Brenner, E.; Baldwin, R. M.; Tamagnan, G. Synthesis of a new precursor to the nicotinic receptor tracer 5-IA-85380 precursor using trimethylsilyl iodide as deblocking agent. *Tetrahedron Lett.* **2004**, *45*, 3607-3610.

(89) Gran, U. Synthesis of a new and versatile macrocyclic NADH model. *Tetrahedron* **2003**, *59*, 4303-4308.

(90) Montaña, A. M.; Grima, P. M. Asymmetry induction on the [4C(4π)+3C(2π)] cycloaddition reaction of C2-functionalized furans: influence of the chiral auxiliary nature. *Tetrahedron* **2002**, *58*, 4769-4786.

(91) Ballistreri, A.; Maccarone, E.; Musumarra, G. The acid dissociation of arenesulphonamides: S_{Het} constants for thia- and oxa-substituents in five-membered *S*-linked heterocycles and effects of substituents in the *N*-linked aromatic ring. *J. Chem. Soc., Perkin Trans. 2* **1977**, *2*, 984-985.

(92) Sweeney, J. B.; Tavassoli, A.; Carter, N. B. and Hayes, J. F. [2,3]-Sigmatropic rearrangements of didehydropiperidinium ylids. *Tetrahedron* **2002**, *58*, 10113-10126.

(93) Thompson, W. J. and Gaudino, J. A general synthesis of 5-arylnicotinates. *J. Org. Chem.* **1984**, *49*, 5237-5243.

(94) Jensen, H. H.; Lyngbye, L.; Jensen, A.; Bols, M. Stereoelectronic substituent effects in polyhydroxylated piperidines and hexahydropyridazines. *Chem. Eur. J.* **2002**, *8*, 1218-1226.

(95) Abramovitch, R. A.; Rogers, R. B. Direct acylamination of 3-substituted pyridine-1-oxides. Directive effect of the substituent. *J. Org. Chem.* **1974**, *39*, 1802-1805.

(96) Bachman, G. B.; Micucci, D. D. Monomers and polymers. V. vinylpyridines and vinylquinolines. *J. Am. Chem. Soc.* **1948**, *39*, 1802-1805.

(97) Müller, P.; Chappellet, S. Asymmetric 1,3-dipolar cycloadditions of 2-diazocyclohexane-1,3-diones and alkyl diazopyruvates. *Helv. Chim. Acta.* **2005**, *88*, 1010-1021.

(98) Prager, R. H.; Smith, J. A.; Weber, B.; Williams, C. M. Chemistry of 5-oxodihydroisoxazoles. Part 18.1 Synthesis of oxazoles by the photolysis and pyrolysis of 2-acyl-5-oxo-2,5-dihydroisoxazoles. *J. Chem. Soc., Perkin Trans. 1.* **1997**, *17*, 2665-2672.

(99) Nienaber, V. L.; Breddam, K.; Birktoft, J. J. A glutamic acid specific serine protease utilizes a novel histidine triad in substrate binding. *Biochemistry* **1993**, *32*, 11469-11475.

(100) McRee, D. E. XtalView/Xfit—a versatile program for manipulating atomic coordinates and electron density. *J. Struct. Biol.* **1999**, 125, 156-165.

(101) Brünger, A. T.; Adams, P. D.; Clore, G. M.; DeLano, W. L.; Gros, P.; Grosse-Kunstleve, R. W.; Jiang, J. S.; Kuszewski, J.; Nilges, M.; Pannu, N. S.; Read, R. J.; Rice, L. M.; Simonson, T.; Warren, G. L. *Crystallography & NMR system*: a new software suite for macromolecular structure determination. *Acta Cryst.* **1998**, *D54*, 905-921.

(102) Allen, F. H. The Cambridge Structural Database: a quarter of a million crystal structures and rising. *Acta Cryst.* **2002**, *B58*, 380-388.

(103) Koradi, R.; Billeter, M.; Wüthrich, K. MolMol: a program for display and analysis of macromolecular structures. *J. Mol. Graphics* **1996**, 14, 51-55.

(104) *SYBYL*, Tripos Inc.: St. Louis, MO.

(105) Gasteiger, J.; Marsili, M. Iterative partial equalization of orbital electronegativeity-a rapid access to atomic charges. *Tetrahedron* **1980**, *36*, 3219-3228.